ZooKeys 872: 1–12 (2019)
doi: 10.3897/zookeys.872.34594
http://zookeys.pensoft.net

RESEARCH ARTICLE

A peer-reviewed open-access journal
ZooKeys
Launched to accelerate biodiversity research

Three new species of the genus *Falcileptoneta* Komatsu, 1970 (Araneae, Leptonetidae) from Korea

Mingjie Xu[1,2], Seung Tae Kim[3], Jung Sun Yoo[4], Eun Jung Nam[4], Shuqiang Li[2]

1 *Hebei Key Laboratory of Animal Diversity, College of Life Science, Langfang Normal University, Langfang 065000, China* **2** *Institute of Zoology, Chinese Academy of Sciences, Beijing 100101, China* **3** *Life and Environment Research Institute, Konkuk University, Seoul 05029, Korea* **4** *Division of Animal Resources, National Institute of Biological Resources, Incheon 22689, Korea*

Corresponding author: *Jung Sun Yoo* (lycosidae@korea.kr); *Shuqiang Li* (lisq@ioz.ac.cn)

Academic editor: *Dimitar Dimitrov* | Received 17 March 2019 | Accepted 30 July 2019 | Published 20 August 2019

http://zoobank.org/ED1EC51D-7C85-483D-B61C-CCBD6267DA79

Citation: Xu M, Kim ST, Yoo JS, Nam EJ, Li S (2019) Three new species of the genus *Falcileptoneta* Komatsu, 1970 (Araneae, Leptonetidae) from Korea. ZooKeys 872: 1–12. https://doi.org/10.3897/zookeys.872.34594

Abstract

Three new species of the genus *Falcileptoneta* Komatsu, 1970 belonging to the spider family Leptonetidae Simon 1890 are described from Korea. All species were collected from wet leaf litter layers.

Keywords

Diagnosis, morphology, new species, taxonomy

Introduction

The family Leptonetidae Simon, 1890 currently contains 21 genera and 349 species worldwide (World Spider Catalog 2019). Most species are tiny (1–3 mm) and have six eyes with the posterior median eyes located behind the posterior lateral eyes; some species have only four or two eyes or are eyeless. Most species live in irregular sheet webs in leaf litter, caves, or mines. In Korea, there are 42 species in four genera: *Leptoneta* Simon, 1872, *Falcileptoneta* Komatsu, 1970, *Masirana* Kishida, 1942 and *Longileptoneta* Seo, 2015. Komatsu (1970) erected *Falcileptoneta* with *F. striatus* (Oi 1952) as the type species (transferred from *Leptoneta*). Prior to this study, 47 *Falcileptoneta* species have

been described from Korea and Honshu, Shikoku in Japan (Irie and Ono 2007). In this study, three new species of *Falcileptoneta* are illustrated and described.

Materials and methods

All specimens were collected by hand from mountainous districts in northern South Korea. Type specimens are deposited in the National Institute of Biological Resources (**NIBR**) in Incheon, Korea and the Institute of Zoology, Chinese Academy of Sciences (**IZCAS**) in Beijing, China. All spiders were preserved in 95% ethanol and examined under a LEICA M205C stereomicroscope. Images were captured with an Olympus C7070 wide zoom digital camera (7.1 megapixels) mounted on an Olympus SZX12 dissecting microscope, and Helicon Focus image stacking software was used to compile the images. All images were edited with Adobe Photoshop CS8.1. Methods follow those of Wang and Li (2011) and Ledford et al. (2011); terminology follows Wang et al (2017). The map was drawn with the assistance of ArcGIS 10.2 and edited with Adobe Photoshop CS8.1. All measurements are in millimeters (mm). The left male palps are illustrated. Leg measurements are displayed as total length (femur, patella, tibia, metatarsus, tarsus). Leg segments were measured on their dorsal side. Abbreviations of morphological structures are as follows:

At atrium;
E embolus;
MS median sclerite;
SS spermathecae stalk;
PS prolateral sclerite;
SH spermathecae.

Taxonomy

Family Leptonetidae Simon, 1890

Genus *Falcileptoneta* Komatsu, 1970

Type species. *Leptoneta striatus* Oi, 1952

Diagnosis. The genus *Falcileptoneta* is similar to *Leptoneta* and *Longileptoneta* by having fewer sclerites on the bulb but can be distinguished from these two genera by the combination of the following characters: tarsus of male palp with shallow, transverse depression and without spines; tibia with apophyses on the retrolateral apical end; bulb with sickle-like or membranous embolus; complex laminae of the bulb. *Leptoneta* can be distinguished by the tarsus with a branch bearing an apical spine. *Longileptoneta* can be identified by the strong femoral spines, the prolateral curvature bearing a prolateral distal spur on the tarsus, a finger-like median sclerite, and a leaf-like embolus.

Comments. According to the original description, the genus *Falcileptoneta* is similar to *Leptoneta* but can be distinguished by the falcula on the tibia of the male palp. Femur normal. Tibia with three trichobothria, and the apical end with spine-like apophyses. Tarsus with several bristles but no spines and a weak transverse depression. We have added descriptions of the following characters: the shape of the embolus and the laminae of the bulb.

Distribution. Korea, Japan.

***Falcileptoneta baegunsanensis* sp. nov.**

http://zoobank.org/3DAFCF04-0F6A-43D9-B945-6369F2126A10

Figures 1–2, 7

Type material. ***Holotype:*** male (NIBR), Mt. Baegunsan, Seonyudam Valley near the parking area (38.0702°N, 127.4026°E), Dopyeong-ri, Idong-myeon, Pocheon-si, Gyeonggi-do, Korea, 09 October 2018, ZG. Chen, Z. Zhao & MJ. Xu leg. ***Paratypes*:** 1 male and 1 female (IZCAS), same data as holotype.

Etymology. The specific name is an adjective referring to the type locality.

Differential diagnosis. This new species is similar to *F. geumsanensis* Seo, 2016 and *F. boeunensis* Seo, 2015 but can be separated by the shape of the palpal tibial apophyses found retrolaterally, with one apophysis coniform and the other bifurcate, bearing three spines distally (Figure 1D) (vs. a spur-like tibial apophysis located ventrally, a leaf-like medial apophysis, a dorsal beak-like apophysis in *F. geumsanensis*; three tibial spines with the outer spine spur-like, the medial one spine-like, and the inner spine conical in *F. boeunensis*.).

Description. ***Male*** (holotype). Total length 1.40. Prosoma 0.60 long, 0.51 wide. Opisthosoma 0.80 long, 0.55 wide (Figure 1A). Prosoma brown. Eyes six. Median groove, cervical grooves and radial furrows distinct. Clypeus 0.15 high. Opisthosoma gray, ovoid. Leg measurements: I 3.53 (0.94, 0.25,0.99, 0.74, 0.61); II 2.97 (0.88, 0.23, 0.74, 0.62, 0.50); III 2.58 (0.66, 0.19, 0.68, 0.63, 0.42); IV 3.4 (0.98, 0.19, 1.00, 0.81, 0.42). Palp as illustrated in Figure 1C, D: femur lacking strong spine; tibia with three apophyses retrolaterally, with one coniform and the other bifurcate, bearing three spines distally (Figure 1D); tarsus with a transverse depression, and a smooth, distinct earlobe-shaped process. Bulb with triangular black sickle-shaped embolus and three types of sclerites: prolateral sclerite membranous; median sclerite wide and shoehorn-like; retrolateral sclerite transparent and membranous (Figure 1B).

Female (one of the paratypes). Similar to male in color and general features but larger and with longer legs. Total length 1.39 as in Figure 2A, B. Prosoma 0.55 long, 0.46 wide. Opisthosoma 0.84 long, 0.50 wide. Leg measurements: I 3.25 (0.78, 0.18, 0.84, 0.98, 0.47); II 2.29 (0.69, 0.17, 0.60, 0.48, 0.35); III 2.09 (0.56, 0.16, 0.52, 0.45, 0.40); IV2.88 (0.84, 0.22, 0.80, 0.63, 0.39). Internal genitalia as provided in Figure 2C: atrium rectangular, anterior margin of atrium with short hairs, and spermathecae oval.

Habitat. Litter layers in mixed forest.

Distribution. Korea (Gyeonggi-do).

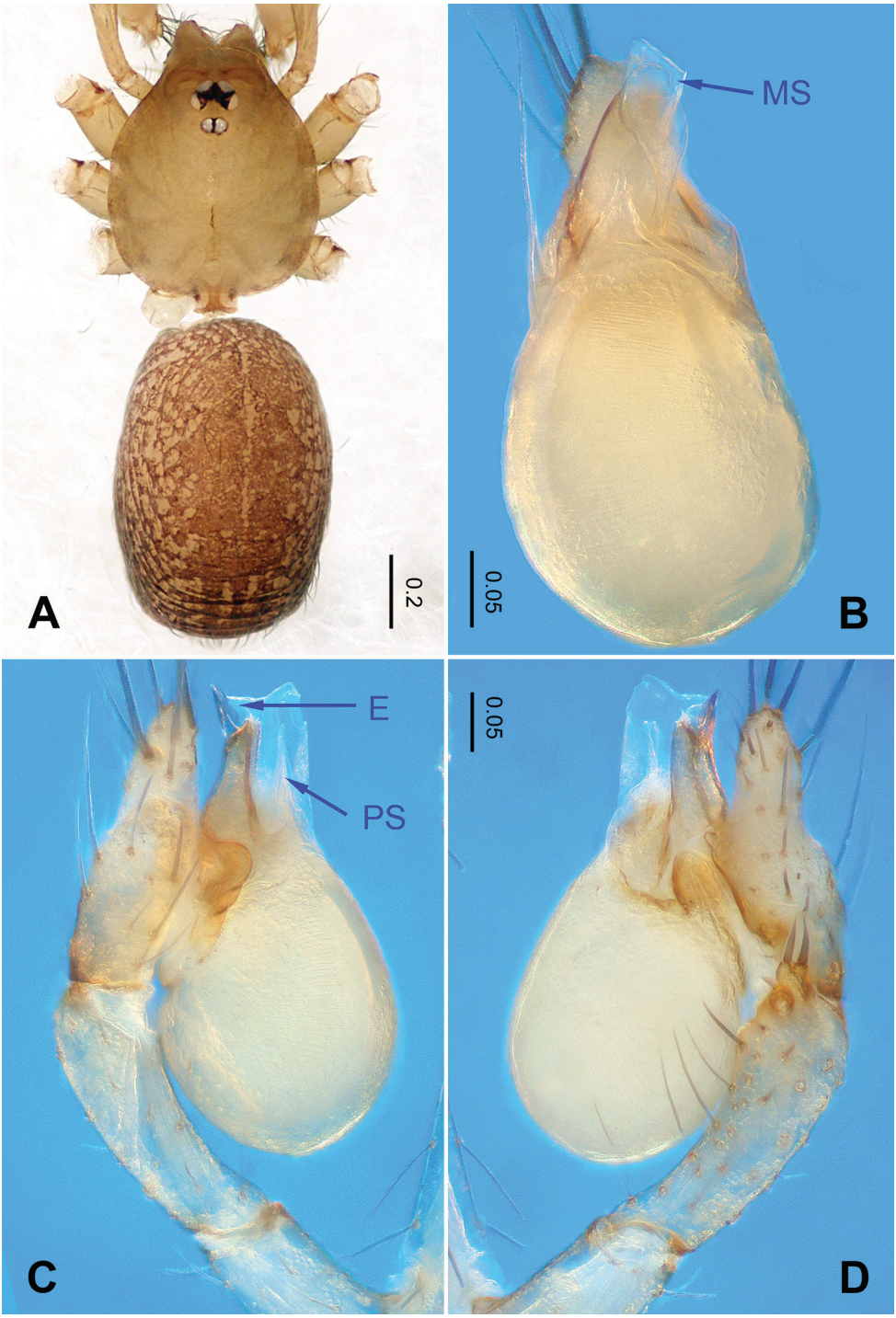

Figure 1. *Falcileptoneta baegunsanensis* sp. nov., male holotype. **A** habitus, dorsal view **B** palpal bulb, ventral view **C** palp, prolateral view **D** palp, retrolateral view. Abbreviations: **PS** = prolateral sclerite; **E** = embolus; **MS** = median sclerite.

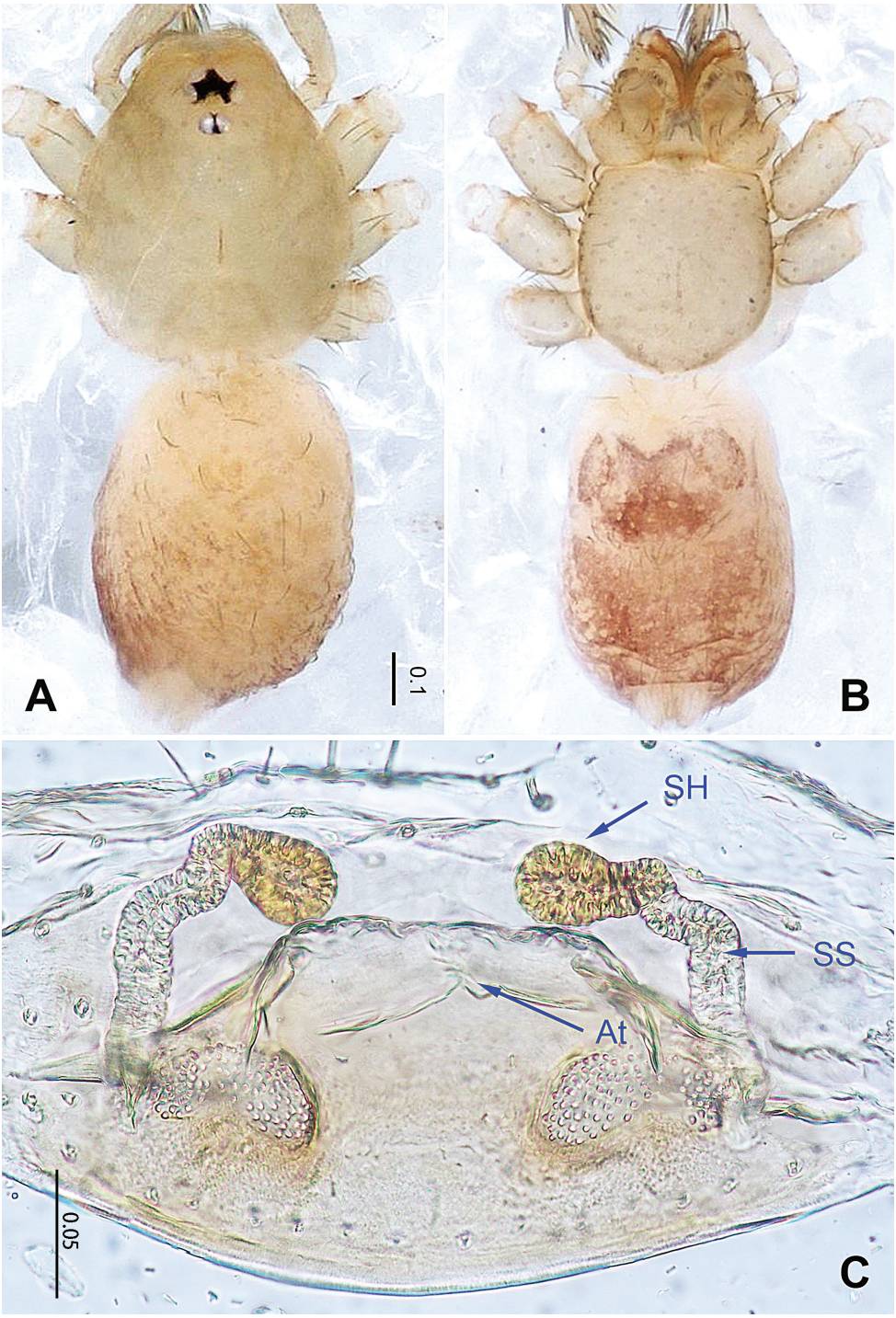

Figure 2. *Falcileptoneta baegunsanensis* sp. nov., female paratype. **A** habitus, dorsal view **B** habitus, ventral view **C** internal genitalia, dorsal view. Abbreviations: **At** = atrium; **SS** = spermathecae stalk; **SH** = spermathecae.

***Falcileptoneta odaesanensis* sp. nov.**
http://zoobank.org/B861FF33-505A-492F-8D88-35C6BB04D47B
Figures 3–4, 7

Type material. ***Holotype*:** male (NIBR), Mt. Odaesan 0.2 km east of Sangwonsa Temple (37.7865°N, 128.5665°E), Jinbu-myeon, Pyeongchang-gun, Gangwon-do, Korea, 18 September 2018, ZG. Chen, Z. Zhao & MJ. Xu leg. ***Paratypes*:** 1 male and 1 female (IZCAS), same data as holotype.

Etymology. The specific name is an adjective referring to the type locality.

Differential diagnosis. This new species is similar to *F. geumdaensis* Seo, 2016, *F. sunchangensis* Seo, 2016 and *F. amakusaensis* Irie & Ono, 2005 but can be separated by the palpal tibia with three distal retrolateral setae (Figure 3D) (vs. tibial apophysis with two whip-shaped hairs bearing minute setae and the main apophysis spiniform in *F. amakusaensis*; tibial apophysis with two spur-like retrolateral apophyses in *F. geumdaensis*; tibial apophysis with two retrolateral spines with the dorsal one thick and spur-like in *F. sunchangensis*).

Description. ***Male*** (holotype). Total length 1.44 (Figure 3A). Carapace 0.63 long, 0.59 wide. Opisthosoma 0.81 long, 0.59 wide. Prosoma brown. Eyes six, reduced to white vestiges. Median groove, distinct cervical grooves and radial furrows. Opisthosoma gray, ovoid. Leg measurements: I 3.27 (0.80, 0.20, 0.91, 0.70, 0.66); II 2.84 (0.75, 0.21, 0.78, 0.60, 0.50); III 2.36 (0.60, 0.18, 0.55, 0.58, 0.45); IV missing. Male palp as in Figure 3C, D: femur without strong spine; tibia with three retrolateral setae distally, arranged in a triangle; tarsus with a transverse depression (Figure 3D). Embolus with a membranous margin and three types of sclerites: prolateral sclerite spine-like; median sclerite shoehorn-like; retrolateral sclerite membranous (Figure 3B).

Female (one of the paratypes). Similar to male in color and general features but larger and with longer legs. Total length 1.61 as in Figure 4A, B. Prosoma 0.63 long, 0.58 wide. Opisthosoma 0.98 long, 0.69 wide. Leg measurements: I 3.27 (0.80, 0.20, 0.91, 0.70, 0.66); II 2.84 (0.75, 0.21, 0.78, 0.60, 0.50); III 2.36 (0.60, 0.18, 0.55, 0.58, 0.45); IV missing. Internal genitalia as in Figure 4C: atrium triangular, genital duct coiled apically, and spermathecae oval.

Habitat. Litter layers in mixed forest.

Distribution. Korea (Gangwon-do).

***Falcileptoneta umyeonsanensis* sp. nov.**
http://zoobank.org/77593E93-102C-4E98-A900-AD3270FF86C0
Figures 5–7

Type material. Holotype: male (NIBR), Mt. Umyeonsan, Seocho-gu, Seoul, Korea, (37.4794°N, 127.0315°E), 03 October 2018, ZG. Chen, Z. Zhao & MJ. Xu leg. **Paratypes:** 1 male and 1 female (IZCAS), same data as holotype.

Etymology. The specific name is an adjective referring to the type locality.

Differential diagnosis. This new species is similar to *F. yebongsanensis* Kim, Lee & Namkung, 2004 and *Leptoneta kwangreungensis* Kim, Jung, Kim & Lee, 2004 but can

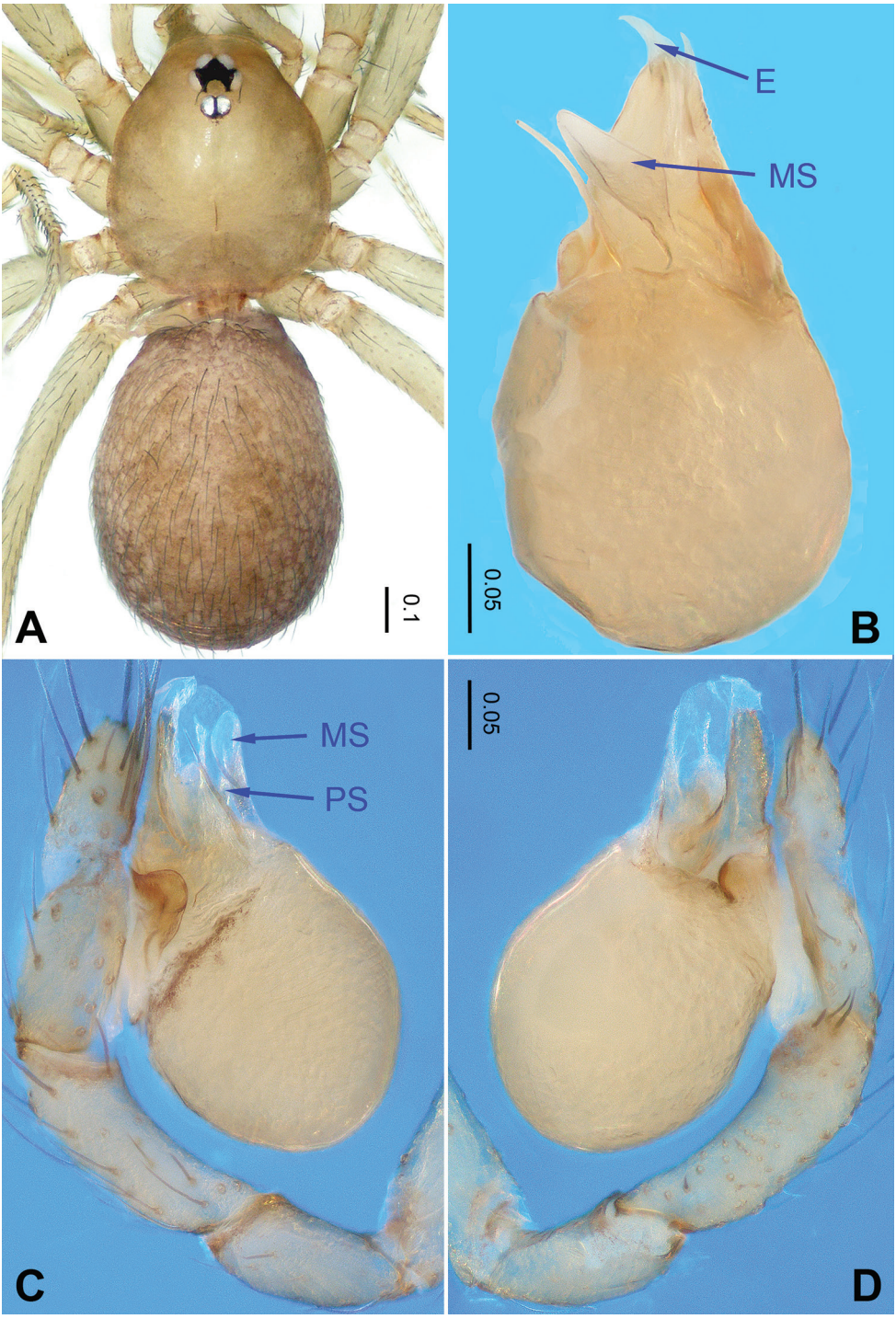

Figure 3. *Falcileptoneta odaesanensis* sp. nov., male holotype. **A** habitus, dorsal view **B** palpal bulb, ventral view **C** palp, prolateral view **D** palp, retrolateral view. Abbreviations: **PS** = prolateral sclerite; **E** = embolus; **MS** = median sclerite.

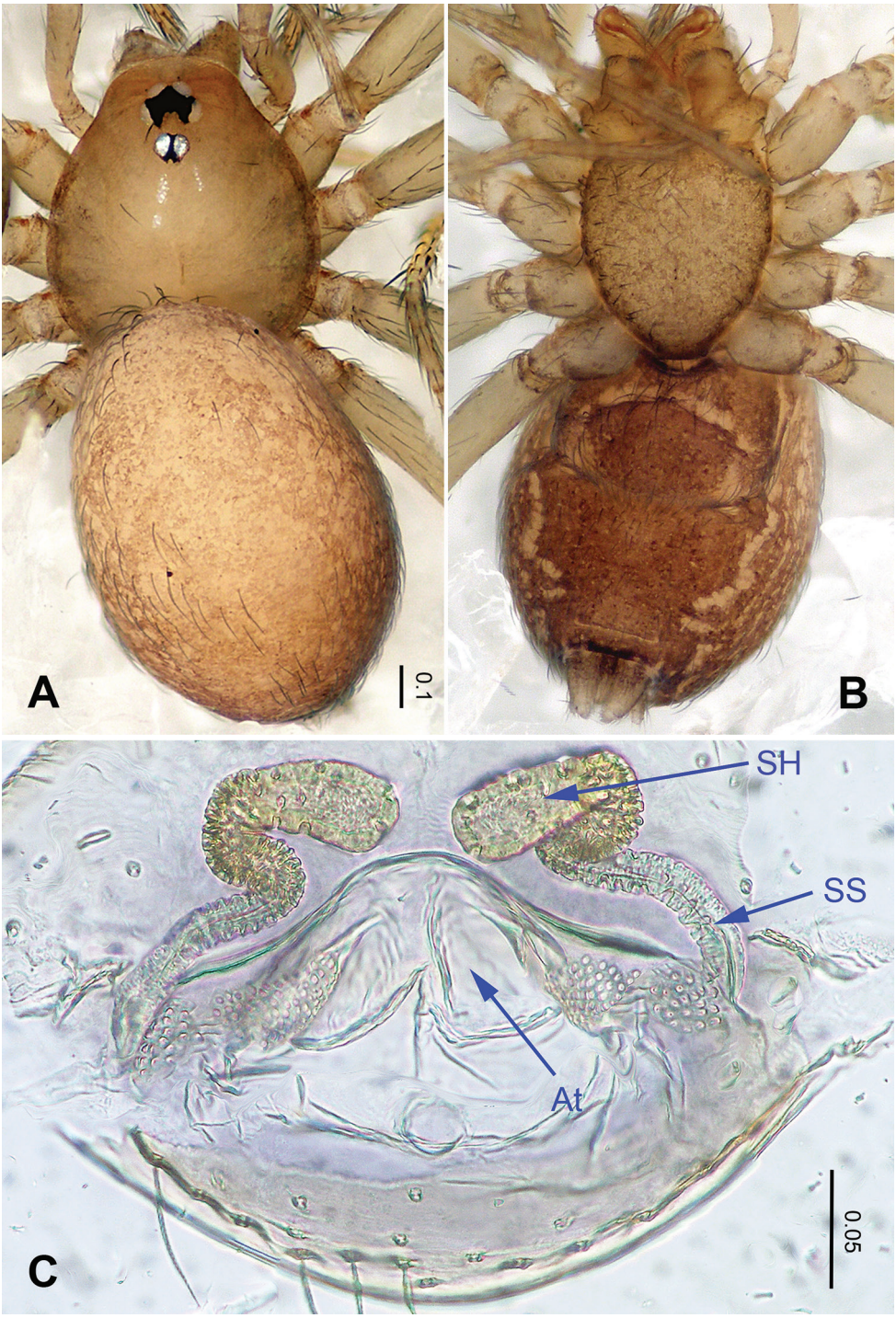

Figure 4. *Falcileptoneta odaesanensis* sp. nov., female paratype. **A** habitus, dorsal view **B** habitus, ventral view **C** internal genitalia, dorsal view. Abbreviations: **At** = atrium; **SS** = spermathecae stalk; **SH** = spermathecae.

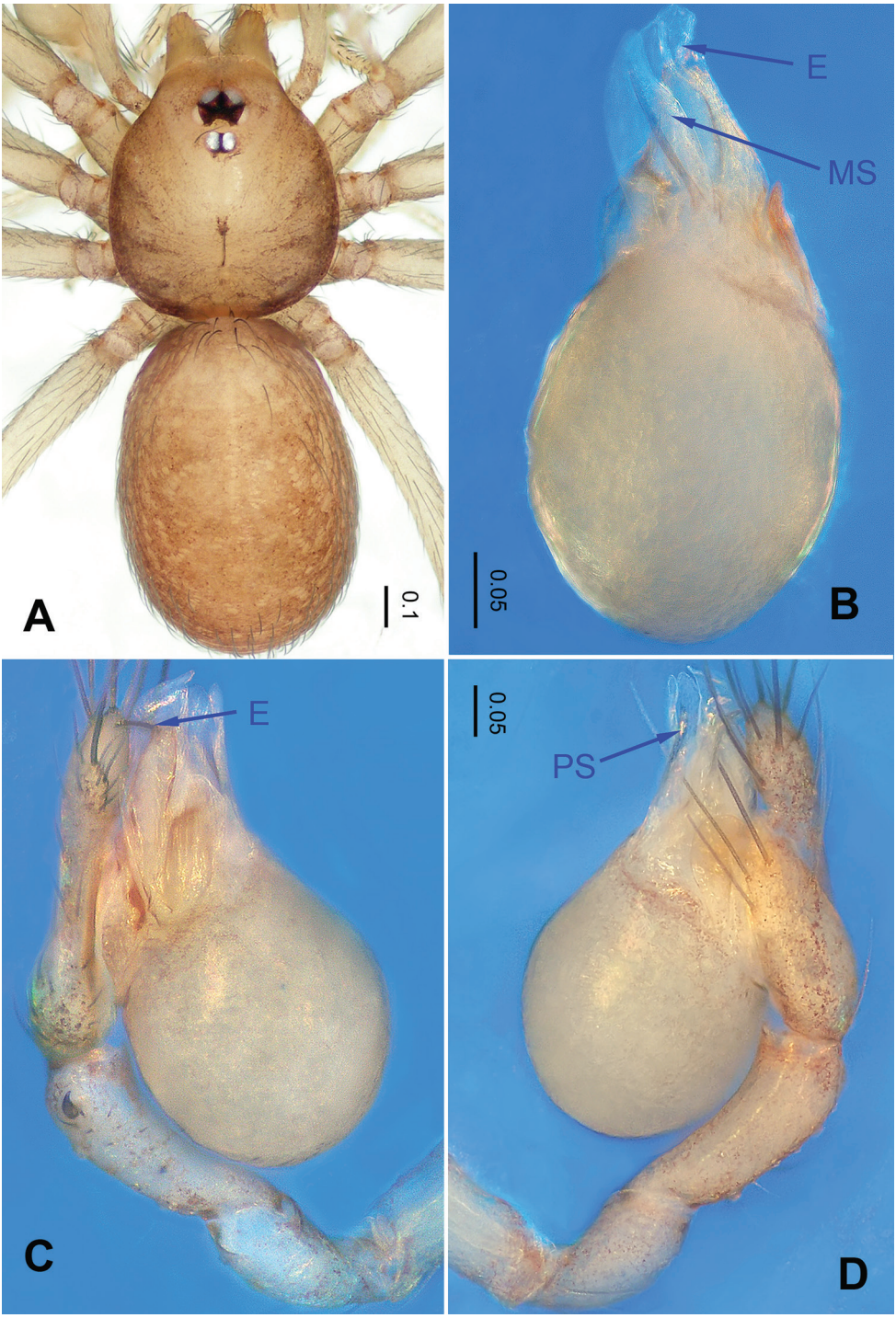

Figure 5. *Falcileptoneta umyeonsanensis* sp. nov., male holotype. **A** habitus, dorsal view **B** right palpal bulb, ventral view **C** right palp, retrolateral view **D** right palp, prolateral view. Abbreviations: **PS** = prolateral sclerite; **E** = embolus; **MS** = median sclerite.

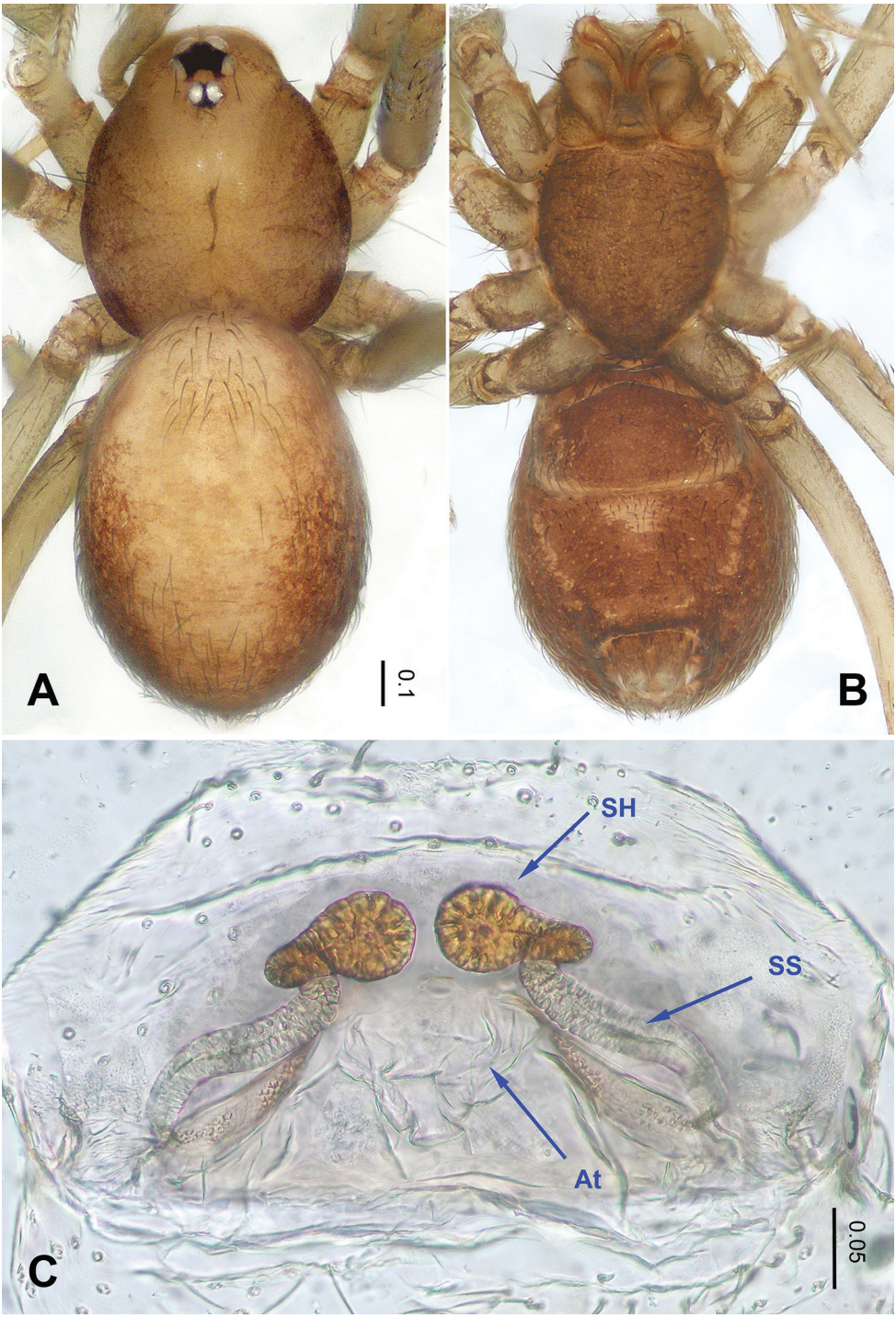

Figure 6. *Falcileptoneta umyeonsanensis* sp. nov., female paratype. **A** habitus, dorsal view **B** habitus, ventral view **C** internal genitalia, dorsal view. Abbreviations: **At** = atrium; **SS** = spermathecae stalk; **SH** = spermathecae.

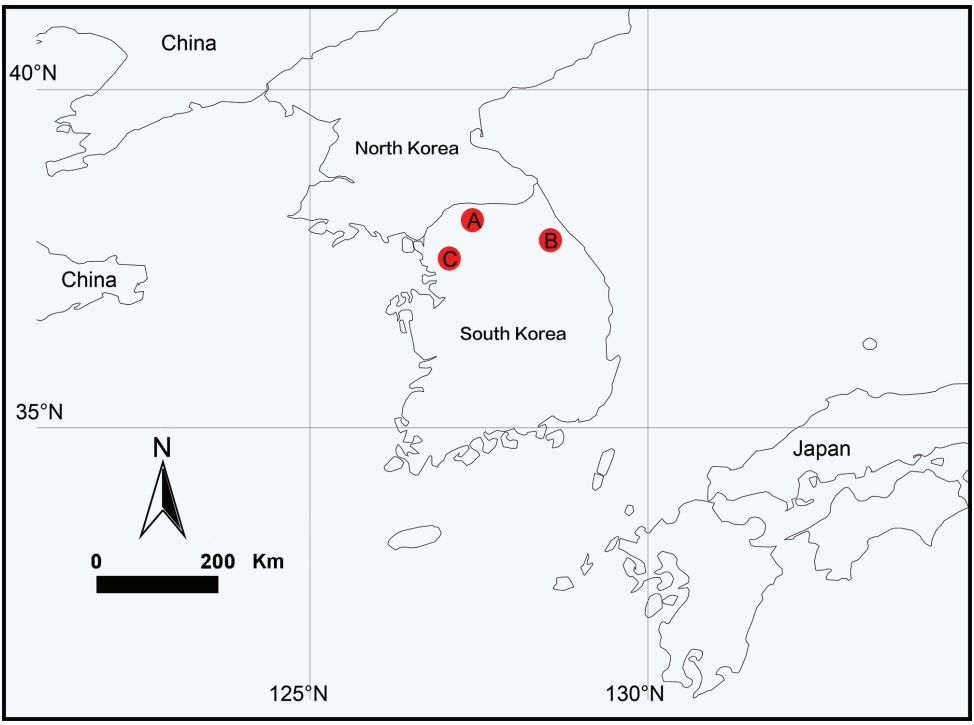

Figure 7. Locality records for three new species of the genus *Falcileptoneta* from Korea. **A** *F. baegunsanensis* sp. nov. **B** *F. odaesanensis* sp. nov. **C** *F. umyeonsanensis* sp. nov.

be separated by one hook-like retrolateral apophysis on the palpal tibia, leaf-shaped median apophysis, and sickle-shaped embolus (Figure 5C) (vs. short tubercle without spines or bristles on tibia, hook-shaped median apophysis and sickle-shaped embolus in *F. yebongsanensis*; spine-shaped embolus and median apophysis in *L. kwangreungensis*).

Description. ***Male*** (holotype). Total length 1.58 (Figure 5A). Carapace 0.64 long, 0.57 wide. Opisthosoma 0.94 long, 0.67 wide. Prosoma brown. Eyes six. Median groove, distinct cervical grooves and radial furrows. Opisthosoma brown, ovoid. Leg measurements: I 3.95 (1.09, 0.19, 1.19, 0.84, 0.64); II 3.06 (0.86, 0.18, 0.86, 0.64, 0.52); III 2.51 (0.71, 0.16, 0.67, 0.59, 0.38); IV 4.28 (1.12, 0.21, 1.29, 0.94, 0.72). Male palp as in Figure 5C, D: femur without a strong spine; tibia with one hook-like retrolateral apophysis (Figure 5C). Embolus with a sickle-shaped tip and three types of sclerites: prolateral sclerite spine-like; median sclerite leaf-like; retrolateral sclerite membranous (Figure 5B).

Female (one of the paratypes). Similar to male in color and general features. Total length 1.51 (Figure 6A, B). Prosoma 0.63 long, 0.55 wide. Opisthosoma 0.88 long, 0.87 wide. Leg measurements: I 3.50 (0.92, 0.20, 0.98, 0.78, 0.62); II 2.84 (0.75, 0.20, 0.76, 0.63, 0.50); III 2.61 (0.69, 0.20, 0.63, 0.61, 0.48); IV 3.71 (0.94, 0.22, 1.00, 0.80, 0.75). Internal genitalia as in Figure 6C: atrium wrinkled, trapezoidal, genital duct coiled apically, and spermathecae round.

Habitat. Litter layers in mixed forest.

Distribution. Korea (Seoul).

Acknowledgements

The manuscript benefitted greatly from comments by Drs Dimitar Dimitrov, Charles Griswold, and Joel Ledford. Sarah Crews kindly checked the language. This work was supported by grants from the National Institute of Biological Resources (NIBR), funded by the Ministry of Environment (MOE) of the Republic of Korea (NIBR201801109). Part of the lab work was supported by the National Natural Sciences Foundation of China (NSFC–31530067).

References:

Irie T, Ono H (2007) Two new species of the genus *Falcileptoneta* (Arachnida, Araneae, Leptonetidae) collected from Chûbu District, Honshu. Bulletin of the National Museum of Nature and Science, Tokyo, Series A 33: 175–180.

Irie T, Ono H (2005) Seven new species of the genera *Falcileptoneta* and *Masirana* (Araneae, Leptonetidae) from Kyushu. Bulletin of the National Museum of Nature and Science, Tokyo, Series A 31: 77–92.

Komatsu T (1970) A new genus and a new species of Japanese spiders (*Falcileptoneta* n. g. and *Sarutana kawasawai* n. sp., Leptonetidae). Acta Arachnologica 23: 1–12. https://doi.org/10.2476/asjaa.23.1

Kim ST, Lee JH, Namkung J (2004) Two new ground-inhabiting *Leptoneta* spiders (Araneae: Leptonetidae) from Korea. Journal of Asia-Pacific Entomology 7: 257–261. https://doi.org/10.1016/S1226-8615(08)60225-3

Kim ST, Jung MP, Kim HS, Lee JH (2004) Two new species of litter-inhabiting spiders of the genus *Leptoneta* from Korea (Araneae: Leptonetidae). The Canadian Entomologist 136(5): 639–644. https://doi.org/10.4039/n03-099

Ledford J, Paquin P, Cokendolpher J, Campbell J, Griswold C (2011) Systematics of the spider genus *Neoleptoneta* Brignoli, 1972 (Araneae: Leptonetidae) with a discussion of the morphology and relationships for the North American Leptonetidae. Invertebrate Systematics 25: 334–388. https://doi.org/10.1071/IS11014

Oi R (1952) A new spider of the genus *Leptoneta*. Arachnological News 1: 10–12.

Seo BK (2016) Four new species of the genus *Falcileptoneta* (Araneae, Leptonetidae) from Korea. Journal of Species Research 5(3): 590–595. https://doi.org/10.12651/JSR.2016.5.3.590

Seo BK (2015) Ten new species of the genus *Falcileptoneta* (Araneae, Leptonetidae) from Korea. Korean Journal of Environmental Biology 33(3): 290–305. https://doi.org/10.11626/KJEB.2015.33.3.290

Wang CX, Li SQ (2011) A further study on the species of the spider genus *Leptonetela* (Araneae: Leptonetidae). Zootaxa 2841: 1–90. https://doi.org/10.11646/zootaxa.2841.1.1

Wang CX, Xu X, Li SQ (2017) Integrative taxonomy of *Leptonetela* spiders (Araneae, Leptonetidae), with descriptions of 46 new species. Zoological Research 38(6): 321–448.

ZooKeys 872: 13–40 (2019)
doi: 10.3897/zookeys.872.35361
http://zookeys.pensoft.net

RESEARCH ARTICLE

A peer-reviewed open-access journal
ZooKeys
Launched to accelerate biodiversity research

The distribution of the genus *Sphecodes* Latreille (Hymenoptera, Halictidae) of the Arabian Peninsula and surrounding countries with description of hitherto unknown female of *S. atlanticus* Warncke, 1992 and male of *S. dathei* Schwarz, 2010

Yulia V. Astafurova[1], Maxim Yu. Proshchalykin[2], Maximilian Schwarz[3]

1 *Zoological Institute, Russian Academy of Sciences, Universitetskaya Nab., 1, Saint Petersburg 199034, Russia* **2** *Federal Scientific Centre for East Asian Terrestrial Biodiversity, Far Eastern Branch of Russian Academy of Sciences, Vladivostok 690022, Russia* **3** *A-4052, Ansfelden, Austria*

Corresponding author: *Maxim Yu. Proshchalykin* (proshchalikin@biosoil.ru)

Academic editor: *Michael S. Engel* | Received 11 April 2019 | Accepted 18 July 2019 | Published 20 August 2019

http://zoobank.org/DCDEFCB1-E33D-476F-90D7-178BC08C311A

Citation: Astafurova YuV, Proshchalykin MYu, Schwarz M (2019) The distribution of the genus *Sphecodes* Latreille (Hymenoptera, Halictidae) of the Arabian Peninsula and surrounding countries with description of hitherto unknown female of *S. atlanticus* Warncke, 1992 and male of *S. dathei* Schwarz, 2010. ZooKeys 872: 13–40. https://doi.org/10.3897/zookeys.872.35361

Abstract

This study summarises all available information on the bees of the genus *Sphecodes* in the Arabian Peninsula and surrounding countries (Israel, Jordan, and Syria). Twenty-six species are currently known from this area, while five species are newly recorded from the Arabian Peninsula: *Sphecodes atlanticus* Warncke, 1992 (Saudi Arabia, Yemen), *S. intermedius* Blüthgen, 1923 (UAE), *S. nomioidis* Pesenko, 1979 (UAE, Oman), *S. puncticeps* Thomson, 1870 (Saudi Arabia), and *S. turanicus* Astafurova & Proshchalykin, 2017 (Saudi Arabia). In addition, twelve species are newly recorded from Jordan, six for Syria, and four for Israel. The female of *S. atlanticus* Warncke, 1992 and the male of *S. dathei* Schwarz, 2010 are here described for the first time and a lectotype is designated for *S. intermedius* Blüthgen, 1923.

Keywords

Anthophila, Apiformes, cleptoparasites, fauna, lectotype, taxonomy

Introduction

The present paper is part of a series of studies dealing with the bees of the genus *Sphecodes* of the territory of the Palaearctic region (Warncke 1992; Bogusch and Straka 2012; Özbek et al. 2015; Astafurova and Proshchalykin 2014, 2015a, b, c, 2016a, b, 2017a, b, c, 2018; Astafurova et al. 2014, 2015, 2018a, b, c, d). The goal of this survey is to improve the knowledge on the taxonomy and distribution of *Sphecodes* in the Arabian Peninsula and surrounding countries (Israel, Jordan and Syria) (Fig. 1) as an essential foundation for advanced biogeographical investigations.

For a long time, the Arabian bee fauna has been one of the lesser sampled faunas of the world. But in recent years significant progress has been made towards a better knowledge of the bees from the Arabian Peninsula, in particular regarding the family Halictidae (Dathe 2009, Engel et al. 2013). A first contemporary inventory of the Halictidae of the Arabian Peninsula was compiled by Ebmer (2008) and Dathe (2009). Later, additional species have been described and recorded by Pesenko and Pauly (2009), Schwarz (2010), Alqarni et al. (2014), Bossert (2017), and Ascher and Pickering (2019) so that there are currently 82 species from 13 genera of family Halictidae known from this area, but the *Sphecodes* fauna of Arabian Peninsula is particularly under-recorded.

Probably the first information on the genus *Sphecodes* Latreille from the Arabian Peninsula and its adjacent lands was published by Lepeletier de Saint Fargeau (Lepeletier de Saint Fargeau and Audinet-Serville 1825), who described *S. olivieri* from 'Arabie'. Almost two centuries later, in his monograph on the Western Palaearctic *Sphecodes*, Warncke (1992) recorded several species from Israel, Syria and Lebanon (Table 1). The list of bees of the Arabian Peninsula published by Dathe (2009) included two *Sphecodes* species: *S. olivieri* and *S. longuloides* Blüthgen. In the recently published third volume of the "Arthropod fauna of UAE", Schwarz (2010) described *S. dathei* and *S. villosulus* and recorded *S. marginatus* Hagens and *S. pinguiculus* Pérez from the United Arab Emirates. In total, nineteen *Sphecodes* species have been recorded from the Arabian Peninsula and its adjacent lands so far (Table 1). The genus *Sphecodes* is not yet documented from Kuwait, Bahrain, or Iraq. Clearly this cosmopolitan genus is present in these countries and it is only a matter of time before the fauna is sampled and recorded.

Based on a comprehensive study of specimens in various collections, we here list 23 species of the genus *Sphecodes*, with five species recorded from the Arabian Peninsula for the first time. Additionally, twelve species are newly recorded from Jordan, six species newly recorded from Syria, and four species newly recorded from Israel. The female of *S. atlanticus* Warncke, 1992 and the male of *S. dathei* Schwarz, 2010 are here described for the first time and a lectotype is designated for *S. intermedius* Blüthgen, 1923.

Materials and methods

The results presented in this paper are based on 235 specimens collected in the Arabian Peninsula and surrounding territories and currently housed in the Natural History Museum (London, UK, NHMUK); the Zoological Institute, Russian Academy

Figure 1. Map of the Arabian Peninsula and surrounding lands.

of Sciences (St. Petersburg, Russia, ZISP); Museum für Naturkunde der Humboldt Universität zu Berlin, Germany (ZMHB), Senckenberg Deutsches Entomologisches Institut, Müncheberg, Germany (SDEI), Oberösterreichisches Landesmuseum, Biologiezentrum, Linz, Austria (OLBL) and the private collection of Maximilian Schwarz (Ansfelden, Austria, OLBL/PCMS). The following acronyms are used for the collections where type specimens are deposited:

BLCU Utah State University, Bee Biology and Systematics Laboratory, Logan, Utah, USA;
ISZP Institute of Systematics and Evolution of Animals, Polish Academy of Sciences, Krakow, Poland;
MNHN Muséum National d'Histoire Naturelle Paris, France;
MRSN Museo Regionale di Scienze Naturali, Torino, Italy;
MZLU Lund University, Lund, Sweden;
NHMUK Natural History Museum, London, UK;
ZMUK University of Copenhagen, Zoological Museum, Copenhagen, Denmark;
ZSN Zoologische Staatssammlung, München, Germany.

Table 1. Checklist of the *Sphecodes* species of the Arabian Peninsula and surrounding lands including distribution by countries.

	Species	Arabian Peninsula					surrounding lands			
		UAE	Oman	Qatar	Saudi Arabia	Yemen	Lebanon	Israel	Jordan	Syria
1	*S. alternatus* Smith							○●	●	○
2	*S. atlanticus* Warncke				●	●				
3	*S. barbatus* Blüthgen									●
4	*S. dathei* Schwarz	○●			●	●				
5	*S. dusmeti* Blüthgen	○								
6	*S. ephippius* (Linnaeus)						○	○		
7	*S. gibbus* (Linnaeus)							○●	●	
8	*S. intermedius* Blüthgen	●						○●	●	
9	*S. longuloides* Blüthgen	○								
10	*S. longulus* Hagens							●	○●	○●
11	*S. majalis* Pérez								●	
12	*S. marginatus* Hagens	○						●	●	
13	*S. monilicornis* (Kirby)							○	○●	●
14	*S. nomioidis* Pesenko	●	●						○	
15	*S. olivieri* Lepeletier	○●	●	○	●			○●	●	
16	*S. pellucidus* Smith								●	●
17	*S. pinguiculus* Pérez	○	●		●			○●		●
18	*S. puncticeps* Thomson				●			○●	●	●
19	*S. rubicundus* Hagens							●		
20	*S. rubripes* Spinola							○	●	○
21	*S. ruficrus* (Erichson)							○	●	
22	*S. rufiventris* (Panzer)							○	●	
23	*S. tadschicus* Blüthgen							●		
24	*S. turanicus* Astafurova & Proshchalykin				●					
25	*S. schenckii* Hagens							○	●	●
26	*S. villosulus* Schwarz	○●			●					
	Total:	9	4	1	7	2	1	16	15	9
				12				20		

White circle – published records (Meyer 1924; Warncke 1992; Dathe 2009; Schwarz 2010; Ascher and Pickering 2019); black circle – current data. Genus *Sphecodes* are not known in Kuwait, Bahrain, and Iraq.

The taxonomy and distribution of species follows that of Warncke (1992), Bogusch and Straka (2012), and Astafurova and Proshchalykin (2017b). Identification keys are available in Warncke (1992), Astafurova and Proshchalykin (2017b) or Astafurova et al. (2018b), except for the two recently described new species (*S. dathei* and *S. villosulus*). A detailed synonymy can be found in Astafurova and Proshchalykin (2016b, 2017b). Morphological terminology follows that of Engel (2001) and Michener (2007). The ventral surface of some flagellomeres bear a distinctive patch of sensilla trichodea A (sensu Årgent and Svensson 1982), which we refer to as 'tyloids', easily observable under the microscope. Abbreviations F, T, and S are used for flagellomere, metasomal tergum and metasomal sternum respectively. The density of integumental punctures is described using the following formula: puncture diameter (in μm) / ratio of distance between punctures to average puncture diameter, e.g., 15–20 μm / 0.5–1.5. Integumental sculpture other than distinctive surface punctation is described following Harris (1979): areolate – coarse, contiguous punctures; reticulate – superficially net-like or network of raised lines; rugose – irregular, nonparallel, wrinkled raised

lines (rugae); rugulose – minutely rugose; strigate – narrow, transverse or longitudinal streaks (strigae), variety of parallel lineations; tessellate – regular network of shallow grooves with flat interspaces.

Specimens were studied with a Leica M205A stereomicroscope and photographs taken with a combination of stereomicroscope (Olympus SZX10) and digital camera (Canon EOS70D). Final images are stacked composites using the program Helicon Focus 6. All images were post-processed for contrast and brightness using Adobe Photoshop.

New distributional records are noted with an asterisk (*).

Taxonomy

List of species

Sphecodes alternatus Smith, 1853

Sphecodes alternatus Smith, 1853: 36, ♀ (syntypes: ♀♀, Albania; NHMUK).
Sphecodes punctiventris Hagens, 1882; *S. gracilior* Morawitz, 1893; *S. antigae* Tournier, 1901; *S. reticulatus* var. *algeriensis* Alfken, 1914; *S. alternatus lindbergi* Pittioni, 1950 (Synonyms).

Diagnosis. See Astafurova et al. 2018a: 6.

Material examined. ISRAEL: 1 ♀, Rehovot s.l., 29.IV.1975, K.M. Guichard (NHMUK 013380375); JORDAN: 1 ♀, 10 km N Petra, 3.V.1996, M. Halada (OLBL/OLBL/PCMS).

Published records. Warncke 1992: 47, map (Israel, Syria); Ascher and Pickering 2019 (Israel).

Distribution. Israel, *Jordan, Syria; North Africa, South and Central Europe, Russia (east to Khakassia Republic), Turkey, Caucasus, Iran, Central Asia, Kazakhstan, NW China.

Sphecodes atlanticus Warncke, 1992

Figures 5, 9, 10, 19, 22

Sphecodes atlanticus Warncke, 1992: 25, Abb. 17, ♂ (holotype: ♂, Algeria: Hoggar-Geb., Guelta; OLBL/PCMS), examined.

Diagnosis. This species is similar to the Trans-Palaearctic *Sphecodes scabricollis* Wesmael, 1835 owing to the flat genal area, the developed preoccipital lateral carina, the densely punctate head and mesoscutum, the size and shape of male antennal tyloids, and in the similar gonostylar shape. However, *S. atlanticus* differs from *S. scabricollis* by a number of characters outlined in Table 2. In addition to presence of preoccipital lateral carina, *S. atlanticus* clearly differs from the *gibbus* species group (*S. anatolicus* Warncke, 1922, *S. gibbus* (Linnaeus, 1758), *S. nippon* Meyer, 1922, *S. rufiventris*

(Panzer, 1798), *S. schenckii* Hagens, 1882, *S. tadschicus* Blüthgen in Popov, 1935; see Astafurova et al. 2018a) by a short distance from top of head to upper margin of lateral ocellus (2 lateral ocellar diameters as seen in dorsal view, versus those with a long vertex where this distance is at most 2.5–3.0 diameters).

Description of hitherto unknown female. Total body length 6.5–8.5 mm. Head (Fig. 5) black (except reddish mouthparts); transverse, 1.3 times as wide as long; vertex elevated, distance from top of head to upper margin of lateral ocellus ca. one lateral ocellar diameter as seen in frontal view and ca. two lateral ocellar diameters as seen in dorsal view; F1 and F2 transverse, 0.7–0.8 times as long as wide; F3 as long as wide; face with fine contiguous punctures (10–20 μm), clypeus with shiny interspaces between punctures separated by 0.1–0.5 of a puncture diameter; mandible with an inner tooth; paraocular areas and upper part of gena with dense adpressed, snow-white, plumose pubescence obscuring the integument.

Mesosoma black; mesoscutum with coarse punctures (25–50 μm) separated by at most a puncture diameter (Fig. 10); mesoscutellum with irregular punctures separated by 0.1–4 puncture diameters; mesepisternum densely reticulate-rugose; propodeal triangle coarsely reticulate-rugose with large shiny, smooth interspaces between wrinkles (Fig. 10); lateral parts of propodeum finely and densely strigate or strigate-rugose with granulate interspaces between wrinkles; vertical part of propodeum smooth with coarse and dense punctures; legs reddish or dark brown. Hind wing costal margin with 9–10 hamuli.

Metasoma (Fig. 19) with colouration varying from red on T1–T4 to entirely dark-brown; tergal discs with coarse and dense punctures (20–30 μm/ 0.5–2, sparser on anterior third of T1), marginal zone impunctate except on T1 with dense punctures (10–20 μm / 0.5–2); sterna finely tessellate with coarse setae pores; pygidial plate dull, as wide as metabasitarsus.

Material examined. SAUDI ARABIA: 6 ♂♂, Wadi Majarish (below Taif), 12.II.1983, K. Guichard (NHMUK 013380451, 013380453, 013380460, 013380462, 013380466, 013380459); 4 ♂♂, Fayfa, 200 m, 29.I. 1983, K. Guichard (NHMUK 013380452, 013380461, 013380463, 013380464); 1 ♂, Lodar, 800 m, 16.V.1967, K. Guichard (NHMUK 0133804446); 1 ♂, Abu Arish, 26.III.1980, K. Guichard (NHMUK 013380465); 2 ♀♀, 1 ♂, Abu Arish, Jizzan Hot Springs, 25.III.1980, K. Guichard (NHMUK 013380458, 013380441, 013380454), 1 ♂, idem, 28.I.1983 (NHMUK 013380450); 1 ♀, Wadi Maraba, 25.I.1983, 1000 m, K. Guichard (NHMUK 013380457); 1 ♀, Jeddah, Locust Research Station, 17.I.1972, A. Basha (NHMUK 013380442); YEMEN: 1 ♂, Usaifira, 1 mile N Ta'izz, 4.500 ft, 21.XII.1937, H. Scott, E. Britton (NHMUK 013380468), 1 ♂, Wadi Maytam, 12 km SE Ibb, 1600 m, 13°53'N, 44°18'E, 27.X.2005, J. Halada (OLBL/PCMS); 2 ♀♀, 3 ♂♂, Hawf NE Albhaydah, 200–730 m, 16°53'N, 53°05'E, 14.X.2005, J. Halada (OLBL/PCMS); 2 ♀♀, 4 ♂♂, 20 km S Taizz, 1200 m, 13°30'N, 43°57'E, 24.X.2005, J. Halada (OLBL/PCMS); 2 ♂♂, Jabal Bura, NEE Al Hudaydah, 200–800 m, 14°52'N, 43°24'E, 30.X-1.XI.2005, J. Halada (OLBL/PCMS); 1 ♂, Wadi Aniz, SSW Sana, 1520 m, 14°60'N, 44°09'E, 7.X.2005, J. Halada (OLBL/PCMS).

Distribution. *Saudi Arabia, *Yemen; Algeria, the Canary Islands.

Table 2. Differences between *Sphecodes atlanticus* Warncke, 1992 and *S. scabricollis* Wesmael, 1835.

Characters	*Sphecodes atlanticus*	*Sphecodes scabricollis*
Both sexes		
Distance from top of head to upper margin of lateral ocellus as seen in frontal and dorsal views	about one lateral ocellar diameters (Fig. 5)	about two lateral ocellar diameters (Fig. 3)
Propodeal triangle/metaposnotum	equal (in female) or longer (in male) than mesoscutellum (Figs 9, 10)	distinctly shorter than mesoscutellum (Figs 8)
Metasomal terga	with coarser and denser punctures (Fig. 19)	with fine and sparser punctures, especially on T1 (Fig. 18)
Male		
Mesoscutum	punctures separated by at most 1.5–2.0 puncture diameters; polished between punctures (Fig. 9)	areolate (Fig. 8)
Genitalia	gonocoxite dorsally with weak impression; gonostylar process longer (Fig. 22)	gonocoxite dorsally without impression; gonostylar process shorter (Fig. 23)
Female		
Paraocular areas	with dense pubescence obscuring integument (Fig. 5)	with sparse pubescence not obscuring integument (Fig. 3)

Sphecodes barbatus Blüthgen, 1923

Figures 4, 17

Sphecodes barbatus Blüthgen, 1923: 497–498, ♀ (holotype: ♀, Turkey, Ak-Chehir; ZSM).

Diagnosis. *Sphecodes barbatus* is very similar to *S. majalis*. The two species are easily separable in the female, but males are difficult. The female *S. barbatus* differs from *S. majalis* by denser, distinctly plumose pubescence on paraocular areas and clypeus (Fig. 4) (sparser, weakly plumose or simple pubescence in *S. majalis*, Fig. 2) and by a distinctly (Fig. 17) punctate T1 (sparse and tiny punctures in *S. majalis*, Fig. 16).

Material examined. SYRIA: 1 ♀, Syria, 40 km NE Damaskus, 22.V.1996, H. Halada (ZISP); 2 ♂♂, Slenfe, 1200 m, 19.IV.1986, K.M. Guichard, (NHMUK 013380371, 013380372).

Distribution. *Syria; Greece, Turkey.

Remarks. Warncke (1992) interpreted *Sphecodes barbatus* as a subspecies of *S. majalis* Pérez, 1903, but later this taxon was restored as a valid species (Bogusch and Straka 2014a).

Sphecodes dathei Schwarz, 2010

Figures 12–15, 24

Sphecodes dathei Schwarz, 2010: 483–486, ♀, plates 1–12 (holotype: ♀, United Arab Emirates, Wadi Shawkah, 25°06'N, 56°02'E, 9–24.VI.2007, in water trap, A. van Harten leg.; SDEI), examined.

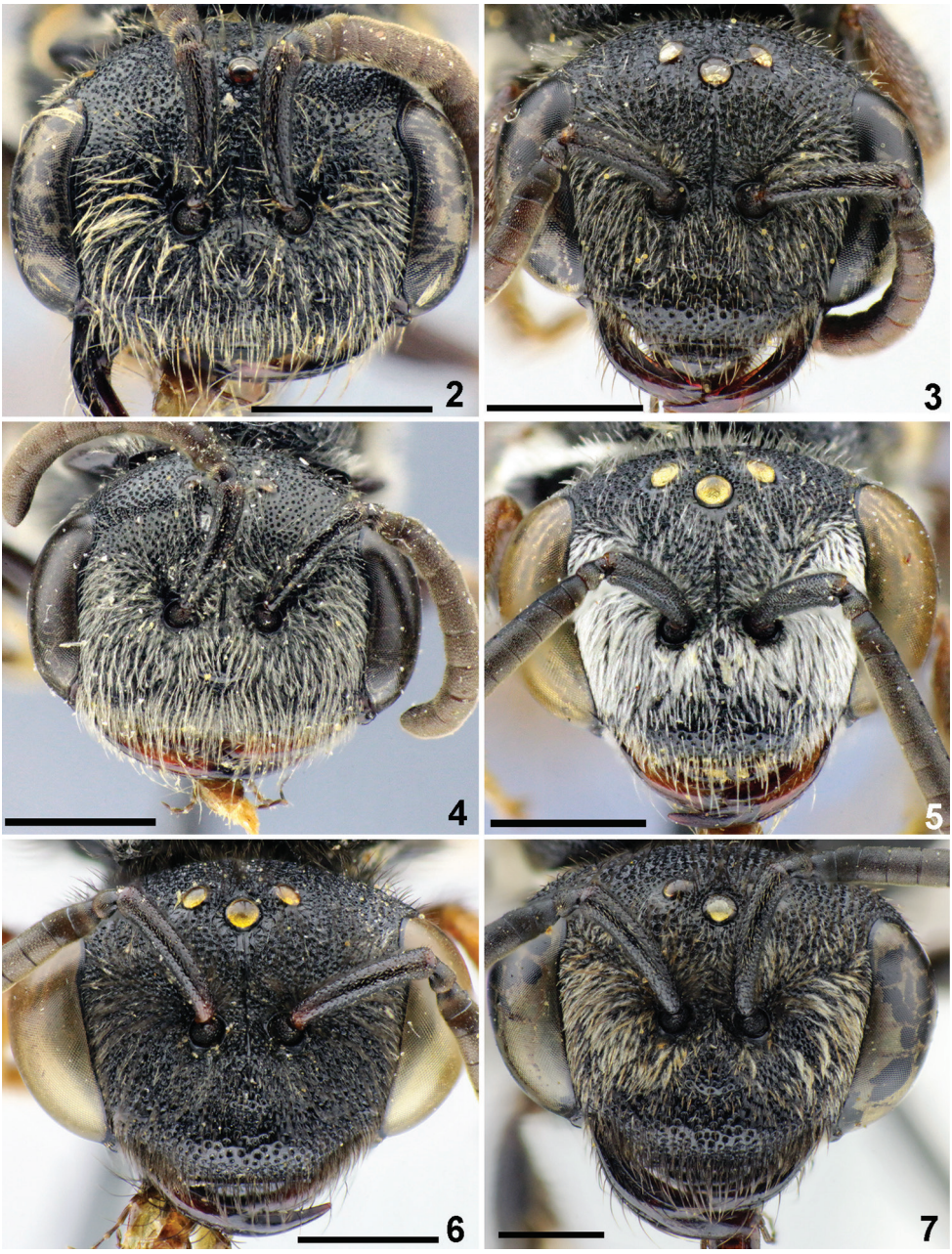

Figures 2–7. Head, females, frontal view. **2** *Sphecodes majalis* Pérez **3** *S. scabricollis* Wesmael **4** *S. barbatus* Blüthgen **5** *S. atlanticus* Warncke **6** *S. rubripes* Spinola **7** *S. albilabris* (Fabricius). Scale bars: 1.0 mm.

Diagnosis. The species is similar to *Sphecodes crassus* Thomson, 1870 owing to the wide female metafemur (strongly enlarged in the basal half); strongly transverse female head; sparsely punctate mesoscutum in both sexes, weakly developed male antennal

tyloids (usually covering less than 1/3 of ventral flagellar surfaces). The female of *Sphecodes dathei* differs from *S. crassus* by dense, apressed, snow-white, plumose pubescence obscuring integument in paraocular areas (sparse, simple pubescence not obscuring integument in *S. crassus*); the male differs by densely and relatively coarsely punctate T1 (in *S. crassus* T1 usually with a few fine punctures, rarely with relatively coarse and dense punctures). Both species have similar gonostylar shape, but *S. dathei* has a narrower, trapezoidal membranous portion of the gonostylus (wider, close to oval in *S. crassus*, Fig. 25).

Description of hitherto unknown male. Total body length 5.0–6.5 mm. Head (Fig. 12) black (except reddish mouthparts and brownish antenna); weakly transverse, 1.1 times as wide as long; vertex not elevated; distance from top of head to upper margin of lateral ocellus ca. two lateral ocellar diameters as seen in dorsal view; antenna (Fig. 13) reaches posterior margin of mesoscutum; F1 transverse, 0.6 times as long as wide; F2 long, 1.7 times as long as wide; remaining flagellomeres 1.2–1.3 times as long as wide; tyloids weakly developed (on F2–F4 covering less than 1/6 of ventral flagellar surfaces and from F5 onward covering less than 1/3); clypeus, frons, supraclypeal and paraocular areas with fine contiguous punctures (10–20 μm); ocello-ocular area and gena with shiny interspaces, punctures separated by 0.5–1 a puncture diameter; face below and above the antennal toruli with dense adpressed snow-white plumose pubescence obscuring integument; gena with similar pubescence, but not obscuring integument.

Mesosoma (Fig. 14) black; mesoscutum and mesoscutellum with punctures (20–25 μm) separated by 0.5–4 puncture diameters; mesepisternum and hypoepimeral area densely reticulate-rugose; propodeal triangle (Fig. 14) and vertical part of propodeum coarsely reticulate-rugose with shiny, smooth interspaces between wrinkles; lateral parts of propodeum coarse reticulate- to strigate-rugose with shiny interspaces between wrinkles; legs dark brown, but tarsi and partially tibia yellow or reddish. Hind wing costal margin with 5 hamuli.

Metasomal T1–T3 red (T1 black basally, T3 – apically); tergal discs (Fig. 15) with dense punctures (10–15 μm / 0.5–1), becoming sparse along marginal zone on T1; marginal zones smooth, impunctate; sterna with numerous microscopic setae pores; gonocoxite dorsally with a deep impression; membranous portion of gonostylus small, trapezoidal (Fig. 24).

Material examined. SAUDI ARABIA: 1 ♀, Wadi Majarish, 800 m, 12.II.1983, K. Guichard (NHMUK 013380455); UNITED ARAB EMIRATES: 1 ♀, Hatta, 24.IV.1992 (NHMUK 013380414); 1 ♂, idem, 19–20.V.1988 (NHMUK 013380431); 7 ♂♂, idem, 14.IV.1990, I. Hammer (NHMUK 013380428, 013380429, 013380430, 013380432, 013380433, 013380434, 013380430); YEMEN: 1 ♀, Lawdar, NE Aden, 1140 m, 13°53'N, 45°48'E, 28.X.2005, J. Halada (OLBL/PCMS).

Published records. Schwarz 2010: 483 (United Arab Emirates).

Distribution. United Arab Emirates, *Saudi Arabia, *Yemen.

Figures 8–11. Mesosoma (**8–10**), dorsal view; lectotype labels (11). **8** *Sphecodes scabricollis* Wesmael, male **9, 10** *S. atlanticus* Warncke (**9** – male, **10** – female) **11** *S. intermedius* Blüthgen, label of lectotype. Scale bars: 1.0 mm.

Sphecodes gibbus (Linnaeus, 1758)

Sphex gibba Linnaeus, 1758: 571, ♀ (syntypes: ♀♀, Sweden; ZMUK).
Apis glabra Füessly, 1775; *Andrena ferruginea* Olivier, 1789; *Apis gibbosa* Christ, 1791; *Melitta sphecoides* Kirby, 1802; *M. picea* Kirby, 1802; *Andrena austriaca*

Figures 12–15. *Sphecodes dathei* Schwarz, male. **12** Head, frontal view **13** antenna, frontal view **14** mesosoma, dorsal view **15** T1, dorsal view. Scale bars: 1.0 mm.

Fabricius, 1804; *Dichora analis* Illiger, 1806; *Sphecodes apicatus* Smith, 1853; *S. nigripennis* Morawitz, 1876; *S. sutor* Nurse, 1903; *S. gibbus* var. *rufispinosus* Meyer, 1920; *S. g.* var. *turkestanicus* Meyer, 1920; *S. castilianus* Blüthgen, 1924; *S. pergibbus* Blüthgen, 1938; *S. lustrans* Cockerell, 1931; *S. angarensis* Cockerell, 1937 (Synonyms).

Diagnosis. See Astafurova et al. 2018a: 17.

Material examined. JORDAN: 1 ♀, Jordan Valey, Dayr Alla, 27.IV.1996, M. Halada (OLBL/PCMS); 1 ♀, N. Shuna env., 20–22.IV.1996; 1 ♀, idem, 29–30. IV.1996, M. Halada (OLBL/PCMS); SYRIA: 1 ♂, 20 km NE Latakia, 25.V.1996, M. Halada (OLBL/PCMS); ISRAEL: 1 ♀, Rehovot s.l., 29.IV.1975, K.M. Guichard (NHMUK 1975-248, 013380378); 1 ♀, Ein Gedi, 200 m, 11.III.1975, K.M. Guichard (NHMUK 1975-154, 013380379); 1 ♂, Jericho (Wadi Quilt), 250 m, 13–22.V.1975, K.M. Guichard (NHMUK 1975-248, 013380373); 1 ♀, Jericho, 200 m, 6–27.III.1975, K.M. Guichard (NHMUK 1975-154, 013380374).

Published records. Warncke 1992: 30 (Israel).

Distribution. Israel, *Jordan; North Africa, Europe (north to 63°), Russia (east to Yakutia), Turkey, Iran, Pakistan, Central Asia, Kazakhstan, Mongolia, NW China, India.

Sphecodes intermedius Blüthgen, 1923

Figure 11

Sphecodes intermedius Blüthgen, 1923: 500 (lectotype (**designated here**): ♂, Type <red label> // Caucas Portz // Sph. intermedius ♂, Type., P. Blüthgen det. // <blue circle> // Lectotypus, *Sphecodes intermedius* Blüthgen, 1923, ♂, des. Astafurova & Proshchalykin, 2018; paralectotype: ♀, Type <red label> Sph. intermedius ♀, Type, P. Blüthgen det. // Paralectotypus, *Sphecodes intermedius* Blüthgen, 1923, ♀, des. Astafurova & Proshchalykin, 2018; ISZP, examined, Fig. 11).

Sphecodes lactipennis Meyer, 1925 (Synonym).

Diagnosis. See Astafurova et al. 2018a: 20.

Material examined. UNITED ARAB EMIRATES: 1 ♂, Hatta (Hotel), 28. IV.1989, (NHMUK 013380370); 1 ♂, idem, 23.VIII.1991 (NHMUK 013380409); 1 ♂, idem, 14.IV.1990, I. L. Hamer [D. Baker det., 1992 as *S. punctatissimus* Meyer] (NHMUK 013380361); ISRAEL: 1 ♀, Jerusalim, 16.VII.1930, S. Bodenheimer [det. Blüthgen] (MNHB); 1 ♀, Tiberias, 200 m, 22.III.1975, K.M. Guichard (NHMUK 013380410); 1 ♀, Jericho (Hisham Palace), 200 m, 8.III.1975, K.M. Guichard (NHMUK 1975-248, 013380408); JORDAN: 1 ♀, N. Shuna env., 20–22.IV.1996; 1 ♀, idem, 29–30.IV.1996, M. Halada (OÖLM)

Published records. Ascher and Pickering 2019 (Israel)

Distribution. *United Arab Emirates, Israel, *Jordan; North Africa, South Europe (east to Ukraine), Russia (south of the European part, Urals), Caucasus, Turkey, Kazakhstan, Central Asia, Pakistan, China (Gansu).

Remarks. *Sphecodes intermedius* Blüthgen, 1923 was described from specimens of both sexes collected in "Caucas" [Caucasus] (Fig. 11). There are two specimens (female and male) in ISZP from this locality, which correspond to the original description of P. Blüthgen. One of these specimens (male) is designated here as a lectotype of *S. intermedius* to avoid any confusion about the status of the type specimens and to properly diagnose this species.

Sphecodes longulus Hagens, 1882

Sphecodes longulus Hagens, 1882: 226, Fig. 25, ♂ (syntypes: ♂♂, Germany; ? Dominican monastery, Venlo, Nederland).

Sphecodes longulus var. *eupidus* Hagens, 1882; *S. nitidulus* Hagens, 1882; *S. subfasciatus* Blüthgen, 1934; *S. amakusensis* Yasumatsu & Hirashima, 1951; *S. sabulosus* Tsuneki, 1983; *S. crassicornis* Tsuneki, 1983; *S. tsunekii* Haneda, 1994 (Synonyms).

Diagnosis. See Astafurova et al. 2018a: 21.

Material examined. JORDAN: 1 ♀, 30 km N Tafila, 2.V.1996, M. Halada (OLBL/PCMS); 1 ♂, 20 km SW Madaba, 26.V.2007, 400 m, Z. Kejval (OLBL/

PCMS); 1 ♂, Ajlun, 35 km W Jarash, 850 m, Z. Kejval (OLBL/PCMS); 1 ♀, 20 km S North Shuna Tall al Arbatin, 19.IV.1996, M. Halada (OLBL/PCMS); ISRAEL: 1 ♂, Dafna, 27.V.1991, K. Warncke (OLBL/PCMS); 1 ♂, North Galeleya, Nature Reserve "Khule", 23.V.1968, V. Trjapitzin (ZISP); 1 ♀, 5 km W Jericho, Wadi Qelet, St. Georg Mon., 6.V.1996, O. Niehuis (OLBL/PCMS); SYRIA: 1 ♂, Damask, 20–21.V.1980, M. Halada (OLBL/PCMS).

Published records. Warncke 1992: 17 (Syria); Ascher and Pickering 2019 (Jordan).

Distribution. *Israel, Jordan, Syria; Europe (north to Finland, Sweden, Denmark, England), Russia (east to Far East), Turkey, Iran, Central Asia, Kazakhstan, China, Japan.

***Sphecodes majalis* Pérez, 1903**

Figures 2, 16

Sphecodes majalis Pérez, 1903: 219, ♀, ♂, (syntypes: ♀, ♂, France, Spain; MNHN).
Sphecodes gracilior Pérez, 1903; *S. opacifrons* Pérez, 1903; *S. problematicus* Schulz, 1906 (Synonyms).

Diagnosis. Refer to the diagnosis *S. barbarus*, above.

Material examined. JORDAN: 35 ♀ ♀, 5 ♂♂, 10 km N Petra, 3.V.1996, M. Halada (OLBL/PCMS); 2 ♀, 10 km N Jarash, 20.IV.2002, M. Snizek (OLBL/PCMS); 1 ♀, Ajlun S of Anjara, 27.IV.2002, M. Snizek (OLBL/PCMS).

Distribution. *Jordan; North Africa, South Europe, Russia (south of the European part), Turkey, Iran.

***Sphecodes marginatus* Hagens, 1882**

Sphecodes marginatus Hagens, 1882: 223, Fig. 18, ♂ (syntypes: 2 ♂, Germany: Cleve; ? Dominican monastery, Venlo, Nederland).
Sphecodes atratus Hagens, 1882; *S. nigritulus* Hagens, 1882; *S. biskrensis* Pérez, 1903 (Synonyms).

Diagnosis. This species belongs to the *miniatus* species group (*S. creticus* Warncke, 1992, *S. haladai* Warncke, 1992, *S. larochei* Warncke, 1992, *S. marginatus* Hagens, 1882, *S. miniatus* Hagens, 1882, *S. nomioidis* Pesenko, 1979, *S. schawrzi* Astafurova & Proshchalykin, 2014, and *S. sandykachis* Astafurova & Proshchalykin, 2018), with the same length and transverse F1–F3 in females. Among species of this group *S. marginatus* is most close to *S. miniatus* and *S. nomioidis* as they have a similar sculpture and structure of the body. Hence females of the three species are challenging to distinguish, but the male differs from the other two species by smaller triangular gonostylus. Differences between these three species are outlined by Bogusch and Straka (2012) and between females of this species group by Astafurova et al. (2018c).

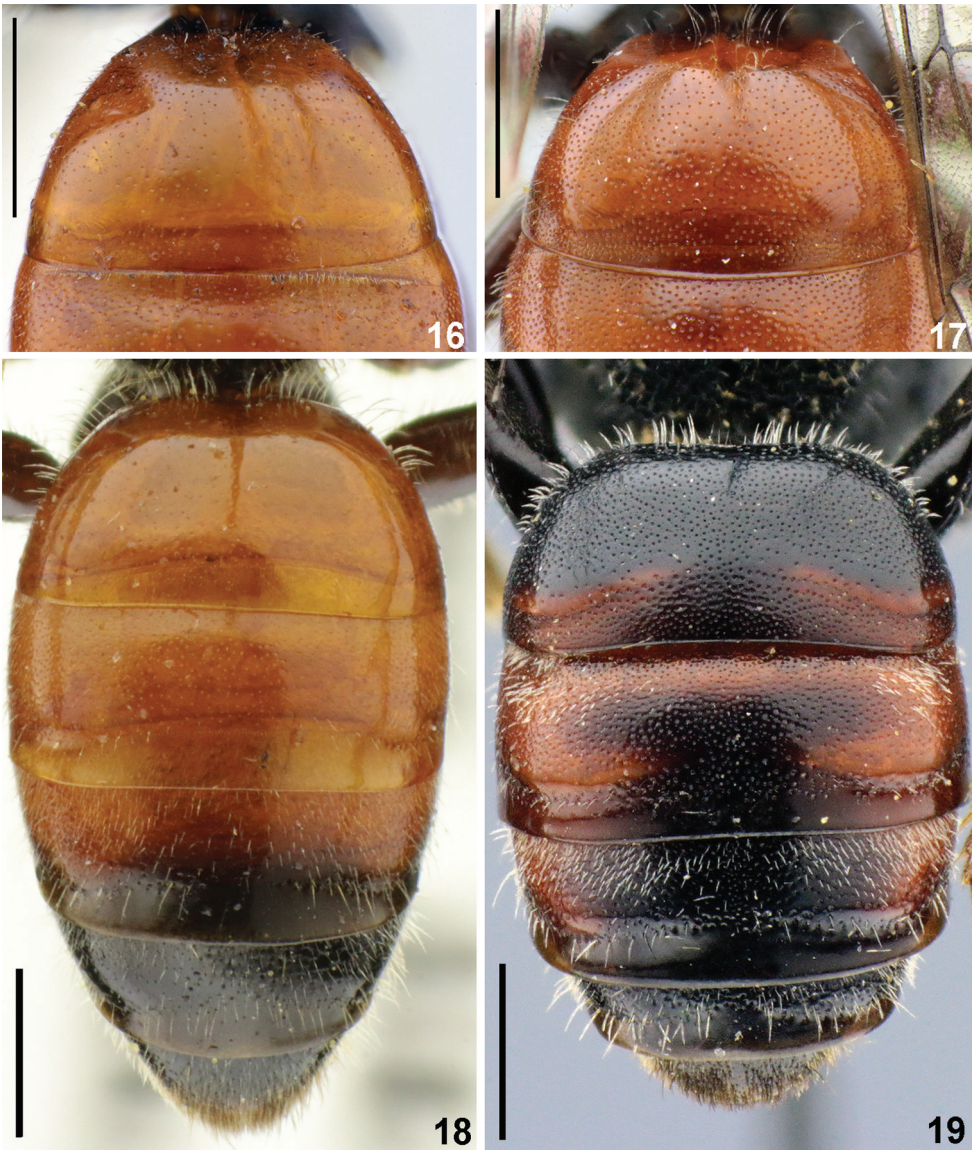

Figures 16–19. T1 (**16, 17**), metasoma (**18, 19**), females, dorsal view. **16** *Sphecodes majalis* Pérez **17** *S. barbatus* Blüthgen **18** *S. scabricollis* Wesmael **19** *S. atlanticus* Warncke. Scale bars: 1.0 mm.

Material examined. ISRAEL: 1 ♀, 1 ♂, Jerusalim, 18.VI.1930; 1 ♂, idem, 10.VI.1931, S. Bodenheimer [det. Blüthgen] (MNHB); JORDAN: 1 ♀, W Jordan Valey, Mubalath, 27.IV.1996, M.Halada (OLBL/PCMS); 1 ♀, n. Shuna, 20–22. IV.1996, M. Halada(OLBL/PCMS); 2 ♂♂, NW of Ailun, 850 m, 20.V.2007, Z. Kejval (ZISP); 1 ♀, Jericho (Wadi Quilt), 250 m, 6.III.1975, K.M. Guichard (NHMUK 1975-154, 013380467).

Published records. Schwarz 2010: 486 (United Arab Emirates); Ascher and Pickering 2019 (United Arab Emirates).

Distribution. United Arab Emirates, *Israel, *Jordan; North Africa, Europe (north to Germany and Denmark, east to Belarus).

Sphecodes monilicornis (Kirby, 1802)

Melitta monilicornis Kirby, 1802: 47, ♂ (syntypes: ♂♂, England, NHMUK).

Sphecodes maculatus Lepeletier de Saint Fargeau, 1841; *S. subquadratus* Smith, 1845; *S. ruficrus* Dalla Torre, 1896; *S. hanuman* Nurse, 1903; *S. monilicornis* var. *nigerrima* Blüthgen, 1927; *S. caucasicus* Meyer, 1920; *S. cephalotes* Meyer, 1920; *S. smyrnensis* Meyer, 1920; *S. monilicornis quadratus* Meyer, 1920; *S. monilicornis berberus* Warncke, 1992; *S. quadratus cephalotiformis* Pittoni, 1950 (Synonyms).

Diagnosis. See Astafurova et al. 2018a: 24.

Material examined. SYRIA: 1 ♀, 50 km W Homs, 12.V.1996, M. Halada (OLBL/PCMS); 1 ♀, 60 km S Damask, Khabab, 14.V.1996, M. Halada (OLBL/PCMS); 1 ♀, 20 km S North Shuna Tall al Arbatin, 19.IV.1996, M. Halada (OLBL/PCMS); 1 ♀, 10 km W Jarasch, 1.V.1996, M. Halada (OLBL/PCMS); 2 ♀♀, Jisr ash Shunhur, 26.V.1996, M. Halada (OLBL/PCMS); 4 ♂♂, 20 km NE Latakia, 25.V.1996, M. Halada (OLBL/PCMS); 1 ♂, 30 km W Damask, 19.VI.2000, M. Halada (OLBL/PCMS); JORDAN: 1 ♀, Jarash env., 1.V.1996, M. Halada (OLBL/PCMS); 1 ♀, 10 km N Jarash, 1.V.1996, M. Halada (OLBL/PCMS); 1 ♂, 16 km WN Aijun, 600 m, 21.V.2077, Z. Kejval (OLBL/PCMS); 1 ♀, 10 km N Petra, 3.V.1996, M. Halada (OLBL/PCMS).

Published records. Ascher and Pickering 2019 (Jordan).

Distribution. Jordan, *Syria; North Africa, Europe (north to 64°), Russia (east to Far East), Caucasus, Turkey, Iran, Pakistan, Central Asia, Kazakhstan, Mongolia, China.

Sphecodes nomioidis Pesenko, 1979

Sphecodes nomioidis Pesenko, 1979: 860, ♀ (holotype: ♀, Ukraine: Donetsk Province, Yenaktsevo, 10.VIII.1978, V. Radchenko leg.; ZISP).

Diagnosis. Refer to diagnosis for *S. marginatus*, above.

Material examined. UNITED ARAB EMIRATES: 4 ♂♂, Hatta, 14.IV.1990, I. Hamer (NHMUK 013380411, 013380415, 013380416, 013380417); OMAN: 1 ♂, Rostaq, 350 m, 21–31.III.1976, K. Guichard (NHMUK 013380443).

Published records. Bogusch and Straka 2012: 14 (Jordan).

Distribution. *United Arab Emirates, *Oman, Jordan; South and Central Europe (west to Austria), Ukraine, Russia (SW of the European part), Turkey.

Sphecodes olivieri Lepeletier de Saint Fargeau, 1825

Sphecodes olivieri Lepeletier de Saint Fargeau in Lepeletier de Saint Fargeau and Audinet-Serville, 1825: 448, ♂ (syntypes: ♂♂, 'Arabie').
Sphecodes collaris Spinola, 1843; *S. hispanicus* var. *abyssinicus* Sichel, 1865; *S. ruficornis* Sichel, 1865; *S. punctulatus* Sichel, 1865; *S. subpunctulatus* Sichel, 1865; *S. rufithorax* Morawitz, 1876; *S. verticalis* Hagens, 1882; *S. desertus* Nurse, 1903; *S. chionospilus* Cockerell, 1911; *S. chionospilus* var. *sanguinatus* Cockerell, 1911; *S. tenuis* Meyer, 1920; *S. olivieri* var. *niveatus* Meyer, 1925 (Synonyms).

Diagnosis. See Astafurova et al. 2018a: 25.

Material examined. UNITED ARAB EMIRATES, 1 ♂, Digdaga, 8.VIII.1984, J.N. Brown [D. Baker det, 92] (NHMUK 013380368); 1 ♂, Hatta (Hotel), 21.VIII.1987, I.L. Hamer [D. Baker det, 92] (NHMUK 013380366); 1 ♂, Soweihan Rd, 12.IV.1988, I.L. Hamer [D. Baker det, 92] (NHMUK 013380367); 1 ♂, Jebal Ali, 15.II.1991, I.L. Hamer [D. Baker det, 92] (NHMUK 013380361); SAUDI ARABIA, 1 ♀, 1♂, Jeddah, 15.II.1972, K.M. Guichard (NHMUK 013380399, 013380398); 1 ♀, 3 ♂♂, Riyadh area, 16–21.IV.1980, K.M. Guichard (NHMUK 013380456, 013380395, 013380396, 013380397); 1 ♂, Jeddah, 13.IV.1980 (NHMUK 013380393); 2 ♀♀, idem, 15.IV.1980, K.M. Guichard (NHMUK 013380392, 013380394); JORDAN: 1 ♀, 20 km W At Tafila, 1.VI.2007, Z. Kejval (OLBL/PCMS); OMAN, 1 ♀, Wadi Qurvat, Ag. Stn. 500 m, 5.III.1976, K. Guichard (NHMUK 013380383); 2 ♀♀, Tinaf, 650 m, 7.III.1976, K. Guichard (NHMUK 013380381, 013380380); 1 ♀, Rostaq, 350 m, 21–31.III.1976, K. Guichard (NHMUK 013380382);

ISRAEL, 1 ♂, Ein Bokek Zohar, 350 m, 25.V.1975, K.M. Guichard (NHMUK 1975-248, 013380385); ISRAEL: 1 ♀, Jericho (Wadi Kelt), 200 m, 6.III.1975, K.M. Guichard (NHMUK 1975-248, 013380387).

Published records. Lepeletier de Saint Fargeau 1825: 448 ('Arabie'); Warncke 1992: 46, map (Israel); Dathe 2009: 385 (United Arab Emirates); Schwarz 2010: 486 (United Arab Emirates); Ascher and Pickering 2019 (United Arab Emirates, Qatar).

Distribution. United Arab Emirates, *Oman, Qatar, *Saudi Arabia, Israel, *Jordan; North Africa, South Europe, Russia (South of European part), Turkey, Caucasus, Iran, Pakistan, Central Asia, Kazakhstan, NW China.

Sphecodes pellucidus Smith, 1845

Sphecodes pellucidus Smith, 1845: 1014, ♀, ♂ (syntypes: ♀♀, ♂♂, England; NHMUK).
Sphecodes pilifrons Thomson, 1870; *S. brevicornis* Hagens, 1874; *S. volatilis* Smith, 1879; *S. pellucidus* var. *algirus* Alfken, 1914; *S. pellucidus* var. *hybridus* Blüthgen, 1924; *S. pellucidus* var. *niveipennis* Meyer, 1925 (Synonyms).

Diagnosis. See Astafurova et al. 2018a: 27.

Material examined. SYRIA: 1 ♀, 30 km N Dara, Nawa, 18.V.1996, M. Halada (OLBL/PCMS); JORDAN: 1 ♀, Jordan valley, S. Shuna, 17.IV.1996, M. Halada (OLBL/PCMS); 1 ♀, 10 km N Petra, 3.V.1996, M. Halada (OLBL/PCMS).

Distribution. *Jordan, *Syria; North Africa, Europe (north to 66°), Russia (east to Far East), Turkey, Iran, Central Asia, Kazakhstan, Mongolia, China.

Sphecodes pinguiculus Pérez, 1903

Sphecodes pinguiculus Pérez, 1903: CCXX, ♀ (syntypes: ♀♀, Spain: Catalonia; MNHN).

Sphecodes sareptensis Meyer, 1922; *S. excellens* Meyer, 1922; *S. punctatissimus* Meyer, 1922; *S. hungaricus* Blüthgen, 1923; *S. coelebs* Blüthgen, 1923; *S. consobrinus* Blüthgen, 1923; *S. persicus* Blüthgen, 1924; *S. capverdensis* Pauly & La Roche, 2002 (Synonyms).

Diagnosis. See Astafurova et al. 2018a: 30.

Material examined. SYRIA: 1 ♂, 80 km E Palmira, 450 m, 22.IV.1992, K. Warncke (OÖLM); SAUDI ARABIA, 1 ♀, Hofut, 145 m, 21–6.IV.1980, K. Guichard (NHMUK 013380359); 1 ♀, Hatta, 10.IV.1983, I.L. Hamer (NHMUK 013380389); 1 ♀, idem, 6.VI.1986, I.L. Hamer (NHMUK 013380390); 2 ♀♀, Khor-Fakkan, 20.III.1987, I.L. Hamer (NHMUK 013380364, 013380377); 1 ♀, Soweihan Rd, 12.IV.1988, I.L. Hamer (NHMUK 013380391); OMAN, 1 ♀, Wadi Qurvat, Ag. Stn. 500 m, 5.III.1976, K. Guichard (NHMUK 013380407); 2 ♀♀, Rostaq, 350 m, 21–31.III.1976, K. Guichard (NHMUK 013380405, 013380406);

ISRAEL: 1 ♂, Tel-Aviv, 22.IV.1966, Bytinski-Salz (OLBL/PCMS); 3 ♀♀, Jericho (Hisham Palace), 200 m, 8.III.1975, K.M. Guichard (NHMUK 1975-248, 013380408).

Published records. Schwarz 2010: 486 (United Arab Emirates, Israel); Ascher and Pickering 2019 (Israel, United Arab Emirates).

Distribution. United Arab Emirates, *Oman, *Saudi Arabia, Israel, *Syria; Cape Verde Islands, North Africa, South Europe, Russia (east to Buryatia), Turkey, Iran, Central Asia, Kazakhstan, Mongolia, North China.

Sphecodes puncticeps Thomson, 1870

Sphecodes puncticeps Thomson, 1870: 99, ♀, ♂ (syntypes: ♀♀, ♂♂, Sweden; MZLU).

Sphecodes bituberculatus Pérez, 1903; *S. opacifrons* Pérez, 1903; *S. puncticeps* var. *cretanus* Strand, 1921 (Synonyms).

Diagnosis. See Astafurova et al. 2018a: 31.

Material examined. SAUDI ARABIA: 1 ♂, Riyadh area, 16–21.IV.1980, K.M. Guichard (NHMUK 013380403); JORDAN: 1 ♀, Jordan valley, S. Shuna, 17.IV.1996, M. Halada (OLBL/PCMS); 2 ♀, 3 ♂♂, Jordan valley, Dayr Alla, 27.IV.1996, M. Halada (OLBL/PCMS); 1 ♀, 10 km N Petra, 3.V.1996, M. Halada (OLBL/PCMS); 1 ♀, 10 km SE Suwayda Kafr, 19.V.1996, M. Halada (OLBL/PCMS); SYRIA: 1 ♀, Latakia s.l., 17.VI.1986, K. Guichard (NHMUK 013380360); 2 ♀♀, 10 km SE Suwayda Kafr, 19.V.1996, M. Halada (OLBL/PCMS); ISRAEL: 2 ♂♂, Jerusalem, 21.IX.1922, P.A. Buxton (NHMUK 013380401, 013380400); 1 ♂, Rehovot s.l., 29.IV.1975, K.M. Guichard (NHMUK 1975-248, 013380404); 3 ♂♂, Jericho (Wadi Quilt), 250 m, 13–22.V.1975, K.M. Guichard (NHMUK 1975-248, 013380365, 013380376, 013380402).

Published records. Warncke 1992: 19 (Israel); Ascher and Pickering 2019 (Israel).

Distribution. *Saudi Arabia, Israel, *Jordan, *Syria; North Africa, Europe (north to Finland and Sweden), Russia (east to Far East), Turkey, Iran, Central Asia, Kazakhstan, Mongolia.

Sphecodes rubicundus Hagens, 1875

Sphecodes rubicundus Hagens, 1875: 318 (syntypes: ♂♂, ♀♀, Germany; ? Dominican monastery, Venlo, Nederland).
Sphecodes rubicundus altisilesiacus Torka, 1927 (Synonyms).

Diagnosis. The female of this species as well as *S. ruficrus* is most close to *S. pellucidus* and *S. ephippius* owing to a densely punctate head and mesosoma, relative wide pygidial plate and impunctate T1, but differs by having a distinctly elevated vertex with the distance between vertex and upper margin of lateral ocellus at least a lateral ocellar diameter as seen in frontal view (versus 0.2–0.5). *S.rubicundus* differs from *S. ruficrus* by white pubescence of head and mesosoma (with brown setae in *S. ruficrus*) and a less curved basal (M) vein in hind wing. The male most closely resembles *S. pesenkoi* Astafurova & Proshchalykin, 2018 and *S. ruficrus* (Erichson, 1835) owing to a similar gonostylar shape (elongate, spoon-shaped). The male of *S. rubicundus* differs from *S. pesenkoi* by an areolate mesoscutum (versus punctures separated by 1–3 puncture diameters) and coarsely and densely punctate T1 (a few fine punctures in *S. pesenkoi*).

According to the phylogenetic analysis (Habermannová et al. 2013) *Sphecodes rubicundus*, *S. ruficrus*, *S. pellucidus*, and *S. ephippius* belong to the same clade. Relationship between these species also is well supported by morphological characters.

Material examined. ISRAEL, 2 ♂♂, Jerusalem, 800 m, 20.III.1975, K.M. Guichard (NHMUK 1975-154, 013380388, 013380386); 1 ♀, Tiberias, 200 m, 22.III.1975, K.M. Guichard (NHMUK 1975-154, 013380384); 1 ♀, Jerusalem, 20.III.1993, D. Ahal (OLBL/PCMS).

Distribution. *Israel; Europe (north to 56°), Russia (south of the European part), Turkey, Caucasus, Iran.

***Sphecodes rubripes* Spinola, 1839**

Figures 6, 21

Sphecodes rubripes Spinola, 1839: 512, ♀ (syntypes: ♀♀, Cyprus; MRSN).
Sphecodes africanus Lepeletier, 1841; *S. rufipennis* Cockerell, 1931, *S. atrescens* Cockerell, 1931 (Synonyms).

Diagnosis. The female of *S. rubripes* differs from *S. albilabris* by the pubescence of paraocular area (Fig. 6) with brown erect setae not obscuring integument (versus white plumose appressed pubescence obscuring integument usually with admixture of brownish erect setae in *S. albilabris*, Fig. 7). Both sexes also differ by mainly red legs, except brown coxae and trochanters, Fig. 21 (at most reddish tarsi and tibia in *S. albilabris*, Fig. 20). These two species also differ in phenology (males of *S. rubripes* were recorded in the early spring while males of *S. albilabris* were found in the summer) and have different hosts (Bogusch and Straka 2012, Cross 2017). *S. albilabris* is widespread in the Palaearctic from the Atlantic Ocean to Russian Far East; however, the distribution of the species in the Mediterranean Region is unclear due to confusion with *S. rubripes*. The past records of *S. albilabris* from Israel and Syria refer to *S. rubripes*. We examined material of *S. albilabris* from Morocco and Tunisia, but we do not have any specimens of *S. albilabris* from the Arabian Peninsula or surrounding lands.

Material examined. JORDAN: 1 ♀, 10 km N Petra, 3.V.1996, M. Halada (OLBL/PCMS).

Published records. Meyer 1924: 3 (Syria, as *S. fuscipennis rubripes*); Warncke 1992: 31 (Israel, as *S. albilabris rubripes*); Ascher and Pickering 2019 (Israel, as *S. albilabris* (Fabricius)).

Distribution. *Jordan, Israel, Syria; North Africa, South-Western Europe, Cyprus.

Remarks. Mayer (1924) and later Warncke (1992) interpreted *Sphecodes rubripes* as a subspecies of *S. albilabris* (Fabricius, 1793), but this taxon was restored as a valid species (Bogusch and Straka 2014b).

***Sphecodes ruficrus* (Erichson, 1835)**

Dichroa ruficrus Erichson, 1835: 101, ♀, (syntypes: ♀♀, Spain; ZMHB).
Sphecodes hispanicus Wesmael, 1836; *S. rufipes* Smith, 1853; *S. gibbus* var. *tunetanus* Gribodo, 1894; *S. atrohirtus* Pérez, 1903 (Synonyms).

Diagnosis. Refer to diagnosis for *S. rubicundus*, above.

Material examined. JORDAN: 1 ♀, W Jordan Valley, env. of S. Shuna, 17.IV.1996, M. Halada (OLBL/PCMS).

Published records. Warncke 1992: 21 (Israel); Ascher and Pickering 2019 (Israel).

Distribution. Israel, *Jordan; North Africa, southwestern Europe.

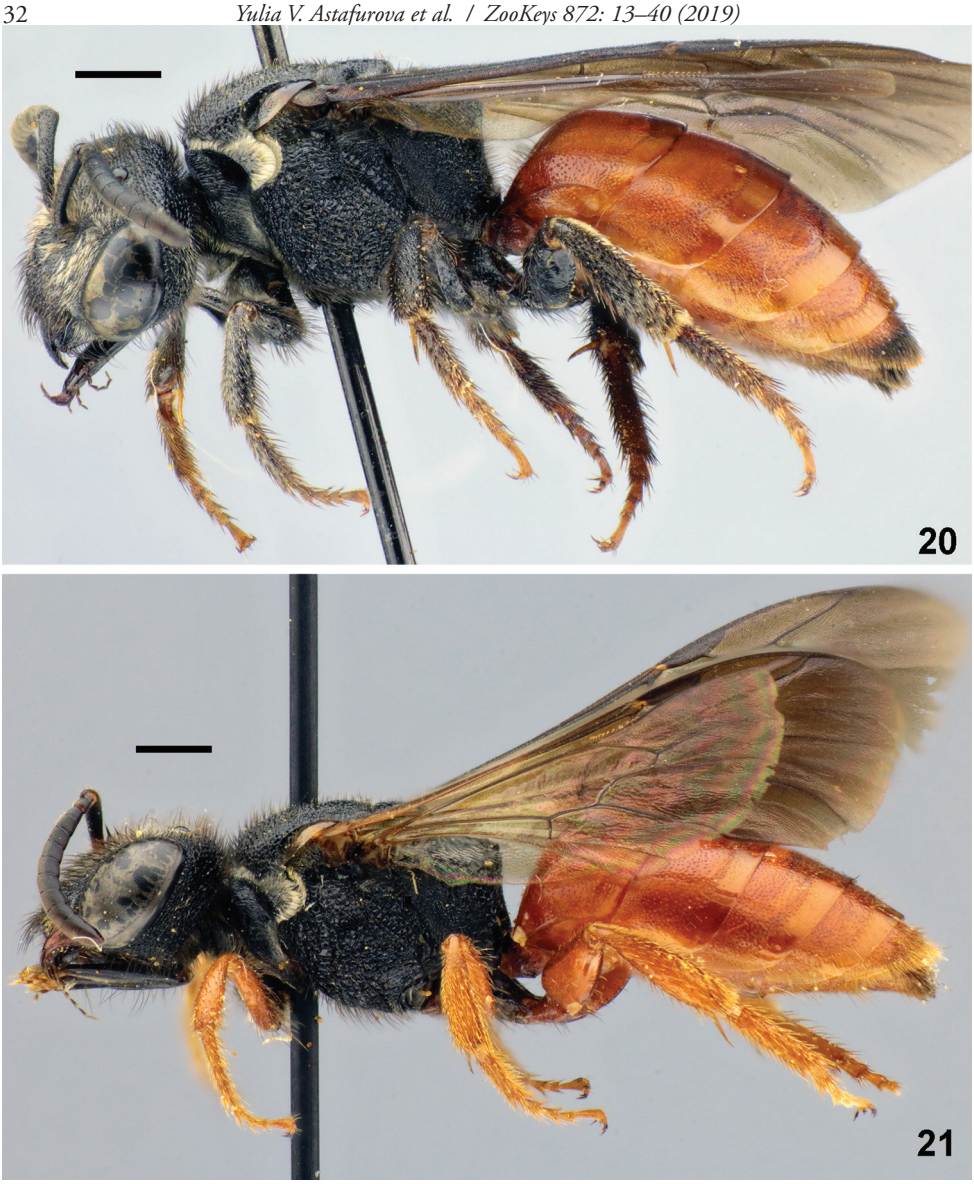

Figures 20, 21. Habitus, females, lateral view. **20** *Sphecodes albilabris* (Fabricius) **21** *S. rubripes* Spinola. Scale bars: 1.0 mm.

Remarks. Russia is mistakenly listed as within the distribution by Bogusch and Straka (2012) as well as Turkey and Armenia by Özbek et al. (2015) due to confusion with *S. ruficrus rubicundus* sensu Warncke (1992).

Sphecodes rufiventris (Panzer, 1798)

Tiphia rufiventris Panzer, 1798: 4, ♀ (syntypes: ♀♀, Germany; ZMHB).

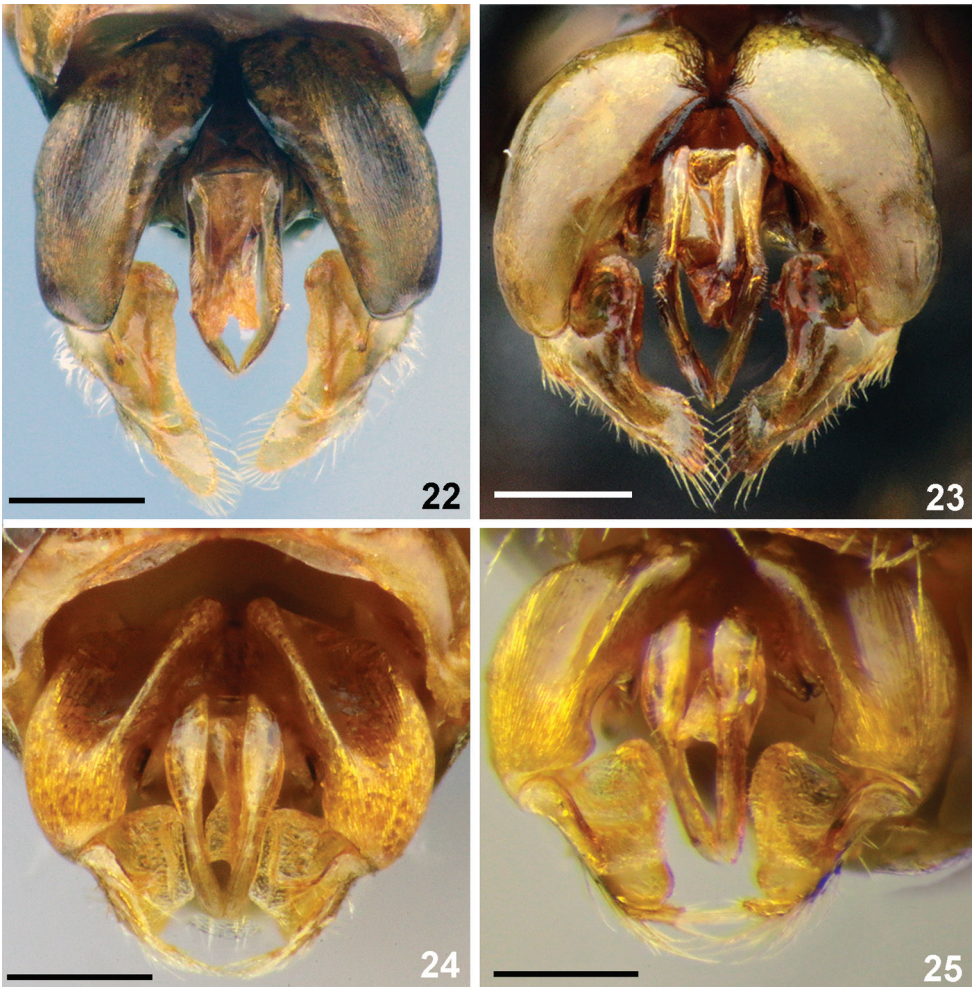

Figures 22–25. Genitalia, males, dorsal view. **22** *Sphecodes atlanticus* Warncke **23** *S. scabri collis* Wesmael **24** *S. dathei* Schwarz **25** *S. crassus* Thomson. Scale bars: 0.25 mm.

Sphecodes subovalis Schenck, 1853; *S. brevis* Hagens, 1875; *S. singularis* Meyer, 1920; *S. combinatus* Blüthgen, 1927; *S. subovalis austrinus* Erlandsson, 1979; *S. rufiventris hethiticus* Warncke, 1992 (Synonyms).

Diagnosis. See Astafurova et al. 2018a: 34.

Material examined. JORDAN: 1 ♂, W Jordan Valey, Mubalath, 27.IV.1996, M. Halada (OLBL/PCMS).

Published records. Ascher and Pickering 2019 (Israel).

Distribution. Israel, *Jordan; North Africa, Europe, (north to 57°), Russia (east to Khakassia Republic), Turkey, Iran, Central Asia, Kazakhstan.

Sphecodes schenckii Hagens, 1882

Sphecodes schenckii Hagens, 1882: 217, ♂ (holotype: ♂, no locality, Rudow leg. [see Blüthgen 1923: 444]; MNHB).
Sphecodes sulcicollis Pérez, 1903; *S. caspicus* Meyer, 1920 (Synonyms).

Diagnosis. See Astafurova and Proshchalykin 2017b: 274.

Material examined. JORDAN: 1 ♂, NW Ajlun, 850 m, 20.V.2007, Z. Kejval (OLBL/PCMS) ; 1 ♀, 10 km N Petra, 3.V.1996, M. Halada (OLBL/PCMS); SYRIA: 3 ♂♂, 20 km NE Latakia, 25.V.1996, M. Halada (OLBL/PCMS).

Published records. Warncke 1992: 27 (Israel, as *Sphecodes schenckii caspicus* Meyer); Ascher and Pickering 2019 (Israel).

Distribution. Israel, *Jordan, *Syria; Europe (north to Germany), Russia (European part), Turkey, Caucasus, ? Iran.

Sphecodes tadschicus Blüthgen, 1935

Sphecodes tadschicus Blüthgen in Popov, 1935: 366, ♂, ♀ (holotype: ♂, near Kulab [Tajikistan], 25.VII.1935, V. Popov leg.; ZISP).

Diagnosis. See Astafurova et al. 2018a: 39.

Material examined. ISRAEL: 1 ♀, 8 ♂♂, Jerusalem, 10–25.VIII.1960, Bytinski (MNHB).

Distribution. *Israel; Turkey, Iran, Central Asia, Kazakhstan.

Sphecodes turanicus Astafurova & Proshchalykin, 2017

Sphecodes turanicus Astafurova & Proshchalykin, 2017b: 274, ♂, ♀ (holotype: ♀, Turkmenistan, Chardzhou, 16.IV.1988, Dialentov leg.; ZISP).

Diagnosis. See Astafurova et al. 2018a: 41.

Material examined. SAUDI ARABIA: 1 ♂, Riyadh, El Ha'ir, 16–21.IV.1980, K.M. Guichard (NHMUK 013380449).

Distribution. *Saudi Arabia; Central Asia, Kazakhstan, China (Gansu).

Sphecodes villosulus Schwarz, 2010

Sphecodes villosulus Schwarz, 2010: 486–491, ♀, ♂ (holotype: ♀, United Arab Emirates, Dubai, Nakhalai, 28–30.IV.1984, in Malaise trap, E. Sugden leg.; BLCU).

Diagnosis. This species differs from other small Palaearctic species with 5–6 hamuli in the hind wing by having a unique combination of simple mandibles and the male gonocoxite dorsally with an impression. The female is closest to *S. armeniacus* owing to dense appressed snow-white pubescence obscuring the integument on face, a transverse head and sparsely punctate mesoscutum, but differs from this species by sparser and finer punctate ocello-ocular area (3–5 μm / 2–3 versus 5–10 μm / 1–2) and strongly transverse F3 (almost square in *S. armeniacus*). The male of *S. villosulus* recalls *S. miniatus* in the rectangular gonostylar shape, but clearly differs from this species by the less developed tyloids on the flagellomeres extending to approximately a half of ventral flagellar surfaces (versus those across 4/5).

Material examined. UNITED ARAB EMIRATES: 1 ♀, 1♂, Abu Dhabi, 30.I.1987, I. Hamer (NHMUK 013380419, 013380423); 1 ♀, 2♂♂, Abu Dhabi, 31.III.1987 (NHMUK 013380418, 013380421, 013380420); 1 ♀, idem, 10.IV.1987, I. Hamer (NHMUK 013380422); 1 ♀, Hatta, 20.XII.1990 (NHMUK 013380424); 2 ♂♂, idem, 23.VIII.1991 (NHMUK 013380426, 013380427); 1 ♀, idem, 5.III.1993, I. Hamer (NHMUK 013380425); 3 ♀♀, North Ras, Al Khaimah, 17.II.2018 (M. Mokrousov) (ZISP); SAUDI ARABIA: 1 ♀, Riyadh, El Ha'ir, 19.III.1980, K.M. Guichard (NHMUK 013380448); OMAN: 1 ♀, Rostaq, 350 m, 21–31.III.1976, K.M.Guichard (NHMUK 013380444).

Published records. Schwarz 2010: 486 (United Arab Emirates); Ascher and Pickering 2019 (United Arab Emirates).

Distribution. United Arab Emirates, *Oman, *Saudi Arabia.

Discussion

In total, 26 species of *Sphecodes* are recorded from the Arabian Peninsula and surrounding lands (Israel, Jordan and Syria) (Table 1). This is a comparable number to the Iranian fauna, but distinctly less in comparison with the adjacent fauna of Turkey, North Africa and Central Asia (Table 3).

The *Sphecodes* fauna of the Arabian Peninsula and surrounding lands is a complex of Mediterranean, Sahara-Gobian, endemic, and species widespread in the Palaearctic region. Eight species, namely *S. alternatus*, *S. ephippius*, *S. gibbus*, *S. longulus*, *S. monilicornis*, *S. marginatus*, *S. pellucidus*, and *S. puncticeps* are widespread from north to south of the Palaearctic region and occur in biomes ranging from forest to desert. However, two of these (*S. marginatus* and *S. puncticeps*) are recorded from the Arabian Peninsula and the remainder all are found only in Mediterranean areas.

Sphecodes majalis, *S. schenckii* Hagens, *S. rubicundus*, and *S. nomioidis* are steppe species, distributed in Europe, Turkey and the Caucasus to Iran. Of them, only *S. nomioidis* is recorded from the Arabian Peninsula.

Sphecodes olivieri, *S. intermedius*, *S. rufiventris*, and *S. pinguiculus* are widespread from steppe to desert in the Western Palaearctic. Of these only *S. rufiventris* is not recorded from the Arabian Peninsula.

Table 3. List of *Sphecodes* species recorded in Arabian Peninsula and surrounding lands (AP+SL), Turkey, Iran, North Africa (Morocco, Algeria, Libya, Tunisia, Egypt) and Central Asia (Kazakhstan, Kyrgyzstan, Uzbekistan, Turkmenistan, Tajikistan).

	Sphecodes species	AP+SL	Turkey	Iran	North Africa	Central Asia
1	*S. albilabris* (Fabricius, 1793)	–	+	+	+	+
2	*S. alternatus* Smith, 1853	+	+	+	+	+
3	*S. anatolicus* Warncke, 1992	–	+	+	–	+
4	*S. armeniacus* Warncke, 1992	–	+	–	+	+
5	*S. atlanticus* Warncke, 1992	+	–	–	+	–
6	*S. atlassa* Warncke, 1992	–	–	–	+	–
7	*S. barbatus* Blüthgen, 1923	+	+	–	–	–
8	*S. crassanus* Warncke, 1992	–	+	–	–	+
9	*S. crassus* Thomson, 1870	–	+	+	+	+
10	*S. cristatus* Hagens, 1882	–	+	–	–	+
11	*S. croaticus* Meyer, 1922	–	+	+	+	+
12	*S. dathei* Schwarz, 2010	+	–	–	–	–
13	*S. dusmeti* Blüthgen, 1924	+	+	–	+	–
14	*S. ebmeri* Astafurova & Proshchalykin, 2018	–	–	+	–	–
15	*S. ephippius* (Linné, 1767)	+	+	+	–	+
16	*S. ferruginatus* Hagens, 1882	–	+	–	–	+
17	*S. geoffrellus* (Kirby, 1802)	–	+	–	+	+
19	*S. gibbus* (Linnaeus, 1758)	+	+	+	+	+
20	*S. hakkariensis* Warncke, 1992	–	+	–	–	+
21	*S. haladai* Warncke, 1992	–	–	+	+	+
22	*S. hyalinatus* Hagens, 1882	–	–	–	–	+
23	*S. hirtellus* Blüthgen, 1923	–	–	–	+	–
24	*S. intermedius* Blüthgen, 1923	+	+	–	+	+
25	*S. longulus* Hagens, 1882	+	+	+	–	+
27	*S. longuloides* Blüthgen, 1923	+	–	–	+	–
28	*S. majalis* Pérez, 1903	+	+	+	+	–
29	*S. marginatus* Hagens, 1882	+	–	–	+	–
30	*S. monilicornis* (Kirby, 1802)	+	+	+	+	+
31	*S. niger* Hagens, 1874	–	+	–	–	–
32	*S. nomioidis* Pesenko, 1979	+	+	–	–	–
33	*S. nurekensis* Warncke, 1992	–	–	–	–	+
34	*S. olivieri* Lepeletier de Saint Fargeau, 1825	+	+	+	+	+
35	*S. pectoralis* Morawitz, 1876	–	–	+	–	+
36	*S. pellucidus* Smith, 1845	+	+	+	+	+
37	*S. pesenkoi* Astafurova & Proshchalykin, 2018	–	–	–	–	+
38	*S. pinguiculus* Pérez, 1903	+	+	+	+	+
39	*S. pseudofasciatus* Blüthgen, 1925	–	+	–	+	–
40	*S. puncticeps* Thomson, 1870	+	+	+	+	+
41	*S. reticulatus* Thomson, 1870	–	+	+	–	+
42	*S. rubicundus* Hagens, 1875	+	+	+	–	–
43	*S. rubripes* Spinola, 1839	+	–	–	+	–
44	*S. ruficrus* (Erichson, 1835)	+	–	–	+	–
45	*S. rufiventris* (Panzer, 1798)	+	+	+	+	+
46	*S. sandykachis* Astafurova & Proshchalykin, 2018	–	–	–	–	+
47	*S. saxicolus* Warncke, 1992	–	–	+	–	+
48	*S. scabricollis* Wesmael, 1835	–	+	+	–	+
49	*S. schenckii* Hagens, 1882	+	+	+	–	–
50	*S. schwarzi* Astafurova & Proshchalykin, 2015	–	–	–	–	+
51	*S. spinulosus* Hagens, 1875	–	+	+	+	+
52	*S. tadschicus* Blüthgen, 1935	+	+	+	–	+
53	*S. trjapitzini* Astafurova & Proshchalykin, 2018	–	–	–	–	+
54	*S. turanicus* Astafurova & Proshchalykin, 2017	+	–	–	–	+
55	*S. zangherii* Noskiewicz, 1931	–	+	–	–	–
56	*S. villosulus* Schwarz, 2010	+	–	–	–	–
	Total:	**26**	**34**	**25**	**26**	**35**

The distribution of Sphecodes species are given according to Özbek et al. 2015 (Turkey), Astafurova et al. 2018d (Iran), Warncke 1992 (North Africa), Astafurova and Proshchalykin 2017b and Astafurova et al. 2018a, c (Central Asia).

Sphecodes barbatus, *S. rubripes*, and *S. ruficrus* are possibly purely Mediterranean species not reaching the Arabian Peninsula. In contrast, *S. atlanticus* turns out to be Sahara-Arabian. *Sphecodes dusmeti* and *S. longuloides* are Mediterranean-Arabian species.

Sphecodes tadschicus and *S. turanicus* are Irano-Turanian species reaching the Arabian Peninsula.

Finally, two species, *S. dathei* and *S. villosulus* are endemic to the Arabian Peninsula.

Although the Arabian fauna of the genus is not fully studied it is now clear that the Arabian fauna differs from that of the Mediterranean; of 26 recorded species only six (*S. olivieri*, *S. intermedius*, *S. marginatus*, *S. nomioidis*, *S. pinguiculus*, and *S. puncticeps*) are common to both and these are all widespread in the Western Palaearctic.

Acknowledgments

We are grateful to Fritz Gusenleitner (OLBL) for help during our visit to Austria, and Andrew Grace (Hastings, UK) for checking the English. We thank Hege Vårdal (NHRS), Lukasz Przybylowicz (ISZP), Michael Ohl, and Viola Richter (ZMHB) for providing *Sphecodes* type specimens. We also thank Michael Engel, Petr Bogusch, and anonymous reviewer for their comments and suggestions to streamline and improve the earlier drafts of the manuscript.

This investigation was supported by the Russian Funds for Basic Research (grant numbers 17-04-00259 and 19-04-00027) and the state research project (№ АААА-А19-119020690101-6).

References

Alqarni AS, Hannan MA, Engel MS (2014) New records of Nomiine and Halictine bees in the Kingdom of Saudi Arabia (Hymenoptera: Halictidae). Journal of the Kansas Entomological Society 87(3): 312–317. https://doi.org/10.2317/JKES140405.1

Årgent L, Svensson B (1982) Flagellar sensilla on *Sphecodes* bees (Hymenoptera, Halictidae). Zoologica Scripta 11: 45–54. https://doi.org/10.1111/j.1463-6409.1982.tb00517.x

Ascher JS, Pickering J (2019) Discover Life bee species guide and world checklist (Hymenoptera: Apoidea: Anthophila). http://www.discoverlife.org/mp/20q?guide=Apoidea_species [Accessed 20 March 2018]

Astafurova YuV, Proshchalykin MYu (2014) The bees of the genus *Sphecodes* Latreille 1804 of the Russian Far East, with key to species (Hymenoptera: Apoidea: Halictidae). Zootaxa 3887(5): 501–528. https://doi.org/10.11646/zootaxa.3887.5.1

Astafurova YuV, Proshchalykin MYu (2015a) Bees of the genus *Sphecodes* Latreille 1804 of Siberia, with a key to species (Hymenoptera: Apoidea: Halictidae). Zootaxa 4052(1): 65–95. https://doi.org/10.11646/zootaxa.4052.1.3

Astafurova YuV, Proshchalykin MYu (2015b) New and little known bees of the genus *Sphecodes* Latreille (Hymenoptera: Halictidae) from Mongolia. Far Eastern Entomologist 289: 1–9.

Astafurova YuV, Proshchalykin MYu (2015c) The bees of the genus *Sphecodes* Latreille, 1804 (Hymenoptera: Halictidae) of the Eastern Palaearctic Region. Proceedings of the Russian Entomological Society 86(2): 17–21. [In Russian]

Astafurova YuV, Proshchalykin MYu (2016a) To the knowledge of the genus *Sphecodes* Latreille (Hymenoptera: Halictidae) of Caucasus. Euroasian Entomological Journal 5(Suppl. 1): 15–9. http://www.eco.nsc.ru/EEJ_contents/15/2016150102.pdf

Astafurova YuV, Proshchalykin MYu (2016b) The bees of the genus *Sphecodes* Latreille (Hymenoptera: Halictidae) of the European part of Russia. Far Eastern Entomologist 321: 1–21. http://www.biosoil.ru/Files/FEE/00000526.pdf

Astafurova YuV, Proshchalykin MYu (2017a) To the knowledge of the *Sphecodes hyalinatus* species-group (Hymenoptera, Halictidae). Entomological Review 97(5): 664–671. https://doi.org/10.1134/S0013873817050104

Astafurova YuV, Proshchalykin MYu (2017b) The genus *Sphecodes* Latreille 1804 (Hymenoptera: Apoidea: Halictidae) in Central Asia. Zootaxa 4324(2): 249–284. https://doi.org/10.11646/zootaxa.4324.2.3

Astafurova YuV, Proshchalykin MYu (2018) A new species of a bee of the genus *Sphecodes* Latreille (Hymenoptera, Halictidae) from Kazakhstan. Entomological Review 98(6): 743–747. https://doi.org/10.1134/S0013873817060118

Astafurova YuV, Proshchalykin MYu, Engel MS (2018a) The cuckoo bee genus *Sphecodes* Latreille, 1804 in Kazakhstan (Hymenoptera: Halictidae). Far Eastern Entomologist 369: 1–47. https://doi.org/10.25221/fee.369.1

Astafurova YuV, Proshchalykin MYu, Niu Z-Q, Zhu C-D (2018b) New records of bees of the genus *Sphecodes* Latreille (Hymenoptera, Halictidae) in the Palaearctic part of China. ZooKeys 792: 15–44. https://doi.org/10.3897/zookeys.792.28042

Astafurova YuV, Proshchalykin MYu, Schwarz M (2015) New data on the genus *Sphecodes* Latreille (Hymenoptera: Halictidae) from Mongolia. Far Eastern Entomologist 302: 1–9. http://www.biosoil.ru/Files/FEE/00000479.pdf

Astafurova YuV, Proshchalykin MYu, Schwarz M (2018c) New and little known bees of the genus *Sphecodes* Latreille, 1804 (Hymenoptera: Apoidea: Halictidae) from Central Asia. Zootaxa 4441(1): 76–88. https://doi.org/10.11646/zootaxa.4441.1.4

Astafurova YuV, Proshchalykin MYu, Schwarz M (2018d) The cuckoo bee genus *Sphecodes* Latreille (Hymenoptera: Halictidae) in Iran. Journal of Hymenoptera Research 66: 39–53. https://doi.org/10.3897/jhr.66.29269

Astafurova YuV, Proshchalykin MYu, Shlyakhtenok AS (2014) Contribution to the knowledge of bee fauna of the genus *Sphecodes* Latreille (Hymenoptera: Halictidae) of the Republic of Belarus. Far Eastern Entomologist 280: 1–8. http://www.biosoil.ru/Files/FEE/00000437.pdf

Blüthgen P (1923) Beiträge zur Systematik der Bienengattung *Sphecodes* Latr. Deutsche Entomologische Zeitschrift 5: 441–513. https://www.zobodat.at/pdf/Deutsche-Ent-Zeitschrift_1923_0441-0514.pdf

Bogusch P, Straka J (2012) Review and identification of the cuckoo bees of central Europe (Hymenoptera: Halictidae: *Sphecodes*). Zootaxa 3311: 1–41. https://doi.org/10.11646/zootaxa.3311.1.1

Bogusch P, Straka J (2014a) *Sphecodes barbatus*. The IUCN Red List of Threatened Species 2014: e.T47981978A47995455. [Downloaded on 01 April 2019]

Bogusch P, Straka J (2014b) *Sphecodes rubripes*. The IUCN Red List of Threatened Species 2014: e.T47982116A47996274. https://doi.org/10.2305/IUCN.UK.2014-2.RLTS.T47982116A47996274.en [Downloaded on 01 April 2019]

Bossert S (2017) Description of the female of *Clavinomia clavicornis* (Warncke, 1980) (Halictidae: Nomiinae), with the species' taxonomy and first record from the Arabian Peninsula. The Pan-Pacific Entomologist 93(1): 29–34. https://doi.org/10.3956/2017-93.1.29

Cross I (2017) *Eucera nigrilabris* Lepeletier, 1841 is the host of *Sphecodes rubripes* Spinola, 1838 Hymenoptera: Aculeata). Ampulex 9: 1–14. https://www.zobodat.at/pdf/Ampulex_9_0012-0014.pdf

Dathe HH (2009) Order Hymenoptera, superfamily Apoidea. Families Colletidae, Andrenidae, Halictidae, Melittidae, Megachilidae and Apidae. Arthropod fauna of the UAE 2: 335–432.

Ebmer AW (2008) Neue taxa der gattungen *Halictus* Latreille 1804 und *Lasioglossum* Curtis 1833 (Hymenoptera, Apoidea, Halictidae) aus den Vereinigten Arabischen Emiraten. Linzer biologische Beitrage 40(1): 551–580. https://www.zobodat.at/pdf/LBB_0040_1_0551-0580.pdf

Engel MS (2001) A monograph of the Baltic amber bees and evolution of the Apoidea (Hymenoptera). Bulletin of the American Museum of Natural History 259: 1–192. https://doi.org/10.1206/0003-0090(2001)259<0001:AMOTBA>2.0.CO;2

Engel MS, Alqarni AS, Hannan MA (2013) A preliminary list of bee genera in the Kingdom of Saudi Arabia (Hymenoptera: Apoidea). Journal of the Saudi Society of Agricultural Sciences 12: 85–89. https://doi.org/10.1016/j.jssas.2012.08.001

Erichson WF (1835) Beschreibung von 19 neuen Hymenopteren aus Andalusien. In: Waltl J (Ed.) Reise durch Tyrol, Oberitalien und Piemont nach dem südlichen Spanien, nebst einem Anhange zoologischen Inhalts. 2. Auflage. Verlag der Pustetschen Buchhandlung (JF Winkler), Passau, 101–109.

Habermannová J, Bogusch P, Straka J (2013) Flexible host choice and common host switches in the evolution of generalist and specialist cuckoo bees (Anthophila: *Sphecodes*). PLoS ONE 8: e64537. https://doi.org/10.1371/journal.pone.0064537

Hagens J von (1875) Weitere Beiträge zur Kenntniss der deutschen *Sphecodes*-Arten. Deutsche Entomologische Zeitschrift 19(2): 315–319. https://doi.org/10.1002/mmnd.48018750205

Hagens J von (1882) Üeber die männlichen Genitalien der Bienen-Gattung *Sphecodes*. Deutsche Entomologische Zeitschrift 26: 209–228. [pls VI & VII] https://doi.org/10.1002/mmnd.48018820115

Harris RA (1979) A glossary of surface sculpturing. Occasional papers of the Bureau of Entomology of the California Department of Agriculture 28: 1–31. https://www.cdfa.ca.gov/plant/ppd/PDF/Occasional_Papers%20_28.pdf

Kirby W (1802) Monographia Apum Angliae. Vol. 2. J. Raw, Ipswich, 387 pp. https://doi.org/10.5962/bhl.title.10346

Linnaeus C (1758) Systema naturae per regna tria naturae secundum classes, ordines, genera, species, cum characteribus, differentiis, synonymis, locis. T. I. Editio X. Impensis Direct. Laurentii Salvii, Holmiae, 823 pp. https://doi.org/10.5962/bhl.title.542

Lepeletier de Saint Fargeau ALM, Audinet-Serville JG (1825) In: Latreille PA (Ed.) Encyclopédie méthodique ou par ordre des matières. Histoire naturelle.Entomologie, ou histoire

naturelle des crustacés, des arachnides et des insectes. Tome Dixième. Veuve Agasse, Paris, 832 pp. https://doi.org/10.5962/bhl.title.82248

Meyer R (1924 "1925") Zur Bienengattung *Sphecodes*. Archiv für Naturgeschichte, Abteilung A, 90(12): 1–12.

Michener CD (2007) The Bees of the World (2nd edn). Johns Hopkins University Press, Baltimore, 953 pp. [+ 20 pls]

Özbek H, Bogusch P, Straka J (2015) A contribution to the kleptoparasitic bees of Turkey: Part I., the genus *Sphecodes* Latreille (Hymenoptera: Halictidae). Turkish Journal of Zoology 39(6): 1095–1109. https://doi.org/10.3906/zoo-1501-43

Panzer GWF (1798) Fauna insectorum germanicae initia, oder Deutschlands Insecten. Heft 54. Felssecker, Nürnberg, 24 pp. [+ 24 pls]

Pérez J (1903) Espéces nouvelles de Melliféres (paléarctiques). Procés-verbaux de la Société Linnéenne de Bordeaux 58: 78– 93, 208–236.

Pesenko YuA (1979) A new species of cleptoparasitic bees of the genus *Sphecodes* Latr. from a nest of Nomioides minutissimus (Rossi) (Hymenoptera, Halictidae). Entomologicheskoe obozrenie 58(4): 860. [In Russian]

Pesenko YuA, Pauly A (2009) A contribution to the fauna of the Nomioidine bees of the Arabian Peninsula (Hymenoptera: Halictidae). Fauna of Arabia 24: 217–236. http://www.atlashymenoptera.net/biblio/Pesenko%20&%20Pauly%202009_Arabian_Nomioidinae.pdf

Popov VB (1935) Contributions to the bee fauna of Tajikistan (Hymenoptera, Apoidea). Trudy Tajikskoi Bazy Akademii Nauk SSSR 5: 351–408. [In Russian]

Schwarz M (2010) Order Hymenoptera, family Halictidae. Supplementary records of the genus *Sphecodes* Latreille. Arthropod fauna of the UAE 3: 483–491.

Smith F (1845) Descriptions of the British species of bees belonging to the genus *Sphecodes* of Latreille. Zoologist 3: 1011– 1015.

Smith F (1853) Catalogue of Hymenopterous insects in the collection of the British Museum. Andrenidae and Apidae. Vol. 1. Printed by order of the Trustees, London, 197 pp. [+pls 1–6] https://doi.org/10.5962/bhl.title.20858

Spinola M (1839) Compte-rendu des Hyménoptères recueillis par M. Fischer pendant son voyage en Egypte, et communiqués par. M. le Docreur Waltl. Annales de la Société Entomologique de France 7: 437–546.

Thomson CG (1870) Opuscula entomologica. Vol. 2. Håkan Ohlson, Lund, 222 pp. https://doi.org/10.5962/bhl.title.8248

Warncke K (1992) Die westpaläarktischen Arten der Bienengattung *Sphecodes* Latr. Bericht der Naturforschende Gesellschaft Augsburg 52: 9–64.

ZooKeys 872: 41–55 (2019)
doi: 10.3897/zookeys.872.29815
http://zookeys.pensoft.net

RESEARCH ARTICLE

A peer-reviewed open-access journal
ZooKeys
Launched to accelerate biodiversity research

Close relationship between the genera *Sinhomidia* and *Homidia* (Collembola, Entomobryidae) revealed by adult and first instar characters, with description of a new *Sinhomidia* species

Zhi-Xiang Pan[1], Chen-Chong Si[2], Shu-Sheng Zhang[3]

1 *School of Life Sciences, Taizhou University, Taizhou, Zhejiang province 318000, China* **2** *Taizhou Foreign Language School, Taizhou, Zhejiang 318000, China* **3** *Wuyanling National Nature Reserve, Wenzhou, Zhejiang 325500, China*

Corresponding author: *Zhi-Xiang Pan* (pzx1118@hotmail.com)

Academic editor: *L. Deharveng* | Received 17 September 2018 | Accepted 10 June 2019 | Published 20 August 2019

http://zoobank.org/57276239-43A7-473C-98D7-2A9B80A33B9F

Citation: Pan Z-X, Si C-C, Zhang S-S (2019) Close relationship between the genera *Sinhomidia* and *Homidia* (Collembola, Entomobryidae) revealed by adult and first instar characters, with description of a new *Sinhomidia* species. ZooKeys 872: 41–55. https://doi.org/10.3897/zookeys.872.29815

Abstract

A third species of the genus *Sinhomidia* is described from South China: *S. uniseta* **sp. nov.** This new species can be distinguished from the two other species of the genus by the following characters: colour pattern, single labial chaeta M, chaetotaxy on terga and ventral tube, unguis with three inner teeth, and 15 clypeal ciliated chaetae. Also, the chaetotaxy of the first instar of *Sinhomidia* is described for the first time in the present paper, and confirms the close relationship between *Sinhomidia* and *Homidia*. A key to species of *Sinhomidia* is provided.

Keywords

chaetotaxy, Entomobryinae, *Sinhomidia uniseta* sp. nov., taxonomy

Introduction

The genus *Sinhomidia* was defined by Zhang et al. (2009), based on the type species *Acanthocyrtus bicolor* (Yosii, 1965). This genus is characterised by 8+8 eyes; scales pointed with coarse striations; dental spines present on inner dens; clavate tenent hairs;

mucro bidentate with subapical tooth larger than apical one, and basal spine reaching subapical tooth; abdominal segment II/III/IV with 2/3/2 bothriotricha, and bothriotrichal complex with slightly modified accessory microchaetae; abdominal segment IV with anterior eyebrow-like macrochaetae (Zhang et al. 2009). This genus has scales present on the appendages according to *S. bicolor* (Zhang et al. 2009), however, Jin et al. (2017) proposed "scales present or absent on appendage" based on *Sinhomidia guangxiensis* Jin et al., 2017, which lacked such scales.

The genera *Sinhomidia* and *Homidia* Börner, 1906 are closely related, the scaled *Sinhomidia* being recognised as sister group of unscaled *Homidia* (Zhang et al. 2014a). This close relationship is supported by morphological, molecular and ecological evidence. Firstly, these two genera share several morphological characters, such as cephalic chaetotaxy on the dorsal side, eyebrow-like macrochaetae on abdominal segment IV, dens with inner spines in adults, smooth labial chaetae e and l_1, the subapical mucronal tooth larger than the apical one, a bilobed bulb on antennal apex (Zhang et al. 2009, Zhang et al. 2014b), bothriotricha formula (2/3/2 on abdominal segment II/III/IV), and sensory chaetotaxic formula on tergal segments (3, 2/2, 2, 3, ? (sensory chaetae on abdominal segment IV variable), 3). They are easily misidentified as *Homidia* in the field in view of their colour pattern and body form. Secondly, recent molecular phylogenetic analyses revealed a close relationship between them based on mitochondrial, ribosomal and nuclear gene fragments (Zhang et al. 2014a, 2015, 2016). Also, Ding et al. (2019) placed *Sinhomidia* within the clade of *Homidia* based on mitochondrial COI, 16S rRNA and nuclear 28S rRNA D1-2. Thirdly, these two genera live in similar habitat, and are usually found in leaf litter in tropical to subtropical bioclimates. *Sinhomidia* with two known species and the new species described here is much less diversified than *Homidia* which has about 37 species in China (Zhang et al. 2009, Jin et al. 2017, Ma and Pan 2017). *Sinhomidia* can be easily discriminated morphologically from *Homidia* by scales on the terga and slightly modified accessory microchaetae of the bothriotrichal complex (Zhang et al. 2009).

The genus *Sinhomidia* is endemic to China. The type species (*S. bicolor*) was first recorded from Taiwan (Yosii 1965), and subsequently a female specimen was found in Anhui Province (Zhang et al. 2009) and male specimens in Guangxi Province (Jin et al. 2017). To date, only two species of this genus have been described (*S. bicolor* and *S. guangxiensis*), and the chaetotaxy of larvae has not been revealed. Here, a third species from Guangdong Province is described, together with its first instar larva. We provide a detailed comparison between the new species and the two known species, and we compare the first instar chaetotaxy among nine species of family Entomobryidae. In addition, a key to the recorded species of *Sinhomidia* is provided.

Materials and methods

Specimens were sieved from leaf litter onto a tray in the field, collected by an aspirator, and stored in 99% ethanol at -20 °C. Specimens were photographed using a Nikon

DS-Fi1 camera mounted onto a Nikon SMZ1000 stereomicroscope, then cleared in lactic acid, mounted in Hoyer's medium under a coverslip, and examined under phase contrast using a Nikon 80i microscope. Lengths were measured from specimens on slide by NIS-Elements Documentation 3.1 software. Photos, illustrations and labels were enhanced by photoshop CS5 (Abode Systems).

Dorsal chaetotaxy is provided for only one side of the body. The nomenclature of cephalic chaetotaxy follows Szeptycki's system (Szeptycki 1973), labial palp follows Fjellberg (1998), labial chaetae follow Gisin (1967), and dorsal thoracic and abdominal chaetotaxy follows Szeptycki (1979).

Abbreviations:

Abd. abdominal segment;
Ant. antennal segment;
Gr. group;
mac macrochaeta(e);
mic microchaeta(e);
ms specialised microchaeta(e);
sens specialised ordinary chaeta(e);
Th. thoracic segment;
VT ventral tube;

Taxonomy

***Sinhomidia uniseta* sp. nov.**
http://zoobank.org/656D27C0-C669-4E19-9399-9CDBA73CF9E5
Figs 1–45

Description (adult and subadult). ***Size.*** Body length up to 2.51 mm. ***Scales.*** Scales pointed and coarsely striated, present on dorsal side of head, thorax and abdomen (Figs 6, 7), with fewer scales present on antennae and legs. Ventral side of manubrium with longer and narrower scales than those of dorsal side of body (Fig. 8). ***Colour pattern.*** Ground colour whitish in ethanol. Eye patches dark blue. Antennae with dark pigmentation, gradually darker from Ant. I to Ant. IV. A dark band between basal antennae. Lateral and anterior margin of Th. II, posterior half of Abd. II, whole Abd. III, posterior Abd. IV and femurs of the hind leg pigmented (Figs 1–3). Ventral side of body and VT without pigment (Fig. 3). Subadults with the same colour pattern as adults, but Th. II laterally and Abd. IV posteriorly lighter (Fig. 4). ***Head.*** Eyes 8+8, G and H smaller than others and always difficult to observe using a light microscope; three chaetae (p, r, and t) within eye patches, with p largest (Fig. 10). Antenna 2.10–2.45 times as long as cephalic diagonal; antennal segments ratio as I:II:III:IV = 1:1.48–1.91: 1.28–1.56:2.51–3.34. Ant. I basally with 3 dorsal and 4 ventral smooth mic (Fig. 11). Ant. II with 5 basal smooth mic (Fig. 12), and 1 longer (rarely 3) and 1 shorter rod-like distal S-chaetae (Fig. 13). Ant. III organ with 2 rod-like and 3 short guard S-chaetae (Fig. 14). Bulb on apical Ant. IV bilobed (Fig. 15). Prelabral and labral chaetae as 4/5, 5, 4, all smooth; labral papillae absent (Fig. 16). Clypeus with 15 mac in four lines, arranged as 3, 5, 4, 3 (Fig. 17). Cephalic chaetotaxy on dorsal side with 3 antennal (A),

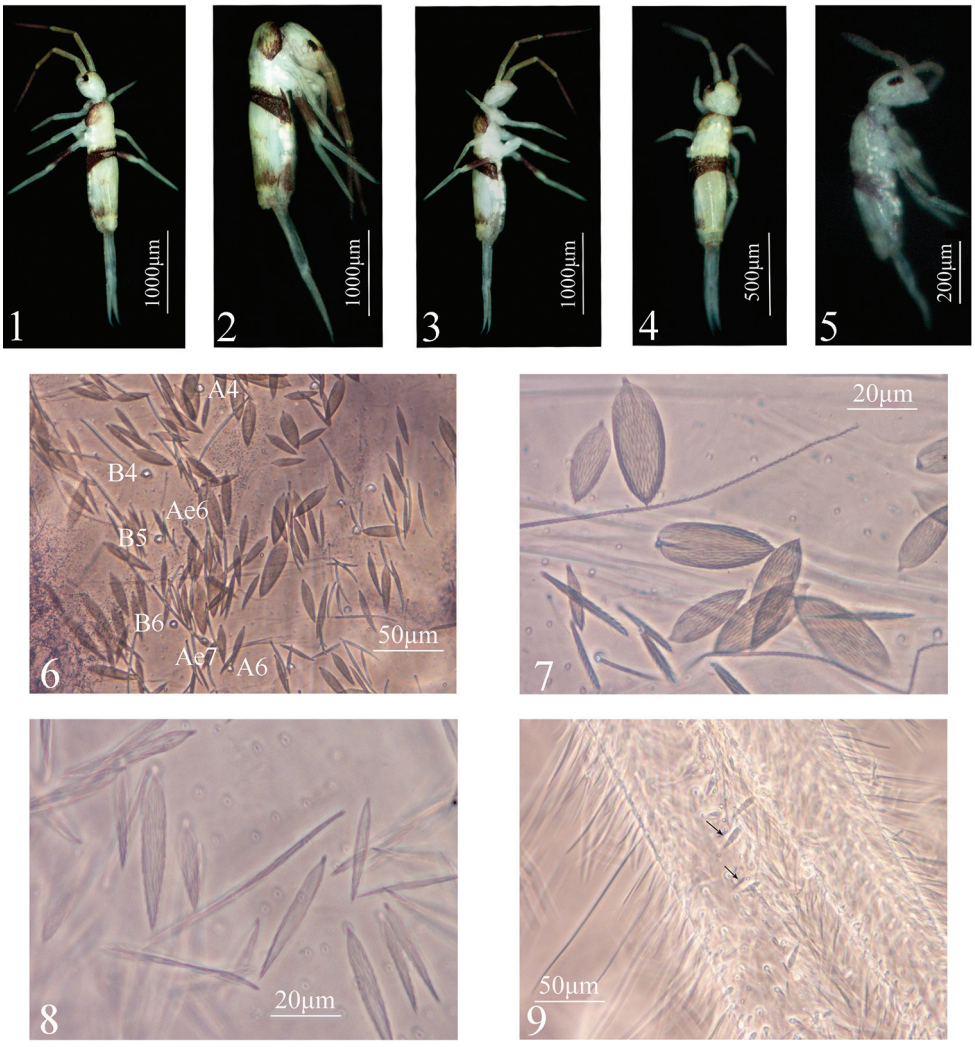

Figures 1–9. *Sinhomidia uniseta* sp. nov. **1–5** Habitus: **1** dorsal view of adult **2** lateral view of adult **3** ventral view of adult **4** dorsal view of subadult **5** lateral view of 1st instar larva **6** postero-median scales on Abd. IV **7** scales and bothriotrichal complex on Abd. III **8** scales on manubrium **9** dental spines.

3 ocellar (O) and 5 sutural (S) mac, Gr. II with 3 mac (Fig. 10). Chaetae on labium basis as $MRel_1L_2$, with e and l_1 smooth; postlabial chaetae not expanded (Fig. 18). Five papillae A–E on labial palp with 0, 5, 0, 4, 3 guard chaetae, respectively; lateral process (l.p.) normal, with tip reaching apex of papilla E; hypostoma with 2 guard chaetae; proximal chaetae 5 (Fig. 19). Maxillary outer lobe with 1 apical chaeta, 1 subapical chaeta and 3 sublobal hairs on sublobal plate, subapical chaeta slightly larger than apical one (Fig. 20). ***Thorax.*** Complete body sens as 2, 2/1, 2, 2, 33, 3, ms as 1, 0/1, 0, 1, 0, 0. Th. II with 4 medio-medial (m1, m2, m2i and m2i2), 3 medio-sublateral (m4, m4i and m4p) mac and 3 S-chaetae (ms antero-internal to sens); posterior with

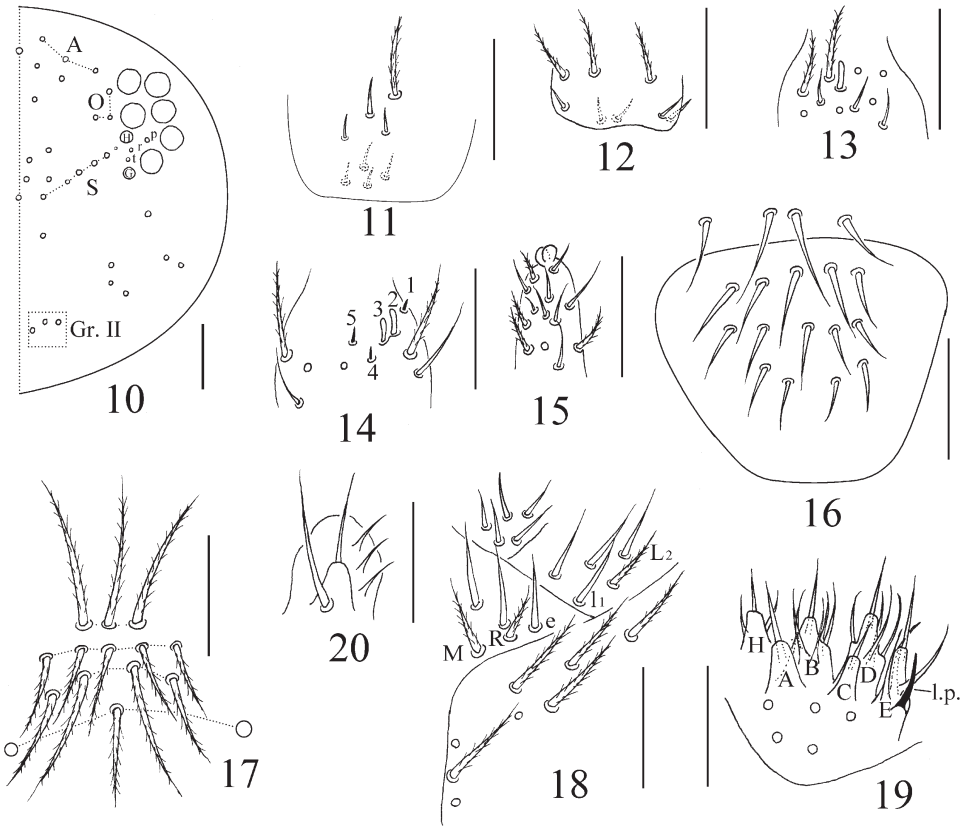

Figures 10–20. *Sinhomidia uniseta* sp. nov. **10** Cephalic chaetotaxy on dorsal side **11** basis of Ant. I **12** basis of Ant. II **13** distal part of Ant. II **14** Ant. III organ **15** distal part of Ant. IV **16** labrum **17** clypeal chaetotaxy **18** labium **19** labial palp **20** maxillary outer lobe **10–16** dorsal view **17–19** ventral view **20** lateral view. Scale bars: 50 μm.

17–19 mac; p6 as mic. Th. III with 17–19 mac and 2 sens; p5, p6 and m6 as mac, p4 as mic (Fig. 21). Coxal macrochaetal formula as 3 (1 pseudopore)/4+1, 3 (3 pseudopores)/ 4+2 (pseudopore(s) unclear) mac (Fig. 22). Trochanteral organ with 24–34 smooth chaetae, 5–6 in ventral and 3–4 in posterior line (Fig. 23). Inner tibiotarsus with slightly ciliated chaetae. Tenent hairs clavate, slightly shorter than inner edge of unguis in length. Unguis with 3 inner and 2 lateral teeth, tooth on outer edge unclear. Unguiculus lanceolate with outer edge slightly serrate and the most basal tooth larger (Fig. 24). ***Abdomen.*** Abd. IV 11–15 times longer than Abd. III along the dorsal axis. Abd. I with 3 mac (m2–4) and 2 S-chaetae (ms antero-external to sens). Abd. II with 5 central (a2, m3, m3e, m3ea and m3ep) and 1 lateral (m5) mac. Abd. III with 1 central (m3) and 4 lateral (am6, pm6, p6 and m7) mac, 2 sens and 1 ms. Abd. IV with 31 elongated and 2 normal length sens, and 10–14 mac arranged in anterior eyebrow-like line; postero-central area with 5 (7) mac (A4, A6, B4–6; Ae6 and Ae7 sometimes

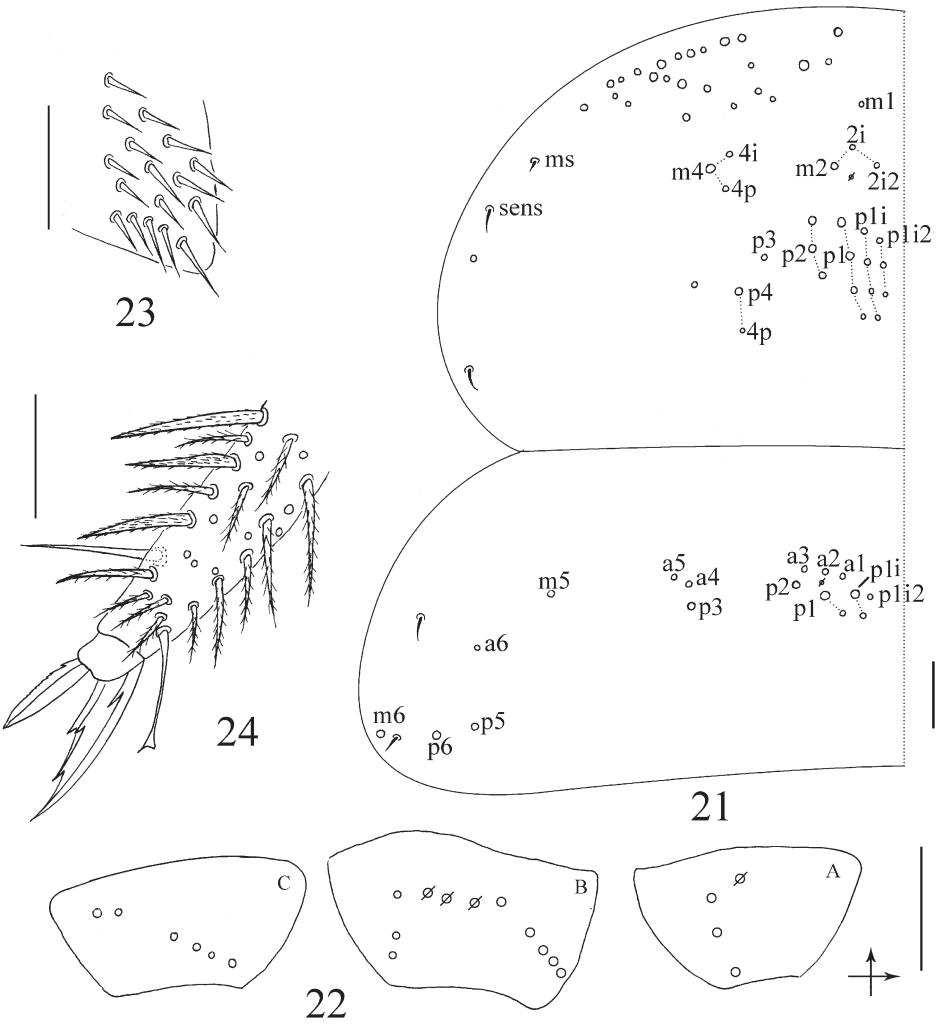

Figures 21–24. *Sinhomidia uniseta* sp. nov. **21** Chaetotaxy of Th. II–III tergites **22** Coxae (**A** fore leg **B** middle leg **C** hind leg) **23** Trochanteral organ **24** Distal part of tibiotarsus and claw of hind leg **21, 24** dorsal view **22, 23** lateral view. Scale bars: 50 μm.

present). Abd. V with 3 sens, the middle one posterior to m3, the lateral one between chaetae a5 and m5 but shifted from anterior to posterior of a5 among the examined specimens; a1, a3, m3, m5, a5, m5, and a6 as mac, m3a sometimes as mac (Fig. 25). Anterior face of VT with many ciliated chaetae, 3+3 of them as mac, in a line connecting proximal (Pr) and external-distal (Ed) mac obliquely to median furrow (Fig. 26); lateral flap with 6–9 smooth and 10–11 ciliated chaetae on each side (Fig. 27); apical smooth chaetae on posterior face variable, five of examined specimens have 5 (2+1+2), one has 7, and another one has 9 (Fig. 28). Tenaculum with 4+4 teeth and 1 large, multi-laterally basally ciliated chaeta (Fig. 29). Manubrial plaque with 3 pseudopores

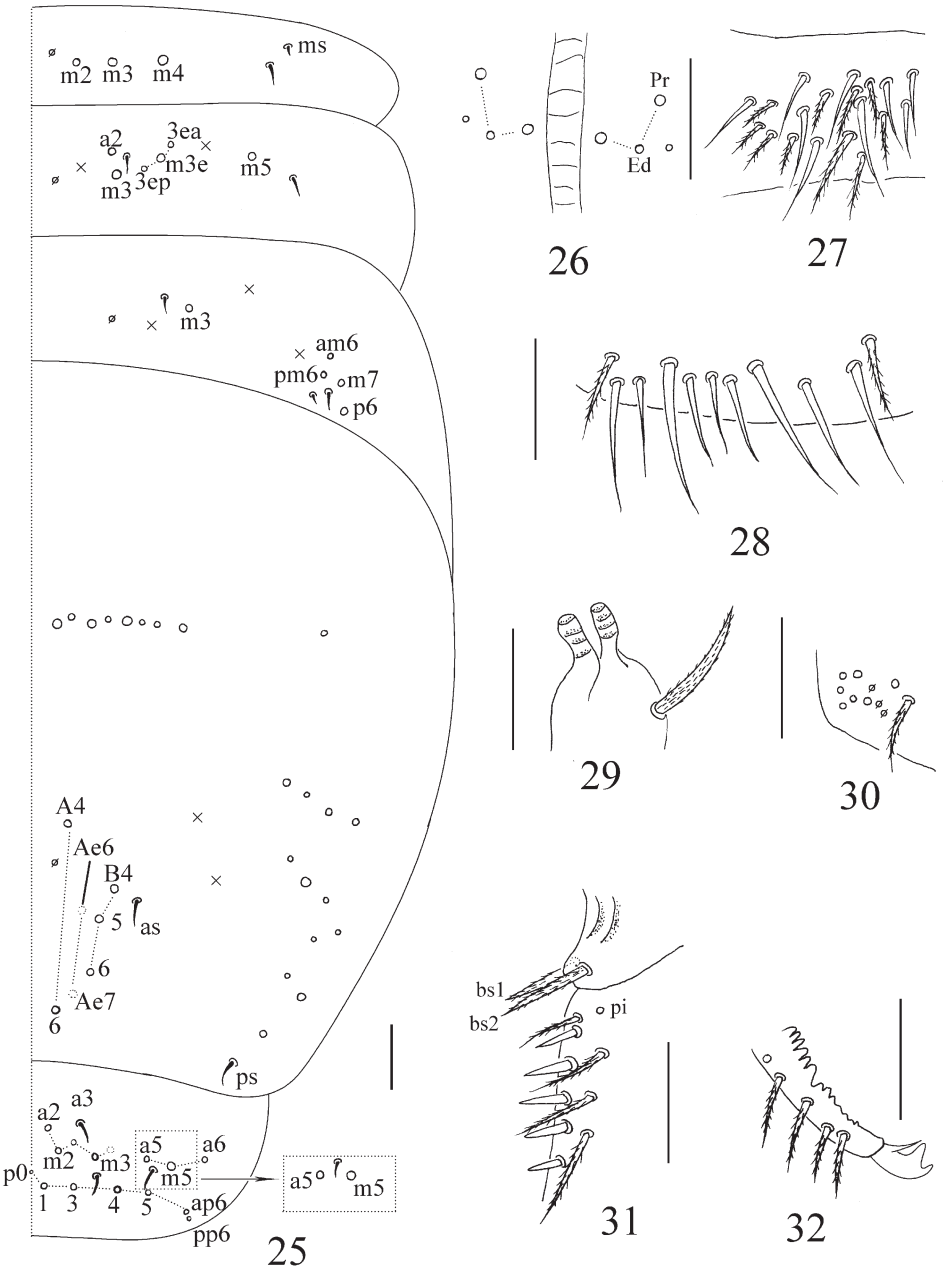

Figures 25–32. *Sinhomidia uniseta* sp. nov. **25** Dorsal chaetotaxy of Abd. I–Abd. V tergites **26** anterior face of ventral tube **27** lateral flap of ventral tube **28** posterior face of ventral tube **29** tenaculum **30** manubrial plaque **31** basal part of dens **32** distal part of dens and mucro **25, 26, 31, 32** dorsal view **28–30** ventral view **27** lateral view. Scale bars: 50 μm.

and 8–10 ciliated chaetae (Fig. 30). Dens with 31–39 inner spines, basal chaetae (bs) spiny and multi-laterally ciliate, bs1 shorter than bs2, the morphology of chaeta pi unclear (Figs 9, 31). Mucro bidentate with subapical tooth larger than apical one; basal spine short, with tip reaching subapical tooth; distal smooth part of dens slightly shorter than mucro (Fig. 32).

Description of the first instar larva. ***Size.*** Body length up to 0.79 mm. ***Colour pattern.*** Ground colour whitish, eye patches dark, antennae and femurs of hind legs with weak pigments, posterior half of Abd. II and whole Abd. III pigmented. The colour pattern is similar to that of adults, but paler overall (Fig. 5). ***Body.*** Body without scales. Complete tergal sens as 2, 2/1, 2, 2, 33, 3, ms as 1, 0/1, 0, 1, 0, 0. Cephalic chaetotaxy on dorsal side with 2 antennal (A), 2 ocellar (O) and 3 sutural (S) mac; eyes 8+8, eye patches with 3 chaetae (p, r, and t; p largest) (Fig. 33). Labium with 3 proximal chaetae, 4 chaetae (M, e, a_1 and a_2) in basomedial field and 5 chaetae (a3–a5, l_1 and L_2) in basolateral field, chaetae M and L_2 ciliate, and others smooth; posterior area of labium with 9 ciliated mac (Fig. 38). Th. II with 7 anterior (a1–7), 6 median (m1–2, m4–7), and 6 posterior (p1–6) primary chaetae arranged in 3 rows; chaetae a7, m2, m5, m7 and p4–6 as mic, others as mac, and with 3 S-chaetae (ms antero-internal to sens). Th. III with 7 anterior (a1–7), 5 median (m1, m4–7), and 6 posterior (p1–6) primary chaetae arranged in 3 rows, and 2 S-chaetae; chaetae a7, m1, m4, m7, and p4–6 as mic, others as mac. Abd. I with 5 anterior (a1–3, a5–6), 5 median (m2–6), and 2 posterior (p5–6) primary chaetae arranged in 3 rows and 2 S-chaetae (ms antero-external to sens); chaetae m2–m4 as mac, others as mic. Abd. II with 6 anterior (a1–3, a5–7), 6 median (m2–7), and 4 posterior(p4–7) primary chaetae arranged in 3 rows, an additional chaeta external to p7 and 2 S-chaetae; chaetae a2, m3 and m5 as mac, a5 and m2 as bothriotricha, others as mic. Abd. III with 6 anterior (a1–3, a5–7), 7 median (m2–5, am6, pm6, m7), and 4 posterior (p4–7) primary chaetae arranged in 3 rows, 4 additional chaetae in lateral region, and 3 S-chaetae (1 ms and 2 sens); chaeta m3, am6 and pm6 as mac, m2, a5 and m5 as bothriotricha, others as mic (Fig. 34). Abd. IV with 5 (A1–4, A6), 6 (B1–6), 4 (C1–4), 7 (T1–7), 3 (D1–3), 3 (E1–3), and 3 (F1–3) primary ciliated chaetae arranged in 7 longitudinal lines, an additional ciliated chaeta between B1 and B2 (shown by arrow in Fig. 35), and 31 elongated and 2 normal sens; T2 and T4 as bothriotricha. Abd. V with 13 primary chaetae (m2, m3 and m5 as mac; a1, a3, a5, a6, p1, p3, p4, p5, ap6 and pp6 as mic) and 3 sens, the median sens posterior to m3. Abd. VI with 16 ciliated chaetae on one side and 2 along the median axis (Fig. 35). ***Appendages.*** Ant. I with 11 ciliated chaetae arranged in one ring and 1 basal smooth chaeta. Ant. II with 26 ciliated chaetae, arranged in 3 rings (8/8/9), basis without smooth spiny chaetae. Ant. III with 38 ciliated chaetae arranged in 4 rings (from basis to apex of Ant. III as 11/12/13/2) and 5 S-chaetae (Ant. III organ). Ant. IV with many S-chaetae (more than two types) and ciliated chaetae, apical bulb bilobed (Fig. 37). Ventral tube with 2 smooth chaetae on the posterior face and on each lateral flap anterior face without chaetae (Fig. 39). Manubrium with 42 ciliated chaetae, dens with numerous ciliated chaetae, without inner dental spines; chaetae bs2 longer than bs1, pi ciliated and similar in length to that of other ciliated chaetae; mucro with sub-

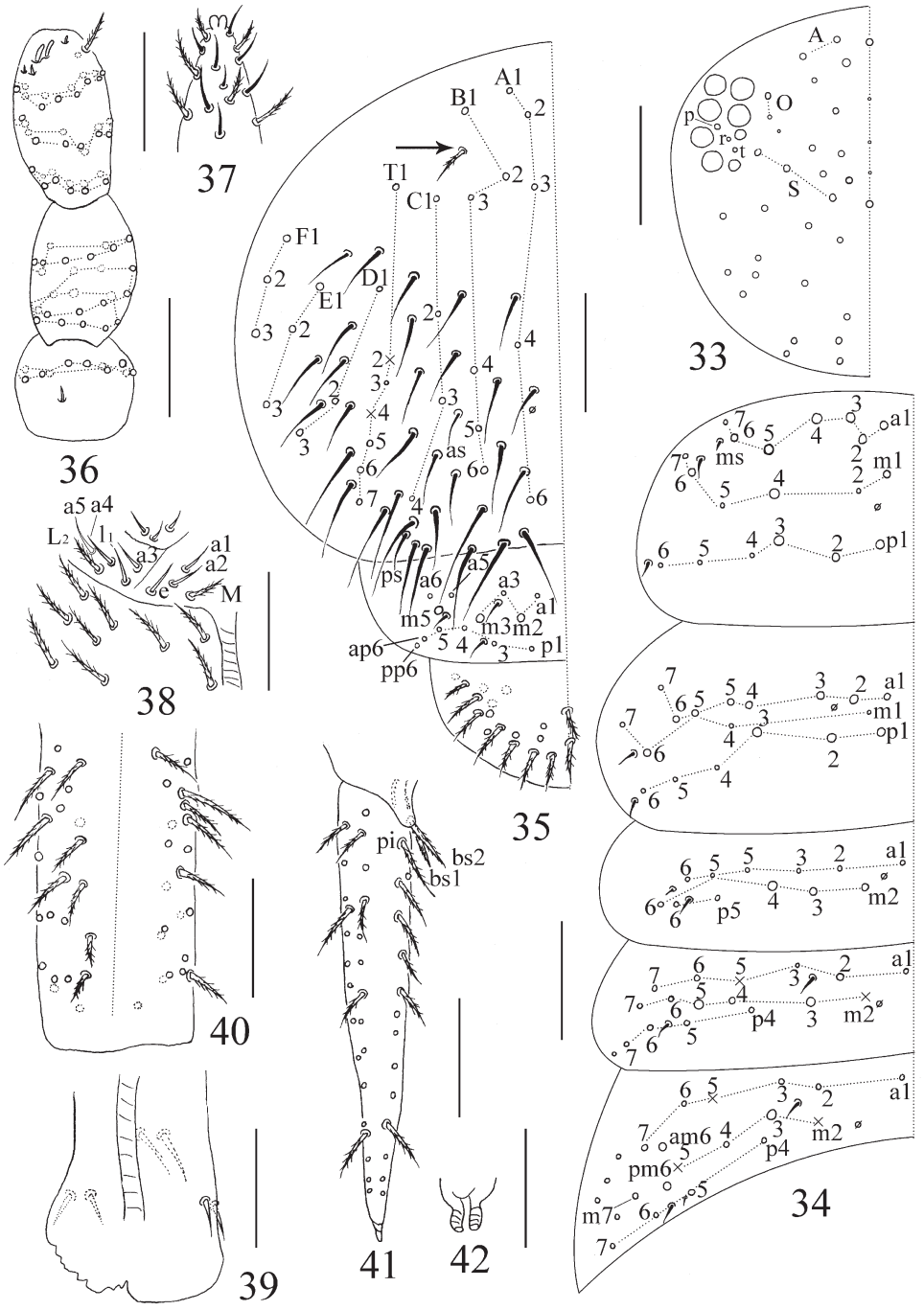

Figures 33–42. The first instar larvae of *Sinhomidia uniseta* sp. nov. **33** Dorsal cephalic chaetotaxy **34** chaetotaxy of Th. II–Abd. III tergites **35** chaetotaxy of Abd. IV–VI tergites **36** chaetotaxy of Ant. I–III **37** distal part of Ant. IV **38** labium **39** ventral tube **40** manubrium **41** dens **42** tenaculum **33–37, 39–42** dorsal view **38** ventral view. Scale bars: 50 μm.

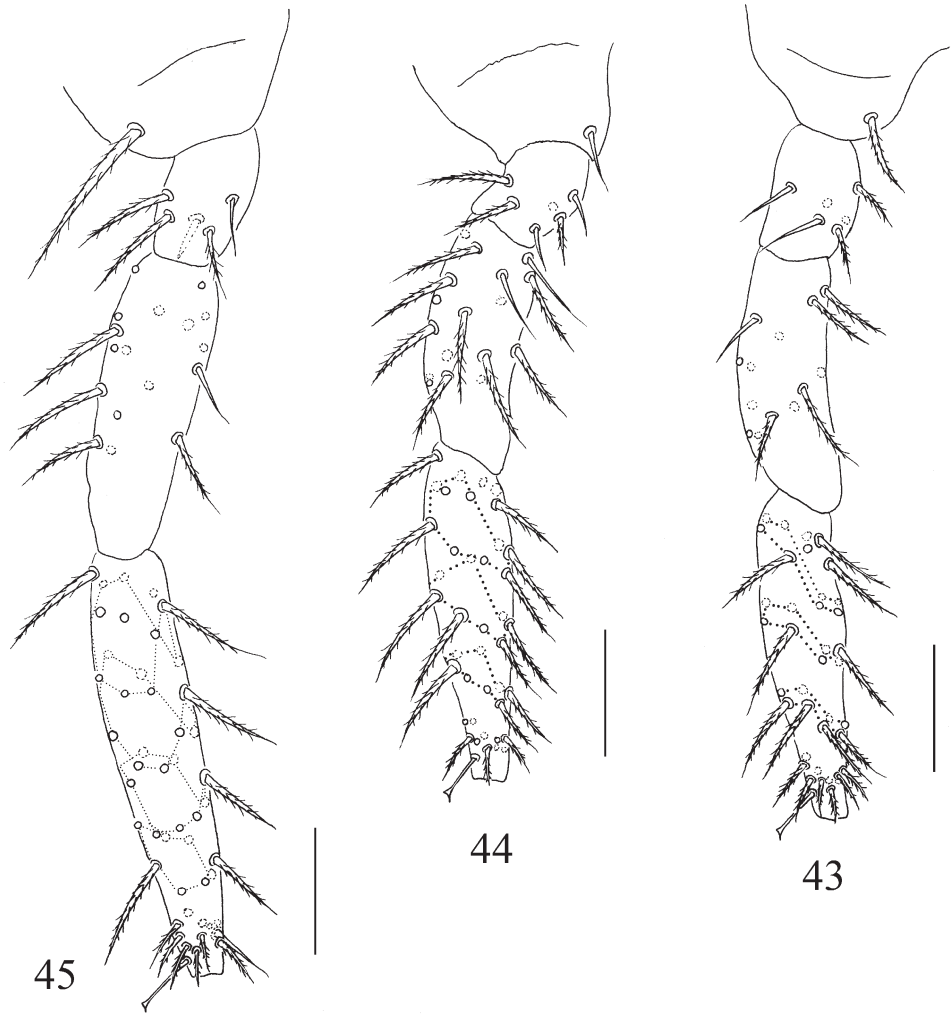

Figures 43–45. Left legs of the first instar of *Sinhomidia uniseta* sp. nov. **43–45** Anterior view of fore leg (**43**), mid leg (**44**) and hind leg (**45**). Scale bars: 50 μm.

apical tooth larger than apical one, basal spine absent (Fig. 41). Tenaculum with 4+4 teeth and without chaetae (Fig. 42). Four segments of fore, middle and hind leg with numerous chaetae, coxae with 1, 1, 1 chaetae, pseudopore unclear; trochanters with 6 (2 smooth), 6 (2 smooth), 5 (1 smooth and 1 spine like) chaetae; femurs with 13 (1 smooth), 17 (2 smooth), 17 (at least 1 smooth) ciliated chaetae; tibiotarsus with 39 (10/8/8/8/4 ciliated and 1 tenent hair), 41 (10/8/8/8/6 ciliated and 1 tenent hair), 48 (10/8/8/8/8/4, 1 tenent hair and 1 inner smooth chaetae) ciliated chaetae (Figs 43–45).

Ecology. Found in leaf litter of *Calamus thysanolepis*.

Holotype. 1♀ on slide, **China**, Guangdong Province, Guangzhou city, Tianhe District, Longdong reservoir, 23°14.134'N, 113°23.94'E, altitude 127±5 m, sample number

Table 1. Detailed differences between the three species of genus *Sinhomidia*.

Characters	*S. uniseta* sp. nov.	*S. bicolor*	*S. guangxiensis*
Colour pattern			
Lateral stripes on head	absent	present	absent
Pigment on Th. II	along lateral and anterior margins, rarely whole	along lateral and anterior margins	whole
Pigment on Abd. I	posterior margin	whole	whole
Middle dark band dorsally on Abd. IV	absent	present	present
Posterior dark band dorsally on Abd. IV	discontinuous	continuous	continuous
Scales on antennae, legs and manubrium	present	present	absent
Maximum body length (mm)	2.5	3.4	2.4
Chaetotaxy			
Chaeta M on labrum	undoubled	doubled	doubled
Chaetae a2 and a5 on Abd. I	absent	absent	present
Chaeta a3 on Abd. II	mic	mic	mac
Postero-medial mac on Abd. IV	5 (7)	9	8
Inner teeth of unguis	3	4	4
Smooth/ciliated chaetae on each lateral flap of ventral tube	5–9/10–11	14/14	3/13

4661, collected by Z-X PAN and S-S ZHANG, 24-III-2018. **Paratypes.** 4♀1♂adults, 1 subadult and 1 first instar larva on slides and 3 adults in ethanol, same data as holotype. All types were deposited at the School of Life Sciences, Taizhou University.

Etymology. Specific epithet refers to the single chaeta M on labial basis (uni + seta).

Remarks. *Sinhomidia uniseta* sp. nov. can be easily distinguished from the other two species of the genus by the dark pigment present on the lateral and anterior margins of Th. II, posterior margin of Abd. II and whole Abd. III, labial single M chaeta, three mac and ms external to sens on dorsal side of Abd. I, 5 (7) mac in postero-median area of Abd. IV, middle sens posterior to m3 on Abd. V, and three teeth on inner side of unguis. Detailed differences between the three species of *Sinhomidia* are listed in Table 1.

Discussion

Close relationship revealed by the chaetotaxy of adults and first instar between *Sinhomidia* and *Homidia*

The genus *Sinhomidia* was named referring to many features shared with *Homidia* (Zhang et al. 2009). *Sinhomidia* is regarded as sister group of *Homidia* (Zhang et al. 2014a), and is considered to be scaled *Homidia* (Zhang et al. 2014b). The genera *Sinhomidia* and *Homidia* share many features, such as colour pattern; chaetotaxy of head, labium, labrum, terga; S-chaetotaxic pattern, bothriotrichal pattern; and morphology of Ant. IV bulb, claw and mucro of adults (Pan et al. 2011, Zhuo et al. 2018).

Table 2. Comparison of the first instar larvae among nine species of Entomobryidae.

Tergite	Chaetae	*S. un*	*H. q*	*H. j*	*S. um*	*S. b*	*O. f*	*H. n*	*E. m*	*P. a*
Th. II	m1	mac	mac	mac	mac	mac	mac	mic	mac	mac
	m2	mic	mic	mic	mic	mic	mic	mic	mic	scale
	p4	mic	mic	mic	mic	mic	mic	mic	mic	mic
	p5	mic	mac	mac	mic	mac	mac	mic	mic	mac
	P6	mic	mic	mic	mic	mic	mic	mic	mic	mic
Th. III	a1	mac	mac	mic	mic	mac	mac	mic	mic	mic
	a2	mac	mac	mac	mac	mac	mac	mic	mic	mic
	a3	mac	mac	mac	mac	mac	mic	mic	mic	mic
	a4	mac	mac	mac	mac	mac	mac	mic	mic	–
	a5	mac	mac	mac	mac	mac	mac	mac	mac	mac
	m1	mic	mic	mic	mic	–	mic	mic	–	–
	m2	–	–	–	–	mac	–	–	mic	mac
	m5	mac	mac	mic	mic	mic	mic	mic	mic	mic
	p1	mac	mac	mac	mac	mac	mac	mac	mic	mac
	p2	mac	mac	mac	mac	mac	mac	mac	mic	mac
Abd. I	a4	–	–	–	–	–	–	–	mic	–
	a5	mic	mic	mic	mic	mic	mic	mic	–	mic
	m2	mac	mac	mac	mic	mac	mac	mac	mic	mac
	m4	mac	mac	mac	mac	mac	mac	mic	mac	mac
	m6	mic	mic	mic	mic	mic	mic	mic	mic	mic
Abd. II	a1	mic	mic	mic	mic	mic	mic	mic	mic	mic
	a2	mic	mic	mic	mic	mac	mac	mic	mic	mac
	a6	mic	mic	mic	mic	mic	mic	mic	–	mic
	a7	mic	mic	mic	mic	mic	mic	mic	mic	–
	m3	mac	mac	mac	mac	mac	mac	mac	mac	mac
	m4	mic	mic	mic	mic	mic	–	–	mic	mic
	m5	mac	mac	mac	mac	mac	mac	mic	mic	mac
	m6	mic	mic	mic	mic	mic	mic	mic	mac	mic
	m7	mic	mic	mic	mic	–	mic	mic	–	mic
	p4	mic	mic	mic	mic	mic	mic	mic	–	–
	p5	mic	mic	mic	mic	mic	mic	–	–	–
Abd. III	a1	mic	mic	mic	mic	mic	mic	mic	mic	mic
	a2	mic	mic	mic	mic	mic	mic	mic	mic	mic
	a7	mic	mic	mic	mic	mic	mic	mic	–	mic
	m4	mic	mic	mic	mic	mic	–	mic	–	mic
	am6	mac	mac	mic	mic	mic	mac	mac	mac	mac
	pm6	mac	mac	mac	mic	mac	mac	mac	mac	mac
	p4	mic	mic	mic	mic	–	mic	mic	mic	–
	p5	mic	mic	mic	mic	mic	mic	–	mic	–
Abd. IV	A4	mac	mic	mic	–	–	–	–	mic	–
	A5	–	mic	–	mic	mic	–	–	–	mic
	A6	mac	mic	mac	mic	mic	–	mic	?	mic
	B4	mac	mac	mic	mac	mic	–	–	mic	mic
	B5	mac	mac	mac	mac	mac	mic	mic	mac	mac
	B6	mac	mic	mic	mic	mic	mic	–	mic	mic
	E2	mac	mac	–	–	mic	mac	mic	–	mic
	E3	mac	mac	mac	mac	mac	–	–	mac	mic

Tergite	Chaetae	*S. un*	*H. q*	*H. j*	*S. um*	*S. b*	*O. f*	*H. n*	*E. m*	*P. a*
Abd. V	a1	mic	mic	mic	mic	mic	mic	mic	mic	mic
	a3	mic	mic	mic	mic	mic	–	–	–	–
	m2	mac	mac	mac	mac	mac	mac	mac	mic	mac
	m3	mac	mac	mac	mic	mac	mac	mac	mic	mac
	a5	mic	mic	mic	mic	mic	mac	mac	–	–
	m5	mac	mac	mac	mic	mac	–	mic	–	mac
	a6	mic	mic	mic	mic	mic	mic	mic	–	mic
	p1	mic	mic	mic	mic	mic	mic	mic	mic	mic
	p2	–	–	–	–	–	–	–	mic	–
	p3	mic	mic	mic	mic	mic	mic	mic	–	mic
	p4	mic	mic	mic	mic	mic	mic	–	mic	mic
	p5	mic	mic	mic	mic	mic	mic	–	–	–
	ap6	mic	mic	mic	mic	mic	mic	mac	mic	mic

Notes: *S. un*: *Sinhomidia uniseta* sp. nov.; *H. q*: *Homidia quadriseta* Pan, 2018; *H. j*: *Homidia jordanai* Pan et al., 2011; *S.um*: *Sinella umesaoi* Yosii, 1940; *S. b*: *Seira barnadi* (Womersley, 1934); *O. f*: *Orchesella flavescens* (Bourlet, 1839); *H. n*: *Heteromurus nitidus* (Templeton, 1836); *E. m*: *Entomobryoides myrmecophila* (Reuter, 1884); *P. a*: *Pseudosinella alba* (Packard, 1873); -: absent; ?: unclear (*H. q* refer to Zhuo et al. 2018; *H. j* refer to Pan et al. 2011; *S. um* and *S. b* refer to Zhang and Deharveng 2015; other four species refer to Szeptycki 1979).

Phylogeny supports this close similarity (Zhang et al. 2014a, b, 2016, Zhang and Deharveng 2015, Ding et al. 2019). Here, we show that chaetotaxy of the first instar larva is also more similar between *Sinhomidia* and *Homidia* than between *Sinhomidia* and the species of the other six genera within family Entomobryidae where it has been described, including the number, morphology and relative location of primary tergal chaetae (Tab. 2).

These two genera differ nevertheless by several characters, such as scales (present in *Sinhomidia* versus absent in *Homidia*) (Figs 6–8), number of guard chaetae on labial papilla E (3 in *Sinhomidia* versus 4 in *Homidia*) (Fig. 19), bothriotrichal complex (slightly modified accessory mic of *Sinhomidia* versus not modified in *Homidia*) (Fig. 7), the relative position of posterior mac (p series) of Th. II–III (close to m series in *Sinhomidia*, versus close to posterior margin in *Homidia*) (Fig. 21), the number of mac on the dorsal side of Abd. I (3–5 in *Sinhomidia* versus 9–11 in *Homidia*), and length ratio Abd. IV/Abd. III (11–15 in the new species, but less than 10 times in *Homidia,* generally) (Zhang et al. 2009, Pan et al. 2011, Pan and Shi 2015, Jin et al. 2017, Zhuo et al. 2018).

Are scales present on appendages of *Sinhomidia*?

Scales are intuitively considered to have evolved from ordinary chaetae, present in many species, and are important diagnostic characters for classification at the subfamilial and tribal levels of the family Entomobryidae. The tribe Willowsiini is well defined by the absence of dental scales (Zhang et al. 2009). However, the presence or absence of body scales for classification is not valid for Willowsiini (Zhang et al. 2014a). *Sinhomidia* is a

member of Willowsiini by the absence of scales on dens, and differs from other genera by its dental spines. Two recorded species of *Sinhomidia* and the new species described here are consistent in the morphology of the scales and tip pointed and fusiform with coarse striations, but they do not agree well between them in whether the scales are present on appendages. They are present on appendages of *S. bicolor* and the new species, but absent on *S. guangxiensis* (Zhang et al. 2009, Jin et al. 2017). Referring to the examined specimens of the new species, a few scales are present on the basal segments of antennae and legs, and ventral side of manubrium; furthermore, scales on the manubrium are narrower and longer than on the dorsal side of the terga, and similar to normal chaetae (Fig. 8). Additionally, scales easily fall off after clearing, and their sockets are difficult to distinguish from those of normal chaetae when checked by light microscope. To confirm if *Sinhomidia* has scales present on appendages in all species, it would be necessary to check the holotype of *S. guangxiensis*.

Key to the species of genus *Sinhomidia*

1 Abd. I entirely dark pigmented, Abd. IV with a middle dark band, claw with 4 inner teeth, labial chaeta M doubled **2**

– Abd. I with posterior margin dark pigmented, Abd. IV without middle dark band, claw with 3 inner teeth, labial chaeta M undoubled ..... ***S. uniseta* sp. nov.**

2 Head with lateral dark stripes, chaetae a2 and a5 absent on Abd. I ..... ***S. bicolor***

– Head without lateral dark stripes, chaetae a2 and a5 present on Abd. I ..... ***S. guangxiensis***

Acknowledgements

This study was supported by the National Natural Science Foundation of China (36101880) and Zhejiang Provincial Natural Science Foundation of China (LY15C040001). Also, thanks given to Professor Shidi SHI who provided comments on this manuscript.

References

Ding YH, Yu DY, Guo WB, Li JN, Zhang F (2019) Molecular phylogeny of *Entomobrya* (Collembola: Entomobryidae) from China: Color pattern groups and multiple origins. Insect Science 26(3): 587–597. https://doi.org/10.1111/1744-7917.12559

Fjellberg A (1998) The labial palp in Collembola. Zoologischer Anzeiger 237(4): 309–330.

Gisin H (1967) Espèces nouvelles at lignées évolutives de *Pseudosinella* endogés (Collembola). Memórias e Estudos do Museu Zoológico da Universidade de Coimbra 301: 5–25.

Jin H, Jia SB, Yan HC, Jordana R (2017) A new species of the Chinese endemic genus *Sinhomidia* (Collembola: Entomobryidae) described and the first description of a male of *Sinhomidia bicolor*. Zootaxa 4358(3): 569–576. https://doi.org/10.11646/zootaxa.4358.3.10

Ma YT, Pan ZX (2017) Two new species of *Homidia* (Collembola: Entomobryidae) from Southwestern China. Zootaxa 4290(3): 519–530. https://doi.org/10.11646/zootaxa.4290.3.6

Pan ZX, Shi SD, Zhang F (2011) New species of *Homidia* (Collembola, Entomobryidae) from eastern China with description of the first instar larvae. ZooKeys 152: 21–42. https://doi.org/10.3897/zookeys.152.1455

Pan ZX, Shi SD (2015) Description of a new *Homidia* species (Collembola: Entomobryidae) with labial chaetae expanded. Entomotaxonomia 37(3): 161–170.

Szeptycki A (1973) North Korean Collembola. I. The genus *Homidia* Börner, 1906 (Entomobryidae). Acta Zoologica Cracoviensia 31(2): 23–39.

Szeptycki A (1979) Morpho-systematic studies on Collembola. IV. Chaetotaxy of the Entomobryidae and its phylogenetical significance. Polska Akademia Nauk, Kraków, 219 pp.

Yosii R (1965) On some Collembola of Japan and adjacent countries. Contributions from the Biological Laboratory Kyoto University 19: 1–71.

Zhang F, Deharveng L, Greensland P, Chen JX (2009) Revision of *Acanthocyrtus* (Collembola: Entomobryidae) with description of a new genus from eastern Asia. Zoological Journal of the Linnean Society 157: 495–514. https://doi.org/10.1111/j.1096-3642.2008.00521.x

Zhang F, Chen Z, Dong RR, Deharveng L, Stevens MI, Huang YH, Zhu CD (2014a) Molecular phylogeny reveals independent origins of body scales in Entomobryidae (Hexapoda: Collembola). Molecular Phylogenetics and Evolution 70: 231–239. https://doi.org/10.1016/j.ympev.2013.09.024

Zhang F, Bedos A, Deharveng L (2014b) Disjunct distribution of *Szeptyckiella* gen. nov. from New Caledonia and South China undermines the monophyly of Willowsiini (Collembola: Entomobryidae). Journal of Natural History 48(21–22): 1299–1317. https://doi.org/10.1080/00222933.2013.859317

Zhang F, Deharveng L (2015) Systematic revision of Entomobryidae (Collembola) by integrating molecular and new morphological evidence. Zoologica Scripta 44(3): 298–311. https://doi.org/10.1111/zsc.12100

Zhang F, Pan ZX, Wu J, Ding YH, Yu DY, Wang BX (2016) Dental scales could occur in all scaled subfamilies of Entomobryidae (Collembola): new definition of Entomobryinae with description of a new genus and three new species. Invertebrate systematics 30(6): 598–615. https://doi.org/10.1071/IS16005

Zhang F, Sun DD, Yu DY, Wang BX (2015) Molecular phylogeny supports S-chaetae as a key character better than jumping organs and body scales in classification of Entomobryoidea (Collembola). Scientific Reports 5: 12471. https://doi.org/10.1038/srep12471

Zhuo PL, Si CC, Shi SD, Pan ZX (2018) Description of a new species and the first instar larvae of *Homidia* (Collembola: Entomobryidae) from Taizhou, Zhejiang Province. Entomotaxonomia 40(2): 148–157.

ZooKeys 872: 57–68 (2019)
doi: 10.3897/zookeys.872.34278
http://zookeys.pensoft.net

RESEARCH ARTICLE

A peer-reviewed open-access journal
ZooKeys
Launched to accelerate biodiversity research

When barcoding fails: development of diagnostic nuclear markers for the sibling caddisfly species *Sericostoma personatum* (Spence in Kirby & Spence, 1826) and *Sericostoma flavicorne* Schneider, 1845

Sonja Darschnik[1], Florian Leese[1,2], Martina Weiss[1,2], Hannah Weigand[1,3]

1 *Aquatic Ecosystem Research, Faculty of Biology, University of Duisburg-Essen, Essen, Germany* **2** *Centre for Aquatic and Environmental Research (ZWU), University of Duisburg-Essen, Essen, Germany* **3** *Musée National d'Histoire Naturelle, Luxembourg, Luxembourg*

Corresponding author: *Florian Leese* (florian.leese@uni-due.de)

Academic editor: *Ana Previšić* | Received 4 March 2019 | Accepted 14 May 2019 | Published 20 August 2019

http://zoobank.org/05EA1F60-A3F4-4F41-A7CB-6FAD040C55E9

Citation: Darschnik S, Leese F, Weiss M, Weigand H (2019) When barcoding fails: development of diagnostic nuclear markers for the sibling caddisfly species *Sericostoma personatum* (Spence in Kirby & Spence, 1826) and *Sericostoma flavicorne* Schneider, 1845. ZooKeys 782: 57–68. https://doi.org/10.3897/zookeys.872.34278

Abstract

The larval stages of the central European sibling caddisfly species *Sericostoma personatum* (Spence in Kirby and Spence, 1826) and *S. flavicorne* Schneider, 1845 are morphologically similar and can only be distinguished by differences in coloration in late larval instars. Identification using the mitochondrial barcoding gene, i.e., the Cytochrome c Oxidase 1, is impossible, as both species share the same highly differentiated haplotypes due to introgression. Nuclear gene markers obtained through double digest restriction site associate sequencing (ddRAD seq), however, can reliably distinguish both species, yet the method is expensive as well as time-consuming and therefore not practicable for species determination. To facilitate accurate species identification without sequencing genome-wide markers, we developed nine diagnostic nuclear RFLP markers based on ddRAD seq data. The markers were successfully tested on geographically distinct populations of the two *Sericostoma* species in western Germany, on known hybrids, and on another sericostomatid caddisfly species, *Oecismus monedula* (Hagen, 1859) that sometimes shares the habitat and can be morphologically confounded with *Sericostoma*. We describe a simple and fast protocol for reliable species identification of *S. personatum* and *S. flavicorne* independent of the life cycle stage of the specimens.

Keywords

Freshwater biodiversity, molecular species identification, RFLP, Sericostomatidae, Trichoptera

Introduction

Macroinvertebrate species are important indicators for the ecological status and water quality of freshwater ecosystems. Correct taxa lists are the basis for bioassessments and hence reliable tools for taxonomic identification of species are essential. However, reliable morphological species identification can be difficult or impossible, especially for closely-related species or early larval stages, because diagnostic characters are lacking or not yet visible. To deal with this problem, DNA-based methods have been developed for species identification, i.e., DNA barcoding (Hebert et al. 2003). Here, species identification is based on comparing sequences of standardized marker genes, in the case of macroinvertebrates typically the mitochondrial Cytochrome c Oxidase 1 gene (CO1), with a reference database. However, using only mitochondrial genes can lead to wrong species delimitation when speciation has occurred relatively recently and rapidly (e.g. Schlick-Steiner et al. 2010; Weiss et al. 2018) or when incomplete lineage sorting (Toews and Brelsford 2012), hybridization and introgression (e.g. Weigand et al. 2017), or selection on maternally inherited traits (Toews et al. 2014; Morales et al. 2015) has led to mito-nuclear discordance patterns.

One taxon that is typically considered in freshwater ecosystem monitoring is the caddisfly family Sericostomatidae (Pitsch 1993; Neu 2018). However, morphological identification in this family is problematic for many species because morphological traits can be very similar between, or highly variable within species, resulting in uncertainties concerning the number of species (Malicky 2005). One example are the two central European sibling caddisfly species *Sericostoma personatum* (Spence in Kirby & Spence, 1826) and *S. flavicorne* Schneider, 1845 (Schmidtke and Brandt 1995; Leese and Wagner 2005; Weigand et al. 2017). Both species are morphologically very similar, yet adults can be typically distinguished by sexual organs and by size differences in the maxilliary palps of males (Malicky 2005). Also, whether the name *S. flavicorne* used here should actually be applied only to a species found in Turkey (Sipahiler 2000) and the central European one should be referred to as *S. schneideri* (Botosaneanu, 2001) cannot be solved. Therefore, we stick to the taxonomic assignment proposed by Malicky (2005) calling the species *S. flavicorne*. Larvae might be discriminated at late larval stages based on mesonotum coloration (Weigand et al. 2017; Neu 2018). Furthermore, conflicting patterns between morphological and mitochondrial data concerning species identity were found (Leese and Wagner 2005) and raised the question if morphospecies or mitochondrial lineages represent valid species. To answer that question, Weigand et al. (2017) analyzed genome-wide nuclear single nucleotide polymorphisms (SNPs) for the two *Sericostoma* sister species in Germany obtained by double digest restriction site associated DNA sequencing (ddRAD seq, Peterson et al. 2012). They also compared results to morphometric traits and CO1 sequences. The analysis revealed that there are two distinct nuclear clusters corresponding to the morphospecies, whereas mitochondrial lineages did not match this pattern, as several haplotypes were shared between the nuclear clusters. Historical introgression and repeated ongoing hybridization among the two sibling species were assumed to be the causes for the mito-nuclear discordance pattern. Yet, the distinct nuclear clusters of specimens occurring in sympatry with only occasional F1 and F2 hybrids (Weigand et al. 2017) suggest that both morphospecies represent two distinctly evolving entities.

While the two species are not assessed individually in current biodiversity assessments of streams because of the difficulty to distinguish them, it is known that they differ in their ecological requirements (Pitsch 1993). Hence, a method allowing to discriminate the two species would improve bioassessment, especially when late larval stages and adults are not available. As traditional DNA barcoding fails to distinguish *S. personatum* and *S. flavicorne* and ddRAD seq is too expensive and time-consuming outside scientific research projects, an alternative delimitation method is needed for routine analyses. One fast, reliable and cheap candidate method is the use of diagnostic restriction fragment length polymorphism (RFLP) markers. The method is based on fixed sequence differences between species in palindromic recognition sites for restriction enzymes so that only the DNA of one species contains the recognition site. After detecting these diagnostic differences, corresponding regions are amplified via PCR, digested with chosen restriction enzymes and fragment lengths can be analyzed using agarose gel electrophoresis, thereby omitting sequencing and speeding up species identification. In this study, we developed a set of nine diagnostic RFLP markers using the nuclear ddRAD seq data as well as the draft genome from Weigand et al. (2017). To assess their reliability and performance for the identification of *S. flavicorne*/*personatum* in Germany, the markers were tested in single and multiplex reactions with samples from two different geographic regions. Additionally, the markers were tested for *Oecismus monedula* (Hagen, 1859), which often co-occurs in the stream habitats and can be mis-identified as *Sericostoma*, especially in early larval stages and when coloring is ambiguous.

Materials and methods

Identification of diagnostic markers

For identification of diagnostic RFLP markers, the ddRAD seq data from Weigand et al. (2017) were used. As ddRAD data and data from the current study originated only from few geographically restricted regions in Germany and no type material was included, the species affiliation to *S. flavicorne* and *S. personatum* may be erroneous (Botosaneanu 2001, Sipahiler 2000). However, it reflects the species hypothesis that is best supported at the moment (Malicky 2005, Neu 2018). For better readability, we will hence refer to the two genetically differentiated species found in Central Germany throughout the article as *S. flavicorne* and *S. personatum*.

As a first step, loci present in at least 50% of all individuals were tested for fixed single nucleotide polymorphisms (SNPs), i.e., diagnostic markers, between the two *Sericostoma* species. The respective scaffolds were extracted from the draft genome. For 217 loci, the sequences were checked for the presence of a palindromic restriction enzyme recognition site at the fixed, diagnostic SNPs. Three restriction enzyme motifs occurring frequently in the analyzed subsets were EcoRV (GATATC), NdeI (CATATG), and PvuII (CAGCTG), respectively. We used in-house python scripts (available on request) to check for the presence of diagnostic sites in the remaining loci with fixed SNPs. Subsequently, primers for amplification of regions containing the selected SNPs were designed with Geneious 6.0.6 (Biomatters Ltd). To enable the later multiplexing of different markers, the primers were chosen to

result in (i) different fragment lengths of the undigested fragments and (ii) different fragment lengths of the digested fragments for markers cut by the same restriction enzyme.

In a final step, the primer sequences were checked for the potential amplification of multiple fragments. Hence, they were mapped against the *Sericostoma* genome (GenBank accession NCQO00000000.1) using the blastn megablast algorithm (Altschul et al. 1990) and primer pairs with multiple hits were excluded from the test set.

Samples

To test the reliability and performance of the potential markers, 80 *Sericostoma* sp. specimens from 17 locations from two different regions in Germany were investigated. Additionally, markers were tested for four *Oecismus monedula* specimens. A detailed list of locations is given in Table 1. Specimens collected in 2013 and 2014 were those studied by Weigand et al. (2017). All specimens were morphologically determined at least to genus level, while samples of 2013, 2014 and 2017 were determined by SD and HW to species level using the diagnostic criteria outlined in Weigand et al. (2017). Samples were stored in 96% Ethanol prior to extraction.

DNA extraction and genus assignment

DNA was extracted using two different protocols: For samples collected in 2018, tissue was taken from legs and thoracic muscle and DNA extracted following a Chelex-based extraction protocol, by incubating tissue samples in 150 µl 10% (w/v) Chelex 100 (Bio-Rad) at 95 °C for 15 minutes in total, vortexing the samples every 5 minutes. For samples from 2013, 2014, and 2017, tissue was taken from the abdomen of specimens. To avoid contamination, gut content was removed before extraction. DNA was extracted according to a salt precipitation protocol (Weiss and Leese 2016) and DNA was eluted in TE minimum or deionized water and stored at 4 °C. For comparison of extraction methods, six samples of 2018 were additionally extracted with the salt precipitation protocol (see Table 1). Assignment of specimens to *S. personatum*/*flavicorne*, or respectively *O. monedula*, was verified by CO1 barcoding. The CO1 gene fragment was amplified via polymerase chain reaction (PCR) using forward primer LCO_mod (5'-TTC TAC AAA TCA TAA AGA TAT TGG AAC -3') and reverse primer FL_rueck1 (5'- TAA GCTCGG GTA TCA ACG TCT AT -3'; Leese 2004, modified after Folmer et al. 1994). PCR for each sample was performed in a 25 µl reaction volume with 1× PCR buffer, 0.2 mM dNTPs, 0.5 µM of each primer, 0.008 U/µl VWR Taq DNA-Polymerase (VWR), and 1 µl of DNA template. Standard thermal cycling conditions were used for CO1 amplification (initial denaturation at 94 °C for 2 min; 38 cycles of 20 s at 94 °C, 30 s at 46 °C, 60 s at 72 °C, and final extension at 72 °C for 5 min). The obtained PCR products were purified as described in Weiss and Leese (2016) and bidirectionally sequenced at GATC-Biotech AG (Cologne, Germany).

Table 1. Overview of sampling sites, number of analyzed specimens per site, DNA extraction method used (SaPr = salt precipitation and/or CH = Chelex), and morphological identification level.

Site	Stream	Coordinates [N/E]	Geographical region	Year	Number of samples	Extraction method	Identification level
Svb	Silvertbach	51.644583 7.230139	North Rhine-Westphalia	2017	7	SaPr	species
D	Diemel	51.420806 8.808667	North Rhine-Westphalia	2017	7	SaPr	species
V	Volme	51.241611 7.531167	North Rhine-Westphalia	2017	2	SaPr	species
1OW	Tributary Lüderbach	50.475897 9.295219	Hesse	2018	5 + 1 *O. monedula*	CH	genus
2KS	Tributary Rammholzer Wasser	50.331768 9.619321	Hesse	2018	5 + 3 *O. monedula*	all samples with CH, 2 *O. monedula* also with SaPr	genus
3OE	Tributary Lohrbach	50.116317 9.462612	Hesse	2018	7	all samples with CH, 2 *Sericostoma* also with SaPr	genus
2OS	Schmale Sinn	50.33576 9.696705	Hesse	2018	6	all samples with CH, 2 *Sericostoma* also with SaPr	genus
Han	Hannebecke	51.30635 8.41007	North Rhine-Westphalia	2014	1	SaPr	species
Val	Valme	51.31553 8.40354	North Rhine-Westphalia	2014	2	SaPr	species
Nie	Nier	51.31380 8.35892	North Rhine-Westphalia	2014	4	SaPr	species
Bra	Brabecke	51.29762 8.40043	North Rhine-Westphalia	2014	3	SaPr	species
Nes	Nesselbach	51.17494 8.41878	North Rhine-Westphalia	2014	3	SaPr	species
Roe	Röhr	51.27247 8.05820	North Rhine-Westphalia	2014	7 + 1 hybrid	SaPr	species
Sch	Schwarze Ahe	51.20499 7.72184	North Rhine-Westphalia	2014	3	SaPr	species
Kru	Krummenau	51.07383 7.71277	North Rhine-Westphalia	2014	9 + 2 hybrids	SaPr	species
Sor	Sorpe	51.19883 8.42851	North Rhine-Westphalia	2013	3	SaPr	species
Sil	Silberbach	51.03180 8.05244	North Rhine-Westphalia	2014	3	SaPr	species

RFLP marker PCR

For RFLP marker validation, a PCR amplification was carried out for all developed primer pairs in separate reactions for 39 samples. Primers are listed in Table 2. Each PCR amplification was conducted in 25 µl reaction volumes with the QIAGEN Multiplex PCR Plus Kit, using 1x MasterMix, 0.5 µM of each primer, and 1 µl of template DNA. Thermal cycler settings were identical for all nine primer pairs (initial denaturation 5 min at 95 °C; 40 cycles of 30 s at 95 °C, 90 s at 50 °C, 90 s at 72 °C, and final extension for 10 min at 65 °C). Amplification success was verified on 1% TBE agarose gels. Subsequently, primers were also tested in multiplex reactions for 58 samples to facilitate the process and make species identification as fast and cheap as possible. When multiplexing, primer pairs EcoRV1 and EcoRV4, EcoRV2 and EcoRV5, NdeI1 and NdeI4, as well as NdeI5 and NdeI8 were combined to avoid overlapping of bands with equal sizes in the agarose gel. The PCR protocol remained the same, primer concentration was 0.5 µM for all primers individually, and the amount of deionized water was reduced accordingly. For the enzyme PvuII only one RFLP primer pair was chosen, hence, no multiplexing was possible.

Table 2. List of primers with corresponding restriction enzymes and expected fragment sizes for *S. flavicorne* (Sf) and *S. personatum* (Sp).

Enzyme	Primer name	Primer sequence (5'-3')	T_m [°C]	Species with restriction site	Fragment size *Sf* [bp]	Fragment size *Sp* [bp]
EcoRV	EcoRV1_fw	GTGCTTCTGTCCTGTTATTC	54.0	Sp	397	229
	EcoRV1_re	TTCAAACTTGCAAAAATGCC	54.1			168
	EcoRV2_fw	AAAGAGGCGATTAACTTTCG	54.0	Sp	542	165
	EcoRV2_re	CACATTATGAACACCACACA	53.8			377
	EcoRV4_fw	AATCACTAAAACTGCCAACC	54.1	Sp	739	217
	EcoRV4_re	CTTGTACCCGTTATCGAGAG	55.1			522
	EcoRV5_fw	GAGTTCTGATCCTGTTTGTG	54.0	Sp	470	129
	EcoRV5_re	TGGCCTAGCTCAATAAATGA	54.1			341
NdeI	NdeI1_fw	TCTTCTGGTTCTAGGGAAAA	54.1	Sp	667	354
	NdeI1_re	ACGAAGACTGAACTCTCAAT	53.2			313
	NdeI4_fw	TCAGCATGACAGGTGAATAT	54.1	Sf	302	440
	NdeI4_re	ACAAAATGAGGCAAGTGAAT	54.0		138	
	NdeI5_fw	TGTTTGATGGATTCCTCAGA	54.0	Sf	379	547
	NdeI5_re	TGCCTCTCATCCTATTGATC	54.0		168	
	NdeI8_fw	TTATTCGCGCCATACTTTAC	53.9	Sf	455	761
	NdeI8_re	ATGGTCTTACCCGTTTAGAG	54.2		306	
PvuII	PvuII2_fw	GCATAACCGACAATGTGTAA	54.0	Sf	564	876
	PvuII2_re	CTAGCTCATTTCCTTTGTGG	54.0		312	

Enzymatic digestion and species determination

All PCR products were digested with the respective enzymes in 30 µl reaction volumes as follows: 10 µl of unpurified PCR product, 2 µl of Green Buffer (to directly load digested PCR products on agarose gels), 1 µl of either FastDigest Eco321 (isoschizomer or EcoRV), FastDigest NdeI or FastDigest PvuII (all Thermo Scientific), and 17 µl deionized water. Incubation was conducted at 37 °C for 5 min for Eco321 and PvuII, and for 60 min for NdeI. Digested PCR products were visualized on 2% TBE agarose gels and compared to a 100 to 1000 bp ladder to determine the size of the fragments. Species were identified by comparing the resulting patterns to the expected fragment lengths (Table 2).

Results

Amplification success differed slightly between candidate markers. Generally, the success rate was high for all tested single and multiplex reactions (Suppl. material 1, Table S1) with primer pairs NdeI5 and PvuII2 showing greatest success of 98.9% (n = 92) across all samples analyzed and NdeI8 showing lowest success rate of 69.2% (n = 94). NdeI8 worked much better in single reactions (89.7%; n = 29) than in multiplex reactions (60.0%; n = 65), which explains its overall lower success rate. The extraction method (Chelex or salt precipitation) did not noticeably influence the success rate. However, visualization of restricted fragments from Chelex extractions resulted in weaker bands than from salt-extracted samples, but the bands were distinctive with both methods (Suppl. material 2, Fig. S1). Further, no evidence for amplification bias between the different sampling regions was found.

A schematic overview of the band patterns predicted after the primer design for both species is shown in Fig. 1. This pattern was supported by laboratory tests. In the following, fragment patterns for the different multiplexed markers plus the single marker PvuII2 are described for both species, and the corresponding fragment lengths are given in Fig. 1. For EcoRV1&4 *S. flavicorne* had uncut fragments for both markers, while four cut fragments were visible for *S. personatum*. A similar pattern was generated with EcoRV2&5. NdeI5&8 generated an inverted pattern, with two intact amplicons for *S. personatum* and four cut fragments for *S. flavicorne*. An intermediate picture was obtained by NdeI1&4, where in *S. flavicorne* NdeI1 remained uncut, while NdeI4 was cut in two fragments. In contrast, for *S. personatum* NdeI4 remained uncut and NdeI1 was cut respectively. Lastly, PvuII2 did not cut in *S. personatum*, but in *S. flavicorne*. For restrictions with FastDigest NdeI, incomplete digestion was observed sometimes, meaning that bands of the original length were still slightly visible on the agarose gel in addition to the expected smaller cut fragments. For three specimens originating from three different streams (Nier, Brabecke and Sorpe), the EcoRV5 primer pair produced a fragment that was about 200 bp shorter than the expected 470 bp.

When the PCR amplification was successful, enzymatic restriction and species assignment based on the resulting fragment patterns was successful for all *S. flavicorne/personatum* individuals, i.e., all 38 individuals (excluding hybrids) previously identified to species level by ddRAD seq (Weigand et al. 2017) could be unequivocally identified. For each of the 16 individuals identified morphologically (2017 samples) using the criteria by Weigand et al. (2017), the RFLP assignment patterns confirmed the morphological identification.

For the four tested *O. monedula* specimens, PCR was successful only for four primer pairs (EcoRV1, EcoRV2, EcoRV4 and PvuII2): For the PvuII2 primer pair a product of ~550 bp was visible when amplified from two of the samples additionally extracted by salt precipitation, while no product was visible when amplified from Chelex extraction (4 individuals). EcoRV1 yielded a fragment of ~900 bp in single marker assessment that was not visible in multiplex tests. In general, bands on the agarose gels were faint in single marker assessment and barely visible in multiplex approaches. EcoRV2 yielded the same pattern after restriction as expected for *S. flavicorne* while EcoRV4 created the same pattern as specimens of *S. personatum*.

The three tested hybrids amplified for all markers but created intermediate results after restriction (Suppl. material 2, Fig. S2). Two hybrids (H2 and H3) were F1 hybrids and the third specimen (H1) was a backcross individual with *S. personatum* according to Weigand et al. (2017). For EcoRV1&2, NdeI1&4 and NdeI5&8 markers, restriction yielded multiband patterns not indicating either of the species, but uncut and cut fragments were present in the same samples, indicating heterozygosity in the hybrid samples. The combination of EcoRV2&5 and PvuII2 indicate the pattern for *S. flavicorne* for H2, but again create multiband patterns for the other two samples. For PvuII2 the pattern created also an additional band at ~950 bp for H1 and H3, which is not expected for any of the species. As expected from the ddRAD data, the inconclusive patterns created here, indicated that the specimens were neither *S. personatum* nor *S. flavicorne*, but rather a hybrid between both.

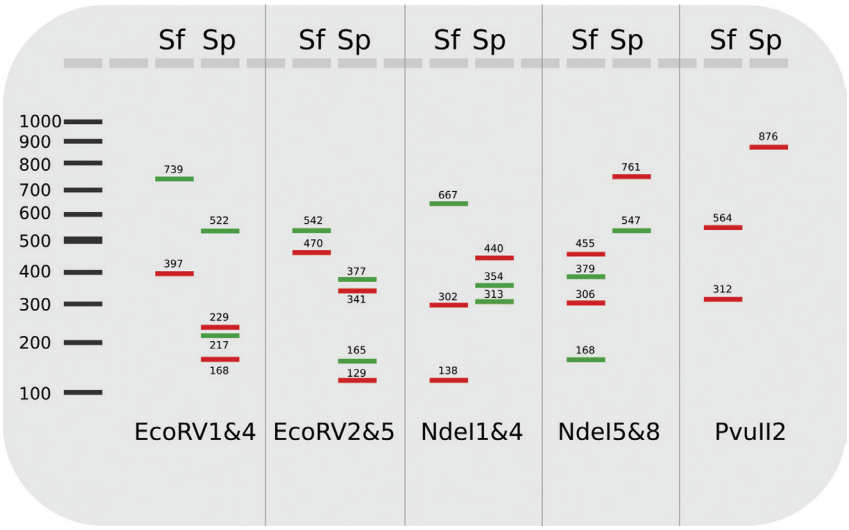

Figure 1. Schematic overview of the different multiplex and single RFLP fingerprints for *S. flavicorne* (Sf) and *S. personatum* (Sp). Fragment lengths are given above/below bands. Red: EcoRV1, EcoRV5, NdeI4, NdeI8, and PvuII2; Green: EcoRV4, EcoRV2, NdeI1, NdeI5.

Discussion

In this study, we developed and tested nine RFLP markers to distinguish the two sibling caddisfly species *S. flavicorne* and *S. personatum* in Germany, which cannot be identified using COI barcoding. An advantage of the RFLP approach is that no sequencing is required and thus species assignment is possible directly after PCR and a short restriction incubation, followed by simple agarose gel visualization. Since all primer pairs amplify with the same PCR settings, all markers can be tested in simultaneous reactions, with the possibility of multiplexing two primer pairs each.

Different factors can impact on the identification success of the RFLP markers. First, good amplification success for the correct amplicons in the PCR is needed to enable subsequent restriction digestion. We found high success rates of ≥ 90% for all single reactions and ≥ 80% for all multiplex reactions, with the exception of NdeI8 (only 60%). For three individuals, an alternative, shorter fragment was amplified for EcoRV5, which might be caused by a local sequence variant. This phenomenon may increase in frequency when extending the geographic range (ascertainment bias). Second, the restriction enzymes need to digest the PCR fragments reliably. While this was the case for FastDigest Eco321 (Isoschizomer of EcoRV) and FastDigest PvuII, incomplete digestion was sometimes observed for FastDigest NdeI, even though incubation time was set to 60 min as advised by the manufacturer. Finally, the DNA extraction method should not influence the reliability of the results in order to provide a robust method for application in different laboratories. The two extraction methods tested here, i.e., the salt precipitation and the Chelex approach, did not systematically impact the amplification or restriction success. Still, DNA extracted with salt precipitation showed

stronger bands on the agarose gels after PCR and after restriction than Chelex extracted samples, indicating a lower yield of PCR products for Chelex extractions. Despite the lower output, the fragments were still successfully amplified. Hence, for a quick and inexpensive *S. personatum*/*flavicorne* identification, Chelex extraction is well-suited, since it is simpler, cheaper and especially much faster than most other extraction methods.

Besides the different technical aspects, we also tested if the RFLP method works for the target species across a broader geographic scale than used in the study of Weigand et al. (2017) (2013/2014 samples – max. distance: 55 km). Therefore, further samples from North Rhine-Westphalia were included (2013/2014 & 2017 samples – max. distance: 112 km), as well as samples from a second region in Germany, Hesse (min. distance to North Rhine-Westphalian samples: 99 km). Between the two regions and within North Rhine-Westphalia, no bias was detected in species identification. This indicates that the markers cannot only be used for species identification for the region in which the markers were developed (2013/2014 samples), but also for specimens from a broader geographical scale. However, we highly recommend to further test the markers with individuals previously identified morphologically or ideally identified using ddRAD seq, when analyzing specimens from other regions or countries.

As the study of Weigand et al. (2017) detected rare hybrids between the two *Sericostoma* species, we evaluated the possibility of misidentifying them as one of the parental species with the RFLP-markers. For the two F1 generation hybrids and the backcross with *S. personatum*, most of the markers showed a heterozygote pattern (meaning cut and uncut fragments per marker), which enables their clear distinction from the parental species. While these results are promising for hybrid detection, the sample size here was small (n=3) and thus results have to be interpreted cautiously.

In addition to *S. flavicorne*/*personatum*, we also tested our RFLP-markers with *O. monedula* samples. These species can co-occur in the streams and can be difficult to distinguish morphologically. In contrast to *S. personatum*/*flavicorne*, amplification success was low for *O. monedula*. No fragments were amplified for several markers, but with EcoRV2 the *S. flavicorne* and with EcoRV4 the *S. personatum* amplicon was generated. Furthermore, two markers (EcoRV1 and PvuII2) generated additional fragments for *O. monedula*, when the DNA was extracted via salt precipitation. These in general weak bands, were almost absent when using DNA from the Chelex extraction or when multiplexing markers. Hence, scoring only individuals successfully amplified for several markers with unambiguous species identification as well as excluding specimens with bands expected only for *O. monedula*, allows to clearly distinguish the two *Sericostoma* species from *O. monedula*. Individuals not fulfilling these criteria cannot be directly assigned to *O. monedula*, especially if only few markers amplify successfully. While the specific PCR products found for *O. monedula* may allow an unambiguous species identification of this species with our markers, our sample size of *O. monedula* is too low for any validation. We currently recommend the use of COI barcoding to clearly assign them to *O. monedula* as for this purpose DNA barcoding works reliably. It should also be noted that the proposed approach does not work for community-based DNA assessments (DNA metabarcoding) but only for individual specimen-based approaches and thus would inquire an additional analysis step.

In summary, the markers introduced in this study are an easy-to-use, cheap, and reliable alternative to CO1 barcoding for determining the problematic sister species *S. personatum* and *S. flavicorne*. They were applied with high amplification and restriction success rates per marker in single and multiplex approaches. The latter allows to halve material costs and reaction times (Zangenberg et al. 1999). By using several markers, reliable results can be obtained even if one primer pair fails to amplify as each marker creates clear and easily distinguishable patterns on its own. Additionally, the probable hybrids between the two *Sericostoma* species can only be clearly identified when using several markers. If for economic reasons only a subset of the here presented markers should be applied, we recommend to select the EcoRV RFLP markers and PvuII2, as they enable the identification of hybrids and the exclusion of *O. monedula* specimens in the dataset evaluated here.

It is important to note that the specimens tested herein only come from a small part of the total species range; therefore, the proven success of identification with the markers is limited to the regions tested. Supposedly, the method will give informative results in different areas as well, which remains to be established in the future.

Acknowledgments

We thank Ana Previšić, Simon Vitecek, and Jean-Luc Gattolliat for valuable remarks and suggestions that greatly improved the manuscript. Furthermore, we thank Cristina Hartmann-Fatu and Sandra Roeser (University of Duisburg-Essen) for laboratory assistance. FL and HW are members of and supported by COST Action CA15219 (DNAqua-Net).

References

Altschul SF, Gish W, Miller W, Myers EW, Lipman DJ (1990) Basic Local Alignment Search Tool. Journal of Molecular Biology 215(3): 403–410. https://doi.org/10.1016/S0022-2836(05)80360-2

Botosaneanu L (2001) *Sericostoma flavicorne* Schneider,1845 and *S. schneideri* Kolenati, 1848: two distinct species and the correct use of their names (Trich., Sericostomatidae).- Bulletin de la Société entomologique de France 106(5): 518–520.

Folmer O, Black M, Hoeh W, Lutz R, Vrijenhoek R (1994) DNA primers for amplification of mitochondrial Cytochrome c Oxidase Subunit I from diverse metazoan invertebrates. Molecular Marine Biology and Biotechnology 3(5): 294–299.

Hagen HA (1859) Die Phryganiden Pictet's. Nach Typen bearbeitet. Entomologische Zeitung des Entomologischen Verein zu Stettin 20: 131–170.

Hebert PDN, Cywinska A, Ball SL, deWaard JD (2003) Biological identifications through DNA Barcodes. Proceedings of the Royal Society B: Biological Sciences 270(1512): 313–321. https://doi.org/10.1098/rspb.2002.2218

Kirby W, Spence W (1826) An introduction to entomology: Or Elements of the Natural History of Insects: With Plates. Longman, Rees, Orme, Brown, and Green, London,1818–26.

Leese F, Wagner R (2005) The "*Sericostoma*-Problem" – Molecular genetic, chemotaxonomic, and autecological approaches (Trichoptera: Sericostomatidae). Lauterbornia 54: 161–63.

Leese F. (2004) Molecular genetic, chemotaxonomic, and autecological investigations of European Sericostomatidae (Insecta: Trichoptera). PhD Thesis, Ruhr-Universität Bochum, Bochum.

Malicky H (2005) Ein kommentiertes Verzeichnis der Köcherfliegen (Trichoptera) Europas und des Mediterrangebietes. Linzer biologische Beiträge 37(1): 533–596.

Morales HE, Pavlova A, Joseph L, Sunnucks P (2015) Positive and purifying selection in mitochondrial genomes of a bird with mito-nuclear discordance. Molecular Ecology 24(11): 2820–2837. https://doi.org/10.1111/mec.13203

Neu PJ (2018) Trichoptera-RP – die Köcherfliegenseiten von P. J. Neu. Informationen zu Ökologie, Taxonomie und Verbreitung der Köcherfliegen in Deutschland. http://www.trichoptera-rp.de [accessed 02.02.2019]

Peterson BK, Weber JN, Kay EH, Fisher HS, Hoekstra HE (2012) Double Digest RADseq: An inexpensive method for de novo SNP discovery and genotyping in model and non-model species. PLoS ONE, 7(5). https://doi.org/10.1371/journal.pone.0037135

Pitsch T (1993) Zur Larvaltaxonomie, Faunistik und Ökologie mitteleuropäischer Fließwasser-Köcherfliegen (Insecta: Trichoptera). Schriftenreihe des Fachbereichs Landschaftsentwicklung Sonderheft S8: 322. http://dx.doi.org/10.14279/depositonce-4809

Schlick-Steiner BC, Steiner FM, Seifert B, Stauffer C, Christian E, Crozier RH (2010) Integrative taxonomy: A multisource approach to exploring biodiversity. Annual Review of Entomology 55(1): 421–438. https://doi.org/10.1146/annurev-ento-112408-085432

Schmidtke R, Brandt S (1995) Ökologische und chemotaxonomische Untersuchungen zur Arttrennung von *Sericostoma flavicorne* Schneider 1845 und *Sericostoma personatum* (Spence in Kirby & Spence 1826) (Trichoptera: Sericostomatidae). Lauterbornia 22: 69–83.

Schneider WG (1845) Verzeichnis der von Prof. Loew im Sommer 1842 in der Türkei und Klein-Asien gesammelten Neuropteren nebst kurzer Beschreibung der neuen Arten. Stettiner Entomologische Zeitung 6: 153-155.

Sipahiler F (2000) Redescription of *Sericostoma flavicorne* SCHNEIDER, 1845 and a new species of genus *Sericostoma* LATREILLE from Turkey (Trichoptera, Sericostomatidae). BRAUERIA (Lunz am See, Austria) 27: 23–25.

Toews DPL, Brelsford A (2012) The biogeography of mitochondrial and nuclear discordance in animals: biogeography of mito-nuclear discordance. Molecular Ecology 21(16): 3907–3930. https://doi.org/10.1111/j.1365-294X.2012.05664.x

Toews DPL, Mandic M, Richards JG, Irwin DE (2014) Migration, mitochondria, and the yellow-rumped warbler. Evolution 68(1): 241–255. https://doi.org/10.1111/evo.12260

Weigand H, Weiss M, Cai H, Li Y, Yu L, Zhang C, Leese F (2017) Deciphering the origin of mito-nuclear discordance in two sibling caddisfly species. Molecular Ecology 26(20): 5705–5715. https://doi.org/10.1111/mec.14292

Weiss M, Leese F (2016) Widely distributed and regionally isolated! Drivers of genetic structure in *Gammarus fossarum* in a human-impacted landscape. BMC Evolutionary Biology 16(1). https://doi.org/10.1186/s12862-016-0723-z

Weiss M, Weigand H, Weigand AM, Leese F (2018) Genome-wide single-nucleotide polymorphism data reveal cryptic species within cryptic freshwater snail species – the case of the *Ancylus fluviatilis* species complex. Ecology and Evolution 8(2): 1063–1072. https://doi.org/10.1002/ece3.3706

Zangenberg G, Saiki RK, Reynolds R (1999) Multiplex PCR. PCR Applications, 73–94. Elsevier. https://doi.org/10.1016/B978-012372185-3/50007-9

Supplementary material 1

Supplementary Table S1

Authors: Sonja Darschnik, Florian Leese, Martina Weiss, Hannah Weigand

Data type: molecular data

Explanation note: Overall amplification success (%) of primer pairs, multiplex, and single reaction approaches combined.

Link: https://doi.org/10.3897/zookeys.872.34278.suppl1

Supplementary material 2

Supplementary figures

Authors: Sonja Darschnik, Florian Leese, Martina Weiss, Hannah Weigand

Data type: molecular data

Explanation note: Figure S1 – three hybrid samples (H1, H2, H3) after restriction for all markers. Figure S2 – comparison of six samples (two of each *S. personatum*, *S. flavicorne* and *O. monedula*) with assessed with PvuII2 after restriction, salt extraction protocol on the left and Chelex extraction on the right.

Link: https://doi.org/10.3897/zookeys.872.34278.suppl2

ZooKeys 872: 69–75 (2019)
doi: 10.3897/zookeys.872.35378
http://zookeys.pensoft.net

RESEARCH ARTICLE

A peer-reviewed open-access journal
ZooKeys
Launched to accelerate biodiversity research

Chyromyidae (Diptera, Acalyptrata) of Turkey

M.J. Ebejer[1], M. Barták[2]

1 *Entomology Section, Department of Natural Sciences, National Museum of Wales, Cathays Park, Cardiff, UK*
2 *Department of Zoology and Fisheries, Faculty of Agrobiology, Food and Natural Resources, Czech University of Life Sciences Prague, Kamýcká 129, 165 00 Praha-Suchdol, Czech Republi*

Corresponding author: *M. Barták* (bartak@af.czu.cz)

Academic editor: *Rudolf Meier* | Received 11 April 2019 | Accepted 30 June 2019 | Published 20 August 2019

http://zoobank.org/8E3CAE13-B2F9-4F23-BD75-D480471D99E4

Citation: Ebejer MJ, Barták M (2019) Chyromyidae (Diptera, Acalyptrata) of Turkey. ZooKeys 872: 69–75. https://doi.org/10.3897/zookeys.872.35378

Abstract

The Chyromyidae of Turkey are reviewed and all 15 species known from the country are listed. The following are new records: *Chyromya miladae* Andersson, 1976, *Gymnochiromyia inermis* (Collin, 1933), *Aphaniosoma approximatum* Becker, 1903, *A. micromacro* Carles-Tolrá, 2001, *A. propinquans* Collin, 1949 and *A. proximum* Ebejer, 1998.

Keywords

Brachycera, faunistics, Schizophora, West Palaearctic

Introduction

The Chyromyidae is a poorly recorded family from several countries around the Mediterranean despite this family of acalyptrate Diptera being very diverse in this region. Until recently this family was poorly represented in most collections. Ebejer (2009) detailed what little is known about the biology and ecology of these flies.

A review of *Aphaniosoma* Becker, 1903 included some records and descriptions of four new species of this genus from Turkey (Ebejer 1998a). Each of two papers on *Gymnochiromyia* Hendel, 1933 added one new record of species in this genus (Ebejer 1998b, 2010). No other literature records of Chyromyidae from Turkey are known to us. In particular, it must be noted that there are no Chyromyidae known from the north, central, and eastern provinces of the country. There is likely to be an interest-

ing diversity probably enriched by species from Central Asia from where many species were described (Ebejer 2006). Species of *Aphaniosoma* have been found at high altitudes in Central Asia where the climatic and ecological conditions are rather different from those typical of the Mediterranean, but to some extent are similar to those in mountainous eastern Turkey. In this paper we collate what is known about Turkish Chyromyidae and add new records.

Materials and methods

Most of the new material presented in this paper originated from Muğla Province (Akyaka, Toparlar, Dalyan, and Muğla university campus). Akyaka (Fig. 1) represents a typical habitat for *Aphaniosoma*. It is a wet salty meadow, partly influenced by tides. However, this locality was severely destroyed after 2015 by agricultural and recreational development. The saline meadow at Dalyan remains relatively unaffected (farm and orchard sites are situated close to this wetland). A small proportion of specimens originates from Aydın Province (Çine) where specimens were collected from the banks of a river flowing out of a dam, ensuring year-round flow of water. Many other rivers in southern Turkey dry out in summer, supporting only very poor dipteran populations.

All species are listed below in alphabetical order under each subfamily and genus. Additional new data for each species are included where these are available and new records for Turkey are indicated. The material that has been examined for this paper was collected by M. Barták and Š. Kubík, unless otherwise stated, and by using yellow

Figure 1. Wetland in Akyaka, SW Turkey. The locality inhabited by the maximum number of Chyromyidae, ten species.

water pan traps (PN), hand held sweep nets (SW), and Malaise traps (MT). Depositories of specimens are in M. Barták collection, Czech University of Life Sciences, Prague, unless otherwise stated and given in parenthesis at the end of each data entry thus: **MJE** = M.J. Ebejer collection, Cowbridge, UK; **SMOC** = Silesian Museum Opava, Czech Republic.

Results

Aphaniosominae
Aphaniosoma **Becker, 1903**
Aphaniosoma approximatum **Becker, 1903**

Material examined. 7♂♂, Muğla Province, Akyaka, river bank, salty meadow, 37°03'16"N, 28°19'57"E, 16–27.v.2011; 1♂, same data (MJE).

This is the first confirmed record in the Mediterranean north of Egypt from where it was described. It is known from most of the Arabian Peninsula. Old records from Southern Europe and the Mediterranean are likely to refer to other similar species.

Aphaniosoma brevivittatum **Ebejer, 1995**

Recorded by Ebejer (1998a).

Material examined. 1♂, Akyaka, pasture, 6 m, SW, 37°03'19"N, 28°20'07"E, 28.iv–8.v.2013; 5♂♂, Akyaka, salty meadow, SW+PT, 37°12'45"N, 28°27'42"E, 28.iv–9.v.2013, (1♂, MJE); 2♂♂, Akyaka, pasture, 4 m, 37°03'09"N, 28°20'17"E, 8–14.ix.2014; 1♂1♀, Akyaka, pasture, 4 m, 37°03'09"N, 28°20'17"E, 13–14.ix.2014; 2♂♂, Akyaka, salty meadow, 2 m, 37°01'49"N, 28°20'01"E, 22.vi–1.vii.2015.

Aphaniosoma claridgei **Ebejer, 1995**

Recorded by Ebejer (1998a).

Material examined. 9♂♂7♀♀, Akyaka, river bank, salty meadow, 37°03'16"N, 28°19'57"E, 16–27.v.2011; 4♂♂1♀, Akyaka, pasture, 4 m, 37°03'08.9"N, 28°20'17.4"E, 16–22.ix.2012; 1♂, Akyaka, pasture, 4 m, 37°03'09"N, 28°20'17"E, 23–27.ix.2012; 1♀, Akyaka, salty meadow, SW+PT, 37°12'45"N, 28°27'42"E, 28.iv–9.v.2013; 2♀♀, Akyaka, salty meadow, SW+PT, 37°02'53"N, 28°19'39"E, 28.iv–9.v.2013; 3♂♂, Akyaka, salty meadow, 2 m, 37°01'49"N, 28°20'01"E, 22.vi–1.vii.2015; 1♀, 8 km S of Çine, river bank, 68 m, 37°32'34"N, 28°03'46"E, 29.iv–i.v.2016.

A very common and abundant species described from Greece but found in most of the countries around the Mediterranean.

Aphaniosoma impudens Ebejer, 1998

Described from Turkey. No new material has been examined.

Aphaniosoma melitense Ebejer, 1993

Recorded by Ebejer (1998a).

Material examined. 2♂♂4♀♀, Antalya, Manavgat, 3.5 km S, Titreyen lake, 1 m, 36°45'25"N, 31°27'19"E, 15.v.2011, J. Roháček (SMOC); 40♂♂12♀♀, Akyaka, river bank, salty meadow, 37°03'16"N, 28°19'57"E, 16–27.v.2011; 15♂♂6♀♀, Akyaka, pasture, 4 m, 37°03'08.9"N, 28°20'17.4"E, 16–22.ix.2012; 1♂1♀, Akyaka, salty meadow, 2 m, 37°03'N, 28°20'E, 23–27.ix.2012; 4♂♂2♀♀, Akyaka, pasture, 4 m, 37°03'09"N, 28°20'17"E, 23–27.ix.2012; 1♂, Akyaka, pasture, 6 m, SW, 37°03'19"N, 28°20'07"E, 28.iv–8.v.2013; 8♂♂, Akyaka, salty meadow, SW+PT, 37°12'45"N, 28°27'42"E, 28.iv–9.v.2013; 1♂1♀, Akyaka, salty meadow, SW+PT, 37°02'53"N, 28°19'39"E, 28.iv–9.v.2013; 3♂♂, Akyaka, pasture, 4 m, 37°03'09"N, 28°20'17"E, 8–14.ix.2014; 5♂♂3♀♀, Dalyan, orchard, 4 m, 36°49'37"N, 28°39'39"E, 11.ix.2014; 7♂♂1♀, Toparlar, lowland forest, 8 m, 36°59'27"N, 28°38'50"E, 11.ix.2014; 3♂♂, Akyaka, pasture, 4 m, YPWT, 37°03'09"N, 28°20'17"E, 13–14.ix.2014; 1♂, 8 km S of Çine, river bank, 68 m, 37°32'34"N, 28°03'46"E, 28–30.vi.2015; 12♂♂1♀, Akyaka, salty meadow, 2 m, 37°01'49"N, 28°20'01"E, 22.vi–1.vii.2015; 1♂2♀♀, Mugla, 730 m, university campus, MT, 37°09'19"N, 28°20'07"E, 5–19.viii.2015, H. Kavak; 1♂, Dalyan, farm, MT, 1 m, 36°48'54"N, 28°39'04"E, 8–20.viii.2015, Dursun; 1♀, Akyaka, 40 m, forest, SW, 37°03'19"N, 28°19'36"E, 26.iv.2016.

This common and often abundant species was described from Malta. It is known from most of the countries around the Mediterranean and reaches Britain.

Aphaniosoma micromacro Carles-Tolrá, 2001

Material examined. 1♂, Akyaka, pasture, 6 m, SW, 37°03'19"N, 28°20'07"E, 28.iv–8.v.2013.

This species was described from Spain. New record for Turkey.

Aphaniosoma necopinatum Ebejer, 1998

Described from Turkey. No new material has been examined.

***Aphaniosoma propinquans* Collin, 1949**

Material examined. 1♂1♀, Akyaka, river bank, salty meadow, 37°03'16"N, 28°19'57"E, 16–27.v.2011; 1♀, Akyaka, pasture, 6 m, SW, 37°03'19"N, 28°20'07"E, 28.iv–8.v.2013; 1♂, Akyaka, salty meadow, 37°02'53"N, 28°19'39"E, 28.iv–9.v.2013; 1♀, Akyaka, salty meadow, 37°12'45"N, 28°27'42"E, 28.iv–9.v.2013; 1♂1♀, 8 km S of Çine, river bank, 68 m, 37°32'34"N, 28°03'46"E, 28–30.vi.2015.

Described from Britain, this is a widespread and fairly common species. New record for Turkey.

***Aphaniosoma proximum* Ebejer, 1998**

Material examined. 1♂, Akyaka, pasture, 4 m, 37°03'08.9"N, 28°20'17.4"E, 16–22.ix.2012; 5♀♀, Akyaka, salty meadow, 2 m, 37°03'N, 28°20'E, 23–27.ix.2012; 1♀, Akyaka, salty meadow, SW+PT, 37°12'45"N, 28°27'42"E, 28.iv–9.v.2013; 1♂, Akyaka, pasture, 4 m, 37°03'09"N, 28°20'17"E, 8–14.ix.2014; 5♂♂1♀, Akyaka, salty meadow, 2 m, 37°01'49"N, 28°20'01"E, 22.vi–1.vii.2015.

A common and widespread species around the Mediterranean, extending as far as the United Arab Emirates. Sometimes found in large numbers. A new record for Turkey.

***Aphaniosoma scutellaris* Ebejer, 1998**

Described from Turkey, it has also been recorded from Germany.

***Aphaniosoma verecundum* Ebejer, 1998**

Described from Turkey.

Material examined. 1♀, Akyaka, pasture, 4 m, 37°03'08.9"N, 28°20'17.4"E, 16–22.ix.2012; 1♂2♀♀, Akyaka, salty meadow, 2 m, 37°01'49"N, 28°20'01"E, 22.vi–1.vii.2015; 1♀, Akyaka, salty meadow, 2 m, PT, 37°01'52"N, 28°20'00"E, 27.iv–1.v.2016.

Chyromyinae
***Chyromya* Robineau-Desvoidy, 1830**
***Chyromya miladae* Andersson, 1976**

Material examined. 1♀, Toparlar, lowland wood, 8 m, 36°59'27"N, 28°38'50"E, 22–24.vi.2015.

This species was described from the Czech Republic but it has been found in Britain, Switzerland, and Germany. A new record for Turkey.

Gymnochiromyia Hendel, 1933
Gymnochiromyia flavella (Zetterstedt, 1848)

Recorded by Ebejer (2010).

Material examined. 1♀, Antalya, Manavgat, 4.4 km S, Manavgat rivershore, 1 m, 36°45'01"N, 31°28'03"E, 15.v.2011, J. Roháček (SMOC); 1♀, 8 km S of Çine, river bank, 68 m, 37°32'34"N, 28°03'46"E, 29.iv–i.v.2016.

A common and widespread species throughout Europe extending from Scandinavia to North Africa.

Gymnochiromyia inermis (Collin, 1933)

Material examined. 1♀, Akyaka, river bank, salty meadow, 37°03'16"N, 28°19'57"E, 16–27.v.2011.

This species is a new record for Turkey. There are two other very similar species known from Israel and Lebanon. What is somewhat unusual for this record is the locality where it was found. These three species of *Gymnochiromyia* are most frequently encountered, though not exclusively so, in open woodland dominated by *Quercus*.

Gymnochiromyia mihalyii Soós, 1979

Recorded by Ebejer (1998b).

Material examined. 2♀♀, Akyaka, pasture, 6 m, SW, 37°03'19"N, 28°20'07"E, 28.iv–8.v.2013; 1♂, Akyaka, salty meadow, 37°12'45"N, 28°27'42"E, 28.iv–9.v.2013; 1♀, Akyaka, salty meadow, 37°02'53"N, 28°19'39"E, 28.iv–9.v.2013; 1♂, Akyaka, salty meadow, 2 m, 37°01'49"N, 28°20'01"E, 22.vi–1.vii.2015.

A widespread species in Europe and the Mediterranean, though not as common as *G. flavella*.

Discussion

We list one species of *Chyromya* (a new record), three of *Gymnochiromyia* (two new records), and 11 of *Aphaniosoma* (three new records). Although we found no literature records of *Chyromya flava* (Linnaeus, 1758) this very widespread species certainly occurs in Turkey. *Chyromya britannica* Gibbs, 2007 was described from Britain and later found in France, but even this species is more widespread than previously thought. MJE has seen a specimen from Slovenia collected in 1958 and housed among unsorted material in the Natural History Museum, London, UK. Thus, its distribution may be more widespread than originally thought and it may also occur in Turkey. With regards to *Aphaniosoma*, given the numerous species present in the eastern part of the

Mediterranean, the many undescribed species known to MJE, and the fact that eastern Turkey has not been investigated for this family, it is very likely that the fauna is currently very under represented. We estimate that approximately 30 species should occur in this country.

Acknowledgements

MB thanks staff and students of the Department of Biology, Muğla Sıtkı Koçman University, Muğla, Turkey, namely Hasan Civelek, Oktay Dusun, Hanife Pala, and Hatice Kavak for their help with collecting specimens and for taking care of Malaise traps. Dr J. Roháček kindly offered material that he collected to include in this paper.

References

Ebejer MJ (1998a) A review of the Palaearctic species of *Aphaniosoma* Becker (Diptera, Chyromyidae), with descriptions of new species and a key for the identification of adults. Deutsche Entomologische Zeitschrift 45(2): 191–230. https://doi.org/10.1002/mmnd.19980450208

Ebejer MJ (1998b) A new species of *Gymnochiromyia* Hendel (Diptera: Chyromyidae) from the Mediterranean, with notes, lectotype designations and a key to the species from the West Palaearctic. Studia Dipterologica 5(1): 19–29.

Ebejer MJ (2006) New species of *Aphaniosoma* Becker (Diptera, Chyromyidae) from Central Asia. Studia Dipterologica 10(1): 249–296.

Ebejer MJ (2009) A revision of Afrotropical Chyromyidae (excluding *Gymnochiromyia* Hendel) (Diptera: Schizophora), with the recognition of two subfamilies and the description of new genera. African Invertebrates 50 (2): 321–434. https://doi.org/10.5733/afin.050.0208

Ebejer MJ (2010) The identification of females of the west Palaearctic species of *Gymnochiromyia* Hendel (Diptera: Chyromyidae) and descriptions of five new species from Israel and the United Arab Emirates. Israel Journal of Entomology 40: 145–168.

ZooKeys 872: 77–90 (2019)
doi: 10.3897/zookeys.872.33105
http://zookeys.pensoft.net

RESEARCH ARTICLE

A peer-reviewed open-access journal
ZooKeys
Launched to accelerate biodiversity research

Population structure of *Aphyocypris normalis*: phylogeography and systematics

Xiao-Xia Huang[1], Kui-Ching Hsu[2], Bin Kang[3], Po-Hsun Kuo[4], Wan-Hsin Tsai[5], Chih-Ming Liang[5], Hung-Du Lin[6], Wei-Kuang Wang[5]

1 *Key laboratory of atmospheric environment and processes in the boundary layer over the low-latitude plateau region, Yunnan University, Kunming, 650091, China* **2** *College of Fisheries, Guangdong Ocean University, Zhanjiang 524088, China* **3** *College of Fisheries, Ocean University of China, Qingdao 266003, China* **4** *Department of Industrial Management, National Taiwan University of Science and Technology, Taipei 106, Taiwan* **5** *Department of Environmental Engineering and Science, Feng Chia University, Taichung 407, Taiwan* **6** *The Affiliated School of National Tainan First Senior High School, Tainan 701, Taiwan*

Corresponding author: *Hung-Du Lin* (varicorhinus@hotmail.com); *Wei-Kuang Wang* (wkwang@fcu.edu.tw)

Academic editor: *M. E. Bichuette* | Received 15 January 2019 | Accepted 23 May 2019 | Published 26 August 2019

http://zoobank.org/1FA844E6-A890-413D-8CFE-EC3F23AB1E9A

Citation: Huang X-X, Hsu K-C, Kang B, Kuo P-H, Tsai W-H, Liang C-M, Lin H-D, Wang W-K (2019) Population structure of *Aphyocypris normalis*: phylogeography and systematics. ZooKeys 872: 77–90. https://doi.org/10.3897/zookeys.872.33105

Abstract

Aphyocypris normalis (Teleostei: Cyprinidae) is an endemic species in South China, but little is known about its genetic structure. This study examined the population structure of *A. normalis* using sequences of the mitochondrial DNA control region and cytochrome *b* gene (2,086 bp). In total, 107 specimens were collected from nine populations. All 105 mtDNA haplotypes were identified as belonging to two allopatric phylogroups. The results of a statistical dispersal-vicariance analysis (S-DIVA) suggested that the ancestral populations of *A. normalis* were distributed widely on Hainan Island and east of the Leizhou Peninsula. A comparison of the fixation indices N_{ST} (0.532) and G_{ST} (0.004) revealed that the phylogeny and geography had a significant relationship. Our study found that (1) the Wuzhishan and Yinggeling Mountain Range was an important barrier limiting gene exchange between populations on both sides; (2) cyclic climate changes may have shaped migrations and population differentiations; and (3) different colonization times caused different population diversities between codistributed species. In addition, the inter- and intraspecific diversities of the genus *Aphyocypris* were estimated.

Keywords

Dispersal; Hainan Peninsula; Vicariance; Wuzhishan and Yinggeling Mountains Range

Introduction

Hainan Island is located in the transitional zone between tropical and temperate zones. The island is separated from mainland China to the north by the Qiongzhou Strait and from mainland Vietnam to the west by the Gulf of Tonkin. Hainan Island was first isolated from the mainland by the results of volcanism and rising sea levels approximately 2–2.5 million years ago (mya) (e.g., Zeng and Zeng 1989; Zhao et al. 2007). Based on the ichthyofaunal similarities (Li 1981), Hainan Island was defined as a unit subregion in the South China region. Our study found that some freshwater fishes, e.g., *Glyptothorax hainanensis* and *Opsariichthys hainanensis*, are considered endemic to Hainan Island, but previous studies (Chen et al. 2007; Lin et al. 2016) have found that these two species are also distributed in the Pearl River subregion. Moreover, geological evidence indicates that land bridges repeatedly connected the island to the Asian continent during the Pleistocene glaciations (Voris 2000; Zhao et al. 2007). According to phylogeographic studies of freshwater fishes (e.g., genus *Glyptothorax* see Chen et al. 2007; *Garra orientalis* see Yang et al. 2016; genus *Opsariichthys* see Lin et al. 2016), during Pleistocene glaciations, migrants probably moved between mainland China and island populations. The gene flows were interrupted when Hainan Island was separated from mainland China by the sinking of the Qiongzhou Strait (Morton and Blackmore 2001; Yap 2002).

The Wuzhishan and Yinggeling Mountain Range (WY Range) rises steeply from the central and southern regions of Hainan Island and gives way to a broad plain in the north. Lin et al. (2010) found that the WY Range was an important barrier based on the population structure of the Reeves's butterfly lizard. However, Huang et al. (2013) suggested that WY Range did not act as a barrier to gene flow among populations of oriental garden lizards (*Calotes versicolor*). In addition, the four largest rivers on the island, the Nandu, Changhua, Wanquan, and Linshui Rivers, originate from the WY Range and flow outwards into the Qiongzhou Strait, South China Sea, and Gulf of Tonkin, respectively (Fig. 1). According to the landforms, the WY Range isolated these four rivers into two regions, southern Hainan (Wanquan and Linshui rivers) and northern Hainan (Nandu and Changhua Rivers). Yang et al. (2016) and Zhou et al. (2017) proposed that the WY Range was an important phylogeographic break based on the population structures of the cyprinid fishes *G. orientalis* and *Onychostoma lepturum*. However, Lin et al. (2016) suggested that the WY Range did not act as a barrier to gene flow among populations of another cyprinid, *O. hainanensis*.

Aphyocypris normalis is a small cyprinid fish restricted to Hainan Island and its adjacent area. Thus, this species is an ideal freshwater fish species to study the biological consequences of the geological history of river systems in this area. *Aphyocypris normalis* was named *Nicholsicypris normalis* until 2011. Liao et al. (2011) suggested that *Pararasbora*, *Nicholsicypris*, and *Yaoshanicus* were synonyms of *Aphyocypris* based on previous morphological studies (Chu 1935; Tzeng 1986; Kottelat 2001). Although Tang et al. (2010) supported their close interrelationship with molecular data, the genetic

distances among them were not estimated. Thus, our study examined the taxonomic status of *Pararasbora*, *Nicholsicypris*, *Yaoshanicus,* and *Aphyocypris* based on molecular data. In addition, the species diversity within *Aphyocypris* is very low. Liao et al. (2011) found that there are two species within *Aphyocypris* (*A. chinensis* and *A. kikuchii*), and *Pararasbra* (*P. moltrechti*), *Nicholsicypris* (*N. normalis*), and *Yaoshanicus* (*Y. arcus*) are monotypic. Until now, there were eight species within the genus *Aphyocypris* (Froese and Pauly 2018), and new species were described (Zhu et al. 2013). Thus, our study examined the diversity within *Aphyocypris*.

The major questions in our study are as follows: (1) What are the taxonomic boundaries within *Aphyocypris* and its close relatives? (2) How did *A. normalis* colonize the rivers on the island and mainland? (3) Is there a phylogeographic break in freshwater fish on Hainan Island? To address the aforementioned questions, the mitochondrial DNA cytochrome *b* gene and control region sequences (hereafter mtDNA) were used to evaluate the phylogenetic relationships and population genetic structure (e.g., Chen et al. 2007; Yang et al. 2012, 2016; Chiang et al. 2010, 2013; Hsu et al. 2014). These results will help to establish mtDNA sequence data and develop conservation strategies for freshwater fishes on Hainan Island.

Materials and methods

Sampling and molecular methods

A total of 107 specimens of *A. normalis* was collected from nine localities on Hainan Island and mainland China (Fig. 1, detailed in Table 1). These populations were sorted into five groups based on the landforms. Fishes were collected from field sites with seines and euthanized with MS-222 (Sigma). Samples were fixed and stored in 100% ethanol. Genomic DNA was extracted from muscle tissue using a Genomic DNA Purification Kit (Gentra Systems, Valencia, CA). The entire cyt b gene and control region fragment were amplified by polymerase chain reaction (PCR) using primers from Xiao et al. (2001) and Zhou et al. (2017), respectively. Each 50 μl PCR mixture contained 5 ng template DNA, 5 μl 10x reaction buffer, 5 μl dNTP mix (10 mM), 5 pmol of each primer and 2 U of Taq polymerase (Promega, Madison, WI, U.S.A.). PCR was performed on an MJ Thermal Cycler with the following program: one cycle of denaturation at 95 °C for 4 min, 30 cycles of denaturation at 94 °C for 45 s, annealing at 48 °C for 1 min 15 s and extension at 72 °C for 1 min 30 s, followed by 72 °C extension for 10 min and sample storage at 4 °C. The purified PCR products were sequenced using an ABI 377 automated sequencer (Applied Biosystems, Foster City, CA, U.S.A.). Chromatograms were checked with the Chromas software (Technelysium), and sequences were manually edited using BioEdit 6.0.7 (Hall 1999). Moreover, to examine the taxonomic status among *Pararasbora*, *Yaoshanicus*, *Nicholsicypris* and *Aphyocypris*, the sequences of Opsariichthyinae from GenBank were obtained (see Results).

Table 1. Sampling locations, abbreviation (Abbr.) and summary statistics of *Aphyocypris normalis*. Haplogroups correspond to the haplogroups recover in BEAST phylogeny (Fig. 3).

River	Locations (Abbr.)	Latitude	longitude	Sample size	Haplotype diversity (h)	Nucleotide diversity (%)		phylogroup
						θ_π	θ_ω	
North of Yunkai Mountains								
Dongjiang	Heyuan (HY)	23°44'N	114°42'E	14	0.99	0.23	0.32	I
South of Yunkai Mountains								
East of Leizhou Peninsular								
Moyangjiang	Yangchung (MY)	22°26'N	111°56'E	11	1.00	0.61	0.71	I
Jianjiang	Hexi (HE)	22°21'N	110°56'E	14	1.00	1.12	1.16	I
West of Leizhou Peninsular								
Beilun River	Dongxing (DX)	21°32'N	107°58'E	7	1.00	1.08	1.26	I
Hainan Island								
Northern								
Nandu River	Haikou (HO)	19°57'N	110°19'E	13	1.00	0.97	1.23	I
Wanquan River	Qionghai (QH)	19°09'N	110°18'E	8	1.00	1.43	1.68	I
Zhubijang	Basha (BS)	19°13'N	109°26'E	11	1.00	0.85	0.97	I
Southern								
Lingshui River	Baoting (BT)	18°38'N	109°42'E	20	0.99	0.50	0.52	II
Changhua River	Thanhuna (TH)	18°46'N	109°30'E	9	1.00	0.68	0.78	II
Total				**107**	**1.00**	**1.49**	**2.45**	

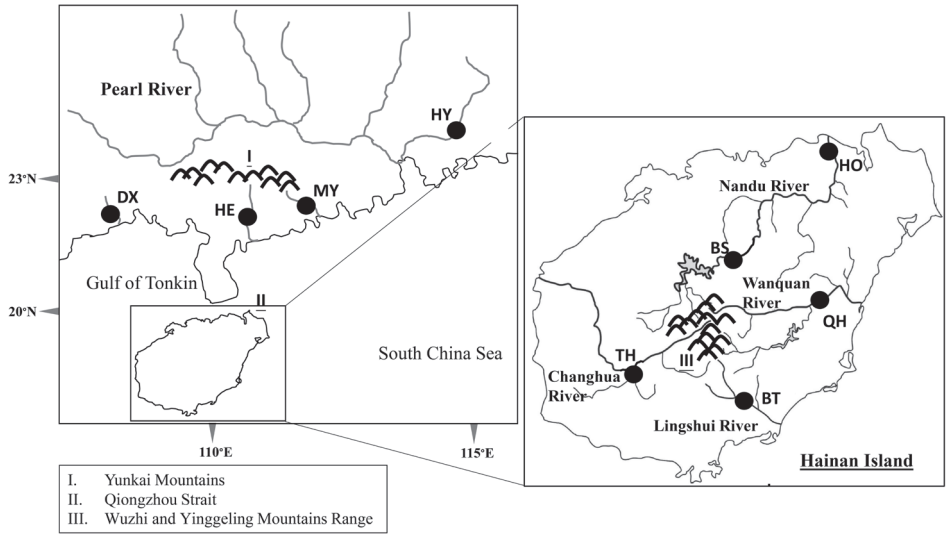

Figure 1. *Aphyocypris normalis* sampling locations on Hainan Island and adjacent areas. All localities sampled in this study are indicated by •.

Sequence alignment and phylogenetic inference

Nucleotide sequences were aligned in Clustal X 1.81 (Thompson et al. 1997). Levels of intrapopulation genetic diversity were estimated by indices of haplotype diversity (*h*) (Nei and Tajima 1983) and nucleotide diversity (θ_π and θ_ω) (Jukes and Cantor 1969) in DnaSP 4.10.8 (Rozas et al. 2003). Comparing estimates generated by these two indices (θ_π, current genetic diversity, and θ_ω, historical diversity) provides insight into population dynamics over recent evolutionary history (Templeton 1993). The existence of phylogeographic structure was examined following Pons and Petit (1996) by calculating two genetic differentiation indices, G_{ST} and N_{ST}, in DnaSP. Pairwise F_{ST} values implemented by DnaSP were used to examine the spatial partitioning of genetic variation among populations. AMOVA (analysis of molecular variance) partitioned were used to the observed variation among samples into within-population (F_{ST}), within-group (F_{SC}) and among-group (F_{CT}) components in Arlequin version 3.5 (Excoffier and Lischer 2010). Arlequin was also used to construct the haplotype network. The program SAMOVA (Dupanloup et al. 2002) was used to identify groups of adjacent sampling locations with the maximum extent of genetic differentiation. These analyses used 500 simulated annealing steps and compared maximum indicators of differentiation (F_{CT}) when the program was instructed to identify K = 2 to K = 8 partitions of the sampling area.

A phylogenetic tree was created by BEAST 1.8.0 (Drummond et al. 2013), which is a Bayesian statistical framework. Phylogenetic relationships were also inferred using maximum-likelihood (ML) in MEGA 6 (Tamura et al. 2013). The GTR+I+G substitution model was selected using the Akaike information criteria (AICc) in jModelTest 2.0 (Darriba et al. 2012). The time to the most recent common ancestor (T_{MRCA}) was also calculated with the software package BEAST. A molecular clock was calibrated using a divergence rate of 2% per million years (Yang et al. 2016). We used a strict clock with a Bayesian skyline tree and estimated the divergence times of the major lineages to the most recent common ancestor (T_{MRCA}). We ran 10^6 generations. The output was visualized in Tracer v1.6 (Rambaut et al. 2013) to verify that convergence and suitable effective sample size were achieved for all parameters. Burn-in and plots for each analysis were visualized using Tracer. The TREEANNOTATOR in the BEAST package was used to summarize tree data, and the tree was viewed using FigTree v1.3 (Rambaut 2014). For ML analysis, bootstrapping was performed with 1000 replications.

In addition, to determine the possible diversification scenarios of *A. normalis*, a statistical dispersal-vicariance analysis (S-DIVA), a program that complements DIVA, was employed to determine statistical support for ancestral range reconstructions (Yu et al. 2010). The tree file formats were generated by the program BEAST with 10^7 Markov Chain Monte Carlo (MCMC) steps and the first 10% as burn-in. The analysis was performed using the 'maxareas = 5' option because the populations were divided into six groups (Table 1).

Table 2. Pairwise p-distance (%) within and among genera and species.

	within	A2	A3	A4	A5	B	B2	C	C2	D	D2	D3	D4	D5	D6	D7
A. Aphyocypris	**3.15**					**15.31**		**16.02**		**18.22**						
A1. *A. normalis*	2.28	5.78	9.74	12.59	12.52											
A2. *A. moltrechti*	1.11		8.92	11.78	11.64											
A3. *A. arcus*	–			11.67	11.58											
A4. *A. kikuchii*	–				2.63											
A5. *A. chinensis*	2.33															
B. Candidia	**8.77**							**12.39**		**16.91**						
B1. *C. barbatus*	–						8.77									
B2. *C. pingtungensis*	–															
C. Nipponocypris	**11.40**									**16.17**						
C1. *N. seiboldii*	–								11.4							
C2. *N. temminckii*	–															
D. Opsariichthys	**10.69**															
D1. *O. bidens*											6.58	12.81	13.25	14.21	12.54	12.46
D2. *O. uncirostris*												13.42	13.33	13.95	13.42	12.63
D3. *O. evolans*													9.21	9.47	9.74	9.12
D4. *O. hainanensis*														7.28	9.47	9.39
D5. *O. minutus*															8.60	9.39
D6. *O. pachycephalus*																4.30
D7. *O. kaopingensis*																

Results

Taxonomic status

Although the genus *Aphyocypris* was included in Danioninae, Liao et al. (2011) reassigned this genus into Opsariichthyinae. Thus, sequences of Opsariichthyinae in GenBank from Chiang et al. (2011), Wang et al. (2011) and Lin et al. (2016) were downloaded (Fig. 2). The ML tree (Fig. 2) showed that all sequences fell into four monophyletic groups corresponding to four genera, *Aphyocypris*, *Candidia*, *Nipponocypris,* and *Opsariichthys*. Among these four genera, the mean pairwise p-distance was 15.84%, with a range of 12.39% to 18.22%. The range of the divergences within these genera was 3.15% to 11.40% (Table 2). In addition, three *Aphyocypris* species, *A. normalis*, *A. moltrechti,* and *A. chinensis*, are also monophyletic groups. The mean intraspecific divergence within these *Aphyocypris* species was 1.91%. The mean interspecific p-distance was 9.89%, with a range of 2.63% to 12.59% (Table 2).

Genetic diversity of *A. normalis*

The complete 1,141 base pairs (bp) of cyt b (MH909846–MH909955) and 945 bp of the control region (MH909956–MH910020) sequences were analyzed. A total of 105 haplotypes (2,086 bp, 270 variable sites and 170 phylogenetic informative sites) were obtained for 107 sequences from nine populations analyzed (Table 1; Fig. 1). Nucleotide sequences were A+T rich (64.9%). Haplotype diversities within populations ranged from 0.99 to 1.00

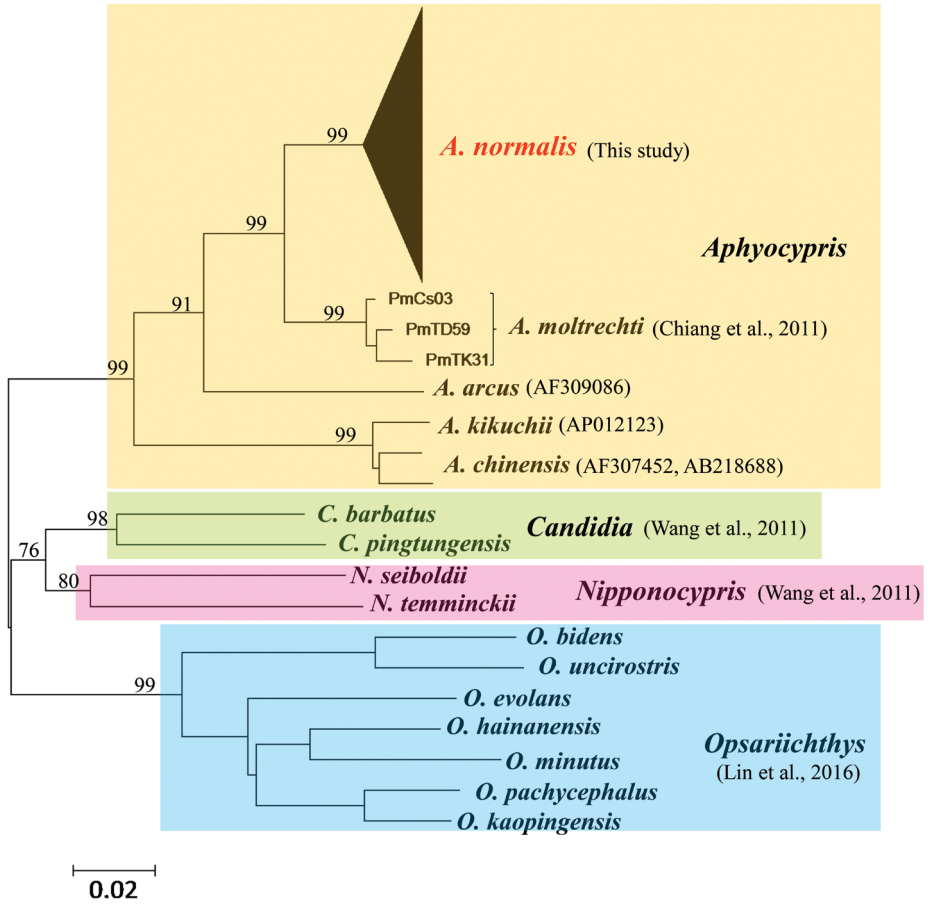

Figure 2. Phylogenetic relationships of the genera *Aphyocypris*, *Candidia*, *Nipponocypris*, and *Opsariichthys* using ML analyses of cyt b gene sequence data. Numbers along the branches indicate the percentage of bootstrap support obtained in the ML analyses.

(Table 1). The nucleotide diversity (θ_π) in the region was the highest in northern Hainan Island (average = 1.20) and the lowest in the northern Yunkai Mountains (population HY, 0.23). At the population level, the nucleotide diversity (θ_π) was the highest in population QH (northern Hainan Island; 1.43) and the lowest in population HY (north of Yunkai Mountains; 0.23). Estimates of the current (θ_π) and historical (θ_ω) genetic diversity per site for each sample indicated that all samples showed a pattern of decline ($\theta_\pi < \theta_\omega$; Table 1).

Population structure and history

All mtDNA haplotypes were population-private haplotypes. Our study found that the sequences were unique, excluding two identical sequences within populations BT and HY. Geographical division assessed by DnaSP indicated significant differen-

Table 3. Matrix of pair-wise F_{ST} (below diagonal) and p values (above diagonal) based on mtDNA in *N. normalis*. Refer to Table 1 for the abbreviations of localities.

	MY	HE	DX	HO	QH	BS	BT	TH
HY	0.67	0.57	0.62	0.56	0.49	0.72	0.82	0.79
MY	0.00	0.38	0.45	0.37	0.29	0.59	0.71	0.67
HE	0.00	0.00	0.27	0.26	0.18	0.46	0.61	0.57
DX	0.00	0.00	0.00	0.29	0.18	0.52	0.64	0.57
HO	0.00	0.00	0.00	0.00	0.14	0.51	0.61	0.58
QH	0.00	0.00	0.00	0.00	0.00	0.41	0.54	0.50
BS	0.00	0.00	0.00	0.00	0.00	0.00	0.73	0.69
BT	0.00	0.00	0.00	0.00	0.00	0.00	0.00	0.44

Table 4. Analysis of molecular variance (AMOVA).

Scheme	Category description	% Var.	Statistic	P
1. Two geological groups (HY+MY+HE +DX) (HO+QH+BS+TH+BT)				
	Among regions	4.54	F_{SC} = 0.54	<0.001
	Among populations in region	51.64	F_{ST} = 0.56	<0.001
	Within population	43.82	F_{CT} = 0.05	<0.001
2. Three geological groups (HY) (MY+HE +DX) (HO+QH+BS+TH+BT)				
	Among regions	4.65	F_{SC} = 0.54	<0.001
	Among populations in region	51.37	F_{ST} = 0.56	<0.001
	Within population	43.98	F_{CT} = 0.05	<0.001
3. Four geological groups (HY) (MY+HE) (DX) (HO+QH+BS+TH+BT)				
	Among regions	-0.16	F_{SC} = 0.55	<0.001
	Among populations in region	55.41	F_{ST} = 0.55	<0.001
	Within population	44.75	F_{CT} = -0.00	<0.01
4. Four geological groups (HY) (MY+HE +DX) (HO+QH+BS) (TH+BT)				
	Among regions	18.82	F_{SC} = 0.39	<0.001
	Among populations in region	32.03	F_{ST} = 0.51	<0.001
	Within population	49.14	F_{CT} = 0.19	<0.01
5. Two phylogroups (HY+HE+MY+DX+QH+BS+HO) (TH+BT)				
	Among regions	31.03	F_{SC} = 0.46	<0.001
	Among populations in region	31.94	F_{ST} = 0.63	<0.001
	Within population	37.03	F_{CT} = 0.31	<0.01
6. Five SAMOVA groups (HY) (HE+MY+DX+QH+HO) (BS) (TH) (BT)				
	Among regions	**34.53**	F_{SC} = 0.37	<0.001
	Among populations in region	24.26	F_{ST} = 0.59	<0.001
	Within population	41.21	F_{CT} = **0.36**	<0.001

tiation among populations (F_{ST} = 0.530). The pairwise F_{ST} values ranged from 0.144 (between populations HO and QH) to 0.820 (between populations HY and BT) (Table 3). After pooling by region (Table 1), the pairwise F_{ST} within the mainland region (mean F_{ST} = 0.493) was smaller than that within island regions (mean F_{ST}

= 0.514) (Table 3). The mean F_{ST} between the mainland and island was similar to that within the island (Table 3). A comparison of the fixation indices N_{ST} (0.532) and G_{ST} (0.004) revealed that N_{ST} was much larger than G_{ST}. This result suggested a strong relationship between phylogeny and geography. These results indicated that the population differentiations were significant.

The Bayesian phylogenetic tree is shown in Figure 3 and is divided into two major phylogroups (I and II). Phylogroup I included seven populations in northern Hainan Island (including) and phylogroup II included only two populations in southern Hainan Island. The best SAMOVA grouping schemes partitioned the sampling area into five groups ($K = 5$; $F_{CT} = 0.35$, $p < 0.001$). All samples were divided into five units: (1) BS, (2) BT, (3) TH, (4) HY and (5) others. The results of AMOVA indicated significant genetic structures at several levels (Table 4), but the most genetic variability was accounted for by between-group differences among five SAMOVA units. Among these five groups, 34.53%, 24.26% and 41.21% variations existed among groups, among populations within groups and within populations, respectively.

The coalescence time of *A. normalis* was estimated to be in the early Pleistocene (T_{MRCA}= 2.33 mya, 1.92 – 2.74). The results of the S-DIVA analysis indicated that possible ancestral populations of *A. normalis* were distributed on Hainan Island and east of the Leizhou Peninsula. The rising of the WY Range on Hainan Island separated the populations into two groups, south and north of the WY Range. After a vicariance event, the populations in the north of the WY Range migrated to the west of the Leizhou Peninsula.

Discussion

Inter- and interspecific diversities within *Aphyocypris*

Today, the genera *Pararasbora*, *Yaoshanicus*, and *Nicholsicypris* are synonymous with the genus *Aphyocypris*. Our study considered that a genus should fulfill two criteria at least, monophyly and distinctness. In this study, the range of the p-distance among the genera *Candidia*, *Nipponocypris* and *Opsariichthys* was 12.39% to 16.17% (mean = 15.16%) (Table 2). The range of the p-distance between the genus *Aphyocypris* and the other three genera ranged from 15.31% to 18.22% (mean = 16.52%) (Table 2). Moreover, the mean interspecific p-distance within the genus *Aphyocypris* was 9.89%, with a range of 2.63% to 12.59% (Table 2). The mean interspecific p-distance within the genus *Opsariichthys* was 10.69%, with a range of 4.30% to 14.21%. Thus, our study determined that the genera boundary was 15.00%. Based on the genetic variations, our study supported the synonymization of *Pararasbora* (*P. moltrechti*), *Yaoshanicus* (*Y. arcus*) and *Nicholsicypris* (*N. normalis*) with *Aphyocypris* (Liao et al. 2011). Moreover, Tzeng (1986) indicated that *A. normalis* is conspecific with *A. moltrechti*, but our results did not support that finding (Fig. 2; Table 2).

Phylogeography of *Aphyocypris normalis*

The geological studies proposed that approximately 2–2.5 mya, Hainan was first isolated from the mainland by the results of volcanism and the ground fall in the current Qiongzhou Strait (e.g., Zeng and Zeng 1989). During the Pleistocene glaciations, migrants probably moved between mainland China and the island by the sinking of the Gulf of Tonkin and Qiongzhou Strait (Morton and Blackmore 2001; Yap 2002). Previous studies (Chen et al. 2007; Lin et al. 2016; Yang et al. 2016) have indicated that during the Pleistocene glaciations, the sea level dropped, and the entire region of the Gulf of Tonkin and the Qiongzhou Strait became part of the coastal plain of the Asian continent (Fig. 1). The strait and exposed continental shelves assisted in population dispersions. Thus, the gene flow among the ancestral populations of Hainan Island and the adjacent areas were unlimited. The results presented here suggest that the ancestral populations of *A. normalis* were distributed widely south of the Yunkai Mountains, including Hainan Island, and east of the Leizhou Peninsula in the early Pleistocene.

Subsequently, our results found that the populations on southern Hainan Island (TH and BT) diverged by a vicariance event. At 0.458 mya, the WY Range arose on Hainan Island and isolated the population in the southern Hainan Island region as lineage II (Fig. 3). This result agrees with previous studies (Yang et al. 2016; Zhou et al. 2017). The WY Range is located in the central and southern regions of Hainan Island and approaches an elevation of 1800 m. The landforms reflect that the rivers on island originate from the central mountainous area and flow outwards. Due to the steep topology of the island, most rivers run directly into the oceans with no connection to the neighboring drainage systems. As in previous phylogeographic studies of freshwater fishes (Yang et al. 2016; Zhou et al. 2017), the WY Range was an important barrier. Zhou et al. (2017) found that the populations of the cyprinid fish *O. lepturum* on Hainan Island could be divided into three units based on their location in the Qiongzhou Strait, the Gulf of Tonkin and the South China Sea. The genetic structure of *A. normalis* on Hainan Island showed the same pattern as that of *O. lepturum* (Zhou et al. 2017). Thus, the WY Range is a phylogeographic break in the phylogeography of *A. normalis*.

Based on previous studies (Chen et al. 2007; Lin et al. 2016; Yang et al. 2016), the populations on Hainan Island and the mainland diverged by a vicariance event, the Qiongzhou Strait. Previous studies (Chen et al. 2007; Lin et al. 2016; Yang et al. 2016) proposed that populations of freshwater fishes migrated from one side of the exposed Qiongzhou Strait to the other, and the populations of the island and the mainland separated into two highly divergent clades due to the rising sea level. Our study found that the populations of *A. normalis* on both sides of the Qiongzhou Strait were a mixture (Fig. 3). Although previous studies (Yap 2002; Zhou et al. 2017) considered that the Qiongzhou Strait is a phylogeographic break of freshwater fishes, we found that the populations of *G. orientalis* (Yang et al. 2016) and *O. hainanensis* (Lin et al. 2016) on both sides of the Qiongzhou Strait were mixed to some extent. In the population structure of *G. orientalis* (Yang et al. 2016), lineage I was only distributed to the north of Qiongzhou Strait, but lineage II was distributed both to the north and south of the

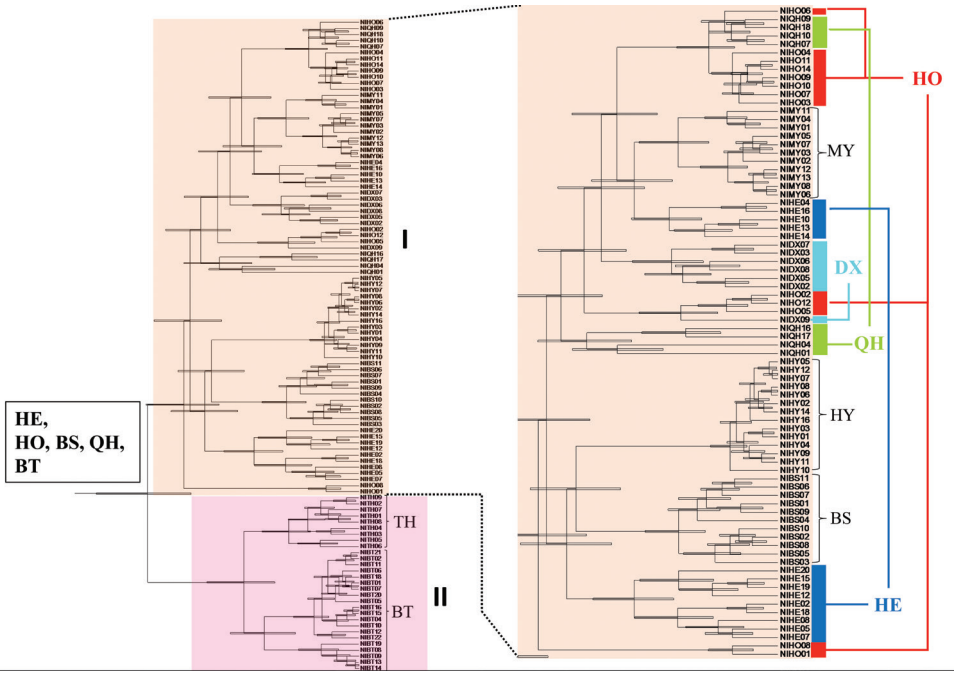

Figure 3. BEAST-derived chronograms of 107 mitochondrial DNA sequences of *Aphyocypris normalis*. The S-DIVA analysis graphical representation of the ancestral distribution is given in the box above the node.

strait. Likewise, the population structure of *O. hainanensis* (Lin et al. 2016) displayed the same pattern as that of *G. orientalis* (Yang et al. 2016). Moreover, geological studies (Voris 2000; Shi et al. 2006; Zhao et al. 2007) suggested that land bridges repeatedly connected the island to the Asian continent. Yang et al. (2016) proposed that when glaciation occurred, the lineages mixed. Thus, the phylogenetic analyses of *A. normalis* (Fig. 3) in the current study revealed a mixed genetic structure across the strait due to cyclic climate changes. When glaciation occurred again after the WY Range rose, some populations retreated from the mainland to the island. Thus, the phylogenetic analysis (Fig. 3) displayed two divergent phylogroups before the divergences among haplotypes included in the ancestral populations.

Our study found that *A. normalis* (this study) and *G. orientalis* (Yang et al. 2016) have similar distribution patterns and that these two species displayed similar phylogeographic patterns. Thus, our study suggested that the effects of environmental changes on Hainan Island and its adjacent area were general patterns. However, the populations of *G. orientalis* showed moderate to high genetic differentiation, but those within *A. normalis* showed a high level of genetic differentiation (Table 2). Although these two species both displayed differentiation, there was no shared haplotype between mainland and island populations, and there was no shared haplotype within *A. normalis*. The haplotype and nucleotide diversities of *A. normalis* are higher than those of *G. orientalis*. Moreover, the genus *Aphyocypris* only includes ten species in East Asia,

but the genus *Garra* contains 138 species in Asia and Africa (Froese and Pauly 2018). Our study found that *A. normalis* and *G. orientalis* had different colonization times, with *A. normalis* in the early Pleistocene and *G. orientalis* in the late Pleistocene. Our study considered that the ancestral populations of these two species originated from different mainland populations. Thus, our future aim is to understand the comparative phylogeography and geological history in Hainan Island and its adjacent area.

Acknowledgments

This work was supported by grants from the Ministry of Science and Technology, Taiwan (MOST107-2221-E-035-006-) and the National Science Foundation of China (No. 41476149 and No. 31560181).

References

Chen XL, Chiang TY, Lin HD, Zheng HS, Shao KT, Zhang Q, Hsu KC (2007) Mitochondrial DNA phylogeographyof *Glyptothorax fokiensis* and *Glyptothorax hainanensis* in Asia. Journal of Fish Biology 70: 75–93. https://doi.org/10.1111/j.1095-8649.2007.01370.x

Chiang TY, Lee TW, Hsu KC, Kuo CH, Lin DY, Lin HD (2011) Population structure in the endangered cyprinid fish *Pararasbora moltrechti* in Taiwan, based on mitochondrial and microsatellite DNAs. Zoological Science 28: 642–651. https://doi.org/10.2108/zsj.28.642

Chiang TY, Lin HD, Shao KT, Hsu KC (2010) Multiple factors have shaped the phylogeography of Chinese spiny loach (*Cobitis sinensis)* in Taiwan as inferred from mitochondrial DNA variation. Journal of Fish Biology 76: 1173–89. https://doi.org/10.1111/j.1095-8649.2010.02589.x

Chiang TY, Lin HD, Zhao J, Kuo PH, Lee TW, Hsu KC (2013) Diverse processes shape deep phylogeographical divergence in *Cobitis sinensis* (Teleostei: Cobitidae) in East Asia. Journal of Zoological Systematics and Evolutionary Research 51: 316–326. https://doi.org/10.1111/jzs.12030

Chu YT (1935) Comparative studies on the scales and on the pharyngeal and their teeth in Chinese cyprinids, with particular reference to taxonomy and evolution. Biol. Bull. St. John's Univ. Shanghai 2, 1–225. https://doi.org/10.2307/1436747

Darriba D, Taboada GL, Doallo R, Posada D (2012) jModelTest 2: more models, new heuristics and parallel computing. Nature Methods 9: 772. https://doi.org/10.1038/nmeth.2109

Drummond AJ, Rambau A, Suchard M (2013) BEAST 1.8.0. http://beast.bio.ed.ac.uk

Dupanloup I, Schneidera S, Excoffier NL (2002) A simulated annealing approach to define the genetic structure of populations. Molecular Ecology 11: 2571–2581. https://doi.org/10.1111/j.1755-0998.2010.02847.x

Excoffier L, Lischer HEL (2010) Arlequin suite version 3.5: a new series of programs to perform population genetics analyses under Linux and Windows. Molecular Ecology Resources 10: 564–567. https://doi.org/10.1111/j.1755-0998.2010.02847.x

Froese R, Pauly D (2018) FishBase. World Wide Web electronic publication. http://www.fishbase.org

Hall TA (1999) BioEdit: a user-friendly biological sequence alignment editor and analysis program for Windows 95/98/NT. Nucleic Acids Symposium Series 41: 95–98.

Hsu KC, Bor H, Lin HD, Kuo PH, Tan MS, Chiu YW (2014) Mitochondrial DNA phylogeography of *Semisulcospira libertina* (Gastropoda: Cerithioidea: Pleuroceridae): implications the history of landform changes in Taiwan. Molecular Biology Reports 41: 3733–3743. https://doi.org/10.1007/s11033-014-3238-y

Huang Y, Guo X, Ho SYW, Shi H, Li J, Li J, Cai B, Wang Y (2013) Diversification and demography of the oriental garden lizard (*Calotes versicolor*) on Hainan Island and the adjacent mainland. PlosOne 8: e64754. https://doi.org/10.1371/journal.pone.0064754

Jukes TH, Cantor CR (1969) Evolution of protein molecules. In: Monro HN (ed.), Mammalian protein metabolism. Academic Press, New York, NY, 21–132. https://doi.org/10.1016/B978-1-4832-3211-9.50009-7

Kottelat M (2001) Freshwater fishes of northern Vietnam. Washington DC: World Bank, 123 pp.

Li SZ (1981) Studies on zoogeographical divisions for fresh water fishes of China. Science Press, Beijing, China (Chinese).

Liao TY, Kullander SO, Lin HD (2011) Synonymization of *Pararasbora*, *Yaoshanicus*, and *Nicholsicypris* with *Aphyocypris*, and Description of a new species of *Aphyocypris* from Taiwan (Teleostei: Cyprinidae). Zoological Studies 50: 657–664.

Lin HD, Kuo PH, Wang WK, Chiu YW, Ju YM, Lin FJ, Hsu KC (2016) Speciation and differentiation of the genus *Opsariichthys* (Teleostei: Cyprinidae) in East Asia. Biochemical Systematics and Ecology 68: 92–100. https://doi.org/10.1016/j.bse.2016.07.001

Lin LH, Ji X, Diong CH, Du Y, Lin CX (2010) Phylogeography and population structure of the Reevese's butterfly lizard (*Leiolepis reevesii*) inferred from mitochondrial DNA sequences. Molecular phylogenetics and Evolution 56: 601–607. https://doi.org/10.1016/j.ympev.2010.04.032 [Epub 2010 Apr 28.]

Morton B, Blackmore G (2001) South China Sea. Marine Pollution Bulletin 42: 1236–1263. https://doi.org/10.1016/S0025-326X(01)00240-5

Nei M, Tajima F (1983) Maximum likelihood estimation of the number of nucleotide substitutions from restriction sites data. Genetics 105: 207–217.

Pons O, Petit RJ (1996) Measuring and testing genetic differentiation with ordered vs. unordered alleles. Genetics 144: 1237–1245.

Rambaut A (2014) FigTree 1.3. Available at: http:tree.bio.ed.ac.uk/software/figtree

Rambaut A, Drummond AJ, Suchard M (2013) Tracer v1.6. http://beast.bio.ed.ac.uk/Trace

Rozas J, Sanchez-DelBarrio JC, Messeguer X, Rozas R (2003) DnaSP, DNA polymorphism analyses by the coalescent and other methods. Bioinformatics 19: 2496–2497. https://doi.org/10.1093/bioinformatics/btg359

Shi YF, Cui ZJ, Su Z (2006) The Quaternary glaciations and environmental variations in China. Hebei Science and Technology Press, Shijiazhuang.

Tamura K, Stecher G, Peterson D, Filipski A, Kumar S (2013) MEGA6: Molecular evolutionary genetics analysis version 6.0. Molecular Biology and Evolution 30: 2725–2729. https://doi.org/10.1093/molbev/mst197

Tang KL, Agnew MK, Chen WJ, Hirt MV, Sado T, Schneider LM, Freyhof J, Sulaiman Z, Swartz E, Vidthayanon C, Miya M, Saitoh K, Simons AM, Wood RM, Mayden RL (2010)

Systematics of the subfamily Danioninae (Teleostei: Cypriniformes: Cyprinidae). Molecular phylogenetics and Evolution 57: 189–214. https://doi.org/10.1016/j.ympev.2010.05.021

Templeton AR (1993) The 'Eve' hypothesis: a genetic critique and reanalysis. American Anthropologist 95: 51–72. https://doi.org/10.1525/aa.1993.95.1.02a00030

Thompson JD, Gibson TJ, Plewniak F, Jeanmougin F, Higgins DG (1997) The Clustal X windows interface: flexible strategies for multiple sequence alignment aided by quality analysis tools. Nucleic acids research 24: 4876–4882. https://doi.org/10.1093/nar/25.24.4876

Tzeng CS (1986) Distribution of freshwater fishes of Taiwan. Journal of Taiwan Museum 39: 127–146.

Voris HK (2000) Maps of Pleistocene sea levels in Southeast Asia: shorelines, river systems and time durations. Journal of Biogeography 27: 1153–1167. https://doi.org/10.1046/j.1365-2699.2000.00489.x

Wang CF, Hsieh CH, Lee SC, Wang HY (2011) Systematics and Phylogeography of the Taiwanese endemic minnow *Candidia barbatus* (Pisces: Cyprinidae) based on DNA sequences, allozymic, and morphological analyses. Zoological Journal of the Linnean Society 161: 613–632. https://doi.org/10.1111/j.1096-3642.2010.00646.x

Xiao W, Zhang Y, Liu H (2001) Molecular systematics of Xenocyprinae (Teleostei: Cyprinidae): taxonomy, biogeography, and coevolution of a special group restricted in East Asia. Molecular Phylogenetics and Evolution 18: 163–173. https://doi.org/10.1006/mpev.2000.0879

Yang JQ, Hsu KC, Liu Z, Su LW, Kuo PK, Tang WQ, Zhou ZC, Liu D, Bao BL, Lin HD (2016) The population history of *Garra orientalis* (Teleostei: Cyprinidae) using mitochondrial DNA and microsatellite data with approximate Bayesian computation. BMC Evolutionary Biology 16: 73. https://doi.org/10.1186/s12862-016-0645-9

Yang JQ, Tang WQ, Liao TY, Sun Y, Zhou ZC, Han CC, Liu D, Lin HD (2012) Phylogeographical analysis on *Squalidus argentatus* recapitulates historical landscapes and drainage evolution on the island of Taiwan and mainland China. International Journal of Molecular Sciences 13: 1405–1425. https://doi.org/10.3390/ijms13021405

Yap SY (2002) On the distributional patterns of Southeast-East Asian freshwater fish and their history. Journal of Biogeography 29: 1187–1199. https://doi.org/10.1046/j.1365-2699.2002.00771.x

Yu Y, Harris AJ, He X (2010) S-DIVA (statistical dispersal-vicariance analysis): a tool for inferring biogeographic histories. Molecular phylogenetics and Evolution 56: 848–850. https://doi.org/10.1016/j.ympev.2010.04.011

Zeng ZX, Zeng XZ (1989) Physical geography of Hainan. Science Press, Beijing.

Zhang HN, Chen CG, Huang KR, Li ZQ, Zhang FL, Chen GZ (1990) The new geological structures, tectonic movements and geological environment in coastal line of South China. Earthquake Press, Beijing (in Chinese).

Zhao HT, Wang LR, Yuan JY (2007) Origin and time of Qiongzhou Strait. Marine Geology and Quaternary Geology 27: 33–40.

Zhou TQ, Lin D, Hsu KC, Kuo PH, Wang WK, Tang WQ, Liu D, Yang JQ (2017) Spatial genetic structure of the cyprinid fish *Onychostoma lepturum* on Hainan Island. Mitochondrial DNA Part A 28: 901–908. https://doi.org/10.1080/24701394.2016.1209193

Zhu Y, Zhao Y, Huang K (2013) *Aphyocypris pulchrilineata*, a new miniature cyprinid species (Teleostei: Cypriniformes: Cyprinidae) form Guangxi, China. Ichthyological research 60: 232–236. https://doi.org/10.1007/s10228-013-0338-y

ZooKeys 872: 91–99 (2019)
doi: 10.3897/zookeys.872.35137
http://zookeys.pensoft.net

SHORT COMMUNICATION

A peer-reviewed open-access journal
ZooKeys
Launched to accelerate biodiversity research

Transfer of the assassin bug *Helonotus pallidulus* Walker to the genus *Heza* Amyot & Serville (Hemiptera, Heteroptera, Reduviidae, Harpactorinae, Harpactorini)

Hélcio R. Gil-Santana[1], Michael D. Webb[2]

1 *Laboratório de Diptera, Instituto Oswaldo Cruz, Av. Brasil, 4365, 21040-360, Rio de Janeiro, Brazil* **2** *Department of Life Sciences (Insects), The Natural History Museum, Cromwell Road, London SW7 5 BD, UK*

Corresponding author: *Hélcio R. Gil-Santana* (helciogil@uol.com.br)

Academic editor: *Guanyang Zhang* | Received 3 April 2019 | Accepted 26 July 2019 | Published 23 August 2019

http://zoobank.org/BE4692DE-5F51-493A-96ED-EA88BCE44189

Citation: Gil-Santana HR,Webb MD (2019) Transfer of the assassin bug *Helonotus pallidulus* Walker to the genus *Heza* Amyot & Serville (Hemiptera, Heteroptera, Reduviidae, Harpactorinae, Harpactorini). ZooKeys 872: 91–99. https://doi.org/10.3897/zookeys.872.35137

Abstract

Based on examination of its holotype, *Helonotus pallidulus* Walker, 1873 is transferred to the genus *Heza* Amyot & Serville, 1843 with the resulting new combination: *Heza pallidula* (Walker, 1873), **comb. nov.** (Hemiptera, Heteroptera, Reduviidae, Harpactorinae, Harpactorini). A comparison with the similar *Heza ventralis* Stål,1872 is provided.

Keywords

Ecuador, Neotropical region, new combination, *Ploeogaster pallidulus*

Introduction

Harpactorinae is the largest subfamily of Reduviidae and is represented by the tribes Apiomerini and Harpactorini in the Neotropical region (Gil-Santana et al. 2015). Harpactorini is the most diverse Reduviidae tribe with 53 recognized genera in the

Neotropical region (Forero et al. 2008, McPherson and Ahmad 2011, Forero 2011, 2012, Swanson 2012, Gil-Santana 2015, Gil-Santana et al. 2015, Zhang et al. 2016, Lapischies et al. 2019). The only key to separate the genera is by Stål (1872), now badly out of date (Forero 2011). Of all genera of Harpactorini in the Neotropical region, just a few have been revised taxonomically or redescribed.

Walker (1873) described *Helonotus pallidulus* Walker, 1873 based on a specimen (described as a male) from "Cuenca", thereby placing a New World species in the Old World genus, *Helonotus* Amyot & Serville, 1843. In the catalog of Lethierry and Severin (1896) this species was included among the Harpactoridae "Genera et species Harpactoridarum subfam. incerti loci systematici". Distant (1903) included it in the New World genus *Ploeogaster* Amyot & Serville, 1843, stating that he had "not sufficiently compared this [*Ploeogaster pallidulus*] with other species of the genus [*Ploeogaster*] to say that it is not a synonym." Since then, *Ploeogaster pallidulus* has only been cited in catalogues (Wygodzinsky 1949, Maldonado Capriles 1990).

In the current work, we confirm that the holotype of *Helonotus pallidulus*, deposited in the Natural History Museum, London, does not belong to either *Helonotus* or *Ploeogaster*. The main differences being that in *P. pallidulus* a postantennal spine is present (rather than a short tubercle in *Ploeogaster* or both absent in *Helonotus*) and the disc of the hind lobe of the pronotum has a pair of spines in *P. pallidulus* (rather than a pair of tubercles in *Ploeogaster* and one or two pairs of tubercles in *Helonotus*) (Amyot and Serville 1843, Malipatil 1986, 1991). However, as commented in detail below, the above characteristics observed in the holotype of *H. pallidulus* are entirely concordant with members of the New World genus *Heza* Amyot & Serville, 1843, a genus revised by Maldonado Capriles (1976, 1983).

Material and methods

For the present study, the holotype of *Helonotus pallidulus*, deposited in the Natural History Museum, London, United Kingdom (BMNH), was directly examined (Figs 1–6).

After imaging the specimen (Figs 1, 3–5), the antennae were relaxed and moved forward in order to obtain a clearer image of the postantennal spine. Additional photographs were taken for a better visualization of the pronotum and postantennal spines (Figs 2, 6).

General morphological terminology mainly follows Schuh and Slater (1995). However, the [visible] segments of the labium are numbered as II to IV, given that the first segment is lost or fused to the head capsule in Reduviidae (Weirauch 2008, Schuh et al. 2009).

When describing label data, a slash (/) separates the lines and a double slash (//) different labels.

Results

Taxonomy

Subfamily Harpactorinae
Tribe Harpactorini

***Heza pallidula* (Walker, 1873), comb. nov.**
Figs 1–6

Helonotus pallidulus Walker, 1873: 90 [description]; Lethierry and Severin 1896: 200 [catalog, among "Genera et species Harpactoridarum subfam. incerti loci systematic"].
Ploeogaster pallidulus; Distant 1903: 251 [checklist]; Wygodzinsky 1949: 44 [catalog]; Maldonado Capriles 1990: 259 [catalog].

Notes. This species was described from a single specimen (holotype) for which Walker (1873) provided the following data: "*a.* Cuenca. From Mr. Fraser's collection". The reference to 58/132 on the label noted above (Fig. 4) refers to an entry in the BMNH register for 1858 132: Cuenca (Province of Ecuador) collected by Fraser. The type specimen, originally recorded as male is in fact female (Fig. 3).

Material examined. *Helonotus pallidulus*, female **holotype**, [Ecuador]: 5. Helonotus pallidulus. // *a.* Cuenca. // Cuenca [opposite side of same label]: 58/132// Holo- / type [rounded label with red circle] // ♀ // Type [rounded label with blackish circle] // QR CODE / NHMUK 013585371 (BMNH).

Redescription. Female (Figs 1–6). Measurements: total length: 22.0 mm; maximum width of abdomen: approximately 7.5 mm.

Coloration. General color pale brownish to brownish red (Figs 1, 2); pale yellowish on ventral surface of thorax and abdomen (Fig. 3). Antenna with distal fourth of segments I and II darkened (other segments absent). Legs somewhat lighter, with fuscous ill-defined submedian marking on fore femur and submedian and distal markings on remaining femora; apices of femora somewhat darkened. Scutellum darkened, with apex reddish brown. *Hemelytra*: corium with base, apical portion at level of membrane and basal half of clavus reddish, median portion somewhat paler, grayish; membrane pale grayish, approximately basal half of anal and cubital veins and median vein mostly blackish (Fig. 1). Meso and metapleura reddish brown (Fig. 5). Meso and metasterna generally paler; stridulitrum and lateral portions of mesosternum darkened (Fig. 3). *Abdomen*: connexiva faintly darkened dorsally at basal half of segments IV–VII (Fig. 1); sternites generally yellowish to pale orange (Fig. 3).

Structure. *Head* (Figs 5, 6): elongated with a well marked transverse sulcus, shorter than pronotum, and a pair of spines just behind antennal bases; these spines (postantennal spines) are conspicuously bowed with the apex directed slightly anteriad (Fig. 6, pa). Eyes globose, glabrous, projecting laterally, rounded in dorsal view and suboval in lateral view. Ocelli elevated, closer to eyes than to each other. Antennal segments I–II

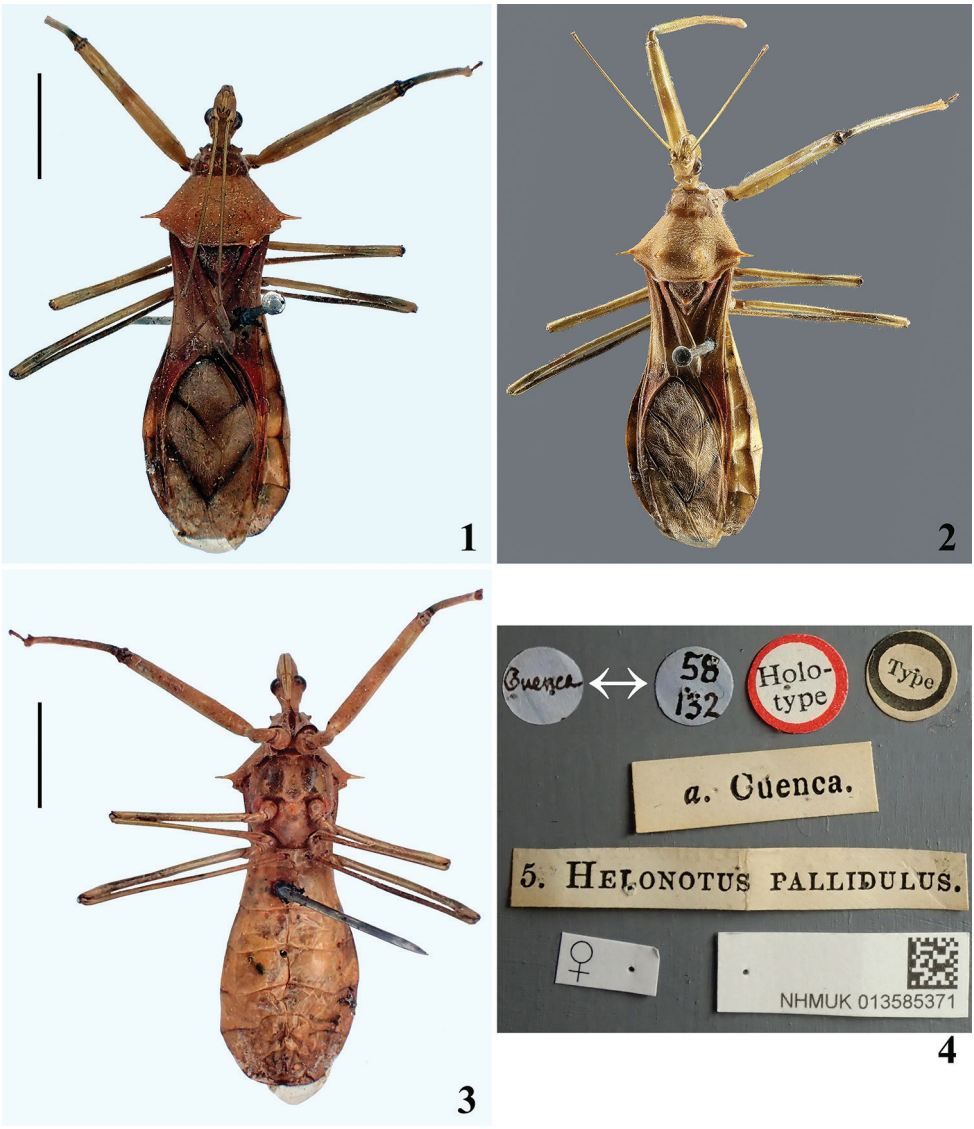

Figures 1–4. *Heza pallidula* (Walker, 1873), comb. nov., female holotype. **1** Dorsal view **2** dorsal view (with antennae and left fore leg repositioned) **3** ventral view **4** labels. Scale bars: 5.0 mm (**1, 3**).

(other absent) straight, slender, segment I somewhat longer than head and pronotum combined; segment II quite shorter than head. Labium stout, moderately curved, segment II (first visible) thickest and longest; segment IV, approximately half as long as segment III, tapering (Fig. 6). *Thorax*. Pronotum: hind lobe approximately two and half times longer than fore lobe, with its maximum width (at posterior margin) somewhat more than twice that of fore lobe; anterior collar inconspicuous; anterolateral angles pronounced; transverse sulcus well marked (Figs 1, 2). Fore lobe divided in two sublobes by shallow median longitudinal depression, with a blunt tubercle on disc of

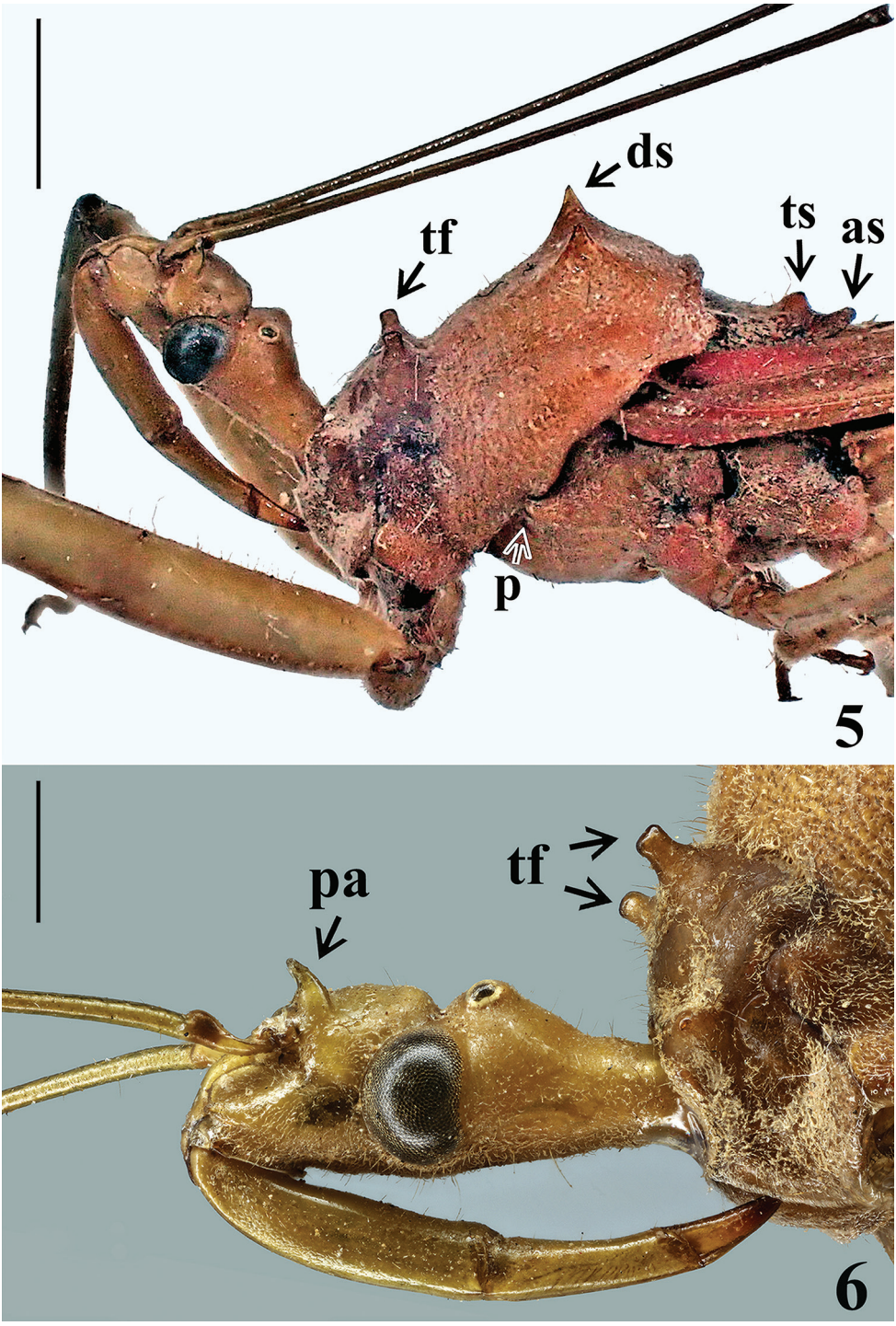

Figures 5, 6. Head and thorax of *Heza pallidula* (Walker, 1873), comb. nov., female holotype, lateral view. **6** Antennae repositioned (**as**, apex of scutellum, **ds**, discal spine of hind lobe, **p**, plica, **pa**, postantennal spine, **tf**, discal tubercle of fore lobe, **ts**, tubercle of disc of scutellum). Scale bars: 2.0 mm (**5**); 1.0 mm (**6**).

each sublobe (Figs 1–2, 5–6, tf). Hind lobe finely transversely corrugate, with four sharp spines (Figs 1, 2); of these, the discal spines (Figs 2, 5, ds) shorter, directed dorsad, larger at base, preceded by an inconspicuous carina; lateral spines relatively long, conspicuous, horizontally directed laterally (Figs 1, 2). Posterior margin curved laterally, with a pair of rounded prominences at level of base of clavus; margin between these prominences slightly curved (Figs 1, 2). Scutellum with a rounded median tubercle on disc (Fig. 5, ts) just before apex, which is rounded and somewhat obliquely elevated (Fig. 5, as). Mesopleura with a well-developed plica (Fig. 5, p), i.e., a small raised tubercle over posterior margin of propleuron. Prosternum almost entirely anterior to fore coxa and shorter than them, with its median portion occupied by stridulitrum. Mesosternum flattened, somewhat depressed at median portion, larger than metasternum. Legs: fore coxae contiguous to each other; middle and hind coxae distant from each other by a distance approximately equivalent to twice width of each coxa (Fig. 3). Apices of all femora with a pair of lateral small tubercles. Femora generally straight; fore femora thickened (Figs 1–3), approximately thrice thicker than middle and hind femora; middle and hind femora slender, slightly dilated subapically; hind femora longest, middle femora shortest. Fore tibiae curved inwards in distal half, somewhat enlarged at apex, with a dorsal spur apically; middle and hind tibiae generally straight, slender. Hemelytra surpassing apex of abdomen for a short distance (Figs 1–3). *Abdomen* spatulate, gradually widening to apex of segment V and then slightly narrowing to form a roughly truncate apex at last segment (Fig. 3). All connexival segments without spines.

Vestiture. Integument generally covered by short thin adpressed setae, more numerous on thorax (Fig. 2). Legs generally covered with longer straight erect setae; fore legs with trochanter, femur and tibia ventrally with a dense pubescence formed by short erect thin setae. Membrane of hemelytra glabrous.

Discussion

The previous placement of this species in *Ploeogaster* by Distant (1903) is incorrect, as some characteristics of the latter are different, such as the absence of postantennal spines (only short postantennal tubercles are present) and the hind lobe of the pronotum without four sharp spines; only with two (lateral) spines, while on the disc, instead of spines, there is a pair of rounded tubercles. Had Distant (1903) "sufficiently compared [*Helonotus pallidulus*] with other described species", he possibly would have placed the species in a different genus.

The transfer of *Helonotus pallidulus* to *Heza* is in accordance with the following features considered as diagnostic for the genus (Amyot and Serville 1843, Maldonado Capriles 1976): head shorter than pronotum, with postantennal spines (Figs 1, 2, 5, 6); pronotum: fore lobe with a pair of blunt or pointed spines on the disc (Figs 5, 6, tf), hind lobe with four sharp spines (Figs 1, 2, 5, ds); mesopleura with a plica (Fig. 5, p); abdomen spatulate, somewhat widened before apex but behind middle of abdomen (Fig. 3).

Besides confirming that the characteristics of *Heza pallidula* are entirely in accordance with those attributed to *Heza*, it is also possible to conclude by consulting

the revision, keys, descriptions and redescriptions provided by Maldonado Capriles (1976, 1983) and Maldonado Capriles and Brailovsky (1983) that this species does not correspond to any previously described species of this genus and must be maintained as a valid species.

Heza pallidula seems to be most similar to *Heza ventralis* Stål, 1872. The latter was described by Stål (1872) and a photo of its type has been made freely available by the Swedish Museum of Natural History (Naturhistoriska riksmuseet, NRM) at http://www2.nrm.se/en/het_nrm/v/heza_ventralis.html. Maldonado Capriles (1976) redescribed *H. ventralis* based only on female specimens. The females of *H. pallidula* and *H. ventralis* share some structural similarity, such as approximate length and shape of the body, similar size of postantennal spines (Fig. 6), and both size and shape of the pronotal spines (Figs 1–3, 5, 6), and the absence of spines on all connexival segments; the three latter characteristics shared with very few species of the genus. Most species of *Heza* have one or more connexival segments spined on its apical angle (Maldonado Capriles 1976, 1983, Maldonado Capriles and Brailovsky 1983). On the other hand, the sericeous white areas on the thorax and more extensively on abdominal sternites are a clear-cut characteristic to separate *H. ventralis* from all other species in the genus, including *H. pallidula*. In *H. pallidula*, the reddish portions of the hemelytra (base and distal portion of corium and basal half of the clavus) and connexivum faintly darkened dorsally at basal half of segments IV–VII (Fig. 1) differ from the uniformly brownish-gray clavus, corium and connexivum of *H. ventralis*. Whereas the postantennal spine is conspicuously bowed with the apex slightly directed anteriad in *H. pallidula* (Fig. 6), it is straight and directed dorsad in *H. ventralis* (Stål 1872, Maldonado Capriles 1976).

The original spelling of the specific name *pallidulus* was changed to *pallidula* in the new combination because, according with the International Code of Zoological Nomenclature (ICZN 1999), if a species-group name is a Latin adjective in nominative singular, it "must agree in gender with the generic name with which it is at any time combined" (Art. 31.2).

Acknowledgements

We thank Ken Merrifield and Stuart Cole (BMNH) for taking the type images. We are also very grateful to Jocelia Grazia (Universidade Federal do Rio Grande do Sul, Brazil), Tadashi Ishikawa (Tokyo University of Agriculture, Japan), Catarina Lopes (Instituto Oswaldo Cruz, Rio de Janeiro, Brazil), Daniel Swanson (University of Illinois at Urbana-Champaign, USA), and Guanyang Zhang (Arizona State University, USA), for their valuable comments and suggestions.

References

Amyot CJB, Serville A (1843) Histoire Naturelle des Insectes. Hémiptères. Librairie Encyclopedique de Roret, Paris, 675 pp.

Distant WL (1903) Rhynchotal Notes. – XVI. Heteroptera: Family Reduviidæ (continued), Apiomerinæ, Harpactorinæ, and Nabinæ. The Annals and Magazine of Natural History, Seventh Series 11: 245–258. https://doi.org/10.1080/00222930308678761

Forero D (2011) Classification of Harpactorinae, assassin bugs Hemiptera: Heteroptera: Reduviidae. Boletín del Museo Entomológico Francisco Luís Gallego 1: 9–24.

Forero D (2012) *Pronozelus*, a new Neotropical harpactorine genus and species from Colombia (Hemiptera: Heteroptera: Reduviidae: Harpactorinae). Entomologica Americana 118: 278–284. https://doi.org/10.1664/12-RA-021.1

Forero D, Gil-Santana HR, Doesburg PH van (2008) Redescription of the Neotropical genus *Aristathlus* (Heteroptera, Reduviidae, Harpactorinae). In: Grozeva S, Simov N (Eds) Advances in Heteroptera research: festschrift in honor of 80th anniversary of Michail Josifov. Pensoft, Sofia-Moscow, 85–103.

Gil-Santana HR (2015) *Parahiranetis salgadoi*, a new genus and species of Harpactorini (Hemiptera: Heteroptera: Reduviidae), with a key to Neotropical wasp-mimicking harpactorine genera. Acta Entomologica Musei Nationalis Pragae 55: 29–38.

Gil-Santana HR, Forero D, Weirauch C (2015) Assassin bugs (Reduviidae excluding Triatominae). In: Panizzi AR, Grazia J (Eds) True bugs (Heteroptera) of the Neotropics, Entomology in Focus 2. Springer Science+Business Media, Dordrecht, 307–351. https://doi.org/10.1007/978-94-017-9861-7_12

ICZN [International Comission on Zoological Nomenclature] (1999) International code of zoological nomenclature. Fourth Edition. London: The International Trust for Zoological Nomenclature.

Lapischies R, Forero D, Barcellos A, Salomão RP (2019). A new species of *Pyrrhosphodrus* (Hemiptera: Heteroptera: Reduviidae) from the Caatinga ecosystem in Brazil, with notes on the genus. Zootaxa 4543: 388–400. https://doi.org/10.11646/zootaxa.4543.3.4

Lethierry L, Severin G (1896) Catalogue général des Hémiptères. Tome III. Hétéroptères. R. Friedländer & Fils, Libraires-Éditeurs, Berlin, 275 pp.

Maldonado Capriles J (1976) The genus *Heza* (Hemiptera: Reduviidae). Journal of Agriculture of the University of Puerto Rico 60: 403–433.

Maldonado Capriles J (1983) Concerning new and old species of *Heza* (Hemiptera: Reduviidae). Journal of Agriculture of the University of Puerto Rico 67: 407–418.

Maldonado Capriles J (1990) Systematic catalogue of the Reduviidae of the World. Caribbean Journal of Science, Special publication No. 1, University of Puerto Rico, Mayagüez, 694 pp.

Maldonado Capriles J, Brailovsky H (1983) Mexican Reduviidae II: Genus *Heza* Amyot & Serville, 1843 (Hemiptera: Harpactorinae). Proceedings of the Entomological Society of Washington 85: 222–225.

Malipatil MB (1986) Revision of the Australian *Helonotus* Amyot and Serville (Heteroptera: Reduviidae). Journal of the Australian Entomological Society 25: 171–175. https://doi.org/10.1111/j.1440-6055.1986.tb01098.x

Malipatil MB (1991) The generic classification of the Australian Harpactorinae (Heteroptera: Reduviidae). Invertebrate Taxonomy 4: 935–971. https://doi.org/10.1071/IT9900935

McPherson JE, Ahmad I (2011) *Parasinea*, a new genus of assassin bug, with description of a new species from Colombia (Hemiptera: Heteroptera: Reduviidae). Annals of the Entomological Society of America 104: 1285–1291. https://doi.org/10.1603/AN11128

Schuh RT, Slater JA (1995) True Bugs of the World (Hemiptera: Heteroptera). Classification and natural history. Cornell University Press, Ithaca, NY, USA, 336 pp.

Schuh RT, Weirauch C, Wheeler WC (2009) Phylogenetic relationships within the Cimicomorpha (Hemiptera: Heteroptera): a total-evidence analysis. Systematic Entomology 34: 15–48. https://doi.org/10.1111/j.1365-3113.2008.00436.x

Stål C (1872) Enumeratio Reduviinorum Americae. In: Enumeratio Hemipterorum. Kongliga Svenska Vetenskaps-Akademiens Handlingar 10: 66–128.

Swanson DR (2012) A new synonym in the Harpactorinae of the New World (Heteroptera: Reduviidae). Proceedings of the Entomological Society of Washington 114: 250–254. https://doi.org/10.4289/0013-8797.114.2.250

Walker F (1873) Catalogue of the specimens of Hemiptera Heteroptera in the Collection of the British Museum (Part VIII). Printed for the Trustees of the British Museum, London, 220 pp.

Weirauch C (2008) From four- to three- segmented labium in Reduviidae (Hemiptera: Heteroptera). Acta Entomologica Musei Nationalis Pragae 48: 331–344.

Wygodzinsky P (1949) Elenco sistematico de los reduviiformes americanos. Instituto de Medicina Regional de la Universidad Nacional de Tucumán, Monografia 1: 1–102.

Zhang G, Hart ER, Weirauch C (2016) A taxonomic monograph of the assassin bug genus *Zelus* Fabricius (Hemiptera: Reduviidae): 71 species based on 10,000 specimens. https://doi.org/10.3897/BDJ.4.e8150

ZooKeys 872: 101–126 (2019)
doi: 10.3897/zookeys.872.36098
http://zookeys.pensoft.net

RESEARCH ARTICLE

A peer-reviewed open-access journal
ZooKeys
Launched to accelerate biodiversity research

New Oligoneuriidae (Insecta, Ephemeroptera) from Iran

Pavel Sroka[1], Jindřiška Bojková[2], Roman J. Godunko[1,3], Tomáš Soldán[1], Javid Imanpour Namin[4], Farshad Nejat[5], Ashgar Abdoli[5], Arnold H. Staniczek[6]

1 *Biology Centre of the Czech Academy of Sciences, Institute of Entomology, Branišovská 31, 37005 České Budějovice, Czech Republic* **2** *Department of Botany and Zoology, Masaryk University, Kotlářská 2, 61137 Brno, Czech Republic* **3** *Department of Invertebrate Zoology and Hydrobiology, University of Łódź, Banacha 12/16, 90237 Łódź, Poland* **4** *Department of Fishery, Faculty of Natural Resources, University of Guilan, POB 1144, Sowmehsara-Rasht, Iran* **5** *Department of Biodiversity and Ecosystem Management, Environmental Sciences Research Institute, Shahid Beheshti University, Daneshjou Boulevard, 1983969411 Tehran, Iran* **6** *Department of Entomology, State Museum of Natural History Stuttgart, Rosenstein 1, 70191 Stuttgart, Germany*

Corresponding author: *Roman J. Godunko* (godunko@seznam.cz)

Academic editor: *L. Pereira-da-Conceicoa* | Received 10 May 2019 | Accepted 11 July 2019 | Published 26 August 2019

http://zoobank.org/74312D7A-5950-447E-B777-CE828E53575A

Citation: Sroka P, Bojková J, Godunko RJ, Soldán T, Namin JI, Nejat F, Abdoli A, Staniczek AH (2019) New Oligoneuriidae (Insecta, Ephemeroptera) from Iran. ZooKeys 872: 101–126. https://doi.org/10.3897/zookeys.872.36098

Abstract

Two new species of the mayfly family Oligoneuriidae are described based on larval specimens recently collected in Iran. The first new species, *Oligoneuriella tuberculata* Godunko & Staniczek, **sp. nov.**, can be distinguished from all its congeners by the presence of pronounced protuberances posteromedially on abdominal terga, highly reduced paracercus, large lamella of gill I, and setation on hind margin of middle and hind femora confined to their basal halves. The second species, *Oligoneuriopsis villosus* Bojková, Godunko, & Staniczek, **sp. nov.**, remarkably belongs to a mostly Afrotropical genus. The new species clearly differs from all its congeners in the shape of setae on the surface of gills and terga, pattern of body colouration, and the shape of posterolateral projections of abdominal segments. Except for the species description, the generic diagnosis of *Oligoneuriopsis* Crass, 1947 is briefly discussed. COI barcode sequences of both new species are provided and molecular species delimitation is tested using distance-based and likelihood-based approaches, with both new species unambiguously recognised as separate lineages. The analysis of COI also corroborates the respective affinities of both new species, estimated based on morphology. The two new species of Oligoneuriidae described herein highlight the importance of the Middle East as a centre of diversity of this mayfly family within the Palaearctic.

Keywords

Barcoding, mayflies, Middle East, *Oligoneuriella*, *Oligoneuriopsis*, taxonomy, new species

Introduction

The mayfly fauna of Iran is still largely unexplored, although considerable progress has been achieved recently. Bojková et al. (2018) summarised the investigations on Iranian mayflies published to date to initiate a more systematic research on the topic. During an extensive field trip in 2017, new material of the family Oligoneuriidae was collected throughout Iran. Within this material, two new species were recognised, attributable to the genera *Oligoneuriella* Ulmer, 1924 and *Oligoneuriopsis* Crass, 1947 (generic concepts according to Bauernfeind and Soldán 2012).

Oligoneuriella occurs in the Palaearctic and comprises 14 species (Sroka et al. 2015). The Middle East hosts a relatively high diversity of *Oligoneuriella*, with six species recorded exclusively in this area (*O. bicaudata* Al-Zubaidi, Braasch & Al-Kayatt, 1987, *O. orontensis* Koch, 1980, *O. tskhomelidzei* Sowa & Zosidze, 1973, *O. magna* Bojková & Soldán, 2015, *O. paulopilosa* Sroka, 2015, *O. pectinata* Bojková & Soldán, 2015) and another two species occurring in large parts of the Palearctic, namely *O. rhenana* (Imhoff, 1852) and *O. pallida* (Hagen, 1855).

Oligoneuriopsis, the second genus, which we found in Iran, is probably closely related to *Oligoneuriella* (Edmunds 1961; Massariol 2017). The former genus includes six species, mostly distributed in the Afrotropics (Bauernfeind and Soldán 2012), with the only exception of *Oligoneuriopsis skhounate* Dakki & Giudicelli, 1980, which is known from the Palaearctic (North Africa and the Iberian Peninsula). It has to be mentioned that the delimitation of *Oligoneuriopsis* is problematic and its separation from *Oligoneuriella* is questionable (see Bauernfeind and Soldán 2012).

As a part of our study, we include new COI barcode sequences of *O. tskhomelidzei* and the two new species. We analyse these sequences to test the delimitation of the newly proposed species and compare them with all *Oligoneuriopsis* and *Oligoneuriella* species, for which COI sequences are available, namely *O. bicaudata*, *O. pallida*, *O. rhenana*, *O. skhounate*, and two unidentified species from Iraq and China.

Materials and methods

Collecting and morphological study

Material used for this study was collected by J. Bojková, R.J. Godunko, J. Imanpour Namin, F. Nejat, M. Pallmann, T. Soldán, and A.H. Staniczek during an investigation of different freshwater habitats in Iran. Samples were obtained by kick sampling and specimens were preserved in 96% EtOH. Environmental variables (pH, conductivity, salinity and temperature) were measured using a HACH sensION 5 portable waterproof conductivity meter and HACH Pocket Pro+ Multi 2. Some specimens were dissected and mounted on slides with HydroMatrix (MicroTech Lab, Graz, Austria) to allow detailed microscopic observations. Drawings were made using a stereomicroscope Olympus SZX7 and a microscope Olympus BX41, both equipped with a draw-

ing attachment. Serial habitus photographs were made with a Leica DMC5400 digital camera on a Leica Z16 APO Macroscope using Leica Application Suite Version 3.1.8 and Helicon Focus Pro to obtain stacked photographs with extended depth of field.

For scanning electron microscopy (SEM), eggs were dissected from female last instar larvae and also mouthparts, legs, and gills were dissected. All parts were subsequently dehydrated through a stepwise immersion in ethanol, dried by critical point drying (Leica EM CPD300), and mounted on SEM stubs. The mounted material was coated with a 5 nm Au/Pd layer (Leica EM ACE200) and subsequently examined and photographed with a Zeiss EVO LS 15 scanning electron microscope. All photographs were subsequently sharpened and adjusted in contrast and tonality in Adobe PhotoshopTM CS6.

Material is deposited in the collections of the Biology Centre CAS, Institute of Entomology, České Budějovice, Czech Republic (**IECA**), State Museum of Natural History, Stuttgart, Germany (**SMNS**), State Museum of Natural History, National Academy of Sciences of Ukraine, Lviv, Ukraine (**SNHM**), and the Natural History Museum and Genetic Resources, Department of Environment, Teheran, Iran (**MMTT_DOE**).

DNA extraction, PCR amplification, and sequencing

For DNA extraction, one severed leg of each specimen was processed with Qiagen DNeasy Blood & Tissue Kit following the manufacturer's instructions for tissue samples. The resulting DNA-elute was used in a PCR reaction with the primer pair of LCO1490 and HCO2198 for COI targeting, utilising a Thermo Scientific™ Phire Tissue Direct PCR Master Mix Kit for samples of *O. tskhomelidzei* and a Qiagen Multiplex PCR Kit for the two new species. The PCR amplification was performed as follows: Initial heat activation at 95 °C for 15 min and 35 cycles of denaturation at 94 °C for 0:30 min. For Thermo Scientific protocol, annealing was performed at 50 °C for 1:30 min and elongation at 68 °C for 0:45 min, for Qiagen protocol, annealing was performed at 56 °C for 1:30 min and elongation at 72 °C for 1:30 min. Both protocols followed a final elongation step at 72 °C for 10 min. The PCR products were enzymatically purified using ExoI/FAP. The purified product was sequenced via the EZ-seq single direct service by Macrogen (Amsterdam, Netherlands). Resulting chromatograms were assembled and final sequences were error checked using Geneious suite version 10.2.3. COI sequences were deposited at Barcode of Life Data Systems (http://www.boldsystems.org) under accession numbers specified in Table 1.

Analysis of sequences

We analysed COI to test the validity of the morphological species concept of both new species. COI of *O. tuberculata* sp. nov., *O. villosus* sp. nov., and *O. tskhomelidzei* were newly sequenced. Remaining sequences used in the analysed dataset were downloaded from GenBank and Bold Systems. Two sequences (one from *Oligoneuriopsis skhounate*

Table 1. List of specimens used for the COI analysis.

Species	Location	Voucher specimen collection code	Bold Process ID	GenBank accessionnumber	Source
O. rhenana	Germany	–	GBEPT372–14	KY261779	GenBank
	Italy	–	GBA22942–15	LN734762	GenBank
	Italy	–	GBA22943–15	LN734763	GenBank
	France	–	GBMIN65367–17	MF458765	GenBank
	Germany	–	GBEPT1975–14	KY261297	GenBank
	France	–	GBMIN65371–17	MF458760	GenBank
	Germany	–	GBEPT344–14	KY262278	GenBank
	France	–	GBMIN65370–17	MF458763	GenBank
	Germany	–	GBEPT1221–14	KY261341	GenBank
	Germany	–	FBAQU839–10	KY262106	GenBank
	Germany	–	FBAQU1261–12	KY262260	GenBank
O. pallida	Hungary	–	–	–	Massariol (2017)
	Hungary	–	GBMIN65365–17	KU609047	GenBank
O. tskhomelidzei	Iran	SMNS_EPH_7724_V_1	EPHIR014–19	–	newly sequenced
	Iran	SMNS_EPH_7596_V_4	EPHIR012–19	–	newly sequenced
	Iran	SMNS_EPH_7596_V_6	EPHIR013–19	–	newly sequenced
O. bicaudata	Iraq	–	BMIKU058–09	–	Bold Systems
	Iraq	–	BMIKU056–09	–	Bold Systems
	Iraq	–	BMIKU054–09	–	Bold Systems
O. tuberculata sp. nov.	Iran	SMNS_EPH_7574_V_1	EPHIR003–19	–	newly sequenced
	Iran	SMNS_EPH_7574_V_2	EPHIR004–19	–	newly sequenced
	Iran	SMNS_EPH_7574_V_4	EPHIR005–19	–	newly sequenced
	Iran	SMNS_EPH_7574_V_5	EPHIR006–19	–	newly sequenced
	Iran	SMNS_EPH_7574_V_6	EPHIR002–18	–	newly sequenced
Oligoneuriella sp. 1	Iraq	–	BMIKU059–09	–	Bold Systems
	Iraq	–	BMIKU040–09	–	Bold Systems
	Iraq	–	BMIKU037–09	–	Bold Systems
	Iraq	–	BMIKU031–09	–	Bold Systems
Oligoneuriella sp. 2	China	–	XJDQD857–18	–	Bold Systems
	China	–	XJDQD856–08	–	Bold Systems
O. skhounate	Spain	–	–	–	Massariol (2017)
O. villosus sp. nov.	Iran	SMNS_EPH_7550_V_2	EPHIR008-19	–	newly sequenced
	Iran	SMNS_EPH_7555_V_3	EPHIR011-19	–	newly sequenced
	Iran	SMNS_EPH_7555_V_2	EPHIR010-19	–	newly sequenced
	Iran	SMNS_EPH_7550_V_4	EPHIR009-19	–	newly sequenced
	Iran	SMNS_EPH_7550_V_1	EPHIR007-19	–	newly sequenced

and one from *Oligoneuriella pallida*) were obtained from Massariol (2017). Identical haplotypes were collapsed. Final alignment was constructed and edited using Geneious 11.0.4 (http://www.geneious.com) and contained fragments 359–655bp long (for details and accession numbers of individual sequences see Table 1).

To split a sequences alignment dataset into candidate species, the alignment was analysed using Automatic Barcode Gap Discovery (ABGD) (Puillandre et al. 2012) (http://wwwabi.snv.jussieu.fr/public/abgd/). This clustering method calculates the distance matrix and identifies the so-called barcode gap that would correspond to the threshold between intra- and interspecific genetic distances (Kekkonen et al. 2015). The settings were default, except for the X value (relative gap width), which was set to 1.0. The Jukes-Cantor (JC69) model was used, selected as best substitution model according to AICc in JmodelTest 2.1.10 (Darriba et al. 2012). The distances within and between recognised species were calculated in MEGA 7 (Kumar et al. 2016).

Species delimitation was also tested using single-loci coalescence based General Mixed Yule Coalescent model (GMYC) (Fujisawa and Barraclough 2013). The GMYC represents a model-based approach, aiming to discover the maximum likelihood solution for the threshold between the branching rates of speciation and coalescent processes on a tree (Kekkonen et al. 2015). The likelihood ratio test assesses if the mixed model fits the data significantly better than a null model that assumes a single coalescent process for the entire tree (Vuataz et al. 2011). Analyses were performed using the SPLITS package for R (http://r-forge.r-project.org/projects/splits).

An ultrametric COI gene tree was reconstructed under a relaxed molecular clock (uncorrelated lognormal distribution) using BEAST 2.4.8 (Bouckaert et al. 2014). An input file was generated in BEAUti 2. The best substitution model (from the models available in BEAST) was determined according to AICc as GTR using JmodelTest 2.1.10. A coalescent constant size tree prior was preferred, because the GMYC null model constitutes a single coalescent cluster (Vuataz et al. 2011, 2013). Other settings were default. MCMC chains were run for 50 million generations sampled every 5000 generations. Convergence and effective sample size were verified using Tracer 1.6. The first 10% of trees (1000) were discarded as burn-in. The maximum clade credibility tree was constructed from 9000 trees using TreeAnnotator 1.8.4 with default settings and visualised using FigTree 1.4.3.

Results and discussion

Oligoneuriella tuberculata **Godunko & Staniczek, sp. nov.**
http://zoobank.org/6CE696BD-36EF-443B-87FC-DB92E0E135C1
Figures 1–4, Table 2

Etymology. The name of the new species refers to the presence of protuberances posteromedially on terga, which is a character unknown for any other species of *Oligoneuriella*. A *tuberculum* is the Latin expression for protuberance.

Type material. ***Holotype*****:** Male larva, IRAN, Kohgiluyeh and Boyer-Ahmad Province, Kata, Marbor River, 31°10.71'N, 51°15.78'E, 1562 m a.s.l., 04.05.2017, leg. Staniczek A.H., Godunko R.J., Pallmann M. & Nejat, F. The holotype is deposited at SMNS under inventory number SMNS_EPH_7574_B_3.

Paratypes**:** 165 larvae, same locality as holotype (40 larvae deposited in SMNS under inventory numbers SMNS_EPH_7574_B_1 and SMNS_EPH_7574_B_2, including DNA voucher specimens with inventory numbers specified in Table 1, 20 larvae deposited in IECA, 100 larvae deposited in SNHM, and 5 larvae deposited in MMTT_DOE).

Localities and biology. The single known locality of *O. tuberculata* sp. nov. in Marbor River is situated in the southeastern part of the Zagros Mountains within the Khersaan River basin (Fig. 9), in close proximity to the Dena Protected Area. The majority of the drainage area is used as pasturage for a small amount of livestock, in nearer surroundings the land use is mainly for farming and rural, residential purposes.

Table 2. Summary of main larval characters of *O. villosus* sp. nov. and *O. tuberculata* sp. nov.

	***O. villosus* sp. nov.**	***O. tuberculata* sp. nov.**
Body length (mm)	13–16	>9–12 (fully mature larvae not available)
Colour pattern	greyish dark brown with distinctive light (yellowish) ornamentation	yellowish-white, light brown to light dirty olivaceous, without marked ornamentation
Compound eyes of male exceeding / not exceeding head margin laterally	slightly exceeding	unknown (fully mature male larvae not available)
Basal setae on paraglossae	sparse, slightly elongated, not arranged in rows	sparse, slightly elongated, not arranged in rows
Setae distally on segment I of labial palps	approx. 15–25, short, hair-like	more than 30, short, hair-like
Hair-like setae proximally on posterior margin of middle- and hind femora	dense and long, forming fringe along all length of femur	dense and long, forming fringe, reaching 1/3–1/2 of femur length
Submedial row of spine-like setae dorsally on fore tibiae	irregular row of bristle-like setae in distal quarter	3–4 setae arranged in irregular row subapically
Presence of posterolateral projections on abdominal segments	II–IX	(II) III–IX
Shape of posterolateral projections of last abdominal segments	bent outwards, apices slightly inwards	nearly straight, slightly diverging from body axis
Posteromedial setae on sterna III-IV	some more than 20× longer than wide	up to 10–15× longer than wide
Size of first gill plate compared to remaining pairs	markedly smaller	significantly larger
Setae on inner distal margin of gill plates II–VII	long	slightly elongated
Setae on ventral surface of gill plates near inner distal margin	present	absent
Paracercus	fully developed	vestigial

Marbor River at the type locality is a small, premontane river, 15–22 m wide, with depths up to 1.5–1.7 m (Fig. 10A). The river bed is braided and formed of coarse and fine gravel, with sparse cobbles. At the type locality the river formed two approximately equal branches with fast, turbulent flow (0.4–0.9 m/s), and a wide alluvium. The larvae inhabited the gravel substratum in the fast flow of the streamline, but were also found in the littoral zone.

Water quality at Marbor River was good, with conductivity 264 μS.cm, salinity 0.1 ‰, and temperature 15 °C.

The emergence of the species can be expected approximately between July and August, as all larvae collected here in May were small and only half-grown with small wing pads. Together with *O. tuberculata* sp. nov., only three other mayfly taxa were collected: *Baetis* (*Rhodobaetis*) sp. (Baetidae), *Rhithrogena* sp. (Heptageniidae) and *Epeorus* sp. (Heptageniidae).

Diagnosis. According to the combination of following diagnostic characters, *O. tuberculata* sp. nov. can be distinguished from all other representatives of the genus *Oligoneuriella* worldwide:

- Body pale, abdominal terga with inconspicuous, pale maculae laterally (Fig. 1A);
- eyes of male laterally not exceeding head margin (Fig. 1A, E);
- dorsal side of foretibia with 3–4 setae arranged into irregular row subapically (Fig. 2G);
- dense rows of long, hair-like setae on posterior margin of proximal 1/3–1/2 of middle- and hind femora (Fig. 2B, C);
- posterolateral processes of abdominal segments relatively narrow (Fig. 3G);
- terga II–IX with unpaired protuberance posteromedially (Fig. 3A, B);

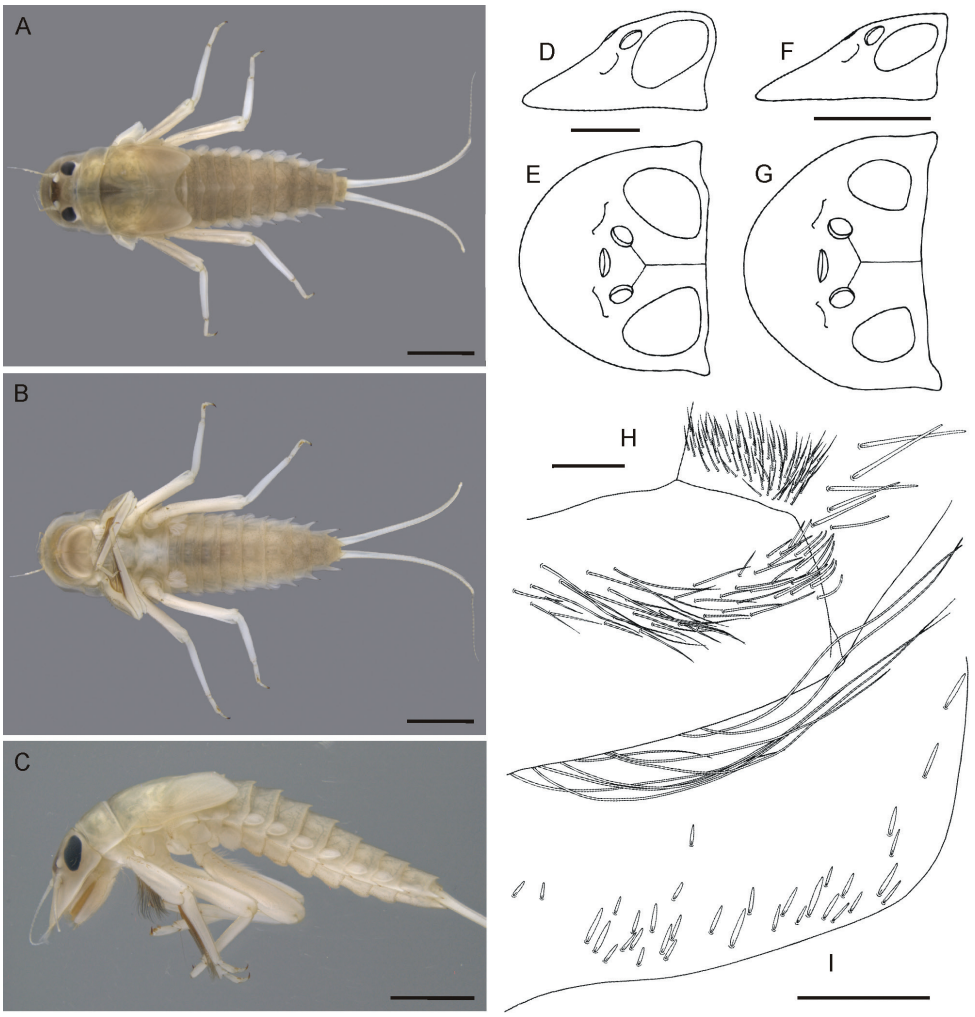

Figure 1. *Oligoneuriella tuberculata* sp. nov., larvae **A** habitus in dorsal view **B** habitus in ventral view **C** habitus in lateral view **D** head of male in lateral view (immature larva) **E** head of male in dorsal view (immature larva) **F** head of female in lateral view **G** head of female in dorsal view **H** detail of setae on distal part of labial palp segment I in dorsal view **I** detail of setae on proximal margin of paraglossae in ventral view. Scale bars: 2.0 mm (**A–C**); 0.5 mm (**D–G**); 0.1 mm (**H**); 0.2 mm (**I**). Same scale bar for **D** and **E**. Same scale bar for **F** and **G**.

- posteromedial flattened setae on sterna III–IV up to 10–15× longer than wide (Fig. 3D, E);
- first gill plate significantly larger than remaining gill plates, without ridge near outer margin dorsally (Fig. 4C, D);
- sparse setation on dorsal and ventral surfaces of gill plates II–VII (Fig. 4A, B, E–H);
- ventral surface of gill plates II–VII with setae sparsely scattered only along outer margin of ventral cavity (Fig. 4B, F, H);
- paracercus vestigial, approximately 5-segmented.

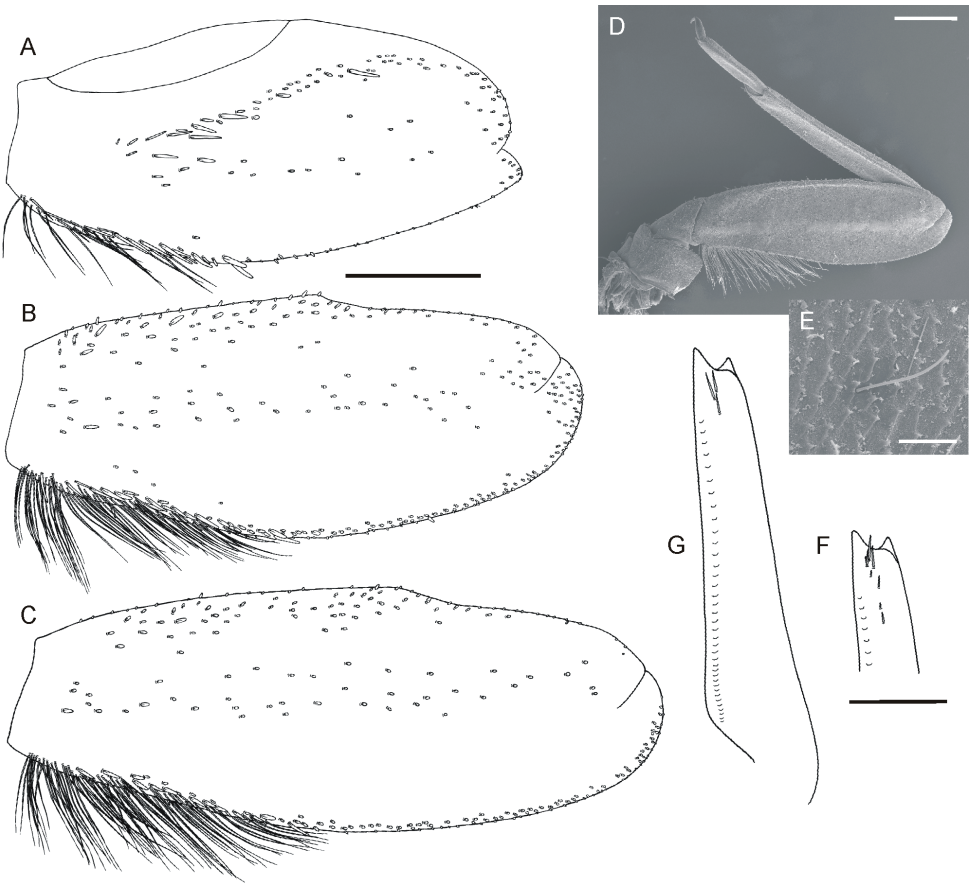

Figure 2. *Oligoneuriella tuberculata* sp. nov., larvae, legs **A** forefemur in dorsal view **B** middle femur in dorsal view **C** hind femur in dorsal view **D** middle leg under SEM in dorsal view **E** micro sculpture of leg cuticula under SEM in dorsal view **F** apical part of foretibia with subapical setae in ventral view **G** shape of foretibia with subapical setae in dorsal view. Scale bars: 0.5 mm (**A–D, F, G**); 0.02 mm (**E**). Same scale bar for **A–C**. Same scale bar for **F** and **G**.

Description. ***Larva.*** Submature larvae: body length 9–12 mm (female), 8–9 mm (male), length of cerci approximately 0.70–0.85× body length, paracercus vestigial, 5-segmented.

Colouration (Fig. 1A–C). General colour pale, yellowish-white, light brown to light dirty olivaceous; dorsal side darker than ventral one; pronotum with 2–3 small, pale, diffuse spots centrally; pro- and mesosternum whitish-yellow; abdominal terga with inconspicuous, pale maculae laterally; sterna uniformly yellowish.

Head. Pale, yellowish-brown to dirty olive, slightly darker centrally; ocellar area brown. Antennae unicoloured, yellow. Head width/length 1 : 1.1–1.3 in submature larvae (Fig. 1D–G). Eyes black, relatively elongated, not exceeding contour of head in dorsal view in male submature larvae (Fig. 1E); distance between eyes 0.5× narrower

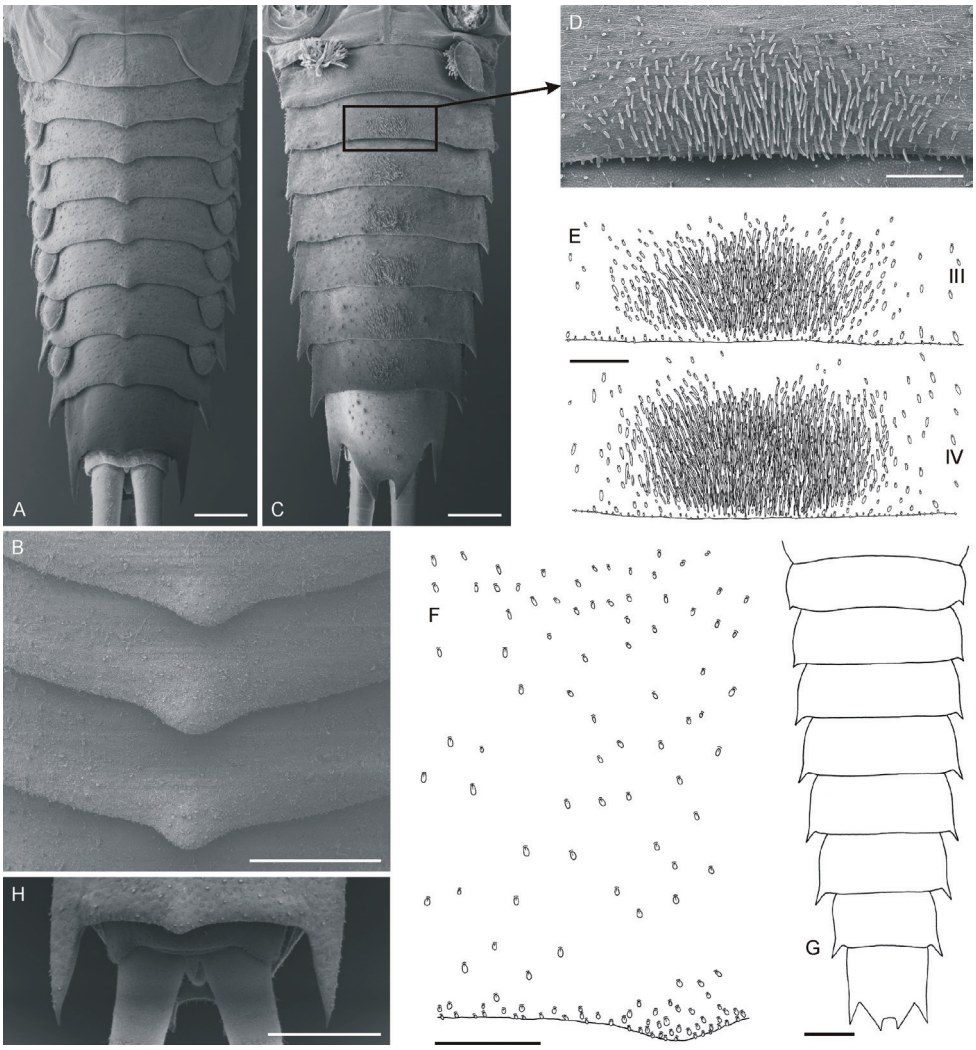

Figure 3. *Oligoneuriella tuberculata* sp. nov., larvae, abdomen **A** abdomen under SEM in dorsal view **B** detail of tergal protuberances under SEM **C** abdomen under SEM in ventral view **D** detail of setae on sternum III under SEM **E** detail of setae on sterna III and IV **F** detail of setae on surface of terga **G** outline of abdomen. **H** detail of abdomen tip under SEM with bases of cerci and vestigial paracercus. Scale bars: 0.5 mm (**A–C, H**); 0.2 mm (**D–F**); 1 mm (**G**).

than eye width in male and about 1.2× than eye width in female. Foremargin of head pale yellow, bordered by dense fringe of long bristle-like setae. Labium ventrally with short, flattened setae maximally 6.5–7.0× longer than wide, irregularly distributed along proximal margin of paraglossae (Fig. 1I). Dorsal side of first segment of labial palp with a group of more than 30 long pointed and short bluntly pointed setae; group of short setae not distinctly separated from long setae situated more proximally on first segment of labial palp (Fig. 1H).

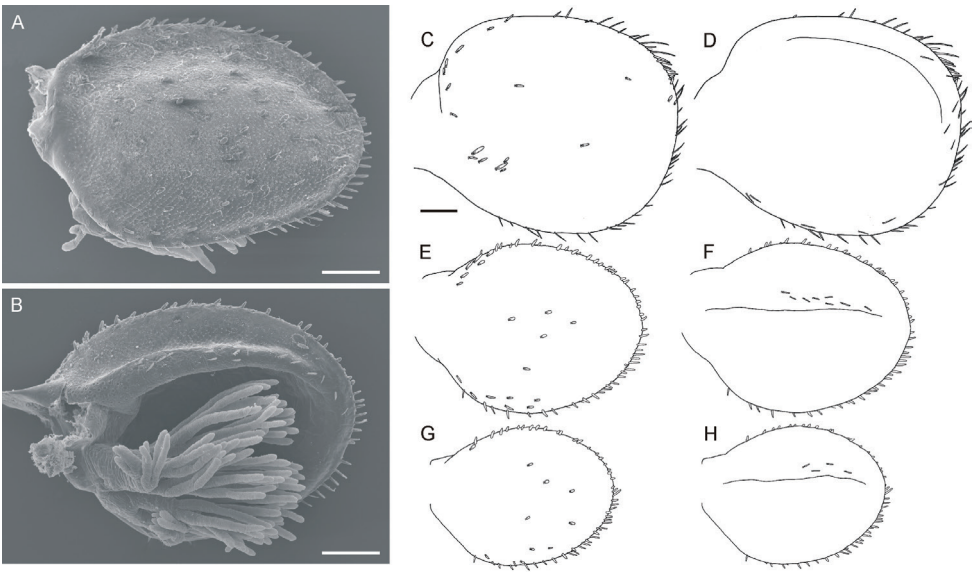

Figure 4. *Oligoneuriella tuberculata* sp. nov., larvae, gills **A** gill IV under SEM in dorsal view **B** gill IV under SEM in ventral view **C** gill plate I in dorsal view **D** gill plate I in ventral view **E** gill plate IV in dorsal view **F** gill plate IV in ventral view **G** gill plate VII in dorsal view **H** gill plate VII in ventral view. Scale bars: 0.1 mm (**A–H**). Same scale bar for **C–H**.

Thorax. Yellowish-brown to light dirty olive; base of wing pads with diffuse whitish maculation; two unclear whitish spots on mesonotum laterally; indistinct elongated maculae centrally. Pleural and ventral side paler than dorsal. Legs pale, whitish-yellow to yellow or slightly olivaceous, without any distinct ornamentation. Coxae and trochanters of same colour as other leg segments. Surface of legs covered with elongated bristles, spatulate and hair-like setae and small setae with star-like distal end (up to 15 μm long). Forecoxae with at least 30 long bristle-like setae distally and at least 20 long stout setae on inner margin. Foretrochanters with tuft of dense, long bristle-like setae distally. Femora unicoloured, occasionally with small diffuse spot distally. Forefemora length 2.0–2.1× of their width; dorsal surface covered with few flattened setae of various length, arranged in irregular sparse rows near filtering setae centrally; sparse row of stout bristle-like setae extends along 1/3–1/4 of length of outer margin, and 13–17 short bluntly pointed setae in submarginal area (Fig. 2A). Filtering setae of femora and tibiae brown, unicoloured. Foretibiae with sparse setae along distal third of ventral side of foretibia (Fig. 2F); dorsal side with 3–4 setae arranged in irregular row in subapical part (Fig. 2G). Foretarsi with 2–3 bluntly pointed setae distally. Foreclaws moderately sclerotised at apex, with 4–5 denticles. Middle and hind coxae and trochanters with sparse setae of different size irregularly on surface. Femora of middle and hind legs with dense rows of long (longer than half of femur width) hair-like setae along 1/3–1/2 of posterior margin of femora; numerous thicker flattened and spine-like setae along posterior margin of proximal half of femora; small sparse spatulate setae scattered on

dorsal surface of femora, forming irregular rows centrally; distal margin with setae of same shape, concentrated proximally and centrally, alternating with few elongated hair-like setae (Fig. 2B–E). Tibiae of middle and hind legs with few short hair-like and spatulate setae irregularly grouped subapically and apically. Tarsi of middle and hind legs with 4–5 elongated bluntly pointed or rounded setae apically, 6–7 hair-like setae along inner margin (as long as tarsi or shorter), alternating with 2–3 shorter stout setae subapically. Claws of middle and hind legs with 5–7 denticles.

Abdomen (Fig. 3). Yellowish-brown to dirty olive; indistinct diffuse pale maculae laterally; terga darker than sterna. Posterolateral processes relatively narrow, present on abdominal segments II–IX; processes on segment II indistinct. Apices of posterolateral processes well sclerotised. Posterolateral processes on segments IV–IX prominent, with outer margins nearly straight, slightly diverging from body axis; posterolateral processes of segment IX largest, with axes nearly parallel to body axis (Fig. 3G). Terga II–IX with unpaired posteromedial protuberance, rounded apically (Fig. 3A, B). Surface of terga covered evenly by very short spatulate setae rounded apically (Fig. 3F); number of setae on surface of terga gradually decreases from tergum II to IV; few flattened spatulate setae rounded apically (8–12 μm long; 9–10 μm wide) cover also posterolateral processes and terga I, V–X. Sterna covered with posteromedial groups of flattened setae, rounded apically (Fig. 3D, E). Length of these setae varies from 15–75 μm on sterna II and III; up to 100 μm on sterna IV–VIII; size of flattened setae gradually increases from sterna II to VII; individual setae are up to 10–15× longer than wide. Large group of setae assembled predominantly posteromedially on sterna II–VIII. Sternum IX covered only with sparse spatulate setae (up to 12 μm long), few elongated flattened setae up to 20 μm long, and numerous hair-like setae. Sternum IX with deep U-shaped incision posteriorly between two pointed, strongly sclerotised processes.

Gills (Fig. 4). Gill I significantly larger than following gills, rounded and symmetric, without ridge near outer margin; gills II–VII circular. Size ratios between gills I and IV approximately 1 : 0.7 (length) and 1 : 0.6 (width). All gill pairs equipped with bundle of whitish filaments, usually shorter than respective gill plate. Dorsal surface of gill I with sparse flattened setae concentrated mainly proximally (Fig. 4C). On lateral margins of gill plates, setae relatively short; setae bordering inner part of distal margin slightly longer (up to 25–30 μm long). Ventral surface of gill I with few isolated submarginal setae distally (up to 25 μm long, Fig. 4D); these setae strongly plumose, similar to setae occurring on ventral surface of following gill pairs. Sparse setation on dorsal and ventral surfaces of gills II–VII; dorsal surface covered with short spatulate setae (Fig. 4A, E, G); ventral surface with relatively short plumose setae sparsely scattered centrally along outer margin of ventral cavity (Fig. 4B, F, H).

Cerci whitish, unicoloured, with inner marginal fringe of fine, hair-like setae. Paracercus vestigial, 5-segmented (Fig. 3H).

Egg, imago, and subimago. Unknown.

Affinities. Among the Palaearctic genera of Oligoneuriidae, attribution of *O. tuberculata* sp. nov. to the genus *Oligoneuriella* is obvious, based on the shape of head, legs, and gills (see Bauernfeind and Soldán 2012). In the worldwide key to Oligoneu-

riidae genera published by Edmunds (1961), *O. tuberculata* sp. nov. erroneously would key out to the Nearctic and Neotropical genus *Lachlania* Hagen, 1868 due to the presence of a highly reduced paracercus. Edmunds (1961) at that time had not been aware of any *Oligoneuriella* species with reduced paracercus, since such species were only described later (Al-Zubaidi et al. 1987, Sroka et al. 2015). Despite the superficial resemblance of *O. tuberculata* sp. nov. to *Lachlania*, they differ in their setation on the anterior head margin. In *O. tuberculata* sp. nov., there are long, bristle-like setae (as in all *Oligoneuriella*). In *Lachlania* these setae are short and spatulate, which represents a crucial larval apomorphy of *Lachlania* (see Kluge 2004). In fact, *Lachlania* phylogenetically represents a quite distant lineage from *Oligoneuriella* and *Oligoneuriopsis* (Massariol et al. 2017). Relatively long setae medially on sterna II–V in *O. tuberculata* sp. nov. suggest a closer relationship with *Oligoneuriopsis*, but a large lamella of gill I and a short row of setae on the posterior margin of femora excludes this attribution (see the discussion on *O. villosus* sp. nov. below).

Within *Oligoneuriella*, the most closely related species to *O. tuberculata* sp. nov. are *O. bicaudata* Al-Zubaidi et al. 1987 from Iraq and *O. pectinata* Bojková & Soldán, 2015 from Turkey. Both species share with *O. tuberculata* sp. nov. the reduction of the paracercus to only a few segments, large lamella of gill I compared to other gill pairs, and the extent of setation on the posterior margin of middle and hind femora forming long and dense fringe. Nevertheless, *O. tuberculata* sp. nov. can be differentiated from both species by several characters:

(i) The first gill plate is markedly larger than gill pairs II–VII, nearly circular and symmetric, without a ridge near the outer margin in *O. tuberculata* sp. nov. In contrast, *O. pectinata* has an oval gill I, only slightly larger than the remaining gill pairs, with an indistinct ridge close to the outer margin (see Fig. 4C, D; Sroka et al. 2015: 341, fig. 46a, b). In *O. bicaudata*, the size ratio of gill I and remaining gill pairs is similar to *O. tuberculata* sp. nov., although the shape of gill plates is slightly different. In *O. tuberculata* sp. nov., the gill plate I is more circular (Fig. 4C, D), whereas in *O. bicaudata* it is rather elongated, narrowing proximally (Al-Zubaidi et al. 1987: fig. 5).

(ii) The setation on the surface of gills: in *O. tuberculata* sp. nov., dorsal and ventral surface of the gill I is equipped with very few flattened setae (Fig. 4C, D), whereas in *O. pectinata* relatively dense setation occurs, especially on the ventral surface (Sroka et al. 2015: 341, fig. 46a, b). The setae on the ventral surface of gills are strongly plumose in both species. However, these setae are shorter (up to 25 μm long) in *O. tuberculata* sp. nov. than in *O. pectinata* (up to 32 μm long) (Sroka et al. 2015: 344, fig. 66a). Lateral margins of the first gill are equipped with rich, long setae in *O. pectinata*, in contrast to *O. tuberculata* sp. nov. with relatively short setae along margins (Fig. 4C, D). Details of gill setation are unknown for *O. bicaudata*.

(iii) All three species can be separated by the shape of abdominal segments. Unpaired posteromedial protuberances on terga are characteristic for *O. tuberculata* sp. nov. (Fig. 3A, B), as they are lacking in *O. pectinata* and Al Zubaidi et al. (1987) did not mention any protuberances on the terga of *O. bicaudata*. Thus, given the conspicu-

ousness of this character, we consider it plausible to assume that the protuberances are absent in this species. Moreover, the protuberances are missing in the material identified as *O. bicaudata* collected near the type locality of this species in Iraq (Al-Saffar, pers. comm). Furthermore, posterolateral processes of the abdominal segments II–VII are relatively narrow, slightly bent outwards in *O. tuberculata* sp. nov. (Fig. 3G), in contrast to relatively robust and straight processes in *O. pectinata*. In *O. bicaudata*, these processes are very thin, curved inward apically, especially on segment IX (Al-Zubaidi et al. 1987, fig. 2).

(iv) All three species have a pale body colouration and an inconspicuous colour pattern on the abdominal terga. However, *O. pectinata* is slightly darker, with a pair of diffuse median spots on terga, whereas *O. tuberculata* sp. nov. is characterised by the presence of diffuse maculae laterally. Abdomen of *O. bicaudata* is pale brown, without any distinct pattern (Al-Zubaidi et al. 1987).

An analysis of diagnostic characters based on adults is impossible at present, as adults are not known for *O. tuberculata* sp. nov. and *O. bicaudata*. The colouration pattern and size of eyes would slightly differ in fully mature larvae from the material described herein.

***Oligoneuriopsis villosus* Bojková, Godunko, & Staniczek, sp. nov.**
http://zoobank.org/3980D827-DA07-40CE-BE30-F997FE5EDBCC
Figures 5–8, Table 2

Etymology. The name of the new species originates from Latin, meaning hairy, and refers to the dense setation along outer margins of femora and tibiae.

Type material. ***Holotype*:** Male larva, IRAN, Khuzestan Province, right tributary of Marun Rud River, W of Bagh Malek, 31°31.23'N, 49°49.31'E (locality no. 93), 585 m a.s.l., 29.04.2017, leg. Bojková J., Soldán T. & Imanpour Namin J. The holotype is deposited in IECA.

***Paratypes*:** 64 larvae, same locality as holotype, deposited in IECA. Eight larvae, IRAN, Khuzestan Province, Balarud River (right tributary of Dez River), N of Andimeshk, 32°35.29'N, 48°17.32'E (locality no. 80), 230 m a.s.l., 26.04.2017, leg. Bojková J., Soldán T., & Imanpour Namin J., deposited in IECA.

70 larvae, IRAN, Hormozgan Province, Shamil River, Shamil, 27°29.66'N, 56°52.25'E, 63 m a.s.l., 30.04.2017, leg. Staniczek A.H., Godunko R.J., Pallmann M., & Nejat F. (20 larvae deposited in IECA, 20 larvae deposited in SNHM, 20 larvae deposited in SMNS under accessory numbers SMNS_EPH_7555_B_1 and SMNS_EPH_7555_B_2, including DNA voucher specimens with inventory numbers specified in Table 1, and 10 larvae deposited in MMTT_DOE).

110 larvae, IRAN, Hormozgan Province, Roudan River, 5 km N of Dehbarez, 27°28.46'N, 57°15.28'E, 217 m a.s.l., 30.04.2017, leg. Staniczek A.H., Godunko R.J., Pallmann M., & Nejat F. (20 larvae deposited in IECA, 70 larvae deposited in SNHM, and 20 larvae deposited in SMNS under inventory numbers SMNS_EPH_7550_B_1

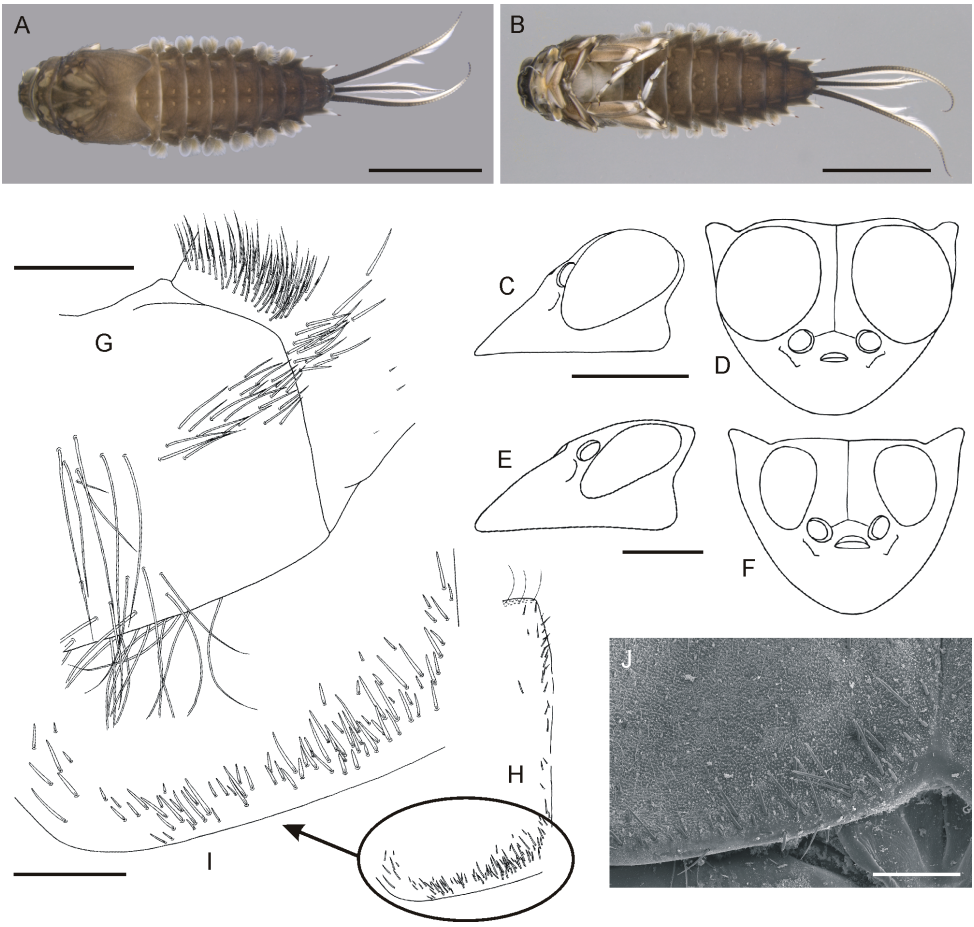

Figure 5. *Oligoneuriopsis villosus* sp. nov., larvae **A** habitus in dorsal view **B** habitus in ventral view **C** head of male in lateral view **D** head of male in dorsal view **E** head of female in lateral view **F** head of female in dorsal view **G** detail of setae on distal part of labial palp segment I in dorsal view **H–I** setae on paraglossae in ventral view **J** detail of basal portion of paraglossae under SEM in ventral view. Scale bars: 5 mm (**A, B**); 1 mm (**C–F**); 0.2 mm (**G–J**). Same scale bar for **C** and **D**. Same scale bar for **E** and **F**.

and SMNS_EPH_7550_V_1–5, including DNA voucher specimens with inventory numbers specified in Table 1).

Localities and biology. Larvae were collected in two rivers at the southern slopes of Zagros Mountains (right tributary of Marun Rud River and Balarud River) and two other localities (Shamil River and Roudan River) in Hormozgan Province at the western edge of Makran, a semi-desert coastal strip, which stretches along the Gulf of Oman (Fig. 9). Extensive land use is present in most parts of the drainage area, mainly for agricultural and residential matters in all localities. In Marun Rud River basin, the agricultural use is more intense than in other localities and there are several urban settlements in the drainage area of this river.

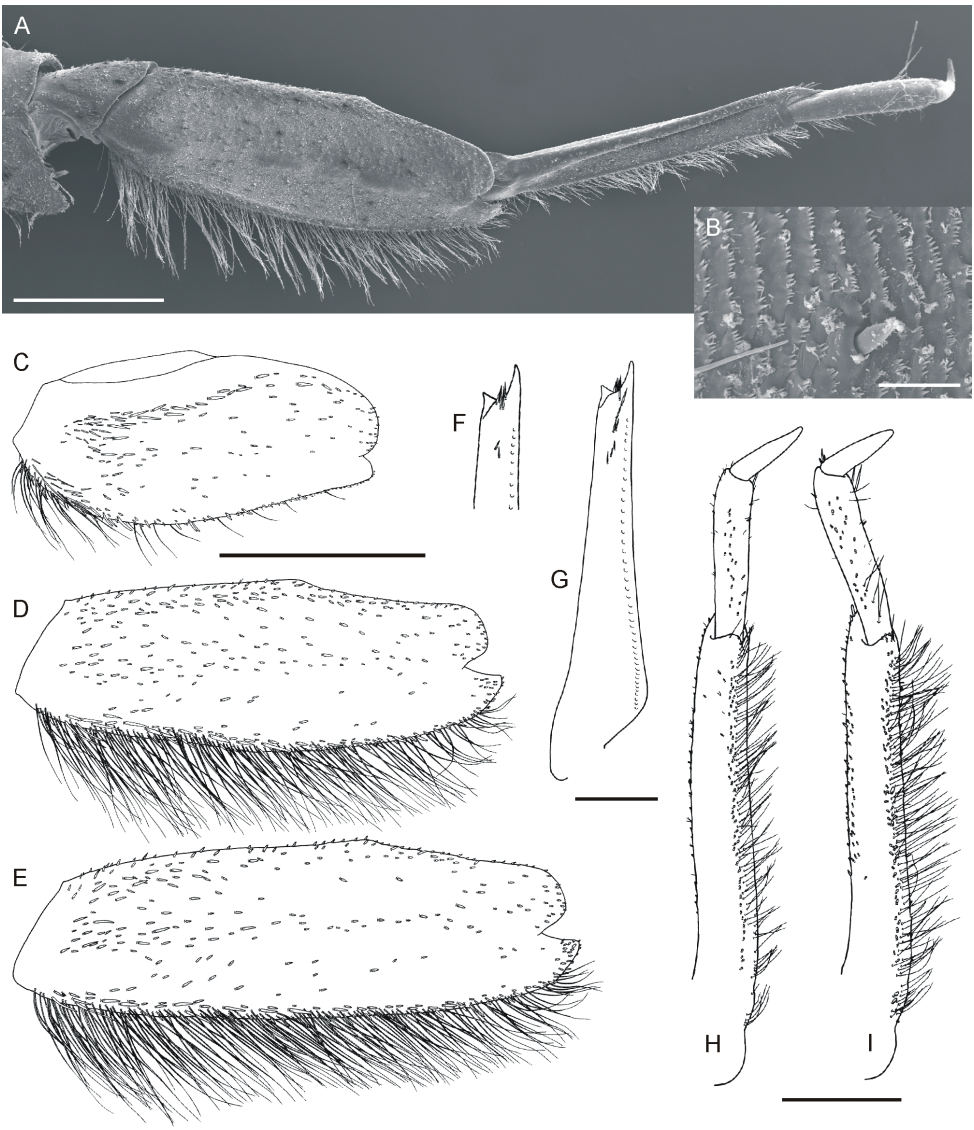

Figure 6. *Oligoneuriopsis villosus* sp. nov., larvae, legs **A** hind leg under SEM in dorsal view **B** micro sculpture of leg cuticula under SEM in dorsal view **C** forefemur in dorsal view **D** middle femur in dorsal view **E** hind femur in dorsal view **F** apical part of foretibia with subapical setae in ventral view **G** shape of foretibia with subapical setae in dorsal view **H** middle tibia and tarsus in dorsal view **I** hind tibia and tarsus in dorsal view. Scale bars: 1 mm (**A, C–E**); 0.02 mm (**B**); 0.5 mm (**F–I**). Same scale bar for **C, D** and **E**. Same scale bar for **F** and **G**. Same scale bar for **H** and **I**.

The species was generally found in shallow river sections (up to 50 cm) with a riverbed composed of coarse and fine gravel, sometimes in combination with cobbles. The localities with the occurrence of this species represented rather small rivers; how-

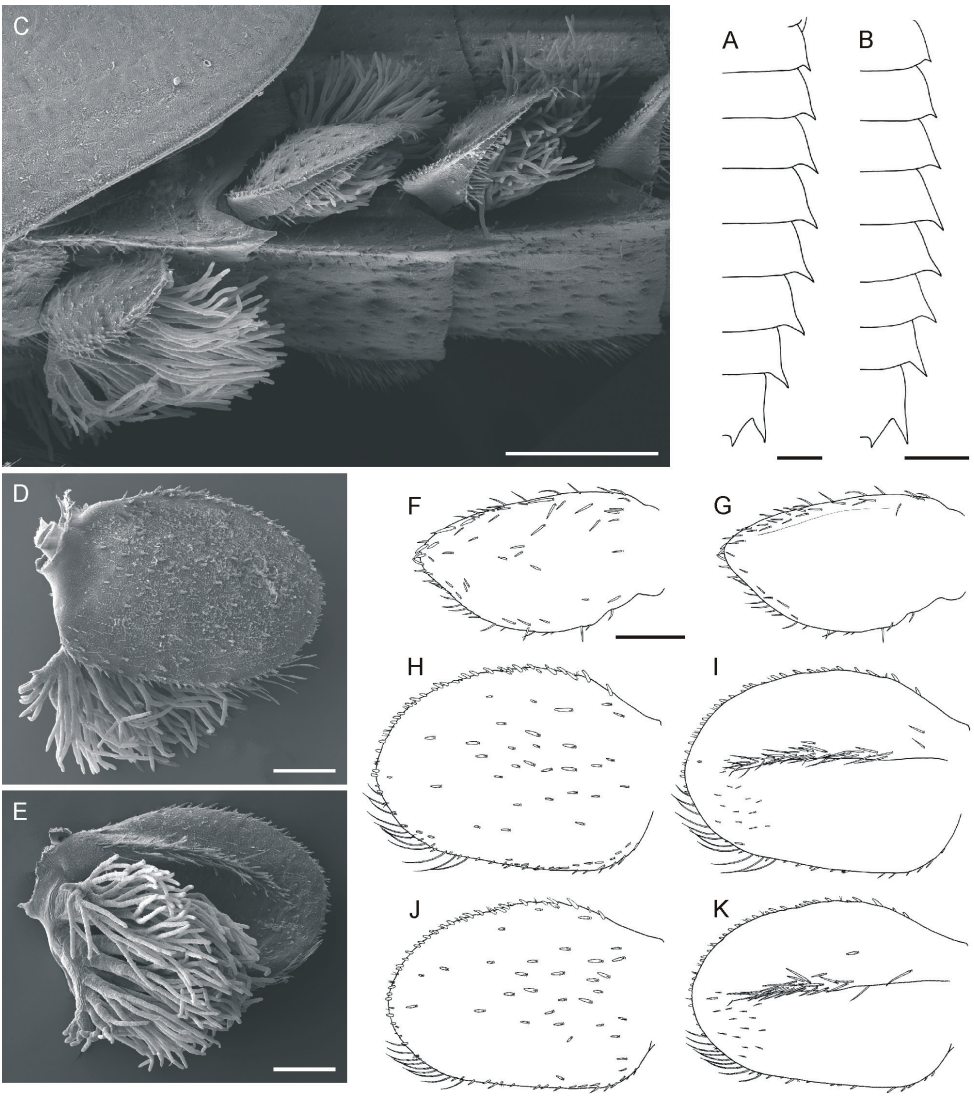

Figure 7. *Oligoneuriopsis villosus* sp. nov., larvae, abdomen and gills **A** abdomen outline, male **B** abdomen outline, female **C** proximal portion of abdomen under SEM in lateral view **D** gill IV under SEM in dorsal view **E** gill IV under SEM in ventral view **F** gill plate I in dorsal view **G** gill plate I in ventral view **H** gill plate IV in dorsal view **I** gill plate IV in ventral view **J** gill plate VII in dorsal view **K** gill plate VII in ventral view. Scale bars: 1 mm (**A, B**); 0.5 mm (**C**); 0.2 mm (**D–K**). Same scale bar for **F–K**.

ever, the stream width varied from 4 to 40 m, depending on the river discharge rates at the end of March (Fig. 10B–D).

Larvae were predominantly distributed in river sections with accelerated current and with a minimum amount of alluvial silt. Large larvae (more than 1 cm) were found along stony margins of riffles, while small and medium-sized larvae (up to 1 cm) dwelt anywhere in the riffles.

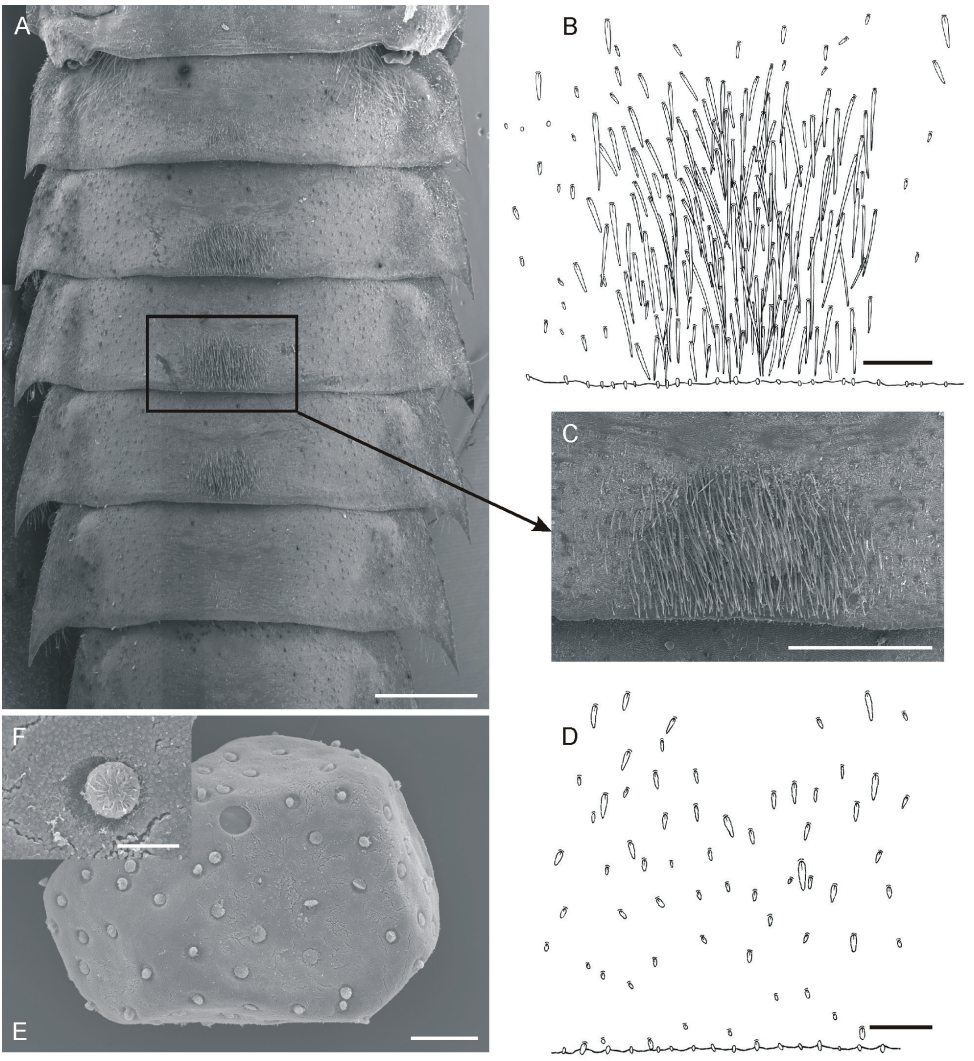

Figure 8. *Oligoneuriopsis villosus* sp. nov., larvae and eggs **A** general view of basal part of abdomen under SEM in ventral view **B** detail of setae on sternum IV **C** detail of setae on sternum IV under SEM **D** detail of setae on surface of terga **E** egg, general view **F** detail of egg chorionic structure. Scale bars: 1 mm (**A**); 0.1 mm (**B, D**); 0.5 mm (**C**); 0.05 mm (**E**); 0.01 mm (**F**).

Water quality at collection sites in Khuzestan Province was good, with pH 8.0–8.4, conductivity 620–760 μS.cm^{-1}, salinity 0.3–0.4 ‰, and temperature 21–29 °C (conductivity and salinity measured on two localities only – the tributary of Marun Rud River and Balarud River). At collection sites in Hormozgan Province, abiotic factors were as following: conductivity 1520-1646 μS.cm, salinity 0.8 ‰, and temperature 32–34 °C.

Emergence of the species can be expected between June and July, as most of larvae occurring in all the localities were small and/or middle-sized at the time of collection. Mayfly taxa found in the same localities included: *Baetis* s. str. (Baetidae), *Labiobaetis*

Figure 9. Map of Iran with localities of *Oligoneuriella tuberculata* sp. nov. (star) and *Oligoneuriopsis villosus* sp. nov. (circles).

sp. (Baetidae), *Nigrobaetis* sp. (Baetidae), *Rhithrogena* sp. (Heptageniidae), *Electrogena* sp. (Heptageniidae), *Choroterpes* sp. (Leptophlebiidae), *Caenis* sp. (Caenidae), and *Prosopistoma* sp. (Prosopistomatidae).

Diagnosis. According to the combination of following diagnostic characters, *O. villosus* sp. nov. can be distinguished from all other representatives of the genus *Oligoneuriopsis* worldwide:

- head widest across posterolateral corners (Fig. 5D, F);
- row of long setae along all length of middle- and hind femora and tibiae (Fig. 6A, D, E, H, I);
- posteromedian projections on abdominal terga absent (Fig. 5A);
- colouration of abdominal terga dark brown with two pale dots medially (Fig. 5A);

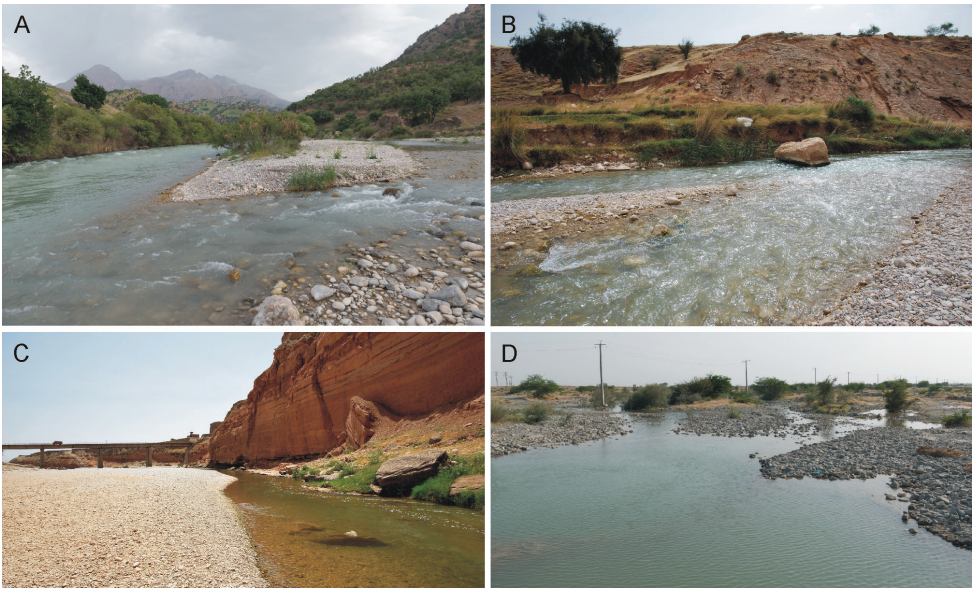

Figure 10. Photos of the localities with occurrence of *Oligoneuriella tuberculata* sp. nov. and *Oligoneuriopsis villosus* sp. nov. **A** Marbor River near Kata (type locality of *O. tuberculata* sp. nov.) **B** right tributary of Marun Rud River near Bagh Malek (type locality of *O. villosus* sp. nov.) **C** Balarud River near Andimeshk (locality of *O. villosus* sp. nov.) **D** Shamil River near Shamil (locality of *O. villosus* sp. nov.).

- setae on surface of terga and gills elongated and bluntly pointed (Figs 7F, H, J, 8D);
- posterolateral projections of abdominal segments diverging from body axis (Fig. 7A, B);
- posteromedial setae on sterna III–IV very long and dense, some more than 20× longer than wide (Fig. 8A–C);
- first gill plate markedly smaller than the remaining pairs (Fig. 7F, G);
- setae on inner distal margin of gill plates II–VII long (Fig. 7H–K);
- setae on ventral surface of gill plates near inner distal margin present (Fig. 7I, K);
- paracercus fully developed (Fig. 5A, B);
- caudal filaments dark in proximal half, distinct dark band in the middle missing (Fig. 5A, B).

Description. ***Larva.*** Mature larvae: body length 13–16 mm (female), 11–12 mm (male), length of cerci approximately 0.4–0.5× body length, paracercus slightly shorter.

Colouration (Fig. 5A, B). Head, thorax and abdomen greyish dark brown with distinctive light (yellowish) ornamentation. When fixed in ethanol, general colouration paler, brown. Legs yellowish with distinctive brown ornamentation forming bands. This colouration apparent only in larger larvae, more than 1 cm long. Smaller larvae uniformly pale, yellowish.

Head. Greyish dark brown, foremargin of head darker, occipital area with yellowish ornamentation forming four longitudinal stripes merging behind ocellar part of head. Antennae yellowish brown proximally, brown distally. Head width/length 1 : 1.2 (Fig. 5C–F). Eyes black, slightly exceeding contour of head in dorsal view in males; distance between eyes 2.2× narrower than eye width in males and 1.5× wider than eye width in females (Fig. 5D, F). Foremargin of head dark, bordered by dense fringe of long bristle-like setae. Labium ventrally with numerous flattened setae of different length not arranged in rows along proximal margin of paraglossae (Fig. 5H–J). Similar setae also situated sparsely along inner margin of paraglossae (Fig. 5H). Dorsal side of first segment of labial palp with group of 15–25 thin setae distally (Fig. 5G).

Thorax. Greyish dark brown, with yellowish spots submedially on prothorax and yellowish spots and longitudinal stripes on mesothorax. Pleural and ventral part of thorax brown. Legs yellowish-brown, with distinct brown ornamentation (Fig. 5B). Coxae and trochanters brown. Proximal half of femora brown, distal half yellowish-brown. Tibiae with narrow brown bands distally and proximally, tarsi with narrow brown band distally. Forecoxae distally with numerous long, bristle-like setae and with about 15 long, thin hair-like setae on inner margin. Foretrochanters distally with numerous long, bristle-like setae. Forefemora length 2–2.5× width; dorsal surface of forefemora covered with scattered flattened setae of various length; dense group of pointed long flattened setae submarginally near filtering setae; outer margin of forefemora bordered by conspicuous fringe of long hair-like setae (Fig. 6C). Filtering setae of femora and tibiae brown. Foretibiae dorsally with irregular row of bristle-like setae in distal quarter (Fig. 6G); ventrally with 2–3 subapical setae and several setae apically (Fig. 6F). Foretarsi distally with groups of pointed setae. Foreclaws heavily sclerotised at apex, with 6–7 denticles. Middle and hind femora and tibiae with dense fringe of long, hair-like setae along entire length of outer margin (Fig. 6A, D, E, H, I). Some hair-like setae present on outer margin of tarsi as well (Fig. 6I). Fringes of hair-like setae on femora and middle and hind tibiae are apparent also in (pale) early-instar larvae.

Abdomen. Greyish dark brown, with pair of submedian smudged yellowish spots and conspicuous sublateral yellowish pattern (Fig. 5A). Ventral part of abdomen greyish dark brown, with conspicuous yellowish pattern (Fig. 5B). Posterolateral processes present on abdominal segments II–IX; bent outwards, apices slightly inwards (Fig. 7A, B). Terga sparsely covered with flattened setae of various sizes mixed with numerous microtrichia, largest setae elongated and bluntly pointed apically (Fig. 8D). Some sterna with densely assembled setae posteromedially (most prominent on sterna III–IV, present also on sternum V). Individual setae distinctly elongated, some more than 20× longer than wide, see Fig. 8A–C). Sternum IX with wide rounded incision posteriorly, equipped with tiny spines.

Gills (Fig. 7). Gill I asymmetric, bluntly pointed apically (Fig. 7F, G), markedly smaller and more elongated than following gills, which are oval and almost symmetric (Fig. 7D, E, H–K). Size ratio between gill I and IV approximately 0.8 : 1 (length) and 0.7 : 1 (width). All gill pairs equipped with bundle of whitish filaments slightly shorter than respective gill plate (filaments are slightly longer in gill I). Dorsal surface of gill

I covered with elongated setae of various size (Fig. 7F). Ventral surface of gill I with submarginal setae only (Fig. 7G). Dorsal surface of gills II–VII with sparsely scattered, elongated, and bluntly pointed setae (Fig. 7D, H, J). Similar setae occurring also on margins of gill plates. Setae bordering inner part of distal margin relatively long (Fig. 7H–K). Ventral surface of gill plates II–VII with numerous hair-like setae along outer margin of ventral cavity (Fig. 7E, I, K). These setae slightly plumose. Second group of minute setae situated near inner distal margin (Fig. 7I, K).

Cerci dark brown, lighter towards apex, with inner marginal fringe of fine hair-like setae. Paracercus reaching approx. 2/3 of cerci length, with dense setation laterally (Fig. 5A, B).

Egg. Shape of eggs studied deformed due to extraction from mature larvae (Fig. 8E). Eggs 250–320 μm long and 190–240 μm wide; chorionic surface covered with circled terminal fibre clusters (diameter 10 μm). Micropyle shallow, circular; sperm guide well apparent (Fig. 8E). Terminal fibre clusters finely sculptured, with leaf-like, flat microstructures (Fig. 8F).

Imago and subimago. Unknown.

Affinities. The establishment of the generic attribution of *O. villosus* sp. nov. is not straightforward, although affinities to the genera *Oligoneuriella* Ulmer, 1924 and *Oligoneuriopsis* Crass, 1947 are obvious based on the shape of head, legs, and gills (see Edmunds 1961; Bauernfeind and Soldán 2012). However, differences between *Oligoneuriella* and *Oligoneuriopsis* are very subtle and the separation of these genera is not clear. The first description of the genus *Oligoneuriopsis* was published by Crass (1947), with the type species *Oligoneuriopsis lawrencei* Crass, 1947, mainly based on the adult stage. Its larva was not described in detail, but briefly commented as being identical to larvae described and depicted earlier by Barnard (1940), who assigned them to "*Elassoneuria trimeniana*". This opinion is followed by later authors, for example Demoulin (1970). Edmunds (1961) considered *Oligoneuriopsis* as closely related to *Oligoneuriella*. In the larval key to genera, the presence of the lamella of gill I in *Oligoneuriella* and its absence in *Oligoneuriopsis* was used as the crucial diagnostic character separating the genera (Edmunds 1961). Nevertheless, Agnew (1980) clearly stated that this character is not valid, since a small lamella is present also in *Oligoneuriopsis*, including the type species *O. lawrencei*. Instead, he proposed the arrangement of the setae medially on abdominal sterna being more developed in *Oligoneuriopsis* than in *Oligoneuriella* as a reliable diagnostic character. Bauernfeind and Soldán (2012) mentioned more conspicuous, very long setae medially on sterna, lamella of gill I reduced, membranous, and cerci with dark band in the middle as diagnostic for *Oligoneuriopsis*. In our view, the length of posteromedial setae on sterna probably mostly represents a reliable character, although it varies, and the setae are reported 3–6× longer than wide in known species of *Oligoneuriella* (Sroka et al. 2015) and even more than 10× longer than wide in *Oligoneuriella tuberculata* sp. nov., described above. However, in *O. villosus* sp. nov., some of these setae are more than 20× longer than wide (Fig. 8B, C), which fulfils the criteria for *Oligoneuriopsis* and roughly also agrees with our observation of setae length in *Oligoneuriopsis skhounate* from North Africa. We observed that the lamella of gill I in *O. skhounate* is small-sized

compared to other gills, but structurally not different. The same condition applies also to *O. villosus* sp. nov. (Fig. 7C). A clearer morphological definition of *Oligoneuriopsis* would be possible after a more thorough study of the Afrotropical material, including the type species *O. lawrencei*, as already pointed out by Bauernfeind and Soldán (2012). Ideally such a study should also include adults, since several adult characters separating *Oligoneuriella* from *Oligoneuriopsis* have been published, mostly concerning wing venation and male genitalia (Bauernfeind and Soldán 2012).

At this time, we consider it justified to assign the new species to *Oligoneuriopsis* based on following characters shared with *O. skhounate* (and presumably also with other Afrotropical representatives of *Oligoneuriopsis*): (i) setae posteromedially on abdominal sterna very long, some more than 20× longer than wide; (ii) lamella of gill I significantly smaller than remaining gill pairs; and (iii) row of setae along entire length of posterior margin of femora and outer margin of tibiae on middle and hind legs. The second and third characters are also depicted in the figures provided by Barnard (1940), presumably representing the larva of *O. lawrencei*, which supports their diagnostic value for the separation of *Oligoneuriopsis* from *Oligoneuriella*.

In the genus *Oligoneuriopsis*, six species have been described up to now (Bauernfeind and Soldán 2012). Five of them are distributed exclusively in the Afrotropics; only a single species, *O. skhounate*, occurs also in the Palaearctic (North Africa and the Iberian Peninsula). The occurrence of Afrotropical species in Iran is extremely unlikely (even more when taking into account that most species are known from South Africa only). Nevertheless, all these species can be morphologically distinguished from *O. villosus* sp. nov. (except *O. dobbsi* (Eaton, 1912) with unknown larva).

Oligoneuriopsis lawrencei Crass, 1947 differs in the shape of head, widest anterior to the eyes (Agnew 1973, fig. 1) contrary to *O. villosus* sp. nov. with the head widest across posterolateral corners (Fig. 5D, F). Furthermore, *O. lawrencei* possesses very long setae on margin of gill plates (Agnew 1980, fig. 8). *O. jessicae* Agnew, 1973 profoundly differs by having posteromedial spine-like projections on abdominal terga (Agnew 1973, fig. 1), missing in *O. villosus* sp. nov. (Fig. 5A). *O. elisabethae* Agnew, 1973 differs from *O. villosus* sp. nov. in colouration. *O. elisabethae* exhibits a uniform light brown colour, without any indication of an abdominal pattern (Agnew 1973), whereas *O. villosus* sp. nov. possesses a distinct pair of submedian, smudged, yellowish spots and a conspicuous, sublateral, yellowish pattern on the dorsal side of abdomen (Fig. 5A).

The nearest distributed congeneric species *O. skhounate* is morphologically similar to *O. villosus* sp. nov. It even shares the colouration pattern of legs with alternating darker and lighter bands (Fig. 5B; Dakki and Giudicelli 1980, figs 28, 29). Nevertheless, several morphological characters allow the separation of these two species: (i) setae on the surface of gills and terga are shorter in *O. skhounate*, longer and more pointed in *O. villosus* sp. nov. (Fig. 8D); (ii) colouration is different, prominent posteromedian pale spot on terga in *O. skhounate* (Dakki and Giudicelli 1980, fig. 20) is missing in *O. villosus* sp. nov. (Fig. 5A). Moreover, the dark band at half length of caudal filaments, depicted for *O. skhounate* (Dakki and Giudicelli 1980; fig. 20), is also missing in *O. villosus* sp. nov. (Fig. 5A, B); (iii) in *O. skhounate*, posterolateral projections of abdomi-

nal segments are oriented parallel to the body axis, and lateral margins of individual segments are convex (Dakki and Giudicelli 1980, fig. 20). In *O. villosus* sp. nov., posterolateral projections of abdominal segments are diverging from the body axis, with lateral margins straight or slightly concave (Fig. 7A, B).

Al-Zubaidi and Al-Kayatt (1986) without further details already reported findings of *Oligoneuriopsis* sp. from north Iraq. An unidentified species of *Oligoneuriopsis* was also collected recently from the same area and deposited in the Bold database as *Oligoneuriopsis* sp. MAA01. This record contains two barcode sequences, which are not publicly accessible, but exhibiting 90.03–90.63% similarity to the haplotypes of *O. villosus* sp. nov. sequenced in the present study. This level of similarity rather corresponds with interspecific distances found in Oligoneuriidae (see Fig. 11C). Therefore, we may assume the existence of more *Oligoneuriopsis* species in the Middle East.

Molecular species delimitation

The ABGD analysis of the COI distance matrix generated 11 stable groups (Fig. 11A). The mean genetic distances within groups generated by ABGD ranged between 0.003 and 0.011 and the mean distances between groups between 0.060 and 0.234; for the histogram of distances see Fig. 11C.

The GMYC model recognised 11 ML entities, with confidence interval 11–11 (Fig. 11A, B). We used single threshold GMYC, since multiple threshold is prone to over splitting species that are not evenly sampled throughout its distributional area (Fujisawa and Barraclough 2013; Hrivniak et al. 2019). The Maximum Likelihood of GMYC model was 197.4186, compared to the likelihood of the null model 181.5407. The likelihood ratio test significantly rejected the null model expecting uniform coalescent branching rates across entire tree (likelihood ratio=31.75579, p=1.271505e-07).

The clusters delimited as distinct species were congruent in both approaches. Both methods of the molecular species delimitation also unambiguously supported the designation of *O. tuberculata* sp. nov. and *O. villosus* sp. nov., which were recovered as distinct units in both analytical approaches. Apart from the two new species described herein, previously known species recognised as distinct entities in both ABGD and GMYC included *O. pallida*, *O. bicaudata*, *O. tskhomelidzei*, and *O. skhounate*. The species identified morphologically as *O. rhenana* was split into three putative COI species, which indicates that this widely distributed taxon (occurring in most of Europe, see Bauernfeind and Soldán 2012) actually represents a species complex. The putative cryptic species within *O. rhenana* were left undescribed for the moment, since extensive material was not at our disposal. Within the dataset, a further two unidentified putative species were recognised, one from China and one from Iraq. These clusters possibly represented a further two undescribed species, left unnamed for the time being.

The analysis of COI corroborated the affinity of *O. villosus* sp. nov. to *Oligoneuriopsis*. From the taxa included, *O. villosus* sp. nov. exhibited the highest sequence similarity with *O. skhounate* from Southern Spain. However, the distance

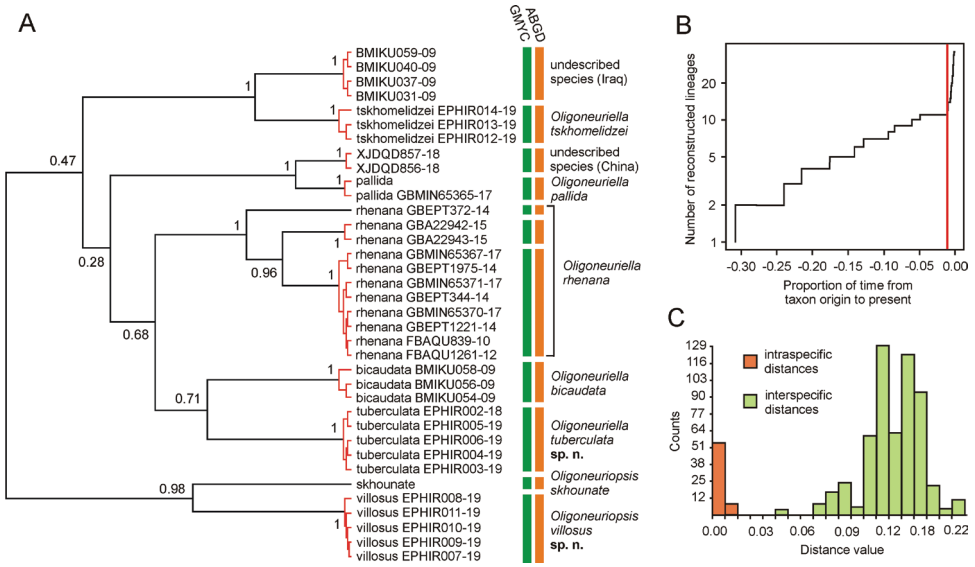

Figure 11. Results of the molecular species delimitation: **A** maximum clade credibility COI gene tree. The red branches represent species delimited by GMYC. Columns on the right illustrate groups delimited by both approaches used **B** lineage through time plot, generated by GMYC. The red vertical line indicates the threshold time between inter- and intraspecific branching **C** distribution of distances calculated by ABGD.

between *O. villosus* sp. nov. and *O. skhounate* clearly separated them into two distinct species. Regarding the affinities of *O. tuberculata* sp. nov., *O. bicaudata* was recovered as the most closely related species from the ones sequenced, which is in accordance with the morphological character distributions.

Acknowledgements

We are grateful to M. Sartori (Musée cantonal de zoologie, Lausanne) for consultations concerning the systematic placement of *O. villosus* sp. nov. and to M. Al-Saffar for information on *O. bicaudata*. The authors are grateful to Milan Pallmann (SMNS) for assistance in the field and to Anne-Kristin Schilling (SMNS) for DNA isolation and sequencing. Two reviewers, Luke Jacobus, Indiana University – Purdue University Indianapolis, USA, and Helen James, Albany Museum, Makhanda, South Africa, provided valuable suggestions and comments that helped to improve the manuscript. We thank the Faculty of Natural Resources of the University of Gilan, the Department of Biodiversity and Ecosystem Management, Environmental Sciences Research Institute, Shahid Beheshti University, Tehran, and the Department of Environment, Natural History Museum and Genetic Resources, Tehran, for collaboration, support, sampling and export permits, and accompanying the authors during field trips. This research was conducted with institutional support RVO: 60077344 for PS, RJG and TS, and was part of the SMNS Research Incentive 2017 to AHS.

References

Agnew JD (1973) Two new species of *Oligoneuriopsis* Crass from the Republic of South Africa (Oligoneuriidae: Ephemeroptera). In: Peters WL, Peters JG (Eds) Proceedings of the first international conference on Ephemeroptera, Florida, August 1970. Brill, Leiden, 114–121.

Agnew JD (1980) Ultrastructural studies on Oligoneuriidae taxonomic applications. In: Flannigan JF, Marshall KE (Eds) Advances in Ephemeroptera Biology. Plenum Press, New York, 353–366. https://doi.org/10.1007/978-1-4613-3066-0_29

Al-Zubaidi F, Al-Kayatt A (1986) A preliminary survey of mayflies from the north of Iraq. Journal of Biological Sciences Research 17(2): 147–151.

Al-Zubaidi F, Braasch D, Al-Kayatt A (1987) Mayflies from Iraq (Insecta, Ephemeroptera). Faunistische Abhandlungen, Staatliches Museum für Tierkunde Dresden 14: 179–184.

Barnard KH (1940) Additional records, and descriptions of new species, of South African alder-flies (Megaloptera), May-flies (Ephemeroptera), caddis-flies (Trichoptera), stone-flies (Perlaria), and dragon-flies (Odonata). Annals of the South African Museum 32: 609–661.

Bauernfeind E, Soldán T (2012) The Mayflies of Europe. Apollo Books, Ollerup, 781 pp.

Bojková J, Sroka P, Soldán T, Imanpour Namin J, Staniczek AH, Polášek M, Hrivniak L, Abdoli A, Godunko RJ (2018) Initial commented checklist of Iranian mayflies (Insecta: Ephemeroptera), with new area records and description of *Procloeon caspicum* sp. n. (Baetidae). ZooKeys 749: 87–123. https://doi.org/10.3897/zookeys.749.24104

Bouckaert R, Heled J, Kühnert D, Vaughan T, Wu C-H, Xie D, Suchard MA, Rambaut A, Drummond AJ (2014) BEAST 2: A Software Platform for Bayesian Evolutionary Analysis. PLoS Computational Biology 10(4): e1003537. https://doi.org/10.1371/journal.pcbi.1003537

Crass RS (1947) The May-flies (Ephemeroptera) of Natal and the Eastern Cape. Annals of the Natal Museum 11(1): 37–110.

Dakki M, Giudicelli J (1980) Éphéméroptères d'Afrique du Nord. 2 – Description d'*Oligoneuriella skoura* n. sp. et d'*Oligoneuriopsis skhounate* n. sp., avec notes sur leur ecologie (Ephem., Oligoneuriidae). Bulletin de l'Institut Scientifique (Rabat) 4: 13–28.

Darriba D, Taboada GL, Doallo R, Posada D (2012) jModelTest 2: more models, new heuristics and parallel computing. Nature Methods 9: 772. https://doi.org/10.1038/nmeth.2109

Demoulin G (1970) Ephemeroptera des faunes Éthiopienne et malgache. South African Animal Life 14: 24–170.

Edmunds Jr GF (1961) A key to the genera of known nymphs of the Oligoneuriidae (Ephemeroptera). Proceedings of the Entomological Society of Washington 63(4): 255–256.

Fujisawa T, Barraclough TG (2013) Delimiting Species Using Single-Locus Data and the Generalized Mixed Yule Coalescent Approach: A Revised Method and Evaluation on Simulated Data Sets. Systematic Biology 62(5): 707–724. https://doi.org/10.1093/sysbio/syt033

Hrivniak Ľ, Sroka P, Türkmen G, Godunko RJ, Kazancı N (2019) A new *Epeorus* (*Caucasiron*) (Ephemeroptera: Heptageniidae) species from Turkey based on molecular and morphological evidence. Zootaxa 4550(1): 58–70. https://doi.org/10.11646/zootaxa.4550.1.2

Massariol FC (2017) Sistemática e Biogeografia de Oligoneuriidae Ulmer, 1914 (Insecta: Ephemeroptera). PhD Thesis, Universidade Federal do Espírito Santo, Vitória.

Kekkonen M, Mutanen M, Kaila L, Nieminen M, Hebert PDN (2015) Delineating Species with DNA Barcodes: A Case of Taxon Dependent Method Performance in Moths. PLoS ONE 10(4): e0122481. https://doi.org/10.1371/journal.pone.0122481

Kumar S, Stecher G, Tamura K (2016) MEGA7: Molecular Evolutionary Genetics Analysis Version 7.0 for Bigger Datasets. Molecular Biology and Evolution 33(7): 1870–1874. https://doi.org/10.1093/molbev/msw054

Puillandre N, Lambert A, Brouillet S, Achaz G (2012) ABGD, Automatic Barcode Gap Discovery for primary species delimitation. Molecular Ecology 21(8): 1864–77. https://doi.org/10.1111/j.1365-294X.2011.05239.x

Sroka P, Bojková J, Soldán T, Godunko RJ (2015) New species of the genus *Oligoneuriella* Ulmer, 1924 (Ephemeroptera: Oligoneuriidae) from Turkey. Zootaxa 4012: 329–350. https://doi.org/10.11646/zootaxa.4012.2.4

Vuataz L, Sartori M, Wagner A, Monaghan MT (2011) Toward a DNA taxonomy of Alpine *Rhithrogena* (Ephemeroptera: Heptageniidae) using a mixed Yule-coalescent analysis of mitochondrial and nuclear DNA. PLos ONE 6(5): e19728. https://doi.org/10.1371/journal.pone.0019728

Vuataz L, Sartori M, Gattolliat J-L, Monaghan MT (2013) Endemism and diversification in freshwater insects of Madagascar revealed by coalescent and phylogenetic analysis of museum and field collections. Molecular Phylogenetics and Evolution 66(3): 979–991. https://doi.org/10.1016/j.ympev.2012.12.003

ZooKeys 872: 127–158 (2019)
doi: 10.3897/zookeys.872.36288
http://zookeys.pensoft.net

RESEARCH ARTICLE

A peer-reviewed open-access journal
ZooKeys
Launched to accelerate biodiversity research

A first phylogenetic study on stoloniferous octocorals off the coast of Kota Kinabalu, Sabah, Malaysia, with the description of two new genera and five new species

Yee Wah Lau[1], James D. Reimer[1,2]

1 *Molecular Invertebrate Systematics and Ecology Laboratory, Graduate School of Engineering and Science, University of the Ryukyus, 1 Senbaru, Nishihara, Okinawa 903-0213, Japan* **2** *Tropical Biosphere Research Center, University of the Ryukyus, 1 Senbaru, Nishihara, Okinawa 903-0213, Japan*

Corresponding author: *Lau YW* (lauyeewah87@gmail.com)

Academic editor: *B.W. Hoeksema* | Received 17 May 2019 | Accepted 12 July 2019 | Published 26 August 2019

http://zoobank.org/BDF92DBF-34CE-4600-939D-2573C7D4F0B4

Citation: Lau YW, Reimer JD (2019) A first phylogenetic study on stoloniferous octocorals off the coast of Kota Kinabalu, Sabah, Malaysia, with the description of two new genera and five new species. ZooKeys 872: 127–158. https://doi.org/10.3897/zookeys.872.36288

Abstract

Sabah, Malaysia, is well known for its extensive and diverse coral reefs. It is located on the northwestern edge of the Coral Triangle, the region with the highest marine biodiversity. Much of the marine fauna here is still unknown, especially inconspicuous animals, such as small stoloniferous octocorals, which are common on coral reefs. Here, we describe two new monospecific genera of the family Arulidae found off the coast of Kota Kinabalu, Sabah, East Malaysia; *Bunga payung* **gen. nov. et sp. nov.** and *Laeta waheedae* **gen. nov. et sp. nov.** As well, the stoloniferan genus *Phenganax* Alderslade & McFadden, 2011 belonging to the family Clavulariidae is expanded with three new species, *P. marumi* **sp. nov.**, *P. subtilis* **sp. nov.**, and *P. stokvisi* **sp. nov.**, which are all sclerite-free. Additionally, we report a possibly undescribed species, closely related to the clavulariid genera *Azoriella* Lopez-Gonzalez & Gili, 2001 and *Cervera* Lopez-Gonzalez et al., 1995. As this and other recent studies have shown, discoveries of small stoloniferous octocorals are helping to fill gaps in our knowledge of the overall systematics of Octocorallia.

Keywords

28S rDNA, Arulidae, biodiversity, Clavulariidae, COI, Coral Triangle, mtMutS, ND6, Stolonifera, systematics, TARP, taxonomy

Introduction

Coral reefs fringe one-sixth of the world's coastlines and constitute the most biologically diverse shallow-water marine ecosystems, supporting thousands of species (Birkeland 1997; Reaka-Kudla 1997; Roberts et al. 2002). The estimated global biodiversity of coral reefs is approximately 950,000 (±40%) species, of which 90% are not yet described (Fisher et al. 2015). One reason marine biodiversity is globally underestimated is that there are many small and cryptic species that are usually overlooked in diversity assessments (Wolf et al. 1983; Hoeksema 2017; Lau et al. 2018, 2019; Sabroux et al. 2019). An estimate from 2002 indicated that 25% of the world's coral reefs have already been severely damaged due to global warming (Goreau et al. 2000; Roberts et al. 2002), pollution, and destructive fisheries methods (dynamite and poison) (Polunin and Roberts 1996; Roberts et al. 2002; Hughes et al. 2017; Heery et al. 2018). Damage continues to accumulate (Hughes et al. 2018), thus threatening coral reef biodiversity and possibly causing the extinction of organisms that have not been scientifically described yet (Carpenter et al. 2008; Hoeksema 2017).

The highest concentrations of coral reef species can be found in the Coral Triangle in the Central Indo-Pacific (Hoeksema 2007, 2017). Continuing analyses have resulted in the boundaries of the Coral Triangle biodiversity hotspot being refined over time (Hoeksema 2007; Huang et al. 2015; Veron et al. 2015; Lane and Hoeksema 2016). The coastline of Sabah, on the northern tip of East Malaysia, is located within the area that makes up the outer western edge of the Coral Triangle (Hoeksema 2007; Waheed and Hoeksema 2013, 2014; Waheed et al. 2015a). Malaysia is known for its extensive coral reefs that cover an area of approximately 4000 km^2 with the majority (>75%) situated in Sabah (Burke et al. 2002; Waheed et al. 2007). Sabah (with its offshore islands) has an extensive history of marine research, focusing mainly on scleractinian diversity and coral cover (Lulofs 1973; Lulofs et al. 1974; Wood 1977, 1979; Mathias and Langham 1978; Nyanti and Johnston 1992; Pilcher and Cabanban 2000; Waheed and Hoeksema 2013, 2014; Reef Check Malaysia 2014, Waheed et al. 2015a, 2015b), and reef fish (Kassem et al. 2012; Reef Check Malaysia 2014; Townsend 2015).

Just off the coast of Kota Kinabalu, the capital of Sabah, there is an assemblage of five islands that make up Tunku Abdul Rahman Park (TARP): Gaya, Manukan, Sapi, Sulug, and Mamutik islands cover an area of approximately 50 km^2, including their surrounding reefs and sea (Spait 2001; Reef Check Malaysia 2014; Waheed and Hoeksema 2014). TARP has been protected since 1977 and is reserved and managed by Sabah Parks. Despite the protection of the coral reefs in the park against destructive fishing and land-based developments (Spait 2001; Waheed et al. 2007), the coral cover in the park has seen a severe decline since 1994 owing to continued anthropogenic influences and a major crown-of-thorns starfish outbreak (Praveena et al. 2012; Waheed and Hoeksema 2014; Heery et al. 2018), emphasizing the urgent need for diversity research and taxonomic documentation.

For the shallow waters of the Indo-Pacific, over 100 genera in 23 families of Alcyonacea (e.g., Alderslade 2001, 2002; Fabricius and Alderslade 2001; Benayahu et al. 2004; van Ofwegen 2005), nine genera in five families of Pennatulacea (Williams

1996), and two genera in two families of Helioporacea have been described (Fabricius et al. 2007; Miyazaki and Reimer 2015). However, compared to scleractinian corals, octocorals have received little research attention and are less well documented (Fabricius and Alderslade 2001; Breedy and Cortés 2008; McFadden et al. 2010; Samimi-Namin and Van Ofwegen 2012). Despite Sabah's location within the area that makes up the outer western edge of the Coral Triangle (Hoeksema 2007; Waheed and Hoeksema 2014; Waheed et al. 2015a), and the fact that octocorals are an abundant and species-rich group on Indo-Pacific coral reefs, relatively little research has been done on octocorals in Sabah (Kassem et al. 2012).

Zooxanthellate octocorals are, however, similarly affected by global climate change and other anthropogenic and natural threats (Prada et al. 2010; Dias et al. 2016; Van de Water et al. 2018). Additionally, octocorals are one of the most widely distributed and common benthic groups, occurring from shallow tropics to the Antarctic deep sea, and are important members of the benthic community, providing refuge and habitat for numerous organisms (Sánchez et al. 2003; Sánchez 2016). Due to their abundance, diverse structural complexity, and symbiotic relationships, octocorals play an important role in the energy transfer between plankton and other benthos (Van de Water et al. 2018) and should receive more research attention. However, research focused on octocorals is still uncommon, and the importance of their taxonomy is underestimated (McFadden and Ofwegen 2012; Benayahu et al. 2017; Conti-Jerpe and Freshwater 2017). This is particularly true for one group of octocorals, namely species of the subordinal group Stolonifera, many of which are inconspicuous, with small polyps (often ~2–3 mm in diameter) and colonies, and are hard to find, one reason for the scant amount of information available for this group (Wolf et al. 1983; McFadden and Ofwegen 2012). In the TARP area, next to sponges, algae, and hard corals, soft corals are the most dominant benthic fauna (Reef Check Malaysia 2014), however, research focusing on octocorals is completely lacking here. Therefore, there may be undescribed species, especially given the geographical location of TARP on the edge of the Coral Triangle.

The present study is the first investigation into the stoloniferous octocorals in and around the TARP area, off the coast of Kota Kinabalu, Sabah, Malaysia, and aims to improve on our understanding of the phylogenetic relationships of stoloniferous octocorals within the Octocorallia radiation. Based on our findings, we formally describe two new monotypic genera within Arulidae and three new species within the genus *Phenganax* Alderslade & McFadden, 2011 within Clavulariidae.

Materials and methods

Specimen collection

A total of 25 stoloniferous octocoral specimens (Table 1) was collected from eight locations (Figure 1) in and around TARP, off the coast of Kota Kinabalu, Sabah, Malaysia, between 20 and 27 March 2018. Specimens were collected at depths of 4–18 m by

Table 1. Overview of stoloniferous octocoral specimens collected from off NW Sabah, used in this study; including GenBank accession numbers and locality. Key: catalogue number: NSMT = National Museum of Nature and Science, Tokyo, Japan; IPMB = Borneo Marine Research Institute, Sabah, Malaysia; n.a. = not available.

Family	Species	Catalogue/ voucher number	Location	GPS (DMS)	GenBank accession numbers			
					28S rDNA	COI	mtMutS	ND6
Arulidae	*Bunga payung* gen. nov. et sp. nov.	IPMB-C 01.00017	Sepangar, E Sepangar Is.	06°03'38.66"N, 116°04'0.65"E	MN164539	n.a.	n.a.	MN164587
	B. payung gen. nov. et sp. nov. (holotype)	NSMT-Co 1679	Sepangar, E Sepangar Is.	06°03'38.66"N, 116°04'0.65"E	MN164540	MN164559	n.a.	MN164588
	Laeta waheedae gen. nov. et sp. nov.	IPMB-C 01.00018	Mid Reef, E Manukan Is.	05°58'35.8"N, 116°00'52.2"E	MN164542	MN164561	MN164583	MN164590
		IPMB-C 01.00019	Gaya Clement Reef, E Gaya Is.	06°01'24.26"N, 116°00'13.55"E		MN164562	MN164584	MN164591
	L. waheedae gen. nov. et sp. nov. (holotype)	NSMT-Co 1680	Udar, W Udar is.	06°4'49.81"N, 116°5'13.16"E	MN164541	MN164560	MN164582	MN164589
	Clavulariidae sp.	NSMT-Co 1686	Edgell Patches, W Sapi Is.	06°00'38.7"N, 115°59'22.2"E	MN164543	MN164563	MN164580	n.a.
		IPMB-C 01.00016	Gaya Clement Reef, W Gaya Is.	06°01'24.26"N, 116°00'13.55"E	MN164544	MN164564	MN164581	n.a.
Clavulariidae	*Phenganax marumi* sp. nov.	IPMB-C 01.00001	Edgell Patches, W Sapi Is.	06°00'38.7"N, 115°59'22.2"E	MN164545	MN164570	n.a.	MN164595
		IPMB-C 01.00002	Mid Reef Slope, E Manukan Is.	05°58'38.08"N, 116°00'52.82"E	MN164546	MN164571	n.a.	MN164596
		IPMB-C 01.00003	Mid Reef Slope, E Manukan Is.	05°58'38.08"N, 116°00'52.82"E	n.a.	MN164572	n.a.	MN164597
		IPMB-C 01.00004	Edgell Patches, W Sapi Is.	06°00'38.7"N, 115°59'22.2"E	MN164547	MN164573	n.a.	MN164598
		IPMB-C 01.00005	Edgell Patches, W Sapi Is.	06°00'38.7"N, 115°59'22.2"E	MN164548	MN164574	n.a.	MN164599
		IPMB-C 01.00006	Gaya Clement Reef, W Gaya Is.	06°01'24.26"N, 116°00'13.55"E	MN164549	MN164575	n.a.	MN164600
		IPMB-C 01.00007	Gaya Clement Reef, W Gaya Is.	06°01'24.26"N, 116°00'13.55"E	n.a.	MN164576	n.a.	MN164601
		IPMB-C 01.00008	Manukan, N Manukan Is.	05°58'46.1"N, 116°00'10.6"E	MN164550	MN164577	n.a.	MN164602
	P. marumi sp. nov. (holotype)	NSMT-Co 1683	Manukan, N Manukan Is.	05°58'46.1"N, 116°00'10.6"E	MN164551	n.a.	n.a.	MN164603
	P. marumi sp. nov.	IPMB-C 01.00009	Manukan, N Manukan Is.	05°58'46.1"N, 116°00'10.6"E	MN164552	MN164578	n.a.	MN164604
		IPMB-C 01.00010	Manukan, N Manukan Is.	05°58'46.1"N, 116°00'10.6"E	MN164553	MN164579	n.a.	MN164605
	Phenganax subtilis sp. nov. (holotype)	NSMT-Co 1684	Sepangar, W Sepangar Is.	06°03'38.66"N, 116°04'0.65"E	MN164554	MN164566	MN164586	n.a.
	P. subtilis sp. nov.	IPMB-C 01.00011	Sepangar II, W Sepangar Is.	06°04'7.38"N, 116°04'6.76"E	MN164555	MN164567	n.a.	n.a.
		IPMB-C 01.00013	Manukan, N Manukan Is.	05°58'46.1"N, 116°00'10.6"E	n.a.	MN164568	n.a.	n.a.
		IPMB-C 01.00012	Manukan, N Manukan Is.	05°58'46.1"N, 116°00'10.6"E	n.a.	MN164569	n.a.	n.a.
	Phenganax stokvisi sp. nov. (holotype)	NSMT-Co 1685	Mid Reef, E Manukan Is.	05°58'35.8"N, 116°00'52.2"E	MN164556	n.a.	n.a.	MN164592
	P. stokvisi sp. nov.	IPMB-C 01.00015	Mid Reef, E Manukan Is.	05°58'35.8"N, 116°00'52.2"E	MN164557	n.a.	n.a.	MN164593
		IPMB-C 01.00014	Mid Reef, E Manukan Is.	05°58'35.8"N, 116°00'52.2"E	MN164558	MN164565	MN164585	MN164594

means of SCUBA and all voucher material was preserved in 70–80% ethanol and subsamples in 95% ethanol. High-resolution in situ images were taken with an Olympus Tough TG-4 in an Olympus PT-056 underwater housing. Vouchers and type material have been deposited at the National Museum of Nature and Science (**NSMT**), Tokyo, Japan (all holotypes) and at the Borneo Marine Research Institute (**IPMB**), Universiti Malaysia Sabah (UMS), Sabah, Malaysia (all paratypes).

Morphological examinations

Sclerites were isolated by dissolving different parts of the specimens (polyp tentacle, calyx, entire polyp and stolon) in 4% hypochlorite (household bleach). Rinsing and visualisation of sclerites followed the same protocol as described in Lau et al. (2018, 2019). Additionally, sclerites from specimens that needed more detailed examination were mounted on scanning electron microscope stubs and coated with Pd/Au for imaging on a JEOL JSM6490LV scanning electron microscope (SEM) operated at high vacuum at 15 kV.

DNA extraction, amplification, and sequencing

DNA was extracted from polyps using a DNeasy Blood and Tissue kit (Qiagen, Tokyo). PCR amplification and sequencing of three mitochondrial markers, cytochrome c oxidase subunit I (COI), mitochondrial mutS-like protein (mtMutS), and the ND6 subunit (ND6), and one nuclear ribosomal marker, 28S ribosomal DNA (28S rDNA) followed the protocols in Lau et al. (2019). The amplified products were visualised by 1% agarose gel electrophoresis. PCR products were treated with Exonuclease I and Alkaline Phosphate (Shrimp) and sent for bidirectional sequencing on an ABI 3730XL (Fasmac, Kanagawa, Japan). Sequences were assembled and edited using Geneious R11 (Kearse et al. 2012) and BioEdit (Hall 1999). COI, mtMutS, and ND6 were checked for introns, exons, and stop-codons in AliView (Larsson 2014).

Molecular phylogenetic analyses

Multiple sequence alignments were performed using MAFFT 7 (Katoh and Standley 2013) and coding markers were aligned using MACSE (Ranwez et al. 2011) under default parameters. To determine the phylogenetic position of the collected specimens, consensus sequences for markers 28S rDNA, COI and mtMutS were aligned to a reference dataset of 121 octocoral genera (n = 127 sequences), including sequences of *Cornularia pabloi* McFadden & van Ofwegen, 2012 and *Cornularia cornucopiae* (Pallas, 1766) as outgroup (total n = 134 sequences). Alignments of 893 bp for 28S rDNA, 717 bp for COI and 923 bp for mtMutS were separately run in Maximum Likelihood (ML)

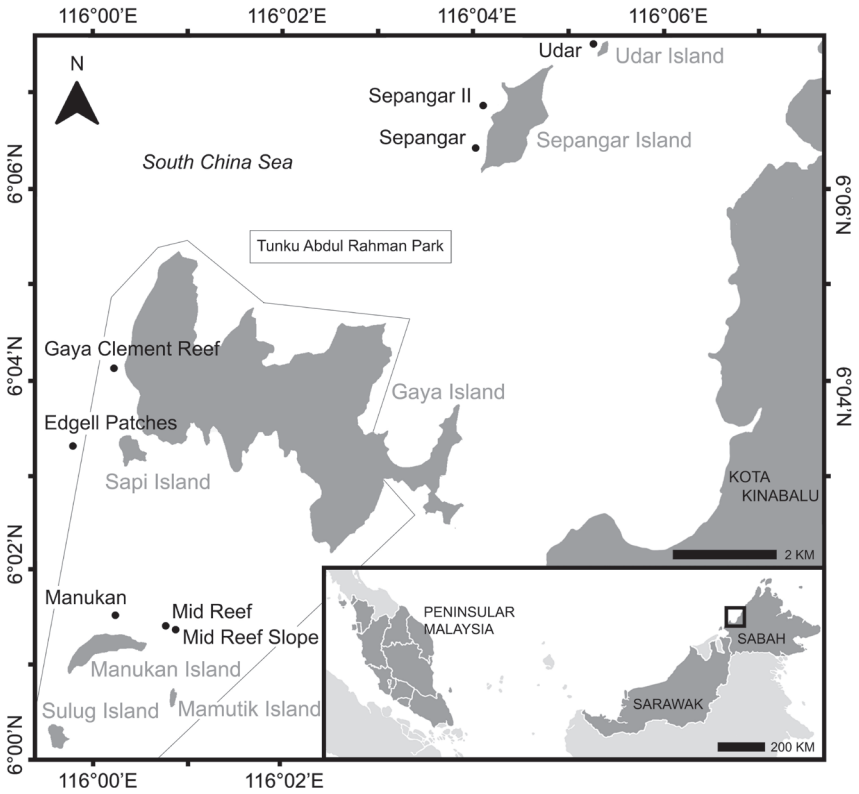

Figure 1. Map of eight sampling locations where stoloniferous octocorals were collected in this study, around Udar and Sepangar Islands and within Tunku Abdul Rahman Park (including Gaya, Sapi, Manukan, Mamutik, and Sulug Islands), Kota Kinabalu, Sabah, Malaysia.

analyses (Suppl. material 1: Figures S1–S3), which were highly congruent with the phylogenetic construction generated with the concatenated three-marker dataset (2533 bp).

A separate phylogenetic analysis was made using a concatenated four-marker dataset to further investigate the phylogenetic position of collected clavulariid and arulid specimens. The four separate markers (28S rDNA, 804 bp; COI, 717 bp; mtMutS, 734 bp; ND6, 441 bp) were also run in ML analyses to check for congruency (Suppl. material 1: Figures S4–S7). The concatenated markers resulted in a 2696 bp dataset with a total of nine reference taxa, including *Hanabira yukibana* Lau, Stokvis, Imahara & Reimer, 2019 as outgroup (total n = 33).

Alignments of the separate markers were all concatenated using SequenceMatrix 1.8 (Gaurav et al. 2011). ML analyses were run with RAX-ML 8 (Stamatakis 2014) using the GTRCAT model. The best ML tree was calculated using the –D parameter. A multi-parametric bootstrap search was performed, which automatically stopped based on the extended majority rule criterion. The Bayesian inference was performed with ExaBayes 1.5 (Aberer et al. 2014) using the GTR substitution model. Four independent runs were run for 10,000,000 generations during which convergence (with a standard deviation of split frequencies <2%) had been reached. Bootstrap supports

and posterior probabilities were depicted on the branches of the best ML tree using P4 (Foster 2004). The resulting tree was visualized in FigTree 1.4.2 (Rambout 2014). Additionally, average distance estimations within species and within genera were computed using MEGA X (Kumar et al. 2018) by analysing pairwise measures of genetic distances (uncorrected *P*) among sequences (Suppl. material 1: Tables S1–S6).

Systematic account

Class Anthozoa
Subclass Octocorallia Ehrenberg, 1831
Order Alcyonacea Lamouroux, 1812
Family Arulidae McFadden & Ofwegen, 2012

Genus *Bunga* gen. nov.
http://zoobank.org/BFF20AFD-A854-48EB-9F6A-EB3AC2066A95

Type species. *Bunga payung* sp. nov., by original designation and monotypy.

Diagnosis. Colony with polyps connected through thin stolons, which are cylindrical in cross-section and loosely attached to hard substrate. Anthocodiae retract into clavate calyces, which do not retract into the stolon. Oral disk expanded to circular membrane, as is characteristic of arulids. Oral disk with eight shallow furrows running from intertentacular margin to mouth of polyp, dividing membrane into eight lobes. Distal two-thirds of tentacles extend from fused margins of oral membrane. Sclerites of anthocodiae are rods. Sclerites of calyx are table-radiates. Sclerites of stolon are fused table-radiates forming a sheet. Sclerites colourless. Zooxanthellate.

Remarks. The main difference between type species *Bunga payung* gen. nov. et sp. nov., with *Arula* McFadden & Ofwegen, 2012 and *Hana* Lau et al., 2018 is found in both polyp morphology and sclerites; the outer margins of the oral membrane are much less pronounced than seen in *Arula* and *Hana*, as well as the lobes, as the furrows appear to be shallower. The 6-radiate sclerite type could not be found in any of the *Bunga* gen. nov. specimens, which are present in the polyp calyx of both *Arula* and *Hana*. *Bunga*, similar to *Hana*, has fused table-radiates that form a sheet in the stolon.

Etymology. From the Malaysian and Indonesian word *bunga*, meaning flower; denoting the shape of the polyps, which resemble flowers. Gender: feminine.

***Bunga payung* sp. nov.**
http://zoobank.org/5DDA8DCE-2333-4C45-8FA4-77021E54A211
Figures 2a–c, 4

Material examined. All specimens are from Sepangar, Sepangar Island, Kota Kinabalu, Sabah, Malaysia (06°03'38.66"N, 116°04'0.65"E), 20 March 2018 and collected by YW Lau. **Holotype**: NSMT-Co 1679, 9 m depth. **Paratype**: IPMB-C 01.00017, 10 m depth.

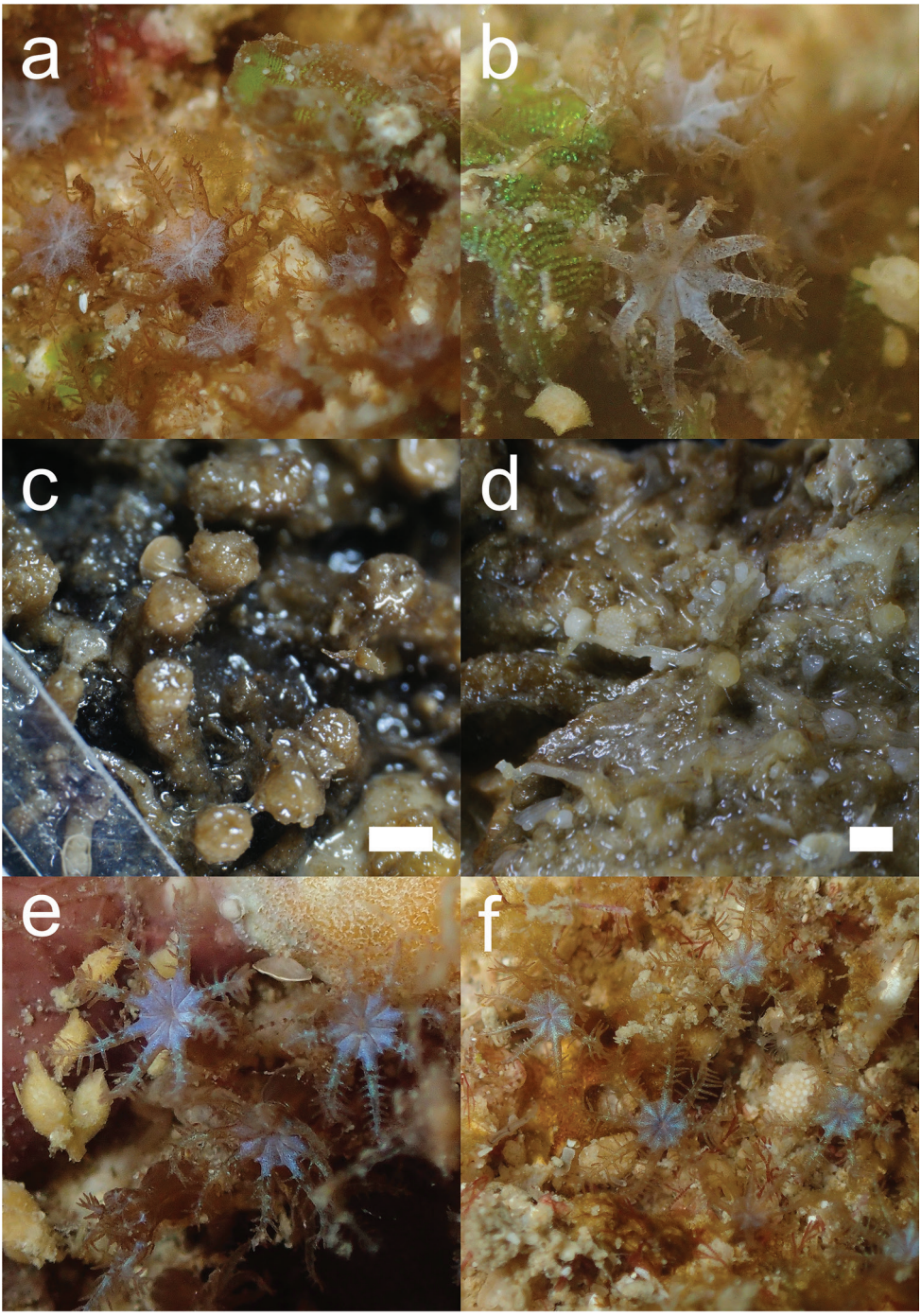

Figure 2. *Bunga payung* gen. nov. et sp. nov.: **a** In situ photograph, holotype (NSMT-Co 1679) **b** In situ photograph, paratype (IPMB-C 01.00017) **c** holotype in ethanol. *Laeta waheedae* gen. nov. et sp. nov. **d** holotype (NSMT-Co 1680) in ethanol **e** In situ photograph, holotype **f** In situ photograph, paratype (IPMB-C 01.00019). Scale bars: 1 mm.

Description. Colony with numerous polyps (total ~70). Polyps connected through stolons attached to rock. Stolons are thin and rounded (circular in cross-section, ~0.3 mm in diameter) and polyps are spaced apart irregularly, either adjacent to one another or spaced apart up to ~5 mm. Expanded polyps are ~2.2–3.0 mm in width and retract fully into calyces of ~1 mm wide and up to ~2 mm in height. Calyces do not retract into the stolon. The oral disk of the polyps is expanded into a circular membrane by fusion of proximal regions of adjacent tentacles (Figure 2a), as is characteristic of arulids. The oral disk has eight shallow furrows that run from intertentacular margin to mouth of polyp, dividing the membrane into eight lobes. The distal two-thirds of the tentacles extend from fused margins of the oral membrane. Tentacles with 6–10 pairs of widely spaced pinnules are arranged in a single row on either side of rachis.

Anthocodial sclerites are smooth rods, with simple tubercles at distal margin ends, 0.1–0.15 mm long (Figure 4a). Calyces contain table-radiates that range 0.06–0.19 mm in length (Figure 4b–d). Sclerites of the stolon are fused table-radiates forming a flat sheet (Figure 4e).

Polyps are brown coloured in life with a whitish oral disk, but yellowish white when preserved in ethanol. Zooxanthellate.

Morphological variation. The paratype is a colony consisting of ~10 polyps. Polyps of the paratype colony show variation in colouration; the whitish colour is not restricted to the oral disk but is also seen in the tentacles. This could be due to differences in sclerite density (Figure 2a), as described in Alderslade and McFadden (2007) and Lau et al. (2019), or it could be due to the position of zooxanthellae in the tissue.

Distribution. Sepangar Island, Kota Kinabalu, Sabah, Malaysia.

Remarks. Anthocodial rods are scarce in *Bunga payung* gen. nov. et sp. nov. The 6-radiate type of sclerite was not observed in this genus but is present in *Arula* and *Hana*, the two other genera in the family Arulidae.

Etymology. From the Malaysian and Indonesian word *payung*, which means umbrella; denoting the shape of the oral disc of the polyps, which resemble the shape of an umbrella.

Genus *Laeta* gen. nov.
http://zoobank.org/02B40F3A-AA78-49A5-ADA8-12F3374CDF21

Type species. *Laeta waheedae* sp. nov., by original designation and monotypy.

Diagnosis. Colony with polyps connected through stolons, which are ribbon-like. Oral disk with eight furrows, running from intertentacular margin to the mouth of the polyp, dividing the membrane into eight shallow lobes. Distal two-thirds of tentacles extend from fused margins of the oral membrane. Sclerites of anthocodiae are rods. Sclerites of calyx are table-radiates and three types of rods; (1) branched rods with high tuberculate processes, (2) club-like rods and (3) table-radiate-like rods. Sclerites of stolon are fused table-radiates, which form a sheet. Sclerites colourless. Zooxanthellate.

Remarks. The main morphological difference between the type species, *Laeta waheedae* gen. nov. et sp. nov., and species of the genera *Arula*, *Hana*, and *Bunga* gen. nov.

is found in the presence of all three types of rods in its calyces. The club-like rod with tubercles at one distal end of the rod is also seen in *Hana hanataba* Lau et al., 2018, however this type of sclerite was only found in the anthocodiae in *Laeta waheedae* and not in the calyx as in *Hana*. Similar to *Bunga*, *Laeta* does not have 6-radiates in the calyx. Similar to *Hana* and *Bunga*, *Laeta* has fused table-radiates in the stolon. Outer margins of the oral membrane are much less pronounced than in *Arula* and *Hana*, and are more similar to margins of the oral disk in *Bunga*.

Etymology. From Latin *laeta*, meaning bright, charming, cheerful. Gender: feminine.

***Laeta waheedae* sp. nov.**

http://zoobank.org/761E7919-D311-4F0B-8B67-17E8ECDEC370

Figures 2d–f, 5

Material examined. All specimens are from Kota Kinabalu, Sabah, Malaysia and collected by YW Lau. **Holotype**: NSMT-Co 1680, Udar, east of Udar Island (06°4'49.81"N, 116°5'13.16"E), 10 m depth. **Paratypes:** IPMB-C 01.00018, Mid Reef, east of Manukan Island, TARP (05°58'46.1"N, 116°00'10.6"E), 8 m depth. IPMB-C 01.00019, Gaya, Gaya Island, TARP (06°01'24.26"N, 116°00'13.55"E), 11 m depth.

Description. The colony consists of ~50 polyps, which are connected through ribbon-like stolons (0.5–0.6 mm width). Polyps are spaced apart quite regularly (~3 mm). Anthocodiae retract fully into low oval to cylindrical calyces (~1 mm in width, ~0.5 mm in height), which do not retract into the stolon. Expanded polyps 3.5–4.0 mm in diameter. Oral membrane with eight shallow furrows running from intertentacular margin to mouth of polyp, dividing the membrane into eight shallow lobes. Distal two-thirds of tentacles extend from fused margins of the oral membrane. Tentacles with 6–8 pairs of widely spaced pinnules are arranged in a single row on either side of rachis.

Sclerites of anthocodiae are small smooth rods, 0.035–0.1 mm in length, with little ornamentation (Figure 5c). Sclerites of calyx are table-radiates, 0.06–0.10 mm (Figure 5d, e, g) and three types of rods: (1) rods branched with high tuberculate processes, 0.08–0.09 mm long (Figure 5f), (2) rods with tubercles at one distal end of the rod, giving it a club-like appearance, 0.1–0.14 mm long (Figure 5a), and (3) rods with table-shaped tubercles, 0.08–0.12 mm long (Figure 5b).

Oral membrane has a blue colour in life (yellowish white when preserved in ethanol). The tentacles are brown in colour, partially with a greenish shimmer. Zooxanthellate.

Morphological variation. The paratype colony consists of ~30 polyps. Tentacles of paratypes show variation in pinnule pairs, partly having nine pairs of widely spaced pinnules arranged in a single row on either side of rachis.

Distribution. Udar Island, Kota Kinabalu, Sabah, Malaysia. Gaya Island, TARP, Kota Kinabalu, Sabah, Malaysia.

Remarks. Polyps of *Laeta waheedae* gen. nov. et sp. nov. have the same blue-purple colour in life as those of *Arula petunia* McFadden & Ofwegen, 2012, but there is a

difference in the outer margins and lobes of the oral membrane; both are more pronounced in *Arula petunia*. The holotype colony was attached to sponge tissue, but this epibiotic relation is not obligate.

Etymology. Named after Dr. Zarinah Waheed, for her dedication to coral reef research and her guidance during fieldwork in Sabah.

Family Clavulariidae Hickson, 1894

Genus *Phenganax* Alderslade & McFadden, 2011

Diagnosis. (after Alderslade & McFadden 2011). Alcyonacea with erect polyps and stolons with encrusting, stoloniferous habit. Sclerites are absent. Zooxanthellate. Distribution tropical, Indo-Pacific. Type species: *Phenganax parrini* Alderslade & McFadden, 2011.

***Phenganax marumi* sp. nov.**
http://zoobank.org/29410835-EB6E-4E9D-9361-CF60FE36ECFD
Figure 3b

Material examined. All specimens are from Kota Kinabalu, Sabah, Malaysia and collected by YW Lau. **Holotype**: NSMT-Co 1683, Manukan, Manukan Island, TARP (05°58'46.1"N, 116°00'10.6"E), 13 m depth. **Paratypes:** IPMB-C 01.00001: Edgell Patches, west of Sapi Island (06°00'38.7"N, 115°59'22.2"E), 16 m depth. IPMB-C 01.00002: Mid Reef Slope, east of Manukan Island, TARP (05°58'38.08"N, 116°00'52.82"E), 13 m depth. IPMB-C 01.00003: Mid Reef Slope, east of Manukan Island, TARP (05°58'38.08"N, 116°00'52.82"E), 11 m depth. IPMB-C 01.00004: Edgell Patches, west of Sapi Island (06°00'38.7"N, 115°59'22.2"E), 19 m depth. IPMB-C 01.00005: Edgell Patches, west of Sapi Island (06°00'38.7"N, 115°59'22.2"E), 16 m depth. IPMB-C 01.00006: Gaya Clement Reef, west of Gaya Island, TARP (06°01'24.26"N, 116°00'13.55"E), 12 m depth. IPMB-C 01.00007: Gaya Clement Reef, west of Gaya Island, TARP (06°01'24.26"N, 116°00'13.55"E), 11 m depth. IPMB-C 01.00008: Manukan, north of Manukan Island, TARP (05°58'46.1"N, 116°00'10.6"E), 12 m depth. IPMB-C 01.00009: Manukan, Manukan Island, TARP (05°58'46.1"N, 116°00'10.6"E), 12 m depth. IPMB-C 01.00010: Manukan, Manukan Island, TARP (05°58'46.1"N, 116°00'10.6"E), 12 m depth.

Description. Colony is attached to rock and sponge and consists of ~15 polyps. Stolons are consistent in width throughout the colony (~0.35 mm). Polyps are spaced apart irregularly (from 0.5 mm up to 6 mm) and retract fully into calyces; calyces do not retract into stolon and are approximately 1 mm in width and 2 mm in height. Expanded polyps 4.0–5.5 mm in width. The pinnules are arranged on either side of the

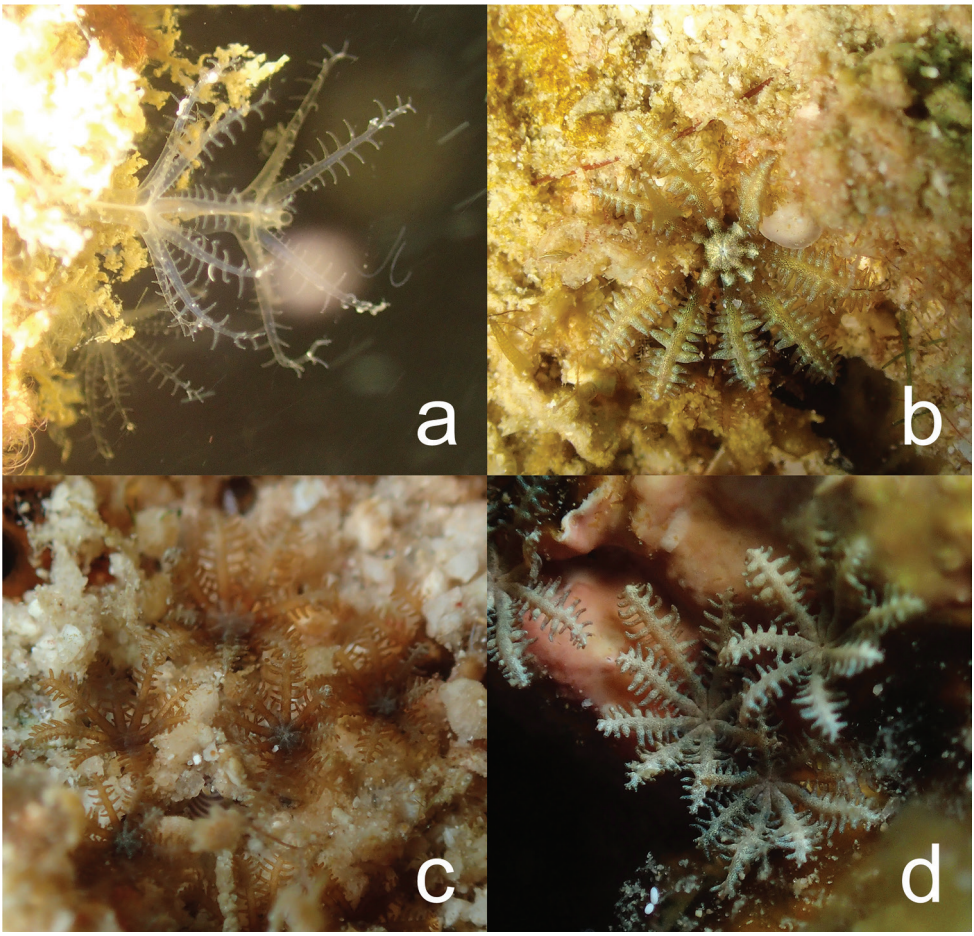

Figure 3. In situ photographs of clavulariids found in and around TARP, Kota Kinabalu, Sabah, Malaysia. **a** Clavulariidae sp., specimen NSMT-Co 1686 **b** *Phenganax marumi* sp. nov., holotype (NSMT-Co 1683) **c** *Phenganax subtilis* sp. nov., holotype (NSMT-Co 1684) **d** *Phenganax stokvisi* sp. nov., holotype (NSMT-Co 1685).

rachis in pairs of 12–15, sometimes spaced apart irregularly. The pinnules give a swollen appearance and are mostly conical shaped, otherwise diamond-shaped. The colony is sclerite-free. Polyps are brownish yellow in colour, with a bright yellowish white oral disk in life (whitish yellow when preserved in ethanol). Tentacles have a greenish colour interrupted with brown specks. Zooxanthellate.

Morphological variation. Paratypes IPMB-C 01.00003 and IPMB-C 01.00007 show variation in the colouration of the polyps, having a paler and pinkish appearance. There is also variation in the number of pinnule pairs (~8 pairs) and the space between the pinnules; pinnules are sometimes so densely packed there is no space between them. Like the holotype, all paratype colonies are small colonies consisting of ~20 polyps.

Distribution. Gaya, Sapi and Manukan Islands, TARP, Kota Kinabalu, Sabah, Malaysia.

Remarks. *Phenganax marumi* sp. nov. resembles *Phenganax parrini* Alderslade & McFadden, 2011 in polyp morphology, but differs in colour. The numerous and densely packed polyps described for a *P. parrini* colony (Alderslade and McFadden 2011) have not been observed in any of the 11 collected *P. marumi* colonies; instead the maximum number of polyps observed in one colony was approximately 35. However, the density of *P. parrini* could be caused by unnatural conditions (aquarium environment) in which it was kept for scientific research purposes (Alderslade and McFadden 2011). *Phenganax marumi* was found on exposed spots on the reef, not sheltered from strong current or light, as opposed to *P. parrini*, which was found in dimly lit, sheltered locations.

Etymology. From the Japanese word *marumi*, which means round or rounded; denoting the plump shape of the polyp tentacles, which give the polyp an overall plump appearance.

***Phenganax subtilis* sp. nov.**

http://zoobank.org/D01BA048-BF0F-4285-B4D3-3D071B9D1653

Figure 3c

Material examined. All specimens are from Kota Kinabalu, Sabah, Malaysia and collected by YW Lau. **Holotype**: NSMT-Co 1684, Sepangar, west of Sepangar Island (06°03'38.66"N, 116°04'0.65"E), 7 m depth. **Paratypes:** IPMB-C 01.00011: Sepangar II, west of Sepangar Island (06°04'7.38"N, 116°04'6.76"E), 7 m depth. IPMB-C 01.00012: Manukan, north of Manukan Island, TARP (05°58'46.1"N, 116°00'10.6"E), 12 m depth. IPMB-C 01.00013: Manukan, north of Manukan Island, TARP (05°58'46.1"N, 116°00'10.6"E), 12 m depth.

Description. The colony consists of ~50 polyps, which are connected through thin rounded stolons with a width of approximately 0.13–0.2 mm, growing over coral rubble. Polyps are partly clustered and spaced apart irregularly (1.0–3.0 mm). Polyps retract into calyces (0.65–0.77 mm width) that are barrel shaped. Expanded polyps are 3.0–3.5 mm in width and have tentacles with pinnules that are widely spaced and arranged in pairs of 12 on either side of the rachis. No sclerites were found in any of the specimens. Polyps are brown coloured in life and whitish yellow when preserved in ethanol. Zooxanthellate.

Morphological variation. Paratypes show variation in the number of pinnules on either side of the rachis (10–13 pairs).

Distribution. Sepangar Island, Kota Kinabalu, Sabah, Malaysia. Manukan Island, TARP, Kota Kinabalu, Sabah, Malaysia.

Remarks. *Phenganax subtilis* sp. nov. differs from *P. parrini* and *P. marumi* sp. nov. mainly in the shape of the pinnules. *Phenganax subtilis* does not have the plump, diamond-shaped pinnules as seen in *P. marumi* and *P. parrini*. Additionally, the colour of *P. subtilis* is different from *P. parrini* and *P. marumi*; brown instead of the more characteristic white-grey.

Etymology. From Latin *subtilis*, meaning simple, subtle, plain; denoting the subtleness of the polyps blending into the reef background. Gender: masculine.

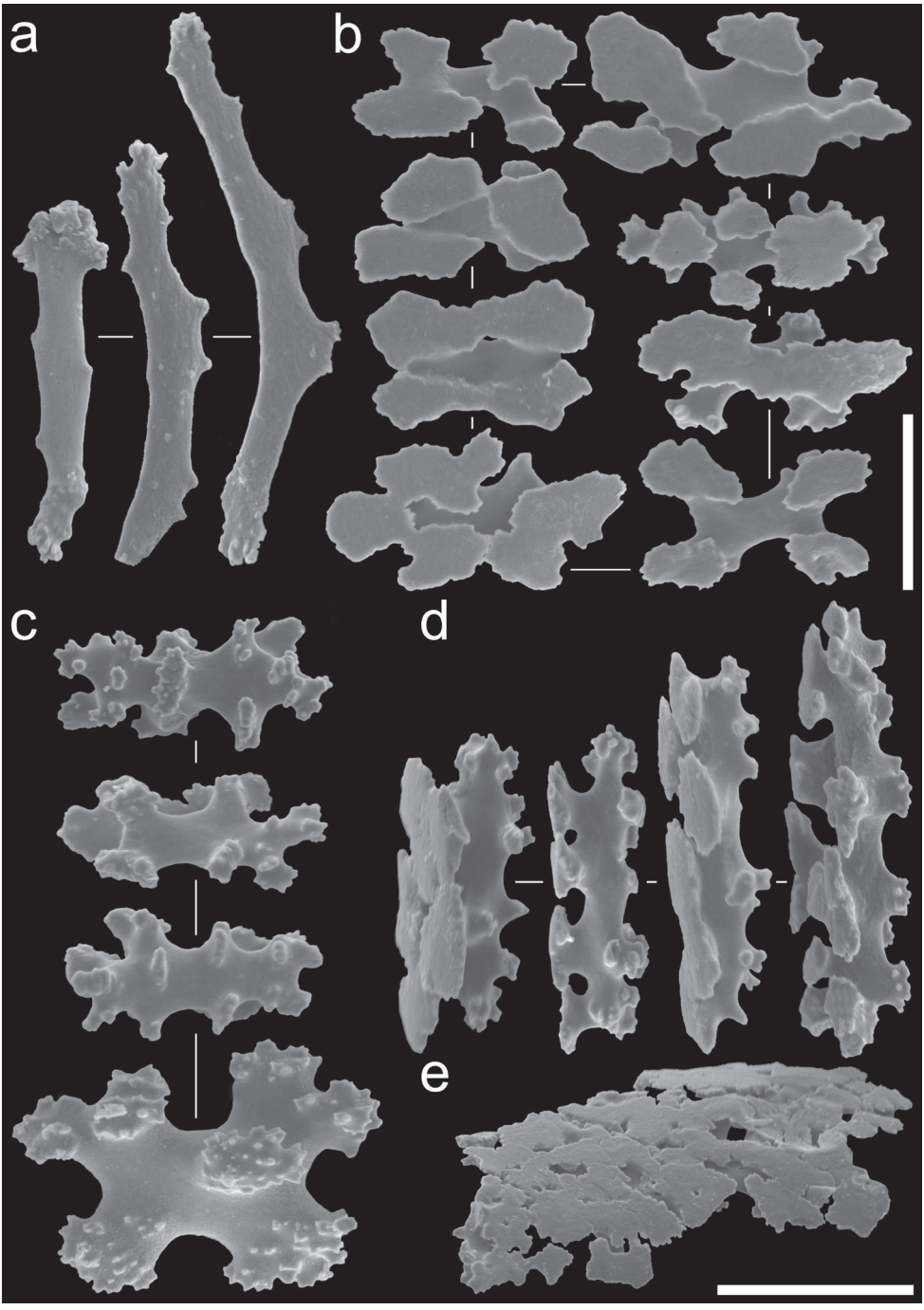

Figure 4. Sclerite types observed in *Bunga payung* gen. nov. et sp. nov., NSMT-Co 1679, holotype: **a** Anthocodial rods **b** table-radiates of calyx, top view **c** table-radiates of calyx, bottom view **d** table-radiates of calyx, lateral view **e** fragment of fused table-radiates of the stolon. Scale bars: 0.05 mm (**a–d**); 0.1 mm (**e**).

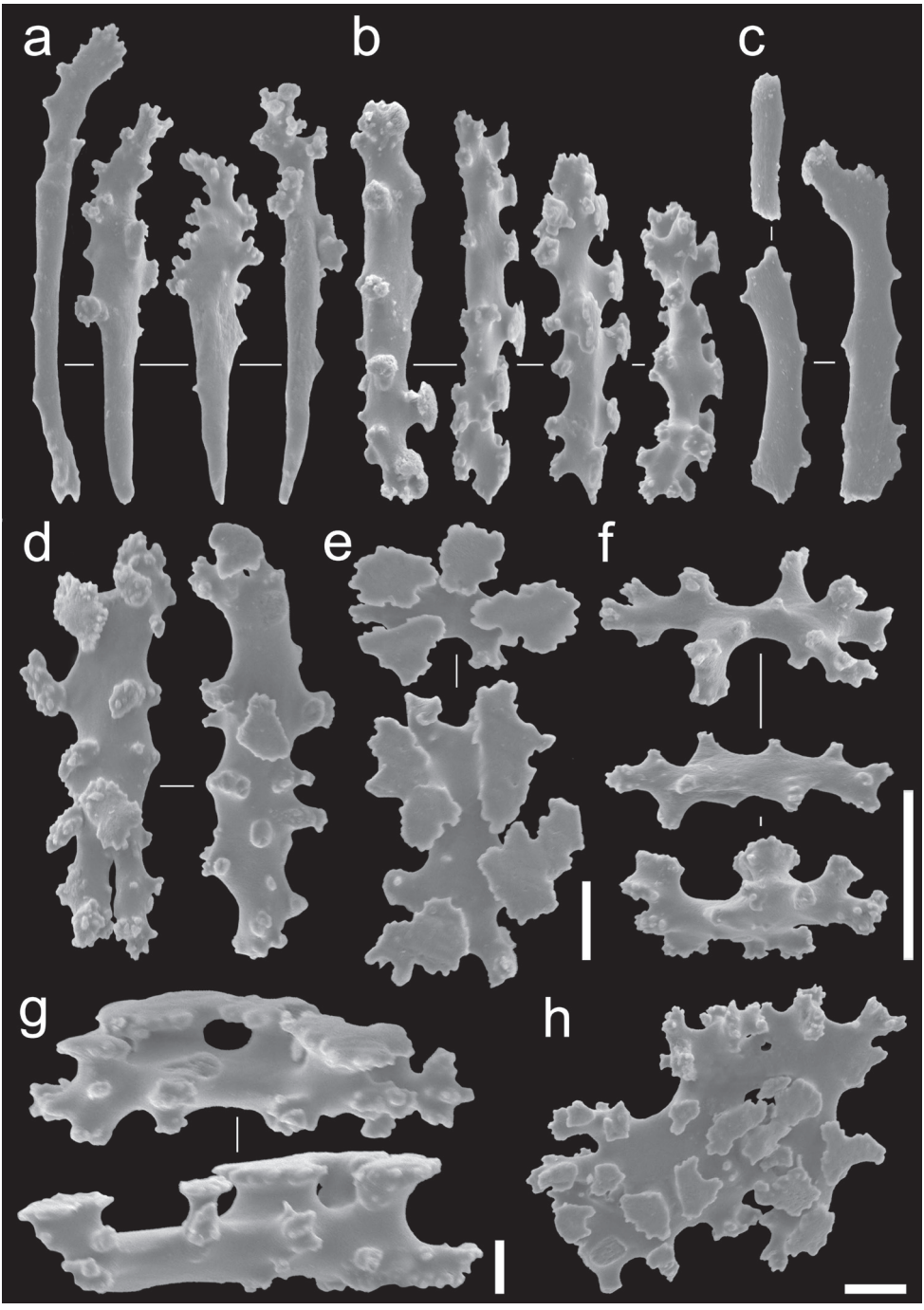

Figure 5. Sclerite types observed in *Laeta waheedae* gen. nov. et sp. nov., NSMT-Co 1680, holotype: **a** rods of calyx **b** rods of calyx **c** anthocodial rods **d** table-radiates of calyx **e** table-radiates of calyx, top view **f** rods of calyx **g** table-radiates of calyx, lateral view **h** fragment of fused table-radiates of the stolon. Scale bars 0.05 mm (**a–c, f**); 0.02 mm (**d–e**); 0.01 mm (**g**); 0.02 mm (**h**).

***Phenganax stokvisi* sp. nov.**
http://zoobank.org/5871284F-05F8-469D-AED1-0BE797C0FEB2
Figure 3d

Material examined. All specimens are from dive location Mid Reef, east of Manukan Island (05°58'35.8"N, 116°00'52.2"E) TARP, Kota Kinabalu, Sabah, Malaysia and collected by YW Lau. **Holotype**: NSMT-Co 1685, 5 m depth. **Paratypes:** IPMB-C 01.00015: 4 m depth. IPMB-C 01.00014 4 m depth.

Description. The colony consists of ~100 polyps which are densely packed and are connected through flattened ribbon-like stolons with irregular width (~0.21–0.55 mm). The colony is fragmented into two pieces with the rock it was attached to. Expanded polyps are approximately 3.0 mm in diameter and have tentacles with pinnules arranged in pairs of ten on either side of the rachis. Polyps are clustered closely together (adjacent to one another) and partly spaced apart (~1.0 mm in between clustered polyps). Polyps retract into calyces (~1.0 mm width) that are barrel shaped. No sclerites were found. Polyps are whitish grey coloured in life (whitish yellow when preserved in ethanol). Zooxanthellate.

Distribution. Manukan Island, TARP, Kota Kinabalu, Sabah, Malaysia.

Remarks. *Phenganax stokvisi* sp. nov. shows similarity to the densely packed *P. parrini*, polyps being in the same size range (2.5–3.0 mm width in *P. parrini*), only showing difference in the number of pinnule pairs and colour of the polyps (possibly due to zooxanthellae).

Etymology. Named after Frank Robert Stokvis, whose passion for octocoral research has never changed since his first study on this topic.

Clavulariidae sp.
Figure 3a

Material examined. All specimens are from Kota Kinabalu, Sabah, Malaysia. NSMT-Co 1686, Edgell Patches, west of Sapi Island (06°00'38.7"N, 115°59'22.2"E), 18 m depth, coll. YW Lau. IPMB-C 01.00016, Gaya Clement Reef, west of Gaya Island, TARP (06°01'24.26"N, 116°00'13.55"E), 11 m depth, coll. YW Lau.

Description. Colonies with 20–30 polyps are connected through flattened stolons, which have a varying width of 0.5–1 mm. Colonies can be loosely attached to sponge or rocky substrates, such as coral rubble. Polyps are transparent and clustered in groups, connected by stolons with lengths up to 4–5 mm. Expanded polyps were ~6.0–7.0 mm in width when alive, with the pharynx visible in all polyps. Polyps retract fully into the calyx, which is cylinder-shaped (~1.3 mm width and up to 1.5 mm tall) and do not retract fully into the stolon. The tentacles have approximately 11 pairs of pinnules, which are widely spaced apart. No sclerites were found in the specimens. Polyps are whitish translucent when alive (yellowish white when preserved in ethanol). Azooxanthellate.

Distribution. West of Sapi and Gaya Islands, TARP, Kota Kinabalu, Sabah, Malaysia.

Remarks. This material, henceforth Clavulariidae sp., can be identified to the family level Clavulariidae Hickson, 1894 by its initial morphological resemblance to the type species *Azoriella bayeri* Lopez-Gonzalez & Gili, 2001 and *Cervera atlantica* Lopez-Gonzalez et al., 1995 in having similar whitish translucent polyps, although, the polyps of *C. atlantica* are translucently orange. However, more diagnostic morphological features and more specimens are necessary before a genus- and species-level distinction can be made.

The main difference between Clavulariidae sp. and *A. bayeri* can be found in the absence of sclerites in Clavulariidae sp. Additionally, both type species *C. atlantica* and *A. bayeri* have polyps that are smaller than in Clavulariidae sp.; *C. atlantica*, ~5.1 mm width, *A. bayeri*, ~3.6 mm width, and Clavulariidae sp., ~6.0–7.0 mm width. As well, *C. atlantica* and *A. bayeri* have more pinnules on either side of the tentacles than seen in Clavularidae sp.; both *C. atlantica* and *A. bayeri* have 12–14 pinnules and Clavulariidae sp. has tentacles with 11 pairs.

Molecular phylogenetic analyses

This study has produced 67 sequences, which were added to the public database GenBank; the 51 clavulariid, and 16 arulid sequences had no previous barcodes. The phylogenies resulting from the ML analyses of the separate markers (Suppl. material 1: Figures S1–S7) were highly congruent with those from the concatenated alignments for both the three- and four-marker datasets (Figures 6–7). ML and Bayesian analyses of the concatenated datasets yielded almost identical tree topologies.

Arulidae from Sabah, Malaysia

Sequences of arulids *Bunga payung* gen. nov. et sp. nov. and *Laeta waheedae* gen. nov. et sp. nov., collected from the north of TARP (Udar, Gaya and Sepangar Islands) formed a completely-supported clade with the arulid genera *Arula* and *Hana*; 100%/1.00 for both the three- and four-marker datasets (Figures 6, 7, respectively). In both phylogenies, *Bunga* was sister to the remaining clade. However, it remains unresolved how *Laeta waheedae*, *Arula*, and *Hana* are related to one another in the four-marker phylogeny reconstruction (21%/0.56). Nonetheless, all genera in the clade have high support values.

Genetic distances (uncorrected *P*, expressed as percentage) between specimens of *Bunga* gen. nov., *Laeta* gen. nov., *Arula*, and *Hana* (between 2.6–4.6% for COI, 5.4–6.1% for mtMutS) indicated that the levels of pairwise differences were well above those observed among congeneric species (McFadden et al. 2011), Suppl. material 1: Table S1.

Morphological data supported the molecular data and justified the description of the two new genera *Bunga* and *Laeta*. There were distinct differences in sclerite features

Figure 6. Phylogenetic relationships among 121 octocoral genera, including seven specimens (highlighted red) collected in and around TARP, Kota Kinabalu, Sabah, Malaysia, using the combined 28S rDNA+COI+mtMutS dataset (total n = 127). The best Maximum Likelihood tree is shown, with values at branches representing bootstrap probabilities (shown when > 70%; top/left) and Bayesian posterior probabilities (shown when > 0.80; bottom/right; A = 1.00, B = 0.95–0.99, C = 0.90–0.94, D = 0.80–0.89). Key: * represents 100%/1.00 for both analyses. Important values concerning target specimens are red. Non-stoloniferous families are shown with family classification only and stoloniferous families are highlighted in grey. Sclerite-free species are indicated with a blue dot. *Cornularia* spp. were used as outgroup.

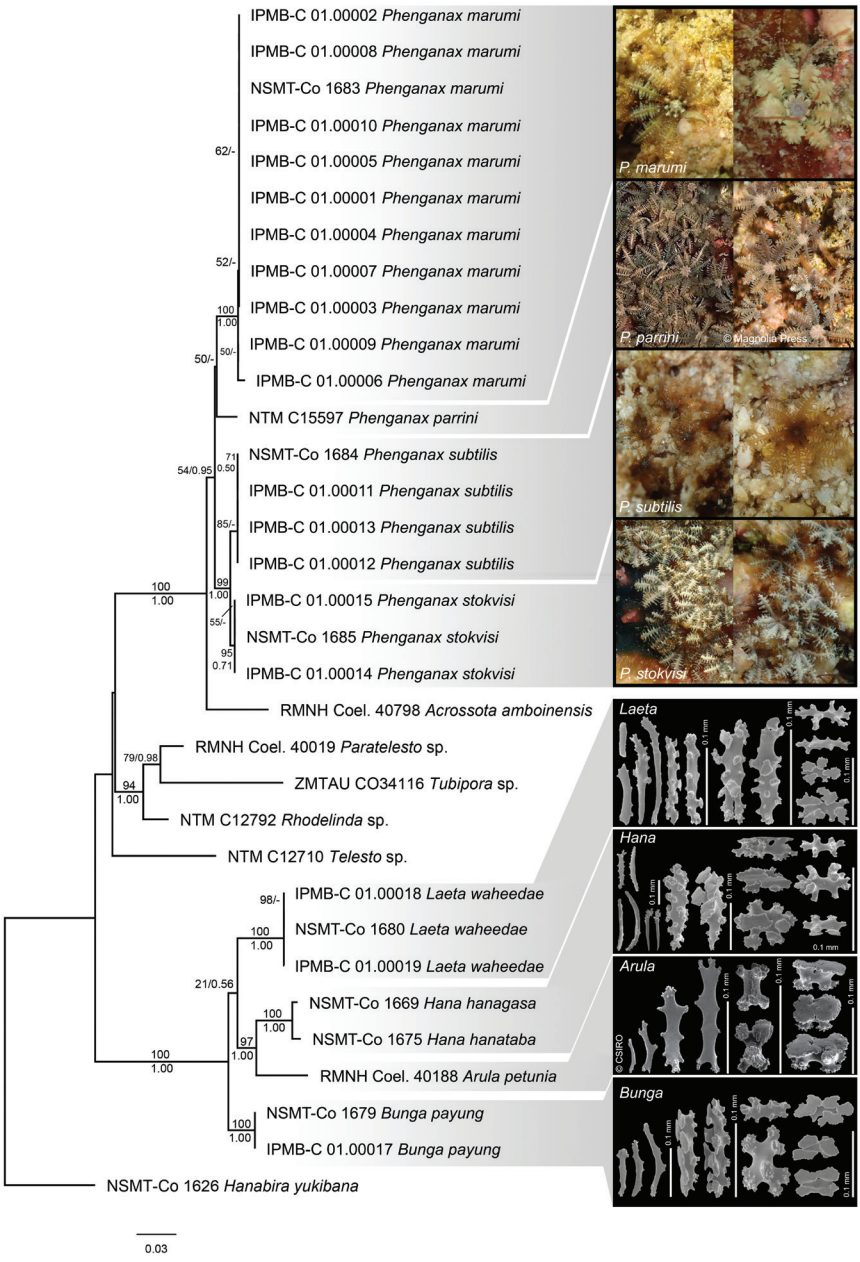

Figure 7. Combined 28S rDNA+COI+mtMutS+ND6 phylogenetic reconstruction for four *Phenganax* species and four arulid genera (*Hana*, *Arula*, *Bunga* gen. nov., and *Laeta* gen. nov.) collected in and around TARP, Kota Kinabalu, Sabah, Malaysia; *Hanabira yukibana* was used as outgroup (total n = 33). The best Maximum Likelihood tree is shown, with values at branches representing bootstrap probabilities (shown when > 50%; top/left) and Bayesian posterior probabilities (shown when > 0.50; bottom/right). Photograph credit: in situ images NTM C15597 *Phenganax parrini*, by Daniel Knop (modified from Alderslade and McFadden 2011, reproduced with permission from copyright holder). Sclerite images RMNH Coel. 40188 *Arula petunia* (modified from McFadden and Van Ofwegen 2012, reproduced with permission from CSIRO Publishing).

between *Bunga*, *Laeta*, *Arula*, and *Hana*, involving the presence and absence of sclerite types in the calyx; three types of rods (branched with high tuberculate processes, club-like rods and table-radiate-like rods), which were only observed in *Laeta* but not in the other sister genera, and the absence of 6-radiates in *Bunga*, which were present in all sister genera. There was also a difference in sclerites of the stolon; *Arula* is the only genus without fused table-radiates, but instead has table-radiates in the calyx. The polyp morphology did not show many obvious differences, although two of them could be observed in the outer margins of the characteristic fused oral membrane; both *Bunga* and *Laeta* had polyps with oral discs that were less pronounced at their outer margins than those of other genera, having a smooth transition from oral disc to the connecting tentacles, while the furrows dividing the oral disc into eight lobes were shallower in both of these genera (Figure 2). The combination of molecular and morphological information supports the erection of two new genera within the Arulidae.

Clavulariidae from Sabah, Malaysia

Sequences of 18 clavulariid specimens grouped together with *Acrossota amboinensis* (Burchardt, 1902) and *Phenganax parrini* Alderslade & McFadden, 2011 in a well-supported clade in both the three-marker and four-marker analyses (Figures 6, 7, respectively), in which *Acrossota* was sister to the remaining clade (100%/1.00). However, there was disparity in the relationships within the remaining clade in the two phylogeny reconstructions and the relationships within the remaining clade were not clearly resolved. The four-marker phylogeny reconstruction, with more specimens, gave a higher resolution (Figure 7) and here, each species had high support values, although it remained unclear how *P. parrini* is related to the other three species (50%/-).

On the other hand, within-genus genetic distances for *Phenganax* were 0.57% for COI and 3.10% for mtMutS, percentages within the range of congeneric species commonly observed in octocorals (Suppl. material 1: Table S3). When comparing pairwise differences between the four species, the values were well above averages for conspecifics; the observed values were in between 0.98–4.09% for COI and between 1.60–4.07% for mtMutS (Suppl. material 1: Table S5), supporting the division into four species (McFadden et al. 2011).

Despite the absence of sclerites, which was characteristic for the entire clade, there were visible differences in morphological polyp features. The main differences were found in tentacle pinnules and colony growth (Figure 3b–d). *Phenganax marumi* sp. nov. was similar to *P. parrini* Alderslade & McFadden, 2011 in polyp morphology, although differing in colour and polyp size; expanded polyp sizes ranged 4.0–5.5 mm in *P. marumi* and 2.5–3.0 mm in *P. parrini*. Additionally, the numerous amounts and densely packed polyps described for a *P. parrini* colony (Alderslade and McFadden 2011) had not been observed in any of the 11 collected *P. marumi* colonies; instead the maximum number of polyps observed for one colony was approximately 30–40. How-

ever, the density of *P. parrini* could be due to unnatural conditions (aquarium environment) in which it was kept for scientific research (Alderslade and McFadden 2011).

Phenganax marumi sp. nov. was found on exposed spots on the reef, not sheltered from strong current or light, opposed to *P. parrini*, which was found in dimly lit, sheltered locations. *Phenganax subtilis* sp. nov. differs from *P. parrini* and *P. marumi* mainly in the shape of the pinnules; *P. subtilis* does not have the plump, diamond-shaped pinnules as seen in *P. marumi* and *P. parrini*. As well, the colour of *P. subtilis* is different from *P. parrini* and *P. marumi*, being brown. *Phenganax stokvisi* sp. nov. shows similarity to the densely packed *P. parrini*, with polyps being in the same size range (2.5–3.0 mm width), but showing differences in the number of pinnule pairs and colour of the polyps (possibly due to the presence of zooxanthellae).

Differences in morphology combined with genetic distances and high support values in the four-marker phylogeny reconstruction supported the erection of the three new sister species of *Phenganax parrini*; *P. marumi* sp. nov., *P. subtilis* sp. nov., and *P. stokvisi* sp. nov.

Clavulariidae sp. had a similar DNA profile to two genera within the Clavulariidae; sequences from the two specimens clustered in a well-supported clade (96%/1.00), together with the genera *Azoriella* (Lopez Gonzalez & Gili, 2001) and *Cervera* Lopez-Gonzalez et al., 1995, with *Cervera* as sister to *Azoriella* and Clavulariidae sp. (Figure 6). Genetic distances between the two specimens and *Azoriella* were 1.41% for COI and 5.09% for mtMutS, values within ranges amongst intergeneric octocoral species (Suppl. material 1: Table S2). However, with the current available molecular data it remains unresolved how Clavulariidae sp. and *Azoriella* are related to one another, as branching was weakly supported (52%/0/70).

Discussion

From surveys at only eight different dive locations, approximately 13 hours of field work, all within approximately 60 km^2 (TARP + area around Udar and Sepangar Islands), five species and two stoloniferan genera new to science were discovered. These results are not completely unexpected, as TARP is located on the outer edge of the Coral Triangle, where studies on stoloniferous octocorals are in their infancy. Of the seven families that are considered to belong to the subordinal group Stolonifera (Cordeiro et al. 2019), three have members that are confirmed to occur in the Indo-Pacific (Alderslade and McFadden 2007, 2011; Fabricius and Alderslade 2011): Acrossotidae Bourne, 1914, Tubiporidae Ehrenberg, 1828 and Clavulariidae Hickson, 1894. Of these, Clavulariidae is the only family that is not monogeneric or even monospecific, and is obviously the most speciose and common. The majority of recent studies on Indo-Pacific Clavulariidae have mainly focused on *Tubipora musica* Linnaeus, 1758, a reef-building alcyonarian species and *Tubipora musica*-sponge associations (Calcinai et al. 2013; Agustiadi and Luthfi 2017). Therefore, it is reasonable to assume that continued surveys in this area and within the Coral Triangle will result in further discoveries

of undescribed stoloniferous octocorals. Such new descriptions could fill knowledge gaps in the overall systematics of Octocorallia, similar as recent discoveries of new small inconspicuous stoloniferan species have done (Alderslade and McFadden 2007, 2011; Benayahu et al. 2017; Lau et al. 2018, 2019).

Arulids of Sabah

There are minor differences in polyp morphology when comparing *Bunga payung* gen. nov. et sp. nov., *Laeta waheedae* gen. nov. et sp. nov., *Arula petunia*, and *Hana* spp.; *Arula* and *Laeta* are similar in colour, having blue colorations in the oral disc and/or tentacles. *Hana* spp. are similar to *Arula petunia* in having a very pronounced oral disc with deep furrows dividing the oral disc into eight distinct lobes, as opposed to *Laeta* and *Bunga*, which both have an oral disc that fuses into the tentacle base and shallow furrows that divides the eight lobes.

It could therefore be proposed that instead of four different genera within Arulidae, *Arula*, *Hana*, *Bunga* gen. nov., and *Laeta* gen. nov. could be five distinct species of *Arula*. However, the erection of a new genus for each new species is justified by the combination of sclerite morphology and molecular information. The four genera of Arulidae are distinguished morphologically by differences in sclerite form and the presence or absence of certain sclerite types in different parts of the colony or being absent completely. The only two sclerite types that all four genera have in common are the rods present in the anthocodiae and the table-radiates in the calyx, which are characteristic to the family Arulidae. *Bunga* is the only genus that has only these sclerites types in the polyps; anthocodial rods and table-radiates in the calyx. *Arula*, *Hana*, and *Laeta* have an additional sclerite type in the calyx; *Arula* and *Hana* have 6-radiates. *Laeta* has three different ornamented rods in the calyx, which are absent in all other genera.

Hana and *Arula* are the two most similar genera in terms of morphology. However, *Arula* is the only genus which has separate table-radiate sclerites in the stolon, and it can also be distinguished from the other genera in having table-radiates that are smaller in size (up to 0.09 mm length) and by not having table-radiates which are elongated in shape; the other three genera all have stolons with fused table-radiates which form a sheet and all have larger table-radiates up to 0.10–0.19 mm length.

Molecular analyses of the concatenated four marker dataset (28s rDNA, COI, mtMutS, and ND6 sequences) resulted in similar phylogenetic positions for *Bunga payung* gen. nov. et sp. nov. and *Laeta waheedae* gen. nov. et sp. nov. when compared to our analyses of the concatenated three marker dataset (28s rDNA, COI, and mtMutS). It should be noted that the two analyses including more specimens for *Bunga* and *Laeta* placed the four genera in slightly different phylogenetic positions. In the three-marker dataset (Suppl. material 1: Figure S8), *Bunga* and *Laeta* formed a clade, although it was not very well supported (74/-). This clade was sister to *Hana* and *Arula*, which also formed a clade. In the four-marker dataset (Figure 7), *Bunga* was sister to all remaining clades. Nonetheless, branches of the four-marker dataset had better support values.

Therefore, we again recommend the use of the extra gene region (ND6) next to the conventional DNA markers (COI, mtMutS, 28S rDNA) commonly used in octocoral phylogenetic analyses (Lau et al. 2018, 2019).

New discoveries and descriptions of stoloniferous octocorals outside of the Coral Triangle have shown surprising octocoral novelty, at the species, genus, and family levels (Alderslade and McFadden 2011; McFadden and Ofwegen 2012; Benayahu et al. 2017; Lau et al. 2018, 2019). Arulidae, the most recently described family of stoloniferous octocorals (McFadden and Ofwegen 2012), is a good example. Arulids have unique morphological features that had not been seen before in octocorals, including an expanded fused oral disc, and a new type of sclerite, table-radiates. The species *Bunga payung* gen. nov. et sp. nov. and *Laeta waheedae* gen. nov. et sp. nov. increase the total number of species within the family Arulidae to five. Moreover, they represent the first confirmed records of arulids in and around the shallow waters of the TARP area in Sabah, Malaysia. The discovery of these two monospecific taxa demonstrates that the recently erected family Arulidae is considerably much more diverse than was originally known. For example, there is photographic evidence of an arulid from the reefs of Bali, Indonesia (McFadden and Ofwegen 2012), and it is possible that other regions in or close to the Coral Triangle harbour unknown stoloniferan diversity.

The distinctive feature of the fused oral membrane seen in arulid polyps and its function is not yet fully understood. It has been proposed by Porter (1976) and Sebens (1979) that an increase in size of the capture surface area of polyps could be positively related to the amount of prey captured (Lasker 1981; Lewis 1982), as has also been suggested for scleractinian corals (Todd et al. 2004; Todd 2008). On the other hand, a large polyp size in scleractinians has been observed to be beneficial for the capture and consumption of large prey items (Alamura et al. 2009; Hoeksema and Waheed 2012; Mehrotra et al. 2014, 2016, 2019; Musco et al. 2018). A study on octocorals by Lasker (1981) showed that there were differences in the number of nematocysts, bigger polyps having relatively less nematocysts, which could influence prey capture. The expanded oral disc seen in arulids could perhaps be an adaptation for feeding and compensation for their relatively small polyp size and lower polyp number per colony, and it would be worthwhile to conduct a study of their nematocysts.

Another compelling hypothesis involves the possibility of these zooxanthellate taxa being heterotrophic, in which an increased light-gathering surface for photosynthesis of symbionts could explain the development of the expanded oral disc. Based on currently available information, the expanded oral disc does not appear to have evolved across the Octocorallia radiation, and is unique to the family Arulidae.

Clavulariids of Sabah

Multiple factors made it initially difficult to establish with certainty if the currently described species were either congeners or possibly already described. The most important factor in this matter is the small number of morphological features that represent

the new *Phenganax* species. The absence of sclerites makes it especially challenging to make confident judgements about evolutionary relationships between species within this genus. Additionally, the available historical literature on described stoloniferous species in the Indo- and northwestern Pacific is in a poor state. There are a number of *Clavularia* species listed by Alderslade and McFadden (2011) that could possibly belong to *Phenganax*, mainly due to the fact that these species also lack sclerites and the described distinguishing characters are alike: namely *Clavularia reptans* Hickson, 1894, *Clavularia reptans* sensu Thomson & Henderson (1906: 402), *Clavularia celebensis* Hickson, 1894, *Clavularia pregnans* Thomson & Henderson, 1906.

The main characteristic morphological difference between the *Phenganax* spp. described in this study and the above mentioned *Clavularia* spp. are the "numerous densely packed pinnules", which are sometimes as many as 30 pinnules per row; all *Phenganax* spp. in the current study have six to 15 pinnules on either side of the tentacle rachis. Not all measurements (for example expanded polyp width) were included in the *Clavularia* spp. (Alderslade and McFadden 2011). *Clavularia reptans* was described as having polyps 7.0–10.0 mm width when expanded, whereas expanded polyp widths of *Phenganax* spp. are within the size range of 2.5–5.5 mm. Further information regarding the colouration of the tentacles and polyp body in combination with colony drawings make it doubtful that these *Clavularia* spp. belong to *Phenganax*. Additional arguments supporting the description of the *Phenganax* species in this study involve ecological aspects. The preferred habitat of *P. parrini* is dimly lit and in sheltered locations, below 10 m depth. The described *Phenganax* spp. in the current study, however, were found at exposed locations above 10 m depth.

Despite the fact that the relationships between the *Phenganax* spp., with emphasis on the position of *P. parrini*, seem to be unresolved, and all species lack sclerites to aid in their identification, the described species all had high support values and could be distinguished based on some features in colony growth form and polyp morphology, namely tentacle pinnules, the density of polyps, polyp size and spacing between polyps in a colony.

Similar to the new genera within Arulidae, the results for the *Phenganax* spp. also demonstrate that more specimens and the extra gene region (ND6) resulted in obtaining higher phylogenetic resolution and increased branch support values, and therefore should represent a more accurate reconstruction of evolutionary relationships. Future octocoral taxonomy will unquestionably build upon a combination of molecular and more traditional morphological techniques (Conti-Jerpe and Freshwater 2017); however, the lack of sclerites has important implications for future studies, as these skeletal parts are one of the major diagnostic features of the group. This emphasizes the need for improved molecular techniques, such as finding an optimum between concatenated marker datasets towards whole-genome mapping, combined with next-generation sequencing to allow more reliance on molecular information when morphological information is scarce.

The current and other recent works show that octocoral species without sclerites are not rarities; the absence of sclerites or other calciferous skeletal parts are known from within seven octocoral families (Acanthoaxiidae, Acrossotidae, Cornulariidae, Dendrobrachiidae, Alcyoniidae, Clavulariidae, Xeniidae) (Alderslade and McFadden

2007, 2011; López-González et al. 1995; Benayahu et al. 2017). Sclerites provide protection against predation, provide support and rigidity to soft colony parts, and are critical in octocoral classification (West 1997; Aharonovich and Benayahu 2012). Sclerites in different species differ in density as well as spatial organisation in the connective tissue, and thus they also differ in the degree to which they offer support and protection (Benayahu et al. 2017). It could be hypothesized that small size and inhabiting small cracks on reefs protects small stoloniferous species from exposure and has eliminated the need for sclerites in some of these species. Alternately, perhaps the absence of predation (e.g., by ovuliids or sea slugs) has made the possession of sclerites unnecessary. However, there is no obvious pattern to be found for this character in the octocoral phylogenetic radiation amongst its smallest members (Figure 6), and more work is needed to confirm this hypothesis. The absence of sclerites is an example of the gaps in our present knowledge about octocorals and indicate how much basic work in alpha taxonomy and documentation remains for this group.

Our results demonstrate that the TARP area, off the coast of Kota Kinabalu, in Sabah, Malaysia, harbours stoloniferous octocoral diversity that was previously unknown to science, which is obvious since it represents one of the first studies focusing on Stolonifera in this region. However, the newly described sclerite-free *Phenganax* spp. as well as Clavulariidae sp. are only small pieces of the puzzle in the needed thorough investigation of the polyphyletic family Clavulariidae (McFadden and Ofwegen 2012; Benayahu et al. 2017; Conti-Jerpe and Freshwater 2017; Lau et al. 2019), and an even smaller step towards a full understanding of the morphological and molecular distinctions amongst clades of Stolonifera and ultimately Octocorallia. Molecular data indicate that the entire Octocorallia classification needs re-structuring, but for now researchers still rely on the traditional morphological classification system (Fabricius and Alderslade 2001; Conti-Jerpe and Freshwater 2017), as evolutionary relationships are still far from being fully resolved (McFadden and Ofwegen 2012; Conti-Jerpe and Freshwater 2017). Integrative taxonomy combining not only morphology and molecular biology but also including ecology and biogeography data appears to be the best way to try to better understand the systematics of such a diverse and important group in marine benthic communities (Perez et al. 2016). To this end, marine parks should include in their goal not only the preservation of commercially important faunal diversity (primarily reef fish), but also of other reef organisms, and in particular, small and inconspicuous cryptic species, as it is these small reef inhabitants that make up the vast majority of the diversity of coral reef communities (Hoeksema 2017).

Acknowledgements

We thank Dr. Z. Waheed (Universiti Malaysia Sabah) for her support regarding research permissions and transport license. Access license to Tunku Abdul Rahman Park (TARP) was granted on authority of Sabah Biodiversity Centre and Sabah Parks (Ref: TTS/IP/100-6/2 Jld.8). The boat crew of Universiti Malaysia Sabah (UMS) is thanked

for their logistic support in the field. Dr. Z. Waheed, M.F.A. Nooramli and S.Q. Pang (UMS) are thanked for help in the field. We thank Prof. E. Hirose (University of the Ryukyus) for providing access to the scanning electron microscope (SEM) used in this work. F.R. Stokvis (Naturalis Biodiversity Center) is thanked for his valuable help and advice concerning the phylogenetic analyses of the octocoral data. Dr. L.P. van Ofwegen is thanked for sharing his expert advice. We thank the reviewers, Prof. C.S. McFadden (Harvey Mudd College) and Dr. O. Breedy (University of Costa Rica), for their thorough and helpful comments, which undoubtedly have contributed to a better manuscript. Finally, we would like to thank Prof. B.W. Hoeksema for helping us with his editorial skills. Fieldwork by the first author in TARP, Kota Kinabalu, Sabah, Malaysia was funded by the Okinawa Research Core for Highly Innovative Discipline Science Projects (ORCHIDS). The first author was supported by a MEXT, Japan Student Services Organization (JASSO) scholarship. All material included in this manuscript was collected under approved collection permits and ethics guidelines.

References

Aberer AJ, Kobert K, Stamatakis A (2014) ExaBayes: massively parallel Bayesian tree inference for the whole-genome era. Molecular Biology and Evolution 31: 2553–2556. https://doi.org/10.1093/molbev/msu236

Agustiadi T, Luthfi OM (2017) Diversity of stoloniferan coral (Stolonifera) at Lirang Island, Southwest Maluku (Moluccas), Indonesia. International Journal of Oceans and Oceanography 11: 21–30.

Aharonovich D, Benayahu Y (2012) Microstructure of octocoral sclerites for diagnosis of taxonomic features. Marine Biodiversity 42: 173–177. https://doi.org/10.1007/s12526-011-0102-3

Alamaru A, Bronstein O, Loya Y, Dishon G (2009) Opportunistic feeding by the fungiid coral *Fungia scruposa* on the moon jellyfish *Aurelia aurita*. Coral Reefs 28: 865. https://doi.org/10.1007/s00338-009-0507-7

Alderslade P, McFadden CS (2007) Pinnule-less polyps: a new genus and new species of Indo-Pacific Clavulariidae and validation of the soft coral genus *Acrossota* and the family Acrossotidae (Coelenterata: Octocorallia). Zootaxa 1400: 27–44. https://doi.org/10.11646/zootaxa.1400.1.2

Alderslade P, McFadden CS (2011) A new sclerite-free genus and species of Clavulariidae (Coelenterata: Octocorallia). Zootaxa 3104: 64–68. https://doi.org/10.11646/zootaxa.3104.1.6

Benayahu Y, Jeng MS, Perkol-Finkel S, Dai CF (2004) Soft corals (Octocorallia: Alcyonacea) from southern Taiwan. II. Species diversity and distributional patterns. Zoological Studies 43: 548–560.

Benayahu Y, McFadden CF, Shoham E (2017) Search for mesophotic octocorals (Cnidaria, Anthozoa) and their phylogeny: I. A new sclerite-free genus from Eilat, northern Red Sea. ZooKeys 680: 1–11. https://doi.org/10.3897/zookeys.680.12727

Birkeland C (1997) Life and death of coral reefs, Chapman and Hall, New York, 536 pp. https://doi.org/10.1007/978-1-4615-5995-5

Breedy O, Cortés J (2008) Octocorals (Coelenterata: Anthozoa: Octocorallia) of Isla del Coco, Costa Rica. Revista de Biologia Tropical 56 (Supplement 2): 71–77.

Burchardt E (1902) Alcyonaceen von Thursday Island (Torres-Strasse) und von Amboina, II. Jenaische Denkschriften fur Medizinsch-naturwessen-schaftliche Gessellschaft zu Jena, 8: 655–682. [pls 54–57]

Burke L, Selig E, Spalding M (2002) Reefs at risk in Southeast Asia. World Resources Institute, USA, 72 pp. https://wriorg.s3.amazonaws.com/s3fs-public/pdf/rrseasia_full.pdf

Calcinai B, Bavestrello G, Bertolino M, Pica D, Wagner D, Cerrano C (2013) Sponges associated with octocorals in the Indo-Pacific, with the description of four new species. Zootaxa 3617: 1–61. https://doi.org/10.11646/zootaxa.3617.1.1

Carpenter KE, Abrar M, Aeby GS, Aronson RB, Banks S, Bruckner A, Chiriboga A, Cortés J, Charles Delbeek JC, DeVantier L, Edgar GJ, Edwards AJ, Fenner D, Guzmán HM, Hoeksema BW, Hodgson G, Johan O, Licuanan WY, Livingstone SR, Lovell ER, Moore JA, Obura DO, Ochavillo D, Polidoro BA, Precht WF, Quibilan MC, Reboton C, Richards Z, Rogers AD, Sanciangco J, Sheppard A, Sheppard C, Smith J, Stuart S, Turak E, Veron JEN, Wallace C, Weil E, Wood E (2008) One-third of reef-building corals face elevated extinction risk from climate change and local impacts. Science 321: 560–563. https://doi.org/10.1126/science.1159196

Conti-Jerpe IE, Freshwater DW (2017) *Hedera caerulescens* (Alcyonacea: Alcyoniidae), a new genus and species of soft coral from the temperate North Atlantic: invasive in its known range? Invertebrate Systematics 31: 723–733. https://doi.org/10.1071/IS16069

Dias TLP, Gondim AI (2016) Bleaching in scleractinians, hydrocorals, and octocorals during thermal stress in a northeastern Brazilian reef. Marine Biodiversity 46: 303–307. https://doi.org/10.1007/s12526-015-0342-8

Fabricius KE, Alderslade P (2001) Soft corals and sea fans: a comprehensive guide to the tropical shallow water genera of the central-west Pacific, the Indian Ocean and the Red Sea. Australian Institute of Marine Science, Townsville.

Fabricius KE, Alderslade P, Williams GC, Colin PL, Golbuu Y (2007) Octocorallia in Palau, Micronesia: Effects of biogeography and coastal influences on local and regional biodiversity. In: Kayanne H, Omori M, Fabricius K, Verheij E, Colin P, Golbuu Y, Yurihira H (Eds) Coral Reefs of Palau. Palau International Coral Reef Centre, Palau, 231 pp.

Fisher R, O'Leary RA, Low-Choy S, Mengersen K, Knowlton N, Brainard RE, Caley MJ (2015) Species richness on coral reefs and the pursuit of convergent global estimates. Current Biology 25: 500–505. https://doi.org/10.1016/j.cub.2014.12.022

Foster PG (2004) Modeling compositional heterogeneity. Systematic Biology 53: 485–495. https://doi.org/10.1080/10635150490445779

Gaurav V, Lohman DJ, Meier R (2011) SequenceMatrix: concatenation software for the fast assembly of multi-gene datasets with character set and codon information. Cladistics 27: 171–180. https://doi.org/10.1111/j.1096-0031.2010.00329.x

Goreau T, McClanahan T, Hayes R, Strong A (2000) Conservation of coral reefs after the 1998 global bleaching event. Conservation Biology 14: 5–15. https://doi.org/10.1046/j.1523-1739.2000.00011.x

Hall TA (1999) BioEdit: a user-friendly biological sequence alignment editor and analysis program for Windows 95/98/NT. Nucleic Acids Symposium Series 41: 95–98. jwbrown.mbio.ncsu.edu/JWB/papers/1999Hall1.pdf

Heery EC, Hoeksema BW, Browne NK, Reimer JD, Ang PO, Huang D, Friess DA, Chou LM, Loke LHL, Saksena-Taylor P, Alsagoff N, Yeemin T, Sutthacheep M, Vo ST, Bos AR, Gumanao GS, Syed Hussein MA, Waheed Z, Lane DJW, Johan O, Kunzmann A, Jompa J, Suharsono, Taira D, Bauman AG, Todd PA (2018) Urban coral reefs: Degradation and resilience of hard coral assemblages in coastal cities of East and Southeast Asia. Marine Pollution Bulletin 135: 654–681. https://doi.org/10.1016/j.marpolbul.2018.07.041

Hoeksema BW (2007) Delineation of the Indo-Malayan centre of maximum marine biodiversity: The Coral Triangle. In: Renema W (Ed.) Biogeography, Time, and Place: Distributions, Barriers, and Islands. Springer, Dordrecht, 117–178. https://doi.org/10.1007/978-1-4020-6374-9_5

Hoeksema BW (2017) The hidden biodiversity of tropical coral reefs. Biodiversity 18: 8–12. https://doi.org/10.1080/14888386.2017.1307787

Hoeksema BW, Waheed Z (2012) It pays to have a big mouth: mushroom corals ingesting salps at Sabah, Malaysia. Marine Biodiversity 42: 297–302. https://doi.org/10.1007/s12526-012-0110-y

Huang D, Licuanan WY, Hoeksema BW, Chen CA, Ang PO, Huang H, Lane DJW, Vo ST, Waheed Z, Amri AY, Yeemin T, Chou LM (2015) Extraordinary diversity of reef corals in the South China Sea. Marine Biodiversity 45: 157–168. https://doi.org/10.1007/s12526-014-0236-1

Hughes TP, Bellwood DR, Connolly SR (2002) Biodiversity hotspots, centres of endemicity, and the conservation of coral reefs. Ecology Letters 5: 775–784. https://doi.org/10.1046/j.1461-0248.2002.00383.x

Hughes TP, Kerry JT, Álvarez-Noriegal M, Álvarez-Romero JG, Anderson KD, Baird AH, Babcock RC, Beger M, Bellwood DR, Berkelmans R, Bridge TC, Butler IR, Byrne M, Cantin NE , Comeau S, Connolly SR, Cumming GS, Dalton SJ, Diaz-Pulido G, Eakin CM, Figueira WF, Gilmour JP, Harrison HB, Heron SF, Hoey AS, Hobbs JPA, Hoogenboom MO, Kennedy EV, Kuo CY, Lough JM, Lowe RJ, Liu G, McCulloch MT , Malcolm HA, McWilliam MJ, Pandolfi JM, Pears RJ, Pratchett MS, Schoepf V, Simpson T, Skirving WJ, Sommer B, Torda G, Wachenfeld DR, Willis BL, Wilson SK (2017) Global warming and recurrent mass bleaching of corals. Nature 543: 373–377. https://doi.org/10.1038/nature21707

Hughes TP, Kerry JT, Simpson T (2018) Large-scale bleaching of corals on the Great Barrier Reef. Ecology 99: 501. https://doi.org/10.1002/ecy.2092

Johnson JY (1861) Notes on the sea-anemones of Madeira, with descriptions of new species. Proceedings of the Zoological Society of London 1861: 298–306.

Kassem K, Hoeksema BW, Affendi YA (2012) Semporna Marine Ecological Expedition. WWF-Malaysia, NCB Naturalis, Universiti Malaysia Sabah. Kota Kinabalu, Malaysia, 267 pp.

Katoh K, Standley DM (2013) MAFFT Multiple sequence alignment software version 7: Improvements in performance and usability. Molecular Biology and Evolution 30: 772–780. https://doi.org/10.1093/molbev/mst010

Kearse M, Moir M, Wilson A, Stones-havas S, Cheung M, Sturrock S, Buxton S, Cooper A, Markowitz S, Duran C, Thierer T, Ashton B, Meintjes P, Drummond A (2012) Geneious

Basic: An integrated and extendable desktop software platform for the organization and analysis of sequence data. Bioinformatics 28: 1647–1649. https://doi.org/10.1093/bioinformatics/bts199

Kumar S, Stecher G, Li M, Knyaz C, Tamura K (2018) MEGA X: Molecular evolutionary genetics analysis across computing platforms. Molecular Biology and Evolution 35: 1547–1549. https://doi.org/10.1093/molbev/msy096

Lane DJW, Hoeksema BW (2016) Mesophotic mushroom coral records at Brunei Darussalam support westward extension of the Coral Triangle to the South China Sea waters of Northwest Borneo. Raffles Bulletin of Zoology 64: 204–212.

Larsson A (2014) AliView: a fast and lightweight alignment viewer and editor for large datasets. Bioinformatics 30: 3276–3278. https://doi.org/10.1093/bioinformatics/btu531

Lasker HR (1981) A comparison of the particulate feeding abilities of three species of gorgonian soft coral, Marine Ecology Progress Series 5: 61–67. https://www.int-res.com/articles/meps/5/m005p061.pdf

Lau YW, Stokvis FR, Ofwegen LP van, Reimer JD (2018) Stolonifera from shallow waters in the north-western Pacific: a description of a new genus and two new species within the Arulidae (Anthozoa, Octocorallia). ZooKeys 790: 1–19. https://doi.org/10.3897/zookeys.790.28875

Lau YW, Stokvis FR, Imahara Y, Reimer JD (2019) The stoloniferous octocoral, *Hanabira yukibana*, gen. nov., sp. nov., of the southern Ryukyus has morphological and symbiont variation. Contributions to Zoology 88: 54–77. https://doi.org/10.1163/18759866-20191355

Lewis JB (1982) Feeding behaviour and feeding ecology of the Octocorallia (Coelenterata: Anthozoa) Journal of Zoology 196: 371–384. https://doi.org/10.1111/j.1469-7998.1982.tb03509.x

López-González PJ, Gili JM (2001) A new genus and species of stoloniferous octocoral from the Azores Archipelago (Cnidaria: Anthozoa). Bulletin of the Biological Society of Washington 10: 130–139.

López-González PJ, Ocaña O, García-Gómez JC, Núñez J (1995) North-eastern Atlantic and Mediterranean species of Cornulariidae Dana, 1846 (Anthozoa: Stolonifera) with the description of a new genus. Zoologische Mededelingen Leiden 69: 261–272.

Lulofs RB (1973) A reef survey of Pulau Gaya and associated islands Part I. World Wide Fund for Nature (WWF) Malaysia, 16 pp.

Lulofs RB, Langham NPE, Mathias JA (1974) A reef survey of Pulau Gaya and associated islands Part II. World Wide Fund for Nature (WWF) Malaysia, 7 pp.

Mathias JA, Langham NPE (1978) Chapter 5: Coral reefs. In: Chua TE, Mathias JA (Eds) Coastal resources of West Sabah. Universiti Sains Malaysia, Penang, 117–151.

McFadden CS, Ofwegen LP van (2012) Stoloniferous octocorals (Anthozoa, Octocorallia) from South Africa, with descriptions of a new family of Alcyonacea, a new genus of Clavulariidae, and a new species of *Cornularia* (Cornulariidae). Invertebrate Systematics 26: 331–356. https://doi.org/10.10071/IS12035

McFadden CS, Sanchez JA, France SC (2010) Molecular phylogenetic insights into the evolution of Octocorallia: a review. Integrative and Comparative Biology 50: 389–410. https://doi.org/10.1093/icb/icq056

McFadden CS, Benayahu Y, Pante E, Thoma JN, Nevarez PA, France SC (2011) Limitations of mitochondrial gene barcoding in Octocorallia. Molecular Ecology Resources 11: 19–31. https://doi.org/10.1111/j.1755-0998.2010.02875.x

Mehrotra R, Scott CM, Rohrer JM, Hoeksema BW (2015) Predation on a sacoglossan gastropod by a mushroom coral. Coral Reefs 34: 517. https://doi.org/10.1007/s00338-015-1285-z

Mehrotra R, Scott CM, Hoeksema BW (2016) A large gape facilitates predation on salps by *Heteropsammia* corals. Marine Biodiversity 46: 323–324. https://doi.org/10.1007/s12526-015-0379-8

Mehrotra R, Scott CM, Monchanin C, Phongsuwan N, Caballer M, Chavanich S, Hoeksema BW (2019) Selective consumption of sacoglossan sea slugs (Mollusca: Gastropoda) by scleractinian corals (Cnidaria: Anthozoa). PLoS ONE 14: e0215063. https://doi.org/10.1371/journal.pone.0215063

Miyazaki Y, Reimer JD (2015) A new genus and species of octocoral with aragonite calcium-carbonate skeleton (Octocorallia, Helioporacea) from Okinawa, Japan. ZooKeys 511: 1–23. https://doi.org/10.3897/zookeys.511.9432

Musco L, Vega Fernandez T, Caroselli E, Roberts JM, Badalamenti F (2018) Protocooperation among small polyps allows the coral *Astroides calycularis* to prey on large jellyfish. Ecology 99: 2400–2401. https://doi.org/10.1002/ecy.2413

Nyanti L, Johnston NA (1992) The coral reefs of the Tunku Abdul Rahman Park, Sabah. Sabah Society Journal 9: 323–348.

Pérez CD, de Moura Neves B, Cordeiro RT, Williams GC, Cairns SD (2016) Diversity and Distribution of Octocorallia. In: Goffredo S, Dubinsky Z (Eds) The Cnidaria, Past, Present and Future. Springer, Cham, 109–123. https://doi.org/10.1007/978-3-319-31305-4_8

Pilcher N, Cabanban AS (2000) The status of coral reefs in eastern Malaysia. In: Global Coral Reef Monitoring Network (GCRMN) Report. Australia Institute of Marine Science, Townsville, 81 pp.

Polunin NVC, Roberts CM (1996) Reef Fisheries, Chapman and Hall, London, 477 pp. https://doi.org/10.1007/978-94-015-8779-2

Porter JW (1976) Autotrophy, heterotrophy and resource partitioning in Caribbean reef building corals. The American Naturalist 110: 731–742. https://doi.org/10.1086/283100

Prada C, Weil E, Yoshioka PM (2010) Octocoral bleaching during unusual thermal stress. Coral Reefs 29: 41–45. https://doi.org/10.1007/s00338-009-0547-z

Praveena SM, Siraj SS, Aris AZ (2012) Coral reefs studies and threats in Malaysia: a mini review, Reviews in Environmental Science and Biotechnology 11: 27–39. https://doi.org/10.1007/s11157-011-9261-8

Rambout A (2014) FigTree.

Ranwez V, Harispe S, Delsuc F, Douzery EJP (2011) MACSE: Multiple Alignment of Coding SEquences accounting for frameshifts and stop codons. PLoS ONE 6: e22594. https://doi.org/10.1371/journal.pone.0022594

Reaka-Kudla ML (1997) The global biodiversity of coral reefs: A comparison with rain forests, 83–108. In: Reaka-Kudla ML, Wilson DE, Wilson EO (Eds) Biodiversity II: Understanding and protecting our biological resources. Joseph Henry Press, Washington, DC, 549 pp. citeseerx.ist.psu.edu/viewdoc/download?doi=10.1.1.466.2268&rep=rep1&type=pdf

Reef Check Malaysia (2014) Status of coral reefs in Malaysia, 2014. Saving our reefs, Research, Education, Conservation, 72 pp. https://data.nodc.noaa.gov/coris/library/NOAA/NonCRCP/Corals/20150320_RCM_Survey_Report_2014.pdf

Roberts CM, Mittermeier CG, Schueler FW (2002) Marine biodiversity hotspots and conservation priorities for tropical reefs. Science 295: 1280–1285. https://doi.org/10.1126/science.1067728

Sabroux R, Hassanin A, Corbari L (2019) Four times more species of sea spiders (Arthropoda: Pycnogonida) in Martinique Island (Lesser Antilles). Marine Biodiversity 49: 1519–1535. https://doi.org/10.1007/s12526-019-00957-9

Samimi-Namin K, van Ofwegen LP (2012) The octocoral fauna of the Gulf. In: Riegl BM, Purkis S (Eds) Coral Reefs of the Gulf: Adaptation to Climatic Extremes. Springer; Netherlands, 225–252. https://doi.org/10.1007/978-94-007-3008-3_12

Sánchez JA (2016) Diversity and evolution of octocoral animal forests at both sides of Tropical America. 20–21. In: Rossi S, Bramanti L, Gori A, Orejas Saco del Valle C (Eds) Marine Animal Forests. Springer, Cham. https://doi.org/10.1007/978-3-319-17001-5_39-1

Sánchez JA, McFadden CS, France SC, Lasker HR (2003) Molecular phylogenetic analyses of shallow-water Caribbean octocorals. Marine Biology 142: 975–9872. https://doi.org/10.1007/s00227-003-1018-7

Sebens KP (1979) The energetics of asexual reproduction and colony formation in benthic marine invertebrates. American Zoologist 19: 683–697. https://doi.org/10.1093/icb/19.3.683

Spait M (2001) Paper 16. Marine park management: Issues and challenges, 6th SITE Research Seminar, 13–14 September 2001: 1–11. https://doi.org/10.1016/S1353-4858(01)01102-3

Stamatakis A (2014) RAxML version 8: a tool for phylogenetic analyses and post-analysis of large phylogenies. Bioinformatics 30: 1312–1313. https://doi.org/10.1093/bioinformatics/btu033

Todd PA (2008) Morphological plasticity in scleractinian corals. Biological Reviews 83: 315–337. https://doi.org/10.1111/j.1469-185X.2008.00045.x

Todd PA, Sidle RC, Lewin-Koh NJI (2004) An aquarium experiment for identifying the physical factors inducing morphological change in two massive scleractinian corals. Journal of Experimental Marine Biology and Ecology 299: 97–113. https://doi.org/10.1016/j.jembe.2003.09.005

Townsend D (2015) First comprehensive list of the coral reef fishes of Tunku Abdul Rahman Park, Sabah, Malaysia (Borneo). Check List 11: 1762. https://doi.org/10.15560/11.7.1762

Van de Water JAJM, Allemand D, Ferrier-Pagés C (2018) Host-microbe interactions in octocoral holobionts – recent advances and perspectives. Microbiome 6: 64. https://doi.org/10.1186/s40168-018-0431-6

Van Soest RWM, Verseveldt J (1987) Unique symbiotic octocoral-sponge association from Komodo. Indo-Malayan Zoology 4: 27–32.

Veron J, Stafford-Smith M, DeVantier L, Turak E (2015) Overview of distribution patterns of zooxanthellate Scleractinia. Frontiers in Marine Science 1: 81. https://doi.org/10.3389/fmars.2014.00081

Waheed Z, Hoeksema BW (2013) A tale of two winds: species richness patterns of reef corals around the Semporna Peninsula, Malaysia. Marine Biodiversity 43: 37–51. https://doi.org/10.1007/s12526-012-0130-7

Waheed Z, Hoeksema BW (2014) Diversity patterns of scleractinian corals at Kota Kinabalu, Malaysia, in relation to exposure and depth. Raffles Bulletin of Zoology 62: 66–82. https://lkcnhm.nus.edu.sg/app/uploads/2017/06/62rbz066-082.pdf

Waheed Z, Adnan FAF, Hwa LCH, Hashim SRM (2007) Status of coral reefs and sedimentation at Kota Kinabalu: a preliminary study at Gaya Bay and Sepangar Bay. Borneo Journal of Marine Science and Aquaculture: 27–43. http://wwwsst.ums.edu.my/data/file/BMzN-Mit3WmB3.pdf

Waheed Z, van Mil HGJ, Syed Hussein MA, Jumin R, Golam Ahad B, Hoeksema BW (2015a) Coral reefs at the northernmost tip of Borneo: an assessment of scleractinian species richness patterns and benthic reef assemblages. PLoS ONE 10(12): e0146006. https://doi.org/10.1371/journal.pone.0146006

Waheed Z, Benzoni F, van der Meij SET, Terraneo TI, Hoeksema BW (2015b) Scleractinian corals (Fungiidae, Agariciidae and Euphylliidae) of Pulau Layang-Layang, Spratly Islands, with a note on *Pavona maldivensis* (Gardiner, 1905). ZooKeys 517: 1–37. https://doi.org/10.3897/zookeys.517.9308

West JM (1997) Plasticity in the sclerites of a gorgonian coral: tests of water motion, light level, and damage cues. The Biological Bulletin 192: 279–289. https://doi.org/10.2307/1542721

Williams RB (1996) The rediscovery of *Cervera atlantica* (Johnson, 1861) (Cnidaria: Octocorallia): notes on its identification, ecology and geographical distribution. Bulletin Zoölogisch Museum Amsterdam 15: 65–74.

Wolf NG, Bermingham EB, Reaka ML (1983) Relationships between fishes and mobile benthic invertebrates on coral reefs, 89–96. In: ML Reaka (Ed.) The ecology of deep and shallow coral reefs, Vol. 1. Washington, DC: National Oceanic and Atmospheric National Undersea Research Program. aoml.noaa.gov/general/lib/CREWS/SaltRiver/salt_river26.pdf

Wood EM (1977) Coral reefs in Sabah: present damage and potential dangers. Malayan Nature Journal 31: 49–57.

Wood EM (1979) Ecological study of coral reefs in Sabah. Technical report, WWF Project Number MYS 15, Petaling Jaya, Malaysia, 163 pp.

Supplementary material 1

Figures S1–S8, Tables S1–S6

Authors: Yee Wah Lau, James D. Reimer

Data type: Adobe Acrobat Document (.pdf)

Link: https://doi.org/10.3897/zookeys.872.36288.suppl1